DOCUMENT RELEASE AND CHANGE FORM

Prepared For the U.S. Department of Energy, Assistant Secretary for Environmental Management
By Washington River Protection Solutions, LLC., PO Box 850, Richland, WA 99352
Contractor For U.S. Department of Energy, Office of River Protection, under Contract DE-AC27-08RV14800

TRADEMARK DISCLAIMER: Reference herein to any specific commercial product, process, or service by trade name, trademark, manufacturer, or otherwise, does not necessarily constitute or imply its endorsement, recommendation, or favoring by the United States government or any agency thereof or its contractors or subcontractors. Printed in the United States of America.

Release Stamp

DATE:
Mar 17,2021
HANFORD RELEASE

1. **Doc No:** RPP-RPT-60101 **Rev.** 00

2. **Title:**
Model Package Report Flow and Contaminant Transport Numerical Model used in WMA A-AX Performance Assessment and RCRA Closure Analysis

3. **Project Number:** T2C25 ☐N/A

4. **Design Verification Required:** ☐Yes ☒No

5. **USQ Number:** ☒ N/A RPP-27195

6. **PrHA Number** **Rev.** ☒ N/A

Clearance Review Restriction Type: public

7. **Approvals**

Title	Name	Signature	Date
Clearance Review	Ayers, Lynn M	*Ayers, Lynn M*	03/17/2021
Document Control Approval	Alvarez, Efren	*Alvarez, Efren*	03/17/2021
Originator	Watson, David (Dj) J	*Watson, David (Dj) J*	09/28/2020
Other Approver	Lungu, Cris C	*Lungu, Cris C*	09/28/2020
Other Approver	Lee, Kearn (Pat)	*Lee, Kearn (Pat)*	10/01/2020
Responsible Manager	Rutland, Paul L	*Rutland, Paul L*	10/01/2020

8. **Description of Change and Justification**

Initial Release

9. **TBDs or Holds** ☒N/A

10. **Related Structures, Systems, and Components**

a. Related Building/Facilities ☒N/A	b. Related Systems ☒N/A	c. Related Equipment ID Nos. (EIN) ☒N/A

11. **Impacted Documents – Engineering** ☒N/A

Document Number	Rev.	Title

12. **Impacted Documents (Outside SPF):**

N/A

13. **Related Documents** ☐N/A

Document Number	Rev.	Title
RPP-CALC-63164	00	WMA A-AX Performance Assessment Contaminant Fate and Transport Process Model to Evaluate Impacts to Groundwater
RPP-CALC-63248	00	WMA A-AX Performance Assessment Flow and Transport Process Model Support of the Sensitivity Analysis
RPP-ENV-61497	00	Preliminary Performance Assessment of Waste Management Area A-AX, Hanford Site, Washington
RPP-ENV-62206	00	Analysis of Post-Closure Groundwater Impacts from Hazardous Chemicals in Residual Wastes in Tanks and Ancillary Equipment at Waste Management Area A-AX at the Hanford Site, Southeast Washington

14. **Distribution**

Name	Organization
Bergeron, Marcel P	CLOSURE & INTERIM MEASURES
Lee, Kearn (Pat)	CLOSURE & INTERIM MEASURES
Singleton, Kristin M	CLOSURE & INTERIM MEASURES
Watson, David (Dj) J	CLOSURE & INTERIM MEASURES

INFORMATION CLEARANCE REVIEW AND RELEASE APPROVAL

Part I: Background Information

Title: Model Package Report Flow and Contaminant Transport Numerical Model Used in WMA A AX Performance Assessment and RCRA Closure Analysis	Information Category: ☐ Abstract ☐ Journal Article ☐ Summary ☐ Internet ☐ Visual Aid ☐ Software ☐ Full Paper ☐ Report ☑ Other Report
Publish to OSTI? ☐ Yes ☑ No	

	Yes	NA
Trademark/Copyright "Right to Use" Information or Permission Documentation	☐	☑

Document Number: RPP-RPT-60101 Revision 0 Date: September 2020

Author: Watson, David (Dj) J

Part II: External/Public Presentation Information

Conference Name:

Sponsoring Organization(s): DOE-ORP

Date of Conference: Conference Location:

Will Material be Handed Out? ☐ Yes ☑ No Will Information be Published? ☐ Yes ☑ No *(If Yes, attach copy of Conference format instructions/guidance.)*

Part III: WRPS Document Originator Checklist

Description	*Yes*	*N/A*	*Print/Sign/Date*
Information Product meets requirements in TFC-BSM-AD-C-01?	☐	☑	
Document Release Criteria in TFC-ENG-DESIGN-C-25 completed? (Attach checklist)	☐	☑	
If product contains pictures, safety review completed?	☐	☑	

Part IV: WRPS Internal Review

Function	*Organization*	*Date*	*Print Name/Signature/Date*
Subject Matter Expert	WRPS	03/11/2021	Watson, David (Dj) J IDMS data attached
Responsible Manager	WRPS	10/05/2020	Rutland, Paul L IDMS data attached
Other:			

Part V: IRM Clearance Services Review

Description	*Yes*	*No*	*Print Name/Signature*
Document Contains Classified Information?	☐	☒	If Answer is "Yes," ADC Approval Required Print Name/Signature/Date
Document Contains Information Restricted by DOE Operational Security Guidelines?	☐	☒	Reviewer Signature: Print Name/Signature/Date
Document is Subject to Release Restrictions? *If the answer is "Yes," please mark category at right and describe limitation or responsible organization below:*	☐	☒	Document contains: ☐ Applied Technology ☐ Protected CRADA ☐ Personal/Private ☐ Export Controlled ☐ Proprietary ☐ Procurement – Sensitive ☐ Patentable Info. ☐ OUO ☐ Predecisional Info. ☐ UCNI ☐ Restricted by Operational Security Guidelines ☐ Other (Specify)
Additional Comments from Information Clearance Specialist Review? Comments incorporated; URLs redacted.	☒	☐	Information Clearance Specialist Approval APPROVED By Lynn M. Ayers at 8:35 am, Mar 15, 2021 Print Name/Signature/Date

When IRM Clearance Review is Complete – Return to WRPS Originator for Final Signature Routing (Part VI)

INFORMATION CLEARANCE REVIEW AND RELEASE APPROVAL

Part VI: Final Review and Approvals

Description	*Approved for Release*		*Print Name/Signature*
	Yes	*N/A*	
WRPS External Affairs	☒	☐	Mc Cune, Hal C - IDMS data attached
WRPS Office of Chief Counsel	☒	☐	Roden, Mari L - IDMS data attached
DOE – ORP Public Affairs/Communications	☒	☐	Tyree, Geoff T - IDMS data attached
Other: DOE OCC	☒	☐	Hellstrom, George W - IDMS data attached
Other: DOE ORP SME	☒	☐	Lobos, Rodrigo A - IDMS data attached

Comments Required for WRPS-Indicate Purpose of Document:

This model package report documents the development of the integrated vadose and saturated zone flow and transport model for the Waste Management Area (WMA) A AX performance assessment. This modeling capability is intended for use in addressing the analysis requirements outlined in Appendix I of the Hanford Federal Facility Agreement and Consent Order (Ecology et al. 1989) for assessment of the radiological impacts of waste residuals in a closed WMA A AX under U.S. Department of Energy O 435.1, Radioactive Waste Management and evaluation of the hazardous chemical impacts for the same wastes under the Resource Conservation and Recovery Act of 1976. The overall objective of the modeling effort is to provide a basis for making informed closure decisions pertinent to WMA A AX. The results of the flow and transport model are intended to provide information regarding the potential long term impact on groundwater of waste residuals left in tanks and associated ancillary equipment (such as pipelines) at closure. Impacts related to past tank waste leaks, losses, and unplanned releases are outside the scope of this modeling effort.

APPROVED
By Lynn M. Ayers at 8:35 am, Mar 15, 2021

Approved for Public Release; Further Dissemination Unlimited

Information Release Station

Was/Is Information Product Approved for Release? ☒ Yes ☐ No

If Yes, what is the Level of Releaser? ☑ Public/Unrestricted ☐ Other (Specify) _____

Date Information Product Stamped/Marked for Release: 03/15/2021

Was/Is Information Product Transferred to OSTI? ☐ Yes ☒ No

Forward Copies of Completed Form to WRPS Originator

- <workflow name="**(LMA) Normal - RPP-RPT-60101 Rev0**" id="**277295503**">
  - <task name="**Clearance Process**" id="**0**" date-initiated="**20201005T0855**" performer="**LYNN M AYERS**" performer-id="**212954838**" username="**h3998817**">
    <comments>**DUE: Monday, October 19 - 9 AM Please review for public release, "Model Package Report Flow and Contaminant Transport Numerical Model Used in WMA A AX Performance Assessment and RCRA Closure Analysis," submitted by DJ Watson. Thank you, Lynn Ayers Information Clearance**</comments>
  </task>
  <task name="**Add XML**" id="**1**" date-done="**20201005T0855**" />
  <task name="**Manager Approval**" id="**41**" date-due="**20201008T0855**" date-done="**20201005T0959**" performer="**PAUL L RUTLAND**" performer-id="**140633218**" username="**h4494439**" disposition="**Approve**" authentication="**true**" />
  <task name="**Document Reviewer1**" id="**54**" date-due="**20201008T0959**" date-done="**20201007T0639**" performer="**HAL C MC CUNE**" performer-id="**226350486**" username="**h7687509**" disposition="**Public Release**" authentication="**true**" />
  - <task name="**Document Reviewer3**" id="**52**" date-due="**20201008T0959**" date-done="**20201123T1526**" performer="**RODRIGO A LOBOS**" performer-id="**232334741**" username="**h2488419**" disposition="**Public Release**" authentication="**true**">
    <comments>**Page 1-4 line 20. "Since the retrieval process has not yet begun, the inventory of tank…" This statement is inaccurate. Tank A-102 has been retrieved, using two technologies, pending to forego the third. Tanks A-104 & A-105 were retrieved years ago when tank damage was discovered. Suggest modifying text to state that the retrieval process is underway or is not complete. Page 1-9 line 33. "Ecology placed DOE under RCRA Corrective Action.." This sentence is incorrect and should be deleted. Text suggestion: " DOE gathered data used in estimating contaminant nature and extent used to evaluate risk to human health and the environment. Documents developed to support this activity relevant to WMA A-AX PA include the following." Page 2-1 line 6. " While there are no Federal requirements for protection of water resources for a radioactive waste disposal facility…" This sentence is incorrect and should be deleted. i.e. At A-AX on Hanford site Federal requirements under CERCLA and applicable ARARs apply including DWS and MCLs for both radionuclides and non-radionuclides. Additionally protectiveness under CERCLA will need to be attained.**</comments>
  </task>
  <task name="**Document Reviewer2**" id="**53**" date-due="**20201008T0959**" date-done="**20210127T0949**" performer="**MARI L RODEN**" performer-id="**262637370**" username="**h0048955**" disposition="**Public Release**" authentication="**true**" />
  - <task name="**Doc Owner Clearance Review**" id="**13**" date-due="**20210128T1009**" date-done="**20210204T0608**" performer="**DAVID J WATSON**" performer-id="**231794240**" username="**h0098416**" disposition="**Send On**" authentication="**true**">
    <comments>**Made red-line/strikeout corrections based on comments from Rod Lobos.**</comments>
  </task>
  <task name="**Milestone 1**" id="**24**" date-done="**20210204T0611**" />
  <task name="**ORP Document Reviewer1**" id="**57**" date-due="**20210208T0611**" date-done="**20210209T1550**" performer="**GEOFFREY T TYREE**" performer-id="**6158846**" username="**h0068565**" disposition="**Public Release**" authentication="**true**" />

```
  <task name="ORP Document Reviewer2" id="58" date-due="20210208T0611"
    date-done="20210310T1711" performer="GEORGE W HELLSTROM" performer-
    id="273013663" username="h8579141" disposition="Public Release"
    authentication="true" />
  <task name="Doc Owner Reviews ORP Comments" id="61" date-
    due="20210311T1710" date-done="20210311T1425" performer="DAVID J
    WATSON" performer-id="231794240" username="h0098416" disposition="Send
    On" authentication="true" />
  <task name="Milestone 2" id="62" date-done="20210311T1425" />
  <task name="Verify Doc Consistency" id="4" date-due="20210312T1425" date-
    done="20210311T1433" performer="LYNN M AYERS" performer-id="212954838"
    username="h3998817" disposition="Cleared" authentication="true" />
</workflow>
```

RPP-RPT-60101
Revision Rev. 0

Model Package Report Flow and Contaminant Transport Numerical Model Used in WMA A-AX Performance Assessment and RCRA Closure Analysis

Prepared by:
W. J. McMahon
CH2M HILL Plateau Remediation Company

R. Khaleel
S. Mehta
R. M. Nell
A. K. Wahi
INTERA, Inc.

M. P. Connelly
TecGeo, Inc.

M. P. Bergeron
R. A. Hiergesell
Washington River Protection Solutions, LLC

Prepared for:
Washington River Protection Solutions, LLC

Date Published: **October 2020**

Prepared for the U.S. Department of Energy
Office of River Protection

Contract No. DE-AC27-08RV14800

Approved for Public Release – Further Dissemination Unlimited

Approved for Public Release;
Further Dissemination Unlimited

ENVIRONMENTAL MODEL PACKAGE REPORT COVER PAGE

Section 1 - Completed by Responsible Manager

Project:
Waste Management Area A-AX Performance Assessment

Date:
4/4/2019

Environmental Model Name and Version:
WMA A-AX PA Tank Residual Flow and Transport Process Model

RELEASE/ISSUE

Section 2 - Completed by Preparer

Document Number: RPP-RPT-60101 Revision No.: _____

Revision History

Revision No.	Description	Date	Affected Pages
0	Initial Release	4/4/2019	All

Section 3 - Completed by Responsible Manager

Document Control	Yes	No
1. Is document intended to be controlled within the Document Management Control System (DMCS)?	◉	○
2. Does document contain scientific and technical information intended for public use?	◉	○
3. Does document contain controlled-use information?	○	◉

Section 4 - Training and Software Installation Approval *(Completed Prior to Model Implementation)*

Modeler-Required Training Completed:

Training Coordinator:

Print First and Last Name	Postion	Signature	Date
William E. Nichols	Scientist (CH-PRC)		4 APR 2019

Implementation Software Installation and Checkout Certified:

Training Coordinator:

Print First and Last Name	Postion	Signature	Date
William E. Nichols	Scientist (CH-PRC)		4 APR 2019

Section 5 - Document Review and Approval

Model Developer:

Print First and Last Name	Postion	Signature	Date
William J. McMahon	Sr. Engineer (CH-PRC)		04/04/19

Model Checker:

Print First and Last Name	Postion	Signature	Date
Amena Mayenna	Scientist (INTERA)		04/04/19

Model Senior Reviewer:

Print First and Last Name	Postion	Signature	Date
Mart Oostrom	Prin. Hydrogeo(INTERA)		4/4/19

Responsible Manager or Designee:

Print First and Last Name	Postion	Signature	Date
Robert A. Hiergesell	Responsible Manager		4/8/19

 A-6006-960 (REV 1)

Supporting Information for

WMA A-AX Model Package Report (RPP-RPT-60101)
Flow and Contaminant Transport Numerical Model Used in WMA A-AX Performance Assessment and RCRA Closure Analysis

1. Identification of Need for RPP-RPT-60101:

This Model Package Report (MPR) provides a description of the development of the primary 3D process model that is utilized in the WMA A-AX Preliminary Performance Assessment to simulate flow and contaminant transport within the fully-linked vadose and saturated zones beneath WMA A-AX. The model incorporates the geologic framework described in RPP-RPT-60101 (*Model Package Report: Geologic Framework Model used in WMA A-AX Performance Assessment and RCRA Closure Analysis*) and assigns representative hydraulic properties to each of the hydrostratigraphic unit. The model develops the basis for constructing the complementary WMA A-AX system model, which is then employed to evaluate the long-term release of contaminants from tank residuals and their migration through the vadose zone and then via the aquifer to a point where the exposure to a member of the public can be calculated.

2. Identification of MPR Document Originators, Checker, and Subject Matter Expert (SME)/Senior Reviewer (SR)

William J. McMahon, CH2M HILL – Plateau Remediation Company

M.S., Agricultural Engineering, Texas A&M University
B.S., Agricultural Engineering, University of California, Davis

Mr. McMahon is a qualified individual for perform and document the STOMP calculations provided in this EMCF. He is a qualified STOMP User at the Hanford and has received training on the WRPS procedures for this environmental model work. He specializes in hydrologic data collection, analysis, and interpretation, and groundwater and vadose zone numerical modeling to support groundwater and vadose remedial projects. He has experience with a number of vadose zone and groundwater modeling packages. His other duties include directing hydrologic data collection efforts, analyzing and interpreting hydrologic data, assessing the effectiveness of groundwater remedial actions, developing work plans for data collection and interpretation, and performing numerical modeling to predict facility impacts to the aquifer to support remediation and construction decisions.

Sunil Mehta, INTERA, Inc.

Ph.D., Earth Sciences (Hydrogeology specialization), University of Kentucky
M.S., Geosciences, University of Louisiana at Monroe
M.Sc., Geology, University of Poona, India
B.Sc., Chemistry, Zoology, and Geology, University of Jodhpur, India

Dr. Sunil Mehta has more than 18 years of experience related to groundwater flow and transport modeling, reactive transport modeling, total system performance assessment, uncertainty analysis, geophysical logging, and well testing. He has worked on projects involving geologic isolation of radioactive wastes, environmental restoration activities, and water resources exploration and evaluation. Dr. Mehta has over 10 years of experience in designing, developing, and applying probabilistic tools to assess the long-term performance of radioactive waste storage and disposal facilities. He has performed reactive transport modeling and groundwater flow modeling to study behavior of contaminants such as uranium and hexavalent chromium in periodically rewetted zones influenced by aquifer-river interactions.

Randy Nell, INTERA, Inc.

PhD, Environmental Chemistry, University of Notre Dame, 2016
BA, Geology, University of Colorado, 2010

Dr. Nell brings applied and theoretical laboratory experience in geochemistry and environmental science, and research expertise in designing and executing experiments pertaining to heavy metal remediation using biotic systems. His experience includes collecting and analyzing data to evaluate metal fate and transformation in microbial ecosystems, developing standard operating procedures for fluorescent microscopy imaging of manganese oxidizing fungi, and preparing biological samples for x-ray adsorption spectroscopy analysis. He also led field data collection and analysis of dioritic rock samples for U-Th/He analysis. Ryan has presented the results of his work at conferences and authored several publications in peer-reviewed journals, including Geochimica et Cosmochimica Acta and Chemical Geology.

Arun Wahi, INTERA, Inc.

M.S., Hydrology, University of Arizona
B.S., Chemical Engineering, Carnegie Mellon University

Mr. Wahi has over 13 years of consulting and research experience in the fields of hydrology, hydrogeology, and chemistry. He has performed fate and transport modeling of radionuclides and organic and inorganic contaminants in support of DOE PAs. He led the pre-retrieval risk assessment of the Hanford Site AX Tank Farm. He has led teams conducting modeling, hydrogeologic, geochemical, forensic, and remediation engineering analyses, as well as field investigations to perform soil and groundwater sampling and aquifer testing.

Michael P. Connelly, TecGeo, Inc

B.S., Geology, University of Utah
M.S., Geology, University of Utah

Mr. Connelly has over 16 years of experience in environmental geohydrology including project management, groundwater modeling, and using computer techniques to analyze and interpret field data for remedial action and site characterization activities.

Marcel P. Bergeron, Washington River Protection Solutions, LCC

M.A., Geology, Indiana University, Bloomington, IN
B. A., Geology, University of Vermont, Burlington, VT

Mr. Bergeron has more than 35 years of experience in a wide variety of subsurface investigations and studies at radioactive and hazardous waste facilities and contaminated sites. He is experienced in planning and implementation of environmental characterization and risk assessment investigations in a variety of roles including as a technical contributor, a project and task manager, and a line manager. He has performed quantitative analysis of subsurface systems using analytical and numerical models and visualization tools. He has significant technical project experience in managing technical teams, schedules, and budgets for multi-disciplinary projects and communication of project results with clients, regulators, and stakeholders.

Raziuddin Khaleel, INTERA, Inc.

Ph.D., Soil and Water Engineering, Texas A&M University
M.S., Water Science and Engineering, Asian University of Technology
B.S., Civil Engineering, Bangladesh University of Engineering and Technology

Dr. Khaleel has over 25 years of experience in groundwater hydrology and numerical simulations of subsurface flow and transport. He was a key contributor to the Hanford Site Performance Assessment for the Disposal of Low-Level Waste in the 200 West Area Burial Grounds, the Performance Assessment for the Disposal of Low-Level Waste in the 200 East Area Burial Grounds, and the Hanford Immobilized Low-Activity Tank Waste Performance Assessment. His contributions have been in the area of conceptual model development, direction of modeling, and in writing the document.

Checker:

Amena Mayenna, INTERA, Inc.
Environmental Scientist, P.E.

M.S. 2008, Environmental Engineering, Washington State University
B.S., 2007, Civil Engineering, Bangladesh University of Engineering & Technology

Amena Mayenna has eleven years of experience in numerical modeling of groundwater in the vadose and saturated zones, model calibration, groundwater management, and geostatistics analysis. She is an experienced programmer and has applied multiple languages and modeling codes including Fortran, MODFLOW, MT3D, MODPATH, PEST, Ground Water Vistas, STOMP, ArcGIS, and Leapfrog Hydro.

Subject Matter Expert/Senior Reviewer:

Mart Oostrom, INTERA, Inc.

PhD, Soil Physics, Auburn University, 1991
MS, Soil Physics and Hydrogeology, Wageningen University, 1986
MA, Teaching (Mathematics), University of Idaho, 2010
BS, Soil Science, Wageningen University, 1984

Dr. Oostrom brings specialized expertise in the development and application of numerical models to evaluate groundwater flow and contaminant transport and the effectiveness of various environmental remediation methods and technologies. Some of his recent experience includes quantifying contaminant flux into groundwater at various deep-vadose zone waste disposal sites; conducting reservoir modeling for enhanced oil recovery and CO2 sequestration; remediating the vadose zone using ammonium injection, soil dessication, and/or pore-water extraction; and developing a circulation method to quantify back-diffusion of dissolved contaminants into permeable sediment. Dr. Oostrom is co-author of the STOMP (Subsurface Flow over Multiple Phase) simulator, a mathematical model used to numerically simulate subsurface (multiphase) flow and transport as well as vadose zone and groundwater remediation. STOMP's target capabilities were guided by proposed or applied remediation activities at sites contaminated with volatile organic compounds and/or radioactive material. The simulator's modeling capabilities address a variety of subsurface environments, including nonisothermal conditions, fractured media, multiple-phase systems, nonwetting fluid entrapment, soil freezing conditions, nonaqueous phase liquids, first-order chemical reactions, radioactive decay, solute transport, dense brines, nonequilibrium dissolution, and surfactant-enhanced dissolution and mobilization of organics. Dr. Oostrom is Associate Editor of the Journal of Contaminant Hydrology and has authored over 100 refereed journal articles and contributed to book chapters on the subjects of multifluid flow, site characterization, remediation, and monitoring.

Responsible WRPS Technical Project Lead:

Robert A. Hiergesell, WRPS
Technical Lead WMA A-AX Performance Assessment

M.Sci., Hydrogeology from Univ. of Nebraska-Lincoln.
B.Sci., Geology at Virginia Polytechnic Institute, Blacksburg, Va.

Mr. Hiergesell has over thirty years of experience in the areas of groundwater monitoring, subsurface flow and transport simulation, environmental remediation and performance assessment for low-level radioactive waste disposal. Prior to joining WRPS, he was employed at the DOE Savannah River National Laboratory where he was the lead technical investigator for numerous environmental restoration and waste management projects.

Robert A. Hiergesell 4/24/2019
Robert A. Hiergesell Date

CHECKER LOG FOR PROCESS MODELS

Project and Environmental Model Calculation Specific Information:

Project: WMA A-AX Performance Assessment

Responsible Manager or Designee, and Position: Robert A. Hiergesell

Originating Group or Department: Date: 03/05/2019

Environmental Model Calculation File Report and Revision No.: RPP-RPT-60101_STOMP3D_MPR_draft_Bver_03

Environmental Model Calculation File Title: Model Package Report Flow and Contaminant Transport Nume

Check: Environmental Model Calculation File Document Elements

	List where Information is Described *(EMCF Section Number)*	Is the Description Correct and Sufficient? Yes	No	If No, describe deficiency:	Checker Signature
Purpose	Section 1	◉	○		
Calculation Approach	Section 2: Model Objective	◉	○		
Assumptions	Appendix A	◉	○		
Inputs *(reference detailed checklist below as well)*	Section 3, 4	◉	○		
Equations used	Section 3, 4	◉	○		
Conclusions	NA	○	◉	NA	
References	Section 8 and References for Appendix A,B and C	◉	○		

Check: Controlled Software Use

	List where Information is Described *(EMCF Section Number)*	Is the Criteria Met? Yes	No	If No, describe deficiency:	Checker Signature
Software used in the calculation is appropriate for application	Section 6	◉	○		
Software use is approved and properly validated in accordance with approved software management plan	Section 6	◉	○		
Software use is properly documented	Section 6	◉	○		
Verify data was input correctly to approved software or spreadsheets	Section 6	◉	○		
If a spreadsheet is used, verify inputs/outputs of calculation(s) to ensure accuracy	sz_boundary_conditions_derivation.xlsx Table_C-1_cross-section-area-calcs.xlsx	◉	○		

Check: Perform Calculation to Verify Free of Errors

	Describe how calculation was performed	List any discrepancies encountered *(If none, enter "None")*	Checker Signature
Perform the environmental	NA	NA	

CHECKER LOG FOR PROCESS MODELS (Continued)

	Describe how calculation was performed	List any discrepancies encountered *(If none, enter "None")*	Checker Signature
model calculation as described to verify it is free of errors			

Check: Process Model Parameterization *(Specify Values and Units in Each Column)*

Model Parameter Type	(1) Input Documented in EMCF?	(2) Values checked against parameter source?	(3) Input in EMCF matches model input file(s)?
Simulation duration: Historic	NA	NA	NA
Simulation duration: Predictive	NA	NA	NA
Boundary conditions: Recharge	Section 3.1.1, section3.1.5 Figure 3-2, Table 3-5	Yes	yes
Boundary conditions: River	NA	NA	NA
Boundary conditions: Head Dependent	Section 3.1.1, Appendix C	Yes	Yes
Boundary Conditions: Specified Flux	Section 3.1.1, Appendix C	yes	yes
Initial Conditions: Hydraulic	Section 3, Appendix C	yes	yes
Initial Conditions: Contaminant	Section 3	NA	NA
Sources and Sinks: Aqueous Mass	NA	NA	NA
Sources and Sinks: Contaminant Mass	NA	NA	NA
Hydraulic Properties: Conductivity	Table 3-9, Appendix C	yes	yes
Hydraulic Properties: Porosity	Table 3-9, Appendix C	yes	yes
Hydraulic Properties: Water Retention *(Vadose Only)*	Table 3-2, Appendix B	yes	yes
Hydraulic Properties: Formation Density	Table 3-4, Appendix B	yes	yes
Transport Properties: Diffusion	section 3.4.1.5.3, Appendix B	yes	yes
Transport Properties: Dispersivity	Table 3-4, Appendix B,C	yes	yes
Transport Properties: Sorption *(typically K_d)*	Table 3-6	yes	yes
Transport Properties: Radioactive Decay Rate	Section C-8 ; Reference:ICRP 2008	NA	NA

Check: Further Checks *(Record additional checks performed and results)*

Model Parameter Type	(1) Input Documented in EMCF?	(2) Values checked against parameter source?	(3) Input in EMCF matches model input file(s)?
Inventory: Radiological Decay Correction. Does the inventory *(source term)* include radionuclides, and if so, is it	NA	NA	NA

CHECKER LOG FOR PROCESS MODELS (Continued)			
Model Parameter Type	(1) Input Documented in EMCF?	(2) Values checked against parameter source?	(3) Input in EMCF matches model input file(s)?
decay-corrected to the appropriate date for inclusion as a source?	NA	NA	NA

EXECUTIVE SUMMARY

This model package report documents the development of the integrated vadose and saturated zone flow and transport model for the Waste Management Area (WMA) A-AX performance assessment. This modeling capability is intended for use in addressing the analysis requirements outlined in Appendix I of the *Hanford Federal Facility Agreement and Consent Order* (Ecology et al. 1989) for assessment of the radiological impacts of waste residuals in a closed WMA A-AX under U.S. Department of Energy O 435.1, *Radioactive Waste Management* and evaluation of the hazardous chemical impacts for the same wastes under the *Resource Conservation and Recovery Act of 1976*. The overall objective of the modeling effort is to provide a basis for making informed closure decisions pertinent to WMA A-AX. The results of the flow and transport model are intended to provide information regarding the potential long-term impact on groundwater of waste residuals left in tanks and associated ancillary equipment (such as pipelines) at closure. Impacts related to past tank waste leaks, losses, and unplanned releases are outside the scope of this modeling effort.

This report discusses the development and translation of the conceptual model for flow and contaminant transport into the WMA A-AX three-dimensional (3-D) numerical flow and transport model evaluated using the Subsurface Transport Over Multiple Phases (STOMP)[1] simulator and the multi-processor capable extreme-scale STOMP (eSTOMP) simulator. The development of representative geologic framework is described along with the implementation of waste release models used to represent contaminant release from waste residuals remaining in tanks and ancillary equipment. The report also provides the technical basis for specific model parameters and boundary conditions, along with description of modeling assumptions.

Model outputs are intended to be generated and used to estimate the possible future concentration in groundwater of various radionuclides and non-radiological contaminants. The methodology used to calculate time-series concentration values (breakthrough curves) and estimate the peak concentrations at designated points of analysis is described in detail. The system modeling (RPP-RPT-60885, *Model Package Report System Model for the WMA A-AX Performance Assessment*) is expected to include the screening methods and results used as a guide to identify the list of key contaminants of potential concern that require specific detailed evaluation in the 3-D numerical flow and transport process model.

This model package report specifically documents the 3-D numerical flow and transport model developed with alternative conceptual model (ACM) 1 of WMA A-AX, along with certain calculations that are necessary to support development of the system model (RPP-RPT-60885). The use of the model to perform U.S. Department of Energy M 435.1-1, *Radioactive Waste Management Manual* base case analysis, to perform sensitivity and uncertainty calculations, and to evaluate other ACMs that remain in development (e.g., ACM 2 and ACM 3) is expected to be documented separately in environmental model calculation files as indicated by the documentation requirements associated with the preparation and issue of environmental model calculations. Although this model package report only addresses one ACM, the model package

[1] Subsurface Transport Over Multiple Phases (STOMP) (and its derivative works, including eSTOMP) is developed and distributed by Battelle Memorial Institute.

report includes the use of the abbreviation ACM 1 to distinguish it from the ACMs that remain in development and are expected in the future.

CONTENTS

1.0 PURPOSE 1-1

1.1 PERFORMANCE ASSESSMENT REQUIREMENTS FOR CLOSURE OF SINGLE-SHELL TANK WASTE MANAGEMENT AREAS 1-2

1.2 PREVIOUS ANALYSIS OF IMPACTS FROM CLOSED WASTE MANAGEMENT AREA A-AX 1-2

1.3 BACKGROUND 1-3

1.3.1 Waste Management Area A-AX Facility Description 1-5
1.3.2 Waste Management Area A-AX Performance Assessment Data Sources 1-8

1.4 DOCUMENT ORGANIZATION 1-10

2.0 MODEL OBJECTIVES 2-1

3.0 MODEL CONCEPTUALIZATION 3-1

3.1 FEATURES, EVENTS, AND PROCESSES 3-1

3.1.1 Model Domain and Boundary Conditions 3-3
3.1.2 Geologic Setting 3-6
3.1.3 Source Term 3-10
3.1.4 Vadose Zone Hydrogeology and Contaminant Transport 3-15
3.1.5 Infiltration and Recharge 3-24
3.1.6 Geochemistry Conceptual Model 3-26
3.1.7 Groundwater Domain 3-34
3.1.8 Points of Calculation, Protectiveness Metric, and Timeframe Considerations 3-37

3.2 NATURE AND EXTENT OF CONTAMINATION 3-44

4.0 MODEL IMPLEMENTATION 4-1

4.1 DISCRETIZATION 4-1

4.2 PARAMETERIZATION 4-7

4.3 MODELING STAGES 4-8

4.4 CALIBRATION 4-9

4.5 SCREENING 4-9

4.6 ALTERNATIVE CONCEPTUAL MODEL 1 ANALYSIS 4-10

4.7 SENSITIVITY AND UNCERTAINTY ANALYSIS.....4-10

5.0 MODEL APPLICATION 5-1

5.1 WASTE MANAGEMENT AREA A-AX PERFORMANCE ASSESSMENT MODEL LIMITATIONS 5-1

5.2 WASTE MANAGEMENT AREA A-AX PERFORMANCE ASSESSMENT MODEL RECOMMENDATIONS 5-1

6.0 SUBSURFACE TRANSPORT OVER MULTIPLE PHASES SOFTWARE 6-1

6.1 SUBSURFACE TRANSPORT OVER MULTIPLE PHASES SOFTWARE QUALITY ASSURANCE..... 6-2

6.2 SUBSURFACE TRANSPORT OVER MULTIPLE PHASES CONTROLLED CALCULATION SOFTWARE..... 6-2

6.3 SOFTWARE INSTALLATION AND CHECKOUT..... 6-4

6.4 STATEMENT OF VALID SOFTWARE APPLICATION 6-5

6.5 MODFLOW AND RELATED CODES SUPPORT SOFTWARE 6-5

7.0 MODEL CONFIGURATION MANAGEMENT 7-1

8.0 REFERENCES 8-1

APPENDICES

APPENDIX A – KEY ASSUMPTIONS IN THE PERFORMANCE ASSESSMENT .....A-i

APPENDIX B – DEVELOPMENT OF VADOSE ZONE HYDRAULIC AND TRANSPORT PROPERTIES FOR WASTE MANAGEMENT AREA A-AX PERFORMANCE ASSESSMENT .....B-i

APPENDIX C – TECHNICAL BASIS FOR WASTE MANAGEMENT AREA A-AX UNCONFINED AQUIFER CONCEPTUAL MODEL.....C-i

APPENDIX D – HORIZONTAL AND VERTICAL SPACING OF THE FINITE DIFFERENCE CELLS IN THE THREE-DIMENSIONAL WASTE MANAGEMENT AREA A-AX FLOW AND TRANSPORT MODEL DOMAIN.....D-i

ATTACHMENT

ATTACHMENT 1 – SOFTWARE INSTALLATION AND CHECKOUT FORMS Att-1-i

FIGURES

Figure 1-1. Waste Management Area A-AX Tanks and Associated Infrastructure and Nearby Liquid Discharge Facilities. 1-6

Figure 3-1. Plan View of Waste Management Area A-AX Performance Assessment Model Domain. 3-4

Figure 3-2. Evolution and Timing of the Surface Condition Changes at Waste Management Area A-AX. 3-5

Figure 3-3. Fence Diagram of Alternative Geologic Models Used in the Performance Assessment for Waste Management Area A-AX. 3-8

Figure 3-4. Example Waste Management Area A-AX Release Functions. 3-13

Figure 3-5. Elevation of Ancillary Equipment Source that Includes the Pipelines in Waste Management Area A-AX Three-Dimensional Model Domain. 3-14

Figure 3-6. Central Plateau Groundwater Model Calibration Results near Waste Management Area A-AX. 3-38

Figure 3-7. Points of Calculation at the Fence Line and 100 meters from Waste Management Area A-AX. 3-41

Figure 3-8. Geologic Cross-Section A-A' through Waste Management Area A-AX. 3-45

Figure 4-1. Horizontal Alignment of Three-Dimensional Model Computational Nodes with Waste Management Area A-AX Single-Shell Tanks. 4-2

Figure 4-2. Horizontal and Vertical Alignment and Distribution of Waste Management Area A-AX Performance Assessment Alternative Conceptual Model 1 Three-Dimensional Model Computational Nodes. 4-3

Figure 4-3. Relative Change in Moisture Content (Volume %) from the Pre-Hanford Steady-State Condition at the Four Vertical Boundaries of the Model at Three Times of Interest: Year 2050, Year 2550, and Year 3050. 4-6

TABLES

Table 1-1. Exposure Scenarios, Performance Objectives and Measures, and Points of Assessment for the Waste Management Area A-AX Performance Assessment. 1-1

Table 3-1. Estimates of Residual Technetium-99 Inventory in Waste Management Area A-AX Tanks and Ancillary Equipment at Assumed Closure in Year 2050....3-12

Table 3-2. Effective Soil Moisture Retention Parameters and Gravel Content for Waste Management Area A-AX Vadose Zone Hydrostratigraphic Units.....3-19

Table 3-3. Optimized Saturated Hydraulic Conductivity and the Pore Connectivity-Tortuosity Coefficient for Different Averaging Schemes for Waste Management Area A-AX Hydrostratigraphic Units. 3-21

Table 3-4. Macrodispersivity and Particle Density Estimates for the Hydrostratigraphic Units at Waste Management Area A-AX.....3-23

Table 3-5. Model Recharge Rate (Net Infiltration) Estimates for Surface Conditions during the Pre-Construction, Operational, and Post-Closure Periods. 3-27

Table 3-6. K_d Value Estimates (mL/g) for Sand in the Waste Management Area A-AX Performance Assessment Models. 3-29

Table 3-7. K_d Value Estimates (mL/g) for Silt in the Waste Management Area A-AX Performance Assessment Models. 3-31

Table 3-8. Gravel-Corrected K_d (mL/g) Values for Mobile Contaminants Included in the Waste Management Area A-AX Residual Inventory Estimates. 3-33

Table 3-9. Waste Management Area A-AX Performance Assessment Unconfined Aquifer Flow and Transport Properties. 3-36

Table 3-10. Dimension of Widths for Point of Calculation Segments at the Fence Line and 100 meters from Waste Management Area A-AX. 3-42

Table 4-1. Summary of Key Elements and Parameters Associated with Site-Specific Model Components for Waste Management Area A-AX..... 4-7

TERMS

2-D	two-dimensional
3-D	three-dimensional
ACM	alternative conceptual model
ASME	American Society of Mechanical Engineers
CA	composite analysis
CCUg	Cold Creek Unit gravel
CCUz	Cold Creek Unit silt
CERCLA	*Comprehensive Environmental Response, Compensation, and Liability Act of 1982*
CFR	*Code of Federal Regulations*
CHPRC	CH2M HILL Plateau Remediation Company
Ci	curie(s)
CLARC	Cleanup Levels and Risk Calculation
cm	centimeter(s)
cm/s	centimeters per second
cm^3/g	cubic centimeters per gram
CPGWM	Central Plateau Groundwater Model
Cr	chromium
DOE	U.S. Department of Energy
DWS	drinking water standards
Ecology	State of Washington Department of Ecology
EHM	equivalent homogeneous medium
EMMA	Environmental Model Management Archive
EPA	U.S. Environmental Protection Agency
ERDF	Environmental Restoration Disposal Facility
eSTOMP	extreme-scale Subsurface Transport Over Multiple Phases simulator
FEPs	Features, Events, and Processes
ft	feet
g	gram(s)
h	hour(s)
H1/HF1	Hanford formation unit 1
H2/HF2	Hanford formation unit 2
H3/HF3	Hanford formation unit 3
HFFACO	*Hanford Federal Facility Agreement and Consent Order*
HLW	high-level waste
HSU	hydrostratigraphic unit
IDF	Integrated Disposal Facility

in.	inch
K_d	distribution coefficient
K_s	saturated conductivity
kg	kilogram(s)
km	kilometer(s)
km^2	square kilometer(s)
m	meter(s)
MCL	maximum contaminant level
m/s	meters per second
µg/L	micrograms per liter
mg/kg	milligrams per kilogram
mg/L	milligrams per liter
mL/g	milliliters per gram
mm/yr	millimeters per year
MPR	model package report
NAVD88	North American Vertical Datum of 1988
NOAA	National Oceanic and Atmospheric Administration
NRC	U.S. Nuclear Regulatory Commission
pCi/g	picocuries per gram
pCi/L	picocuries per liter
PA	performance assessment
PNNL	Pacific Northwest National Laboratory
PUREX	Plutonium Uranium Extraction (Plant)
RCRA	*Resource Conservation and Recovery Act of 1976*
RETC	RETention Curve (software)
Rlm	Ringold Formation Lower Mud Unit
Rwia	Ringold Formation Unit A
Rwie	Ringold Formation Unit E
SSL	Soil Screening Level
SST	Single-Shell Tank
STOMP	Subsurface Transport Over Multiple Phases simulator
TCT	tensorial connectivity-tortuosity
UPR	unplanned release
VSZ	vadose and saturated zone
WAC	*Washington Administrative Code*
WMA	Waste Management Area
WRPS	Washington River Protection Solutions, LLC
yr	year

1.0 PURPOSE

The integrated three-dimensional (3-D) vadose and saturated zone (VSZ) water flow and contaminant transport model for the Waste Management Area (WMA) A-AX performance assessment (PA) provides estimates of future radiological and non-radiological contaminant concentrations in groundwater from WMA A-AX after closure. The purpose of this evaluation is to provide a technical basis for determining the human health and environmental impacts from residual wastes that may remain following the planned WMA A-AX retrieval and closure activities. U.S. Department of Energy (DOE) O 435.1, *Radioactive Waste Management* requires that DOE radioactive waste management activities shall protect the public from exposure to radiation from radioactive materials, protect the environment, and comply with applicable Federal, State, and local laws and regulations and any applicable Executive Orders and other DOE directives. DOE M 435.1-1, *Radioactive Waste Management Manual* identifies specific performance objectives and other performance-related factors that need to be considered in the PA.

Of particular relevance to the 3-D VSZ flow and transport model evaluations are the "All-Pathways" calculation of the highest projected dose or concentration (in groundwater) beyond a 100-m buffer zone surrounding the disposed waste and the requirement to evaluate the impacts to water resources. An extended discussion of the regulatory requirements and other elements of the assessment context is presented in report RPP-RPT-58540, *Assessment Context for the WMA A-AX Closure Performance Assessment*. The performance objectives comprise a combination of DOE O 435.1 and *Resource Conservation and Recovery Act of 1976* (RCRA) closure requirements and State of Washington Department of Ecology (Ecology) requirements. Those performance objectives addressed by the 3-D VSZ model are shown in Table 1-1.

Table 1-1. Exposure Scenarios, Performance Objectives and Measures, and Points of Assessment for the Waste Management Area A-AX Performance Assessment.

Exposure Scenario	Performance Objective and Measures	Point of Assessment	
		Operational and Active Institutional Control Periods[a]	Post-Institutional Control Period
All-Pathways	25 mrem/yr[b]	Facility Boundary	100 m[c]
Water Resources Protection	Ecology requirements on concentration	At the Source and 100 m[c]	100 m[c]
Chemical Toxicity/Risk	Ecology and RCRA Closure requirements related to risk	At the Source and 100 m[c]	100 m[c]

[a] The active institutional control period includes final closure.

[b] Excluding radon in air.

[c] The point of highest projected dose or concentration beyond a 100-m buffer zone surrounding the disposed waste. Additionally, concentrations found in tank residuals will be compared against the standard Model Toxics Control Act (*Revised Code of Washington* 70.105D, "Hazardous Waste Cleanup—Model Toxics Control Act") three-phase model.

Ecology = State of Washington Department of Ecology RCRA = *Resource Conservation and Recovery Act of 1976*

This model package report (MPR) documents the 3-D numerical flow and transport model developed with alternative conceptual model (ACM) 1, along with certain calculations that are necessary to support development of the WMA A-AX system model (RPP-RPT-60885, *Model Package Report System Model for the WMA A-AX Performance Assessment*). The use of the model to perform DOE M 435.1-1 base case analysis, to perform sensitivity and uncertainty calculations, and to evaluate other ACMs is to be documented in environmental model calculation files (EMCFs) as required by the documentation requirements associated with the preparation and issue of environmental model calculations. Although this MPR only addresses one ACM, the MPR includes the use of the acronym ACM 1 to distinguish it from the ACMs that remain in development and are expected to be evaluated in the future.

1.1 PERFORMANCE ASSESSMENT REQUIREMENTS FOR CLOSURE OF SINGLE-SHELL TANK WASTE MANAGEMENT AREAS

Appendix I Section 2.5 "Performance Assessment" of the *Hanford Federal Facility Agreement and Consent Order* (HFFACO) (Ecology et al. 1989) requires that WMA PAs evaluate the risk associated with the individual components of the WMA after retrieval and include the ability to account for the dose and risk of each component relative to the impacts associated with the WMA as a whole. In addition, the PA must include the flexibility to account for new or evolving information as it becomes available. The need for the WMA A-AX PA flow and transport modeling derives from the requirements of DOE O 435.1 and the additional requirements imposed by Appendix I. According to DOE M 435.1 and Appendix I of the HFFACO, the analysis needs to include time history results of the transport of radionuclides and non-radiological contaminants individually and collectively and be suitable for estimating the maximum concentration in the environment. These requirements derive from the specific performance objectives identified in DOE M 435.1-1 Chapter IV Section P "Disposal," as well as other performance measures related to intruder scenarios required by DOE M 435.1-1. In summary, these requirements, as implemented in the WMA A-AX PA flow and transport model, implement the DOE M 435.1-1 requirement that the WMA A-AX PA include calculations of potential doses to representative future members of the public and environmental impacts from potential releases from the tank residuals for a 1,000-year period after closure.

1.2 PREVIOUS ANALYSIS OF IMPACTS FROM CLOSED WASTE MANAGEMENT AREA A-AX

Previous modeling of impacts for a closed WMA A-AX was performed in the Single-Shell Tank (SST) PA (DOE/ORP-2005-01, *Initial Single-Shell Tank System Performance Assessment for the Hanford Site*) and DOE/EIS-0391, *Final Tank Closure and Waste Management Environmental Impact Statement for the Hanford Site, Richland, Washington*. The SST PA evaluated impacts using a two-dimensional (2-D) numerical model representation of WMA C, used as an analogue for WMA A-AX that involves certain simplifications of the detailed conceptual model. The 2-D numerical model for WMA C developed for DOE/ORP-2005-01 assumes that the groundwater flows beneath the WMA parallel to tank row 241-C-103, 241-C-106, 241-C-109, and 241-C-112, consistent with the estimated post-Hanford unconfined aquifer hydraulic gradient. To account

for 3-D aspects, the tank centerline concentration breakthrough curve results were transformed to concentration values across the tank farm fence line according to a linear dilution scalar. These results were then used as a template for WMA A-AX by multiplying the WMA C breakthrough curve results by the WMA A-AX source term(s) to obtain the contaminant concentration for that of those source(s). The SST PA evaluation does not include interaction between radionuclides and non-radiological contaminants from sources located in different parallel rows, or calculation of concentration 100 m downgradient of the WMA A-AX fence line.

The DOE/EIS-0391 approach to the groundwater impact analysis includes integrated use of a single, large-scale saturated zone model with multiple small-scale vadose zone-only models, including two representing each of the SST farms in WMA A-AX. The DOE/EIS-0391 vadose zone models used for the various SST WMAs were implemented in three dimensions to incorporate the spatial variability of geologic and recharge conditions across the Central Plateau of the Hanford Site. The DOE/EIS-0391 performed comparative analysis of alternatives for various waste management and tank closure strategies. This alternatives analysis evaluated impacts of residual wastes from whole tank farms, not from individual tanks, and it included evaluation of impacts from past releases and hypothetical leaks during waste retrieval operations. For the PA to consider the different compositions and potentially different volumes of waste residuals in each SST, it will need to model releases from individual tanks independently, in contrast to the approach in DOE/EIS-0391, which was broader in scope and therefore less detailed with respect to residual releases. DOE/EIS-0391 presents groundwater impact results for polygonal lines of analysis, referred to as "barrier lines of analysis." For example, the A Barrier line of analysis encompasses the impacts from WMA C, WMA A-AX, and all double-shell tank WMAs within the A Complex (consisting of tank farms 241-A, 241-AN, 241-AP, 241-AW, 241-AX, 241-AY, and 241-AZ). However, the A Barrier line of analysis results presented in Appendix O of DOE/EIS-0391 do not distinguish between the groundwater impacts resulting from contaminant sources within WMA A-AX and the impacts resulting from sources within WMA C, or indicate where along Barrier A relative to WMA A-AX the maximum impacts occur.

1.3 BACKGROUND

The main purpose of the WMA A-AX VSZ modeling for the DOE O 435.1 PA is to evaluate the impacts to groundwater and human health associated with waste remaining in tank residuals after closure of WMA A-AX. For purposes of the initial WMA A-AX PA, the time of closure of WMA A-AX, related ancillary equipment, and adjacent double-shell tank farms is assumed to be January 1, 2050, consistent with the assumptions in DOE/EIS-0391. The modeling is conducted in accordance with the DOE G 435.1-1, *Implementation Guide for Use with DOE M 435.1-1, Radioactive Waste Management Manual* PA guidelines. For the WMA A-AX PA evaluation, the modeling provides a detailed evaluation of the groundwater concentrations and radionuclide arrival times during the 1,000-year compliance and 10,000-year sensitivity-uncertainty periods per DOE O 435.1.

The flow and transport model is implemented in three dimensions to account for the lateral movement of water and radionuclides and to maintain consistency with other vadose zone

transport analyses conducted at the Hanford Site. The model evaluates the impacts to groundwater from the WMA A-AX sources both on an individual basis and collectively. In addition, the model includes the flexibility to account for new or evolving information as it becomes available.

This impact analysis from residual waste left in tanks and ancillary equipment at closure does not consider contaminant release during WMA A-AX operations. During its operational history, a number of confirmed or suspected waste release events have occurred at WMA A-AX (RPP-ENV-37956, *Hanford 241-A and 241-AX Tank Farms Leak Inventory Assessment Report*). These confirmed or suspected releases included leaks and releases from tanks, unplanned releases (UPRs) from waste transfer lines and systems, and condensate leaks from the tank farm ventilation system (RPP-ENV-37956). Also, intentional discharges of condensate and other wastes occurred at various liquid discharge sites at or near WMA A-AX (RPP-ENV-37956; RPP-RPT-58693, *Engineered System Data Package for Waste Management Area A-AX*). Although some of the releases during operations could potentially impact groundwater, the evaluation of their impacts to groundwater is outside the scope of this modeling. This evaluation only considers the post-closure impacts to the environment of the radionuclides and non-radiological contaminants remaining in the residual waste.

Since the retrieval process is not complete, the inventory of tank and ancillary equipment waste residuals has been estimated based on anticipated waste retrieval results. RPP-RPT-58293, *Hanford 241-A and 241-AX Farm Tank and Ancillary Equipment Residual Waste Inventory Estimates* provides estimates of residual inventory as of October 1, 2016, and provides the inventory basis for the WMA A-AX PA analysis. The estimates of residual waste inventories will continue to evolve and will be updated as progress on retrieval is made.

The system modeling is expected to include a screening phase with the intent to expedite the process model analysis by limiting the process modeling to those radionuclides sufficiently mobile in the subsurface environment to impact groundwater within the compliance and sensitivity-uncertainty periods. The outcome of the screening phase is to determine the maximum distribution coefficient (K_d) values of contaminants in the WMA A-AX tank residuals associated with them reaching the water table within 1,000 years and within 10,000 years. Contaminants with K_d values greater than the threshold values determined from screening may be excluded from the compliance and sensitivity-uncertainty analyses. To ensure that the screening analysis only excludes those contaminants that do not impact groundwater within the compliance and uncertainty timeframes, screening involves applying the maximum recharge rates associated with each land surface category during each period, and assigning to each hydrostratigraphic unit (HSU) the vadose zone hydraulic properties that produce the highest pore water velocity. This approach to screening follows Federal soil screening guidance and DOE performance assessment guidelines (EPA/540/F-95/041, *Soil Screening Guidance: Fact Sheet*; DOE G 435.1-1, Chapter IV) that approve of the use of site-specific models for risk assessment screening purposes.

1.3.1 Waste Management Area A-AX Facility Description

The 241-A and 241-AX Tank Farms are located within WMA A-AX in the 200 East Area of the Central Plateau of the Hanford Site. The 241-A Tank Farm (A Farm) and 241-AX Tank Farm (AX Farm) were constructed between 1953 and 1955 and between 1963 and 1965, respectively. The 241-A and 241-AX Tank Farms were placed in service in 1955 and 1965, respectively, and both were used to store and transfer waste until mid-1980. The WMA A-AX tank farms are surrounded by several other double-shell tank farms within the A Complex, and SST Farm 241-C (C Farm) is located nearby to the northwest (Figure 1-1). WMA A-AX includes SSTs, catch tanks, diversion boxes, valve pits, pipelines, French drains and UPR sites. Numerous liquid discharge facilities used nearby at various times (cribs, trenches, ditches, septic systems, etc.) surround the WMA.

The tanks in both A Farm and AX Farm were designed for the storage of boiling waste generated from irradiated fuel reprocessing at the 202-A Plutonium Uranium Extraction (PUREX) Plant. The tanks in A Farm were designed to contain liquid and solid wastes at a maximum temperature of 220 °F, later revised to 300 °F, and the tanks in AX Farm were designed to contain liquid and solid wastes at a maximum temperature of 350 °F. The tanks in A Farm have laterals ~10 ft beneath the tanks for leak detection, and the tanks in AX Farm include drain slots within the tank structure leading to leak detection pits. Additional leak detection measures include vertical drywells and in-tank equipment at both tank farms.

The 241-A Tank Farm contains six 75-ft diameter nominally 1,000,000-gal capacity SSTs that consist of a carbon steel liner inside a concrete tank. The tank steel bottoms intersect the sidewalls orthogonally, and the concrete thickness is 0.5 ft minimum on the tank bottom, 1.25 ft to 2 ft on the sidewalls, and 1.25 ft minimum for the tank dome. The concrete tank dome thickness increases to ~3.5 ft along the sidewalls. Each tank was originally equipped with 9 to 11 risers and a 20-in. diameter vapor exhaust pipeline that penetrated the tank dome, and 4 airlift circulators that were operated to suspend solids, mix the tank contents, and dissipate heat.

The 241-AX Tank Farm contains four 75-ft diameter nominally 1,000,000-gal capacity SSTs that consist of a carbon steel liner inside a concrete tank. The tank steel bottoms intersect the sidewalls orthogonally, and the concrete thickness is 1.5 ft minimum on the tank bottom (excluding grout and drain slots), 1.25 ft to 2 ft on the sidewalls, and 1.25 ft minimum for the tank dome. The concrete tank dome thickness increases to ~5 ft along the sidewalls. Each tank was originally equipped with 54 risers that penetrated the tank dome and 22 airlift circulators that were operated to suspend solids, mix the tank contents, and dissipate heat.

By 2004, all the 100-series tanks were declared stabilized on an interim basis, indicating that the tank contains less than 50,000 gal of drainable interstitial liquid and less than 5,000 gal of supernate (HNF-SD-RE-TI-178, *Single-Shell Tank Interim Stabilization Record*). The VSZ modeling addresses the waste remaining in the tanks and ancillary equipment, including pipelines, after retrieval concludes.

Figure 1-1. Waste Management Area A-AX Tanks and Associated Infrastructure and Nearby Liquid Discharge Facilities.

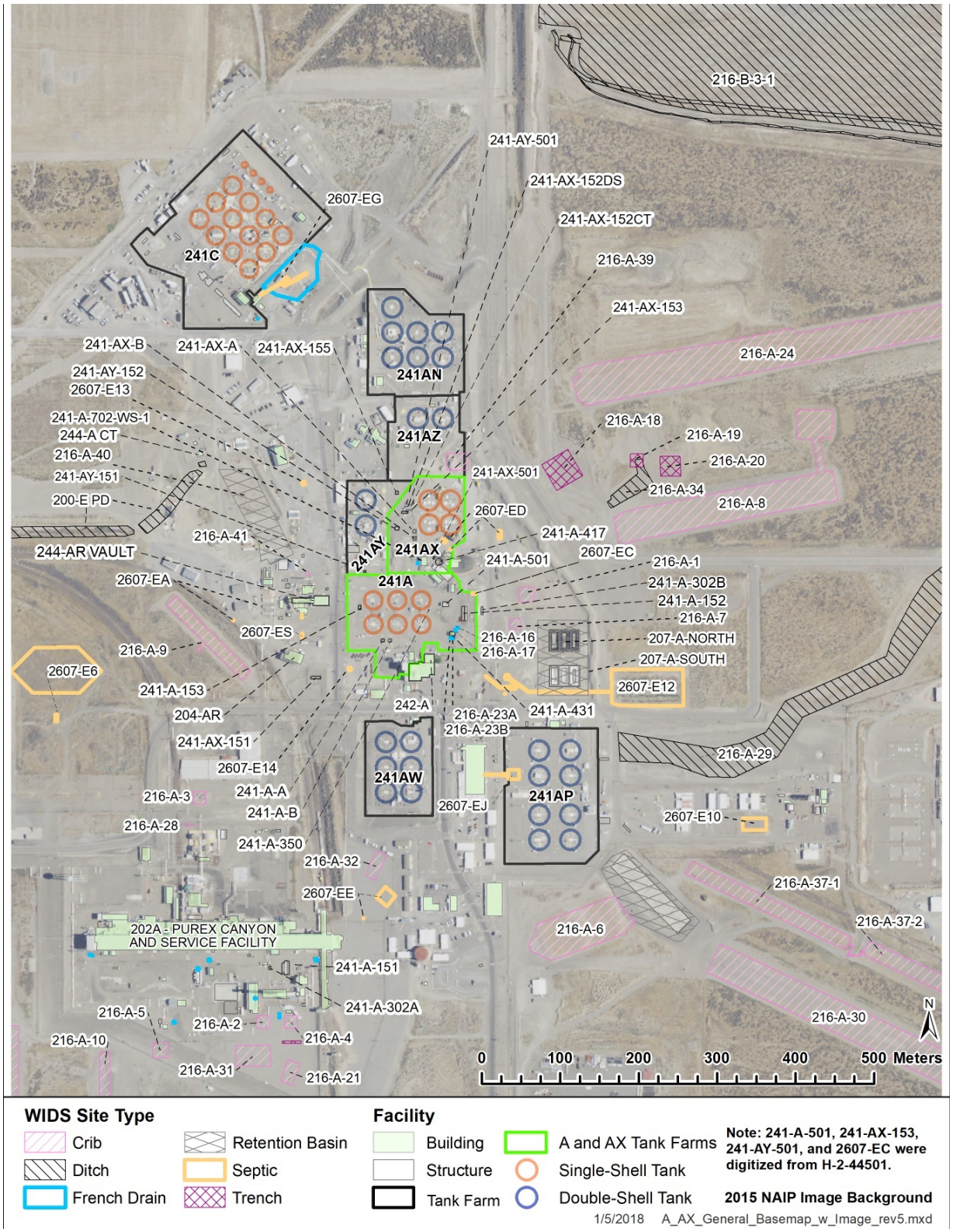

PUREX = Plutonium Uranium Extraction (Plant) WIDS = Waste Information Data System

The 244-AR Vault is located outside of the WMA about 60 m to the west of the tanks in A Farm. The 244-AR Vault facilities constructed in 1966 include a canyon building, a service building, two (filter building) concrete housings, and a change room. The canyon building is a reinforced-concrete, two-level, multi-cell structure. The lower level process cells contain four tanks, a failed equipment cell, and associated piping and equipment. The upper portion of the vault and the lower cells are separated by cover blocks with recessed lifting bails. The unit received waste sluiced from the 241-A and 241-AX Tank Farms. The vault was the focal point for reprocessing and routing of PUREX-generated waste between tank farms and B Plant (via 244-CR Vault) in the late 1960s and between the tank farms and the Waste Encapsulation Storage Facility in the late 1970s. In 1984, the 244-AR Vault received upgrades to allow it to transfer PUREX-generated cladding removal waste between the tank farms and B Plant or the Waste Encapsulation Storage Facility (ARH-374, *244-AR Vault Information Manual*). The last documented waste transfer occurred in 1978, but the site is still covered under the RCRA Part A Permit (WA7 89000 8967, *Hanford Facility Resource Conservation and Recovery Act Permit, Dangerous Waste Portion Revision 8C for the Treatment, Storage, and Disposal of Dangerous Waste*). The facility was isolated from steam and water in 1996, and the vault was interim stabilized in 2003 when the pumpable liquid was removed (RPP-12051, *244-AR Vault Interim Stabilization Completion Report*; RPP-RPT-42231, *Summary of Twenty-Five Miscellaneous Tanks Associated with the Single-Shell Tank System*).

To support the transfer and storage of waste within WMA A-AX SSTs, there is a complex waste transfer system of pipelines (transfer lines), diversion boxes, vaults, valve pits, and other miscellaneous structures. Collectively, these are referred to as ancillary equipment. The diversion boxes are belowground, reinforced-concrete boxes that were designed to contain any waste that leaked from the high-level waste (HLW) transfer line connections. Diversion boxes house jumpers (remote pipeline connectors) that could route waste from one transfer line to another. The following diversion boxes are located in or associated with WMA A-AX (Figure 1-1): 241-A-151, 241-A-152, 241-A-153, 241-AX-151, 241-AX-152DS, 241-AX-153, 241-AX-155, 241-AY-151 and 241-AY-152. If waste leaked into a diversion box, it generally drained by gravity to nearby catch tanks where any spilled waste was stored and then pumped to SSTs (DOE/RL-92-04, *PUREX Source Aggregate Area Management Study Report*).

Four catch tanks exist within the 241-A and 241-AX Tank Farms: 241-A-350, 241-A-417, 241-A-302B, 241-AX-152CT. A fifth catch tank, 241-AX-151CT, is located just outside of A Farm to the southwest. Catch tanks collect spills and/or leaks during waste transfers between processing facilities and tank farms. Catch tanks also received any water from rainfall, snowmelt, or dust that entered the diversion boxes prior to the weatherproofing of the diversion boxes. There are three other catch tanks associated with the 241-A and 241-AX Tank Farms that are located outside of and some distance from the farms: 204-AR-TK-1 (approximately 100 m southwest of the tanks in A Farm), 241-A-302A (just south of PUREX), and 244-A CT (approximately 280 m northwest of the tanks in A Farm).

Multiple levels of piping were installed over time in WMA A-AX. A time line of piping installations is described in RPP-7494, *Historical Vadose Zone Contamination from A, AX, and C Tank Farm Operations*. There are at least 121 transfer pipelines (9.1 miles ± 3 miles) attributed to A Farm, and 119 transfer pipelines (7.9 miles ± 2 miles) attributed to AX Farm.

Pipelines were routinely flushed after use, but some lines in WMA A-AX became plugged in the past, although none are believed to remain plugged.

1.3.2 Waste Management Area A-AX Performance Assessment Data Sources

Details of WMA A-AX relevant to the PA are provided in documents that describe facility characteristics, to-date conditions, geologic and hydrologic interpretations, subsurface contamination approximations, and source term estimates. The list of these data packages and other documents is provided below.

- RPP-RPT-58540, *Assessment Context for the WMA A-AX Closure Performance Assessment* provides information to support and define the regulatory context and assessment process for the WMA A-AX PA.

- RPP-RPT-58693, *Engineered System Data Package for Waste Management Area A-AX* presents information related to major features of the existing engineered system for WMA A-AX, including:

  - SSTs, ancillary equipment, liquid discharge sites, and process facilities

  - Recharge rates in and around WMA A-AX for past, current, and anticipated future near-surface conditions at and following site closure

  - Contaminant source term release parameters for residual wastes in SSTs and ancillary equipment after site closure

  - Corrosion processes for steel components and elements (i.e., tank steel liners and pipelines, and related equipment)

  - Tank structure and emplaced grout/concrete degradation processes and rates and how these processes and rates relate to contaminant release rates from residual wastes.

- RPP-RPT-58291, *Hanford Waste Management Area A-AX Soil Contamination Inventory Estimates* (Rev. 1) presents estimates of contaminated soil inventories at WMA A-AX. These inventory estimates were developed in support of future environmental assessments and potential corrective measure decisions prior to closure and will be updated as additional investigations are completed and additional information is obtained.

- RPP-ENV-58578, *Summary of the Natural System at Waste Management Area A-AX* (Rev. 1) summarizes information relevant to the location, geology, hydrology, and far-field vadose zone and saturated zone properties of WMA A-AX.

- RPP-RPT-58293, *Hanford 241-A and 241-AX Farm Tank and Ancillary Equipment Residual Waste Inventory Estimates* provides supporting information for the WMA A-AX residual inventory estimates in support of the WMA A-AX PA.

- HNF-EP-0182, *Waste Tank Summary Report for Month Ending November 30, 2016*, (Rev. 347 and monthly revisions thereafter) provides information on wastes currently stored at Hanford Site tank farms, including at WMA A-AX, and future revisions are expected to provide regular updates on the state of retrieval operations as they progress. RPP-RPT-58293 relied on HNF-EP-0182 Rev. 347 in establishing residual inventories for subsequent PA calculations. Although later revisions have periodically updated estimates for some parts of the waste inventory (e.g., when different estimation methods are attempted), no waste transfers into or out of the SSTs at WMA A-AX have occurred, and the inventory estimated as of late 2016 is retained as sufficient basis for the initial WMA A-AX PA. The estimated future residual inventory will be replaced with measured residual inventory following retrieval for a final PA.

- RPP-RPT-60171, *Model Package Report: Geologic Framework Model used in WMA A-AX Performance Assessment and RCRA Closure Analysis* was developed in parallel to this MPR, and provides a summary of the development and implementation of alternative geologic models for WMA A-AX.

- RPP-RPT-60885, *Model Package Report System Model for the WMA A-AX Performance Assessment* provides information about the waste release processes and development of the submodels that involve waste form degradation and release from various residual inventory-containing sources at closure (tanks and ancillary equipment, including pipelines).

- RPP-CALC-62319, *Residual Waste Source Inventory Term for the Waste Management Area A-AX Performance Assessment Inventory Case 1* develops and documents the residual inventory estimate of SSTs and ancillary equipment at the assumed closure date of WMA A-AX.

- RPP-ENV-37956, *Hanford 241-A and 241-AX Tank Farms Leak Inventory Assessment Report* (Rev. 3) summarizes information on historical waste loss events associated with tanks and pipelines in the 241-A and 241-AX Tank Farms.

DOE gathered data used in estimating contaminant nature and extent used to evaluate risk to human health and the environment. Documents developed to support this activity relevant to WMA A-AX PA include the following:

- RPP-14430, *Subsurface Conditions Description of the C and A-AX Waste Management Area*

- RPP-35484, *Field Investigation Report for Waste Management Areas C and A-AX*, Rev. 1.

Finally, it is relevant to consider model inputs, assumptions, and design decisions adopted in comparable VSZ modeling assessments of closed tank farms or disposal facilities. In addition to DOE/EIS-0391, the most relevant of such assessments are recently completed PAs for Hanford

Site facilities that have natural or engineered features in common with WMA A-AX. Two particularly relevant PAs include the following:

- RPP-ENV-58782, *Performance Assessment of Waste Management Area C, Hanford Site, Washington*, which assessed human health and environmental impacts from residual wastes remaining in the WMA C SST tank farm ~300 m northwest of WMA A-AX, and

- WCH-520, *Performance Assessment for the Environmental Restoration Disposal Facility, Hanford Site, Washington* (Rev. 1), which assessed impacts from a landfill in a part of the Hanford Site Central Plateau with a sequence of vadose zone HSUs comparable to that at WMA A-AX.

1.4 DOCUMENT ORGANIZATION

This MPR addresses three basic topics: (1) basis for development of the model, including the identification of objectives; (2) software qualifications; and (3) model implementation and parameterization. These topics are organized into the following sections and appendices:

- Section 1.0 provides introductory and background information

- Section 2.0 presents the modeling objectives

- Section 3.0 presents the model conceptualization that includes the geology of WMA A-AX and the relevant Features, Events, and Processes (FEPs) that affect flow and transport in the 200 East Area, along with the modeling assumptions and the source characteristics of the residual contamination

- Section 4.0 describes the modeling implementation details, initial conditions, boundary conditions, and parameter values

- Section 5.0 discusses the Subsurface Transport Over Multiple Phases (STOMP) [2] and the extreme-scale STOMP (eSTOMP) software used to conduct the analysis

- Section 6.0 identifies the limitations of the model, and the applicability of the results

- Section 7.0 provides the details related to configuration management of the model inputs and outputs including the software used

- Appendix A provides a list of all the key assumptions associated with the WMA A-AX PA including the assumptions relevant to the 3-D VSZ modeling

[2] Subsurface Transport Over Multiple Phases (STOMP) (and its derivative works, including eSTOMP) is developed and distributed by Battelle Memorial Institute.

- Appendix B describes the technical basis for the vadose zone conceptual model and parameter selection

- Appendix C describes the technical basis for the aquifer conceptual model and parameter selection

- Appendix D tabulates the horizontal and vertical spacing of the finite difference cells in the 3-D VSZ model.

This page intentionally left blank.

2.0 MODEL OBJECTIVES

The objectives of the WMA A-AX PA vadose zone fate and transport model include the capability to provide results that support the evaluation of human health and environmental impacts at selected point of analysis for the "all-pathways" exposure scenario described in DOE M 435.1-1 Chapter IV Section P. The impacts from the WMA A-AX tank residuals must comply with any applicable State or local law, regulation, or other legally-applicable requirement for water resource protection (DOE G 435.1-1 Chapter IV Section P.[2]). For water resources protection, impacts are assessed based on comparison to Washington State [*Washington Administrative Code* (WAC) 246-290, "Group A Public Water Supplies"; WAC 246-290-310, "Maximum Contaminant Levels (MCLs) and Maximum Residual Disinfectant Levels (MRDLs)"] or Federal Drinking Water Standards (EPA drinking water standards [DWSs] such as maximum contaminant levels [MCLs]), whichever are more restrictive. The point of analysis selected for evaluating comparisons to MCLs should be at the point of highest calculated concentration or dose beyond a 100-m buffer zone surrounding WMA A-AX, although a larger or smaller buffer zone may be used with justification, and some volume averaging based on projected groundwater use may be appropriate (DOE M 435.1-1 Chapter IV Section P, DOE G 435.1-1 Chapter IV Section P). To evaluate compliance with performance objectives and measures in DOE O 435.1, the analysis period is to cover 1,000 years following closure of WMA A-AX. Inherent in the modeling objectives is the expectation that the groundwater impacts or receptor doses do not exceed the performance objectives and measures identified in DOE M 435.1-1 Chapter IV Section P.

Also, included in the modeling objectives is the intent to establish confidence in the outcome(s) of the modeling. The sensitivity and uncertainty analyses are conducted for periods that extend beyond 1,000 years to calculate the maximum dose and other impacts at times beyond the compliance period. The basis and applicability for parametric values used in ACM 1 modeling are identified, explained, and justified, as are model initial conditions, boundary conditions, and changes in properties with time. Establishing confidence also requires identifying, explaining, and if possible, evaluating the significance of the assumptions used in the development of the transport modeling and their relevance to the controlling pathways or scenarios analyzed (NCRP Report No. 152, Performance Assessment of Near-Surface Facilities for Disposal of Low-Level Radioactive Waste). Assumptions necessary to develop inputs to the transport models, address uncertainties or data gaps, or address linkages to other models used in the analysis are identified, justified, and shown to be consistent with the conceptual model (Appendix A). Appendix A presents a listing and explanation of the assumptions made for the modeling analysis, along with a brief discussion about the implications of the assumptions.

This page intentionally left blank.

3.0 MODEL CONCEPTUALIZATION

This section describes the modeling methodology and approach for the determination of the WMA A-AX residual waste impacts to groundwater. A synopsis of the 3-D VSZ conceptual model and conceptual model components and the technical basis and rationale for the selection of parameters is provided here, along with supporting information and rationale in the appendices. This section includes a description of the WMA A-AX vadose zone geology and the pertinent vadose zone physical and chemical characteristics. A summary of the rationale and basis for selection of the Point of Calculation, a protectiveness metric, and the timeframe for compliance is also included in Section 3.1.8.

3.1 FEATURES, EVENTS, AND PROCESSES

DOE O 435.1 requires that DOE radioactive waste management activities protect the public, workers, and the environment from exposure to radioactive materials contained in disposed low-level waste. The international community devised the FEPs Analysis Methodology to develop conceptual models to support nuclear waste disposal system PAs, and the FEPs Methodology, with some modifications that account for Hanford's history of operations, has been successfully implemented at the Hanford Site (e.g., RPP-RPT-58540). DOE/RL-2011-50, *Regulatory Basis and Implementation of a Graded Approach to Evaluation of Groundwater Protection* identifies and describes the FEPs applicable to most vadose zone modeling applications in the 200 Areas and concludes with the development of a "basic" Hanford Site-specific vadose zone conceptual model. This conceptual model provides a basis for identifying the model attributes and criteria that lead to the selection of the appropriate model type (at least two dimensions) and computer code (STOMP or multiprocessor capable eSTOMP) applicable to the particular needs of the WMA A-AX PA.

The following list of key conceptual model components derives from the basic Hanford Site vadose zone conceptual model identified in DOE/RL-2011-50, Rev. 1:

- Model domain and boundary conditions
- Geologic setting
- Source term
- Vadose zone hydrogeology and contaminant transport
- Infiltration and recharge
- Geochemistry and sorption
- Groundwater domain.

These conceptual model components are consistent with those identified in EPA guidelines for the evaluation of the protection of groundwater pathway [EPA 402-R-94-012, *A Technical Guide to Ground-Water Model Selection at Sites Contaminated with Radioactive Substances*; OSWER No. 9200.4-18, "Establishment of Cleanup Levels for CERCLA Sites with Radioactive Contamination"; and HNF-5294, *Computer Code Selection Criteria for Flow and Transport Code(s) To Be Used in Vadose Zone Calculations for Environmental Analyses in the Hanford*

Site's Central Plateau]. The principal FEPs at Hanford associated with these conceptual model components identified in Appendix B of DOE/RL-2011-50, Rev. 1, include the following:

- Relatively thick vadose zone composed of sedimentary deposits (geologic setting conceptual model component)
- Semi-arid region (infiltration/recharge conceptual model component)
- Underlying unconfined aquifer (groundwater domain conceptual model component)
- Relatively limited number of contaminants in the tank and ancillary equipment, including pipelines, residual waste (source term) that have potential impacts to groundwater during the compliance and uncertainty timeframes.

For the evaluation of WMA A-AX closure, the conceptual model components must also account for the source release of radionuclides and non-radiological contaminants from the grouted tanks, contaminant transport through engineered barriers, and contaminant transport through the natural environment, while accounting for decay and in-growth of daughter isotopes. Transport through engineered barriers must consider the degradation of the tank structures, flow of water through the waste in the tanks, and contaminant releases into the vadose zone. These processes include details of physical and chemical mechanisms on a refined local scale.

The particular FEPs identified here contribute to the set of safety functions that attenuate exposure via the groundwater pathway. The safety functions represent multiple and redundant barriers or mechanisms that attenuate the estimated dose received by the public. For example, the relatively thick vadose zone FEP contributes to a safety function involving the duration of transport and the dispersion, retardation, and decay of the radionuclides that occurs during transport. The intent of the WMA A-AX PA is to evaluate the performance of these safety functions, including instances when some of them are lost by degradation over time or by disruptive events. The sensitivity analysis provides a means to determine which FEPs contribute to the safety functions, and which FEPs might affect others in ways that might degrade their function or cause them to act differently than expected.

The sensitivity analyses can be used to explore the implications of the loss of individual or multiple safety functions, while at the same time exploring the implications of aggregated FEPs that might affect a safety function in similar ways. The structure of the PA for WMA A-AX will therefore be to identify sensitivity cases that examine outcomes when the safety functions behave differently than expected, are degraded compared to a base case, or are lost entirely. Particular attention will be given to any FEPs identified that might affect multiple safety functions simultaneously.

The key conceptual model components listed above and their associated FEPs are discussed in the following subsections. The discussion includes the rationale and basis for each of the conceptual model components, the function that each conceptual model component and corresponding FEPs serve in the model, the assumptions associated with model components, and a qualitative assessment of the impact the component has on the model results.

3.1.1 Model Domain and Boundary Conditions

The model domain and boundary conditions establish both a framework and limiting conditions for the numerical model. The model domain for flow and transport in the vadose zone and groundwater (Figure 3-1) is represented numerically in 3-D space with the horizontal axes rotated 45 degrees from the azimuth. The rotation aligns the x-axis in the general or approximate northwest to southeast direction of steady-state groundwater flow forecast by the Central Plateau Groundwater Model (CPGWM; CP-47631, *Model Package Report: Central Plateau Groundwater Model Version 8.4.5*, Rev. 4). Appendix C, Section C.6 provides the detailed explanation of how the CPGWM was used to determine the direction of flow and applicable boundary conditions at WMA A-AX. Aligning an axis with the general direction of groundwater flow allows easier implementation of Neumann and Dirichlet-type boundary conditions to the orthogonal boundaries. The numerical model adapts the physical elements of the conceptual model to a Cartesian grid and assigns numerical values to the parameters used in calculational algorithms to represent the physical and geochemical systems and processes.

Horizontally, the WMA A-AX model domain is 813 m (2,667 ft) northwest to southeast by 1,028 m (3,373 ft) southwest to northeast (Figure 3-1). The model domain is 119.5 m (392 ft) vertically, extending about 24 m (79 ft) below the water table. The southwestern and northwestern corners of the model domain are 574832.05 m, 136075.33 m, and 575544.49 m, 136787.77 m, respectively (Lambert Coordinate system easting, National Oceanic and Atmospheric Administration [NOAA] Manual NOS NGS 5, State Plane Coordinate System of 1983). The southeastern and northeastern corners are 575392.51 m, 135514.87 m, and 576104.94 m, 136227.31 m, respectively. The vertical base elevation of the model is nominally 95.25 m (North American Vertical Datum of 1988 [NAVD88]), although the bottom and top of the active model domain vary spatially according to the top of basalt elevation and surface relief, respectively (RPP-RPT-60171).

A specified-flux boundary condition is applied at the surface and net infiltration rates representing recharge vary spatially and temporally along the upper boundary. The rates depend on temporal changes in assumed site and surface conditions (Figure 3-2), and the location and physical dimensions of WMA A-AX. Recharge parameterization is discussed in Section 3.1.5. The bottom boundary of the unsaturated (vadose) zone is the water table and the bottom of the unconfined aquifer is defined by the underlying basalt bedrock which is assumed to be a vertical no-flow boundary condition. Boundary conditions at the sides of the model domain are also assumed to be no flow in the vadose zone and prescribed flux and prescribed head in the aquifer on the upgradient (northwest) and downgradient (southeast) boundaries, respectively.

Figure 3-1. Plan View of Waste Management Area A-AX Performance Assessment Model Domain.

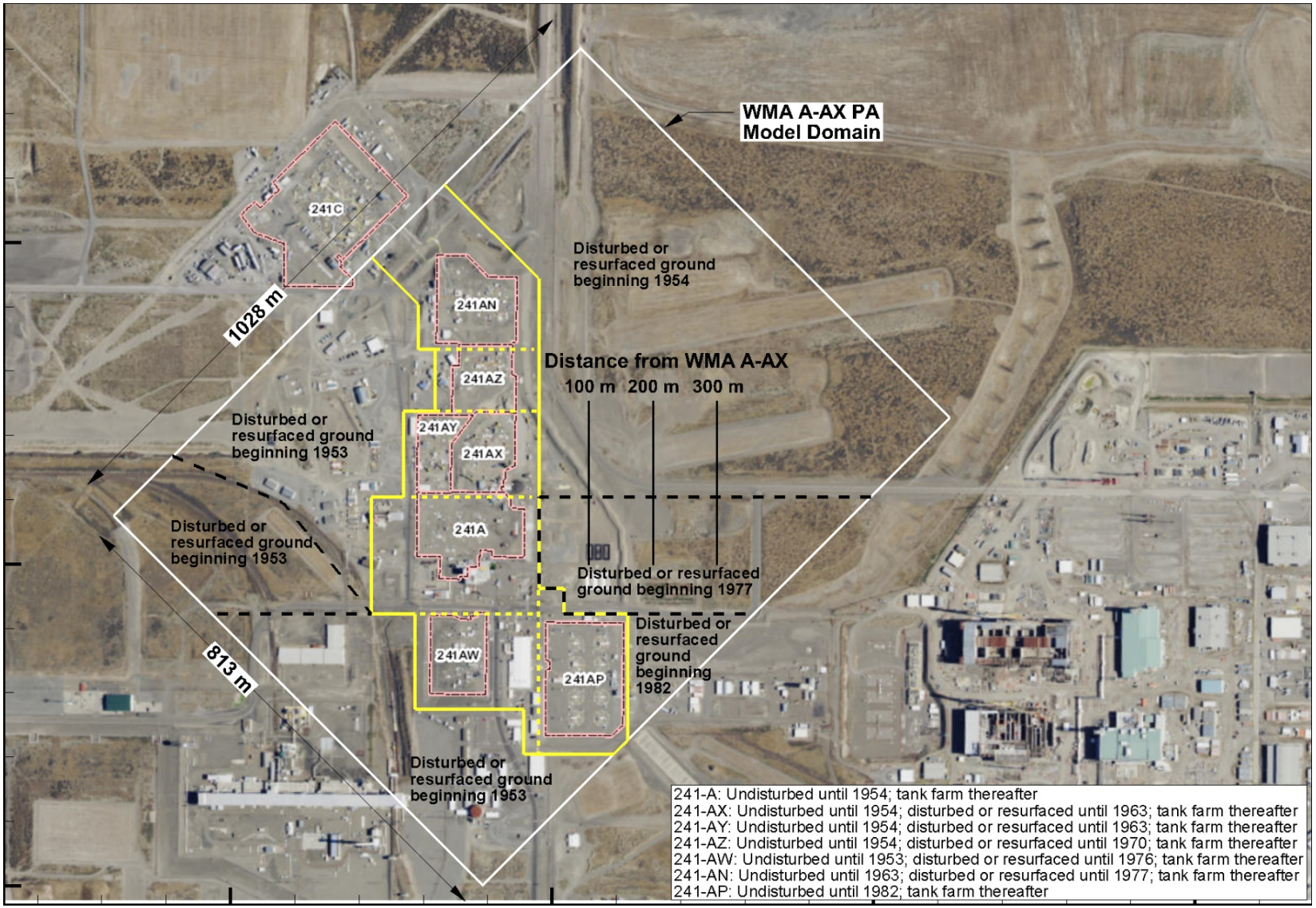

PA = performance assessment WMA = Waste Management Area

Figure 3-2. Evolution and Timing of the Surface Condition Changes at Waste Management Area A-AX.

Phase	Conditions	Duration	Conceptual Cross Section
Pre-operations	Before construction	Until steady-state moisture conditions are achieved.	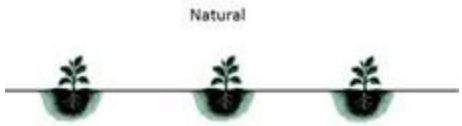
Construction and Operations	Current conditions	~1953 to 2050	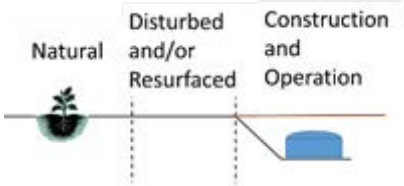
Early Post-Closure	Transition to conditions of restricted recharge due to Modified RCRA C surface barrier	2050 to 2550	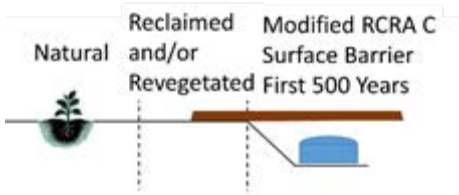
Late Post-Closure	Degraded surface barrier conditions	2550 to 12050 (end of sensitivity and uncertainty analysis evaluation period)	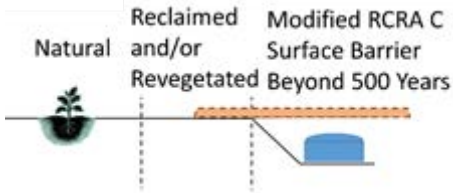

The boundary condition in the aquifer on the upgradient boundary is defined as a prescribed flux calculated based on the flow through the STOMP model domain boundaries estimated from the calendar year 2137 results[3] of the corresponding cells in the CPGWM (Sections C.6 and C.7). Prescribed flux boundary conditions were chosen instead of prescribed head boundary conditions to ensure that the flow through the aquifer matched the flow estimated from the CPGWM. The prescribed flux boundary condition values account for the fact that different hydrogeologic units comprise the aquifer, and that the thickness of the unconfined aquifer varies because of the uneven surface of the underlying basalt. The results of the CPGWM indicate that at steady state in calendar year 2137, approximately 1,052 m^3/day of groundwater flow enters the upgradient boundary of the WMA A-AX model domain (Section C.6). However, the distribution of hydrogeologic units and overall geometry of the aquifer in the CPGWM is not identical to the WMA A-AX model, and the flow must be distributed along the boundary in the WMA A-AX model in a manner consistent with the hydrogeologic units and hydraulic properties specified in the WMA A-AX model.

[3] As described in Sections C.6 and C.7, the relevant CPGWM simulation assumed that discharges and withdrawals of groundwater across the Central Plateau cease in calendar year 2037, with approximate steady-state conditions achieved by the end of the simulation 100 years later.

The prescribed flux boundary conditions in the aquifer account for the different hydraulic properties of the HSUs that comprise the aquifer along the upgradient boundary, the different cross-sectional areas of the HSUs along the boundary, and the non-uniform aquifer thickness throughout the model domain caused by the dip and topography of the underlying basalt boundary. Section C.7 provides a detailed description of the calculations that determined the boundary condition fluxes in the Cold Creek Unit gravel (CCUg) and Ringold Formation Wooded Island Unit A (Rwia, Ringold A) to be 0.139 m/day and 7.64×10^{-6} m/day, respectively. These prescribed fluxes are applied along the northwest boundary of the model domain. These fluxes, divided by the hydraulic conductivities of the two units, produce a hydraulic gradient of -7.6×10^{-6} m/m at the northwest boundary, which is consistent with the long-term steady-state gradient forecast by the CPGWM (-5×10^{-6} m/m across the domain of the STOMP model). The prescribed head on the southeast (downgradient) boundary is equal to 119.4959 m NAVD88 (see Section 3.1.7 and Appendix C for further discussion about the development of this estimate). The boundary conditions along the northeast and southwest boundaries are prescribed head, the values of which are determined from a preconditioning steady-state simulation in which the northeast and southwest boundaries are defined as no-flow. The northeast and southwest boundary conditions involve the results of the preconditioning steady-state simulation and the use of the "initial condition" feature in STOMP.

3.1.2 Geologic Setting

The geological setting information presented here is a summary of the information presented in RPP-ENV-58578, RPP-RPT-58693, and RPP-RPT-60171. Waste Management Area A-AX is located near the eastern edge of the 200 East Area on the Hanford Site on what is known colloquially as the Central Plateau. The vadose zone is ~80 to 90 m (262 to 295 ft) thick, assuming the water table elevation is ~122 m (400 ft) (PNNL-13023, *RCRA Groundwater Monitoring Plan for Single-Shell Tank Waste Management Area A-AX at the Hanford Site*). There are approximately 72 m and 69 m between the base of the A Farm and AX Farm 100-series tanks and the assumed water table elevation, respectively (RPP-RPT-58693). Waste Management Area A-AX lies within the Hanford formation unit 1 (H1) in the vadose zone, although construction of the farms replaced the H1 unit with backfill. Between the base of the unconfined aquifer (i.e., Columbia River Basalt) and ground surface, this area of the Hanford Site has the following lithologic units from the bottom of the aquifer to land surface:

- Columbia River Basalt*
- Ringold Formation Wooded Island Unit A (Rwia, Ringold A)*
- Ringold Formation Wooded Island Lower Mud Unit (Rlm, Ringold mud)*
- Ringold Formation Wooded Island Unit E (Rwie, Ringold E)*
- Cold Creek Unit gravels (CCUg) *
- Cold Creek Unit silt (CCUz)
- Cold Creek Unit sand (CCUs) ACM 2 only
- Hanford formation unit 3 (H3)
- Hanford formation unit 2 (H2)
- Hanford formation unit 1 (H1)
- Eolian sediments
- Backfill.

Lithologic units with asterisks indicate the formation occurs below and above the water table.

The development of the geologic conceptual models and subsurface HSU picks for WMA A-AX involved review, and, in certain cases, reinterpretation of 43 "deep" (penetrated ≥ 150 ft below ground surface) boreholes that had geologic logs or geophysical logs, or both (RPP-RPT-60171). The geologic logs (and geophysical logs, when available) for each of these deep boreholes were reviewed, and the overall quality of the geologic and geophysical logs evaluated. The review based the quality of the available information on the level of detail and completeness of the geologic borehole log, and denoted it as follows:

- "1" (excellent–detailed lithology descriptions and percentage estimates for samples and excellent geophysical logs)

- "2" (fair to good–detailed lithology descriptions and percentage estimates for samples, but may be missing data for some intervals or have poor to incomplete geophysical logs)

- "3" (poor to very bad–no detailed lithology descriptions and percentage estimates for samples [only driller's notes] and no to poor geophysical logs).

Two geologic ACMs, ACM 1 and ACM 2, were developed. ACM 2 differs from ACM 1 in that ACM 2 differentiates between the extent and thickness of the Cold Creek silt and sand beds as separate hydrologic units of the uppermost Cold Creek Unit. Although the WMA A-AX PA is expected to include evaluation of both ACMs, this MPR only addresses ACM 1 because hydraulic parameterization of ACM 2 is not yet complete. The primary difference between the two alternative models is that ACM 2 provides a more detailed lateral extent and thickness of the CCUz, which results from the inclusion of additional borehole data omitted from ACM 1. Interpretation of the additional data also allows the Cold Creek sand unit (CCUs) to be differentiated from the silt in places. The development of ACM 1 included only the geologic data that received a "1" or "2" quality rating, which occurred with 29 of the 43 total boreholes. ACM 2 was developed using geologic data from all 43 deep boreholes. The development of ACM 2 could utilize all the geologic data because the silt and sand of the Cold Creek Unit are distinguishable even in logs of questionable quality. Because this MPR addresses ACM 1, further use of the term Cold Creek silt or the abbreviation CCUz refers to the undifferentiated silt and sand of the Cold Creek Unit unless specifically indicated otherwise. The fence diagrams running southwest to northeast through the center of WMA A-AX for both these models are shown in Figure 3-3.

Figure 3-3. Fence Diagram of Alternative Geologic Models Used in the Performance Assessment for Waste Management Area A-AX. (1 of 2 sheets)

(a) ACM 1

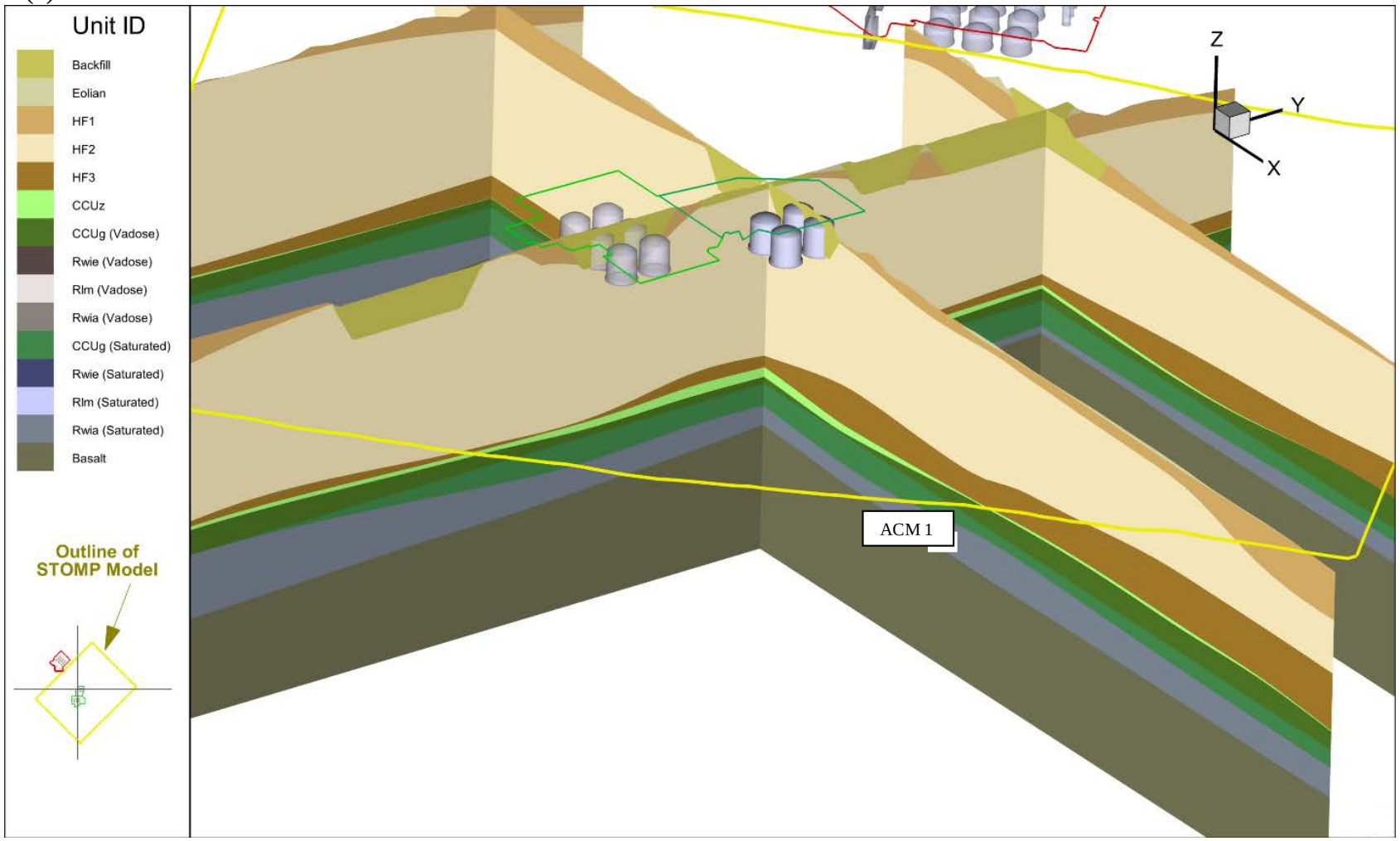

Figure 3-3. Fence Diagram of Alternative Geologic Models Used in the Performance Assessment for Waste Management Area A-AX. (2 of 2 sheets)

(b) ACM 2

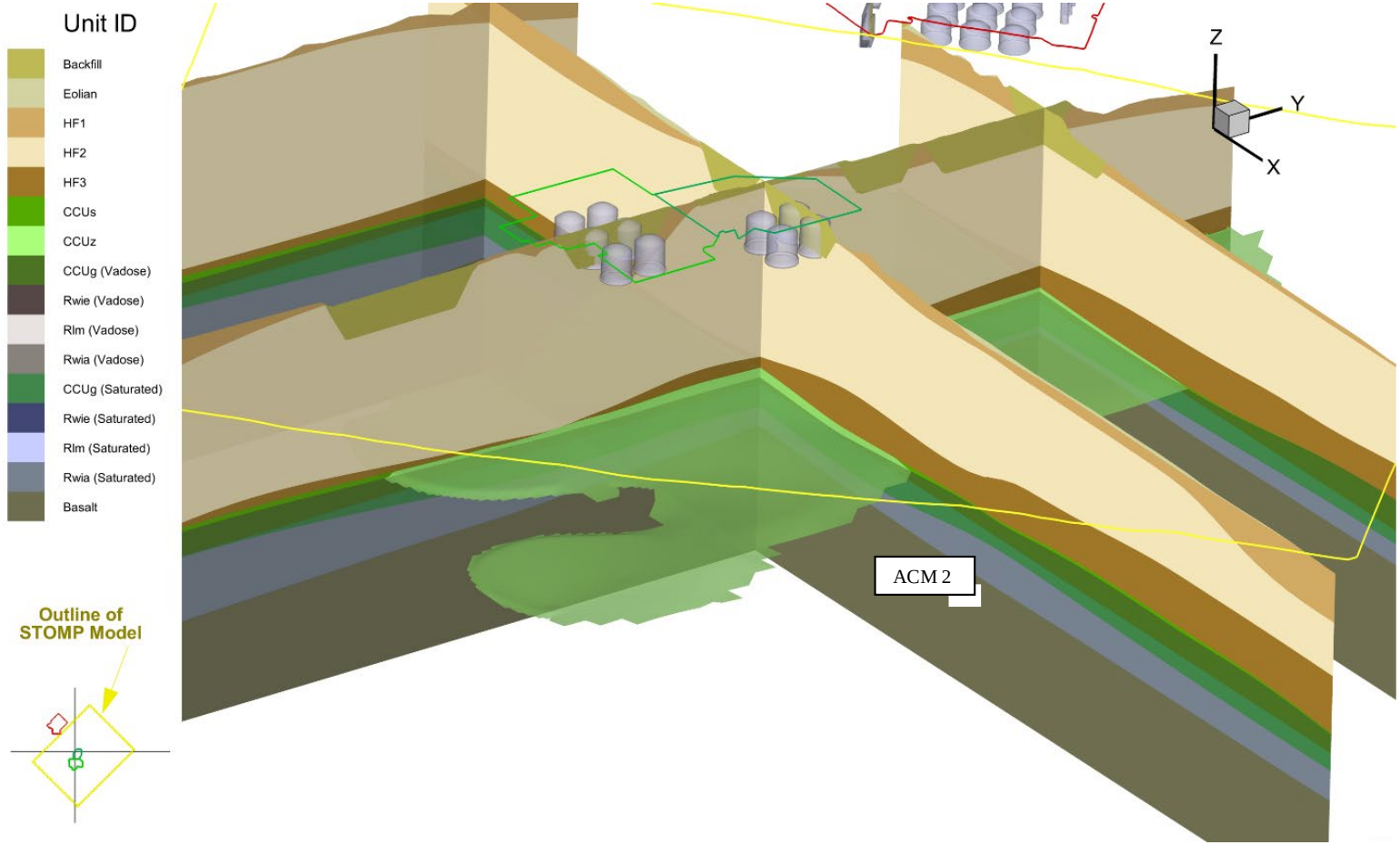

ACM = Alternative Conceptual Model
CCUg = Cold Creek Unit gravels
CCUz = Cold Creek Unit silt
HF1 = Hanford formation unit 1
HF2 = Hanford formation unit 2
HF3 = Hanford formation unit 3
Rlm = Ringold Formation Wooded Island Lower Mud Unit
Rwia = Ringold Formation Wooded Island Unit A
Rwie = Ringold Formation Wooded Island Unit E

Subsurface Transport Over Multiple Phases (STOMP) is developed and distributed by Battelle Memorial Institute.
Reference: RPP-RPT-60171, *Model Package Report: Geologic Framework Model used in WMA A-AX Performance Assessment and RCRA Closure Analysis.*

3.1.3 Source Term

The source term conceptual model component defines the characteristics of the inventory and the release of residual waste from the tanks and ancillary equipment, including pipelines. A closure date of January 1, 2050 is assumed for WMA A-AX, so radionuclides are decayed to that date in documents that estimate inventory for the residual waste. Section 5.1 in RPP-RPT-58693 provides a description of the processes associated with the release of contaminants into the pore waters of the material in the tank and ancillary equipment, and their migration from the residual waste matrix through the surrounding engineered barriers to the vadose zone. RPP-RPT-60885 includes the description of the modeling implemented to estimate the release of contaminants from the waste form (source) to the near field just outside the tanks and ancillary equipment.

RPP-CALC-62319 includes the assumptions and methodology used to estimate the post-retrieval inventory. Table 3-1 presents the current estimates of the residual inventory of ^{99}Tc in the WMA A-AX tanks and ancillary equipment, including pipelines (RPP-CALC-62319).

Figure 3-4 presents a graphical depiction of hypothetical rates of release of ^{99}Tc from each source. Figure 3-4 only represents a test case to support development of the process model until RPP-RPT-60885 includes the base case release functions. It is further anticipated that as WMA A-AX proceeds toward closure, the inventory estimates will be updated to address pertinent new information including measured volumes and compositions of waste residuals.

The release functions developed in RPP-RPT-60885 represent annualized contaminant mass rate releases (i.e., grams per year) from the individual sources. To apply these release functions in the STOMP flow and transport model, the mass rate is apportioned to the release nodes associated with each source. In the STOMP flow and transport model, the grouted residual releases are assumed to occur uniformly across the entire base of the tank. The nodes representing the tank structures are inactive within the flow and transport model domain, so the releases are located in the vadose zone nodes immediately below the structures. The base of each 100-series tank consists of 32 nodes. Thus, the quantity that the release functions indicate is released from the 100-series tanks is divided by 32. The waste residual releases from ancillary equipment sources that include the waste transfer pipelines are assumed to occur uniformly throughout the approximate area occupied by the WMA A-AX 100-series tanks. The ancillary equipment sources pipelines are assumed to be at the depth where the 100-series tanks begin to dome upward (Figure 3-5). This places the ancillary equipment releases approximately 12 m (39 ft) above the tank releases. The ancillary equipment area nodes are located in the backfill, excluding the nodes occupied by the tank domes because those nodes are inactive. The ancillary equipment area represents approximately 11,032 m^2 in A Farm and occupies 539 backfill nodes, and approximately 6,640 m^2 in AX Farm and occupies 323 backfill nodes in the model.

Table 3-1. Estimates of Residual Technetium-99 Inventory in Waste Management Area A-AX Tanks and Ancillary Equipment at Assumed Closure in Year 2050.

Source	Technetium-99	
	(Ci)	(g)
241-A-101	2.25	131
241-A-102	2.51	147
241-A-103	1.82	106
241-A-104	12.4	724
241-A-105	15.8	923
241-A-106	3.27	191
241-A Tank Farm Ancillary Equipment, including Pipelines	8.36E-05	0.005
241-AX-101	2.09	122
241-AX-102	0.568	33
241-AX-103	1.78	104
241-AX-104	7.48	437
241-AX Tank Farm Ancillary Equipment, including Pipelines	1.94E-05	0.001

Note: The specific activity of technetium-99 is 0.01712 Ci/g, as given in the RT Module of GoldSim (GoldSim Contaminant Transport Module User's Guide [GoldSim Technology Group 2017]) implementation of the radioactive decay properties in "ICRP Publication 107: Nuclear Decay Data for Dosimetric Calculations" (ICRP 2008).

Reference: Tables 7-3 and 7-4 of RPP-CALC-62319, *Residual Waste Source Inventory Term for the Waste Management Area A-AX Performance Assessment Inventory Case 1*, Rev. 0.

GoldSim© simulation software is copyrighted by GoldSim Technology Group LLC of Issaquah, Washington.

Figure 3-4. Example Waste Management Area A-AX Release Functions.

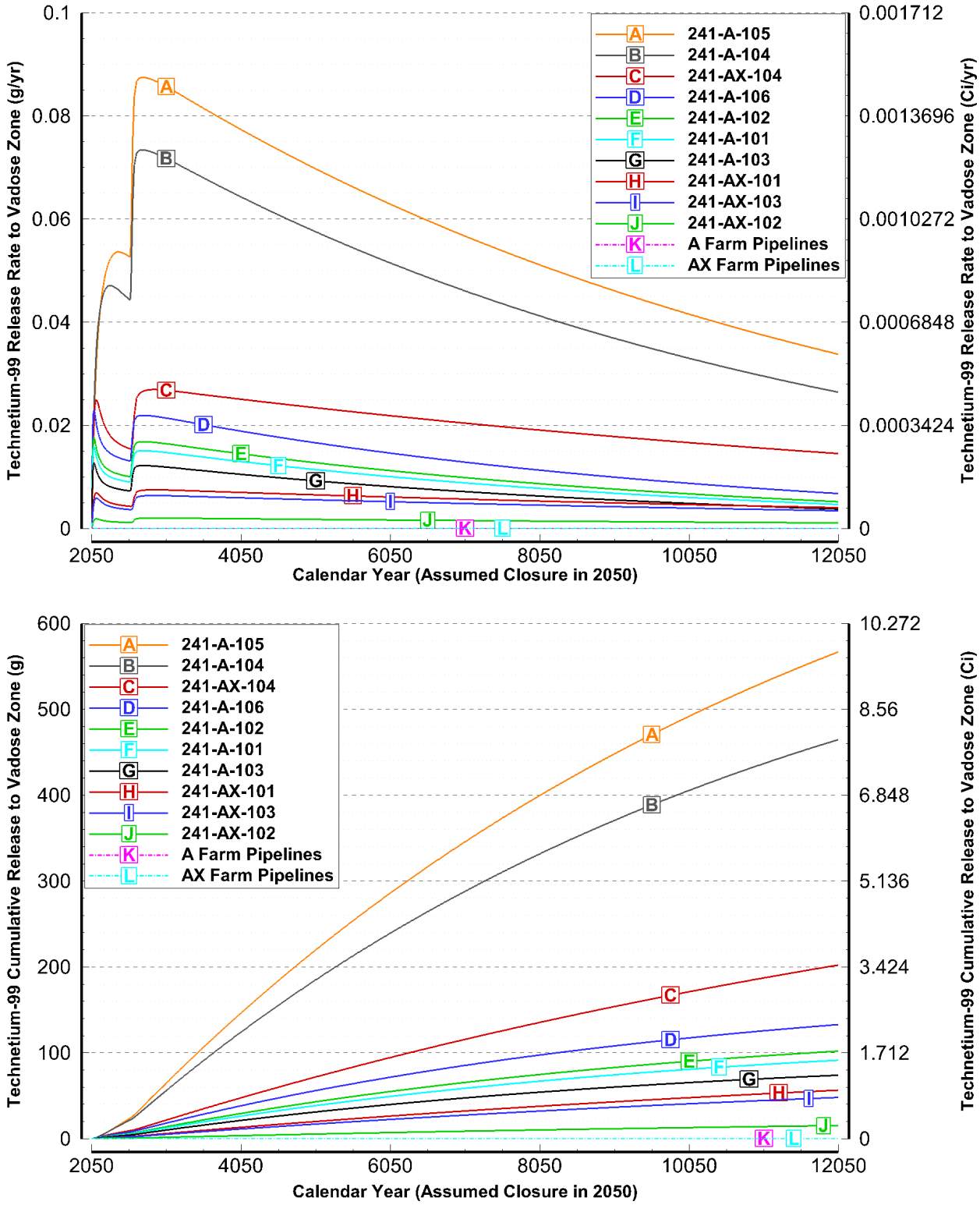

A Farm = 241-A Tank Farm AX Farm = 241-AX Tank Farm

Figure 3-5. Elevation of Ancillary Equipment Source that Includes the Pipelines in Waste Management Area A-AX Three-Dimensional Model Domain.

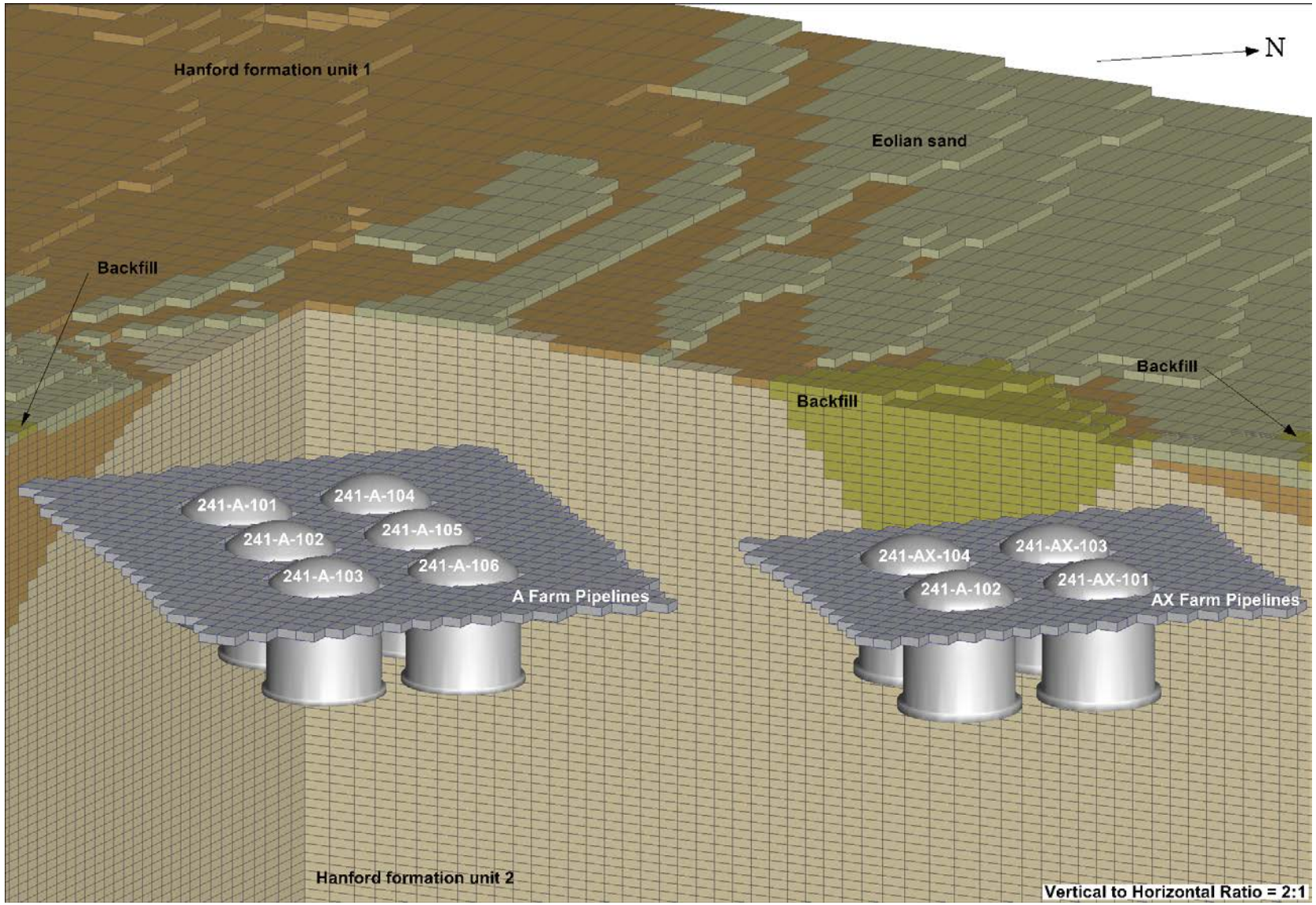

3.1.4 Vadose Zone Hydrogeology and Contaminant Transport

The WMA A-AX PA vadose zone contaminant fate and transport modeling is based on the porous media continuum assumption (DOE/RL-2011-50). The vadose zone hydrogeology and transport information presented here is a summary of the information presented in Appendix B. This section is organized as follows:

- Overall modeling approach (Section 3.1.4.1)
- Constitutive relations for hydraulic properties (Section 3.1.4.2)
- Effective moisture retention (Section 3.1.4.3)
- Variable anisotropy model (Section 3.1.4.4)
- Effective transport parameters (Section 3.1.4.5).

3.1.4.1 Overall Modeling Approach. Within the 200 Areas of the Hanford Site, vadose zone sediments are heterogeneous at a variety of scales. For the WMA A-AX PA fate and transport modeling, an equivalent homogeneous medium (EHM) model is used to represent the subsurface flow through the heterogeneous Hanford sediments. Further details on the EHM modeling approach are provided in Appendix B. Briefly, the EHM modeling represents the expected values in the context of ensemble averaging over numerous realizations. The EHM modeling does not capture the distinct variation in the field data, which is considered as a single realization. However, the EHM model representation does capture the mean or the bulk flow characteristics of the vadose zone moisture plumes ("Simulating field-scale moisture flow using a combined power-averaging and tensorial connectivity-tortuosity approach" [Zhang and Khaleel 2010]; "Estimation of effective unsaturated hydraulic conductivity tensor using spatial moments of observed moisture plume" [Yeh et al. 2005]).

The vadose zone properties which are of special interest in modeling are soil moisture retention and unsaturated as well as saturated hydraulic conductivity for various HSUs. For WMA A-AX PA modeling, following the EHM modeling approach, small-scale core measurements are used to predict the large, field-scale flow behavior (Appendix B). Because site-specific data are lacking, the existing database on sediment physical and hydraulic properties for the broader 200 Areas was queried for information regarding sediment particle size distribution (PSD), moisture retention, and saturated as well as unsaturated hydraulic conductivity. The following three-step process was used to develop the hydraulic properties and transport parameters for the WMA A-AX PA modeling (Appendix B):

- **Breakdown** of hydraulic properties by HSUs
- **Constitutive model** parameters for laboratory, core-scale hydraulic properties
- **Upscaling** for macroscopic, field-scale flow and transport parameters.

The **breakdown** of hydraulic properties by HSU was done as follows.

- Based on the ROCSAN database (Appendix B) and the PSD of the sediment samples, the properties for the HSUs at WMA A-AX are categorized as three combined groupings of units (i.e., sand-dominated units, gravel-dominated units, and fine-textured units).

- Sand-dominated units: AX Farm backfill, Eolian sand, H1, and H2.

- Gravel-dominated units: A Farm backfill, H3, CCUg, and Ringold A.

- Fine-textured units: CCUz, Cold Creek Unit sand (CCUs, ACM 2 only), and Ringold mud.

Within the 200 Areas, unlike the sand-dominated (H2) sediments, both H1 and H3 sediments typically are comprised of a significant gravel fraction and considered as "gravel-dominated." However, the ROCSAN sieve data indicate that the Hanford H1 unit at WMA A-AX is similar to the sand-dominated H2 unit with respect to gravel content (Appendix B, Section B.4.1). The average gravel contents for H1 and H2 units are about 16% and 14% (by weight), respectively. Because of this similarity, the WMA A-AX H1 unit is assigned the hydraulic properties of the Hanford H2 unit.

The criteria and database for development of **constitutive model** parameters for core-scale hydraulic properties are as follows:

- Selected laboratory, core-scale samples having data on PSD, saturated hydraulic conductivity, moisture retention and unsaturated hydraulic conductivity

- For nearly all samples, both moisture retention and unsaturated hydraulic conductivity data were used to derive the constitutive model (van Genuchten-Mualem) parameters for core samples

- The parametrization using RETC (RETention Curve) computer program (EPA/600/2-91/065, *The RETC Code for Quantifying the Hydraulic Functions of Unsaturated Soils*) for the core-scale samples was based on a simultaneous fit of the moisture retention as well as unsaturated hydraulic conductivity data

- For some fine-textured samples without unsaturated conductivity measurements, the saturated conductivity and the moisture retention data were used to estimate the unsaturated conductivity

- The laboratory database for core samples (Appendix B, Sections B.4.2 through B.4.4) is based on published reports for 200 Areas (i.e., RPP-20621, *Far-Field Hydrology Data Package for the Integrated Disposal Facility Performance Assessment*; PNNL-23711, *Physical, Hydraulic, and Transport Properties of Sediments and Engineered Materials Associated with Hanford Immobilized Low-Activity Waste*; WHC-EP-0883, *Variability and Scaling of Hydraulic Properties for 200 Area Soils, Hanford Site*; WHC-EP-0645, *Performance Assessment for the Disposal of Low-Level Waste in the 200 West Area Burial Grounds*).

As discussed in Appendix B, for the laboratory measurements, moisture retention experiments are based on standard methods (i.e., hanging column method, Tempe pressure cell, and vapor adsorption). Unsaturated hydraulic conductivity experiments are based on steady-state head

control method, the multistep or the centrifuge method (Appendix B). A gravel (>2-mm size fraction) correction (if needed) is applied to laboratory measurements ("Correcting Laboratory-Measured Moisture Retention Data for Gravels" [Khaleel and Relyea 1997]). As stated above, the van Genuchten-Mualem ("A Closed-form Equation for Predicting the Hydraulic Conductivity of Unsaturated Soils" [van Genuchten 1980]; "A New Model for Predicting the Hydraulic Conductivity of Unsaturated Porous Media" [Mualem 1976]) model parameterization for nearly all core samples was biased toward the relatively dry end of the moisture regime to avoid inaccurate predictions of conductivity estimates (e.g., "Evaluation of van Genuchten-Mualem Relationships to Estimate Unsaturated Hydraulic Conductivity at Low Water Contents" [Khaleel et al. 1995]).

Upscaling for macroscopic, field-scale flow and transport parameters was accomplished as follows (Appendix B):

- Vadose zone heterogeneous geologic media is conceptualized as being comprised of multiple EHM
- Each heterogeneous HSU is treated as an anisotropic EHM having its individual upscaled (effective) flow and transport properties
- Upscaled flow properties and the macroscopic anisotropy for the field scale are based on a variable moisture-dependent anisotropy model
- Macrodispersivity estimates for various HSUs are based on a combination of numerical simulation results, stochastic solutions, and 200 East Area tracer experiments (Appendix B).

The constitutive model parameters and data tables for laboratory, core-scale hydraulic properties for the sand-dominated, gravel-dominated, and fine-textured units are provided in Appendix B. Details on the upscaling process and variable moisture-dependent anisotropy are provided in Appendix B.

3.1.4.2 Constitutive Relations for Hydraulic Properties. The soil matric potential-moisture content relationships are described for each HSU using the following empirical relationship (van Genuchten 1980):

$$\theta(h) = \theta_r + (\theta_s - \theta_r)\{1 + [\alpha h]^n\}^{-m} \tag{3-1}$$

where $\theta(h)$ is the moisture content, here expressed explicitly as a function of the soil matric potential h, and the other terms are defined as follows:

θ_r = residual moisture content (dimensionless)
θ_s = saturated moisture content (dimensionless)
α = a fitting parameter (cm^{-1})
n = a fitting parameter (dimensionless)
m = $1 - 1/n$.

Combining the van Genuchten model with Mualem's (1976) model produces the following relationship for unsaturated hydraulic conductivity, K:

$$K(S_e) = K_s S_e^l \left\{1 - \left(1 - S_e^{(1/m)}\right)^m\right\}^2 \tag{3-2}$$

where S_e =effective saturation= $(\theta-\theta_r)/(\theta_s-\theta_r)$, K_s is the saturated hydraulic conductivity (cm/s), and l is a pore-connectivity parameter (dimensionless) that Mualem (1976) estimated as being about 0.5, representing an average of 45 samples. For the WMA A-AX PA, l is treated as being directional and pore-interaction terms l_{xx}, l_{yy}, and l_{zz} are defined to characterize the large, field-scale variable, moisture-dependent anisotropy invoked as part of EHM modeling. While other constitutive relations are available and programmed in STOMP and eSTOMP, the van Genuchten-Mualem formulation is used because of the existence of an extensive database for Hanford sediments using this formulation (e.g., WHC-EP-0883).

3.1.4.3 Effective Moisture Retention. A simple averaging of laboratory data listed in Appendix B, Sections B.4.2, B.4.3, and B.4.4 was used to define the effective saturated and residual moisture contents (θ_s^e and θ_r^e, respectively) for the sand-dominated, gravel-dominated, and fine-textured units. A linear averaging scheme ("Upscaled soil-water retention using van Genuchten's function" [Green et al. 1996]) was used to describe the effective saturation S^e at a given pressure head h. The effective van Genuchten parameters n^e and α^e were fit to the laboratory-measured retention data. Table 3-2 lists the upscaled effective retention parameters for the HSUs at WMA A-AX. The gravel content data that are used to identify and group the HSUs as sand- or gravel-dominated at WMA A-AX are presented in Appendix B, Section B.4.1. The gravel content of the sediment samples used to develop the hydraulic property estimates for the different HSUs at WMA A-AX are included in the subsections of Appendix B, Section B.4.2 that describe the HSUs individually. The gravel content of these sediment samples provides the basis for the gravel correction factor applied to the contaminant distribution coefficients.

The effective moisture retention curve parameter estimates for the HSUs do not require gravel correction. The H2 unit and other sand-dominated units parameter estimates (Table 3-2) are based on laboratory experiments run on the bulk samples with an average gravel content of about 5% (by weight) (RPP-20621). For other gravel-dominated HSUs, the parameter estimates already include the effects of the gravel content, and no further gravel correction is needed.

3.1.4.4 Variable Anisotropy Model. As described in Appendix B, Section B.3, variable, moisture-dependent anisotropy in unsaturated soils is an effective, large-scale (macroscopic) flow property. For the large-scale, macroscopic vadose zone, the EHM modeling provides a framework to upscale small-scale measurements to field-scale properties for the large-scale, macroscopic vadose zone.

For WMA A-AX PA, a tensorial connectivity-tortuosity (TCT) model is used to evaluate and characterize the large, field-scale variable, moisture-dependent anisotropy ("A Tensorial Connectivity–Tortuosity Concept to Describe the Unsaturated Hydraulic Properties of Anisotropic Soils" [Zhang et al. 2003]). The TCT model assumes that the anisotropy is

determined not only by directional saturated hydraulic conductivity, but also by the directional connectivity-tortuosity coefficients, L_i, corresponding to the three principal directions.

Table 3-2. Effective Soil Moisture Retention Parameters and Gravel Content for Waste Management Area A-AX Vadose Zone Hydrostratigraphic Units.

Hydrostratigraphic Unit		Gravel Content[a] (% weight)	θ_s^e (cm^3/cm^3)	θ_r^e (cm^3/cm^3)	α^e (1/cm)	n^e
Backfill	241-A Tank Farm	58[b]	0.174	0.0038	0.0886	1.271
	241-AX Tank Farm	7[b]	0.384	0.0290	0.0642	1.698
Sand-Dominated Units, excluding backfill: (Eolian sand, H1[c], and H2)		5[c]	0.384	0.0290	0.0642	1.698
Gravel-Dominated Units, excluding backfill: (H3, CCUg, Ringold E, and Ringold A)		66[d]	0.174	0.0038	0.0886	1.271
Fine-Textured Units: (CCUz and Ringold mud)		0[f]	0.435	0.0761	0.006545	1.815

CCUg = Cold Creek Unit gravel
CCUz = Cold Creek Unit silt
H1 = Hanford formation unit 1
H2 = Hanford formation unit 2
H3 = Hanford formation unit 3
Ringold A = Ringold Formation Unit A
Ringold E = Ringold Formation Unit E
Ringold mud = Ringold Formation Lower Mud Unit

[a] Gravel content of the samples used to represent the hydraulic properties for the Waste Management Area A-AX units; these numbers are not necessarily same as those based on the ROCSAN sieve data (Section B.4.1).

[b] Gravel content for the 241-AX Tank Farm backfill unit is 7% (by weight) versus 58% (by weight) for the 241-A Tank Farm backfill (ARH-LD-127, *Geology of the 241-A Tank Farm*; ARH-LD-128, *Geology of the 241-AX Tank Farm*). The H2 sand-dominated effective retention curve (average gravel content ~5% [by weight], range ~0 to 32% [by weight] [RPP-20621, *Far-Field Hydrology Data Package for the Integrated Disposal Facility Performance Assessment*]) is assumed to be representative of hydraulic properties for the 241-AX Tank Farm backfill.

[c] Based on the average gravel content for the 44 samples used to represent the sand-dominated hydrostratigraphic units (HSUs) (RPP-20621); average ~5% (by weight), range ~0 to 32% (by weight). Based on the ROCSAN data (Section B.4.1), the average gravel contents for H1 and H2 units around Waste Management Area A-AX are about 16 and 14% (by weight), respectively; the typically "gravel-dominated" H1 unit is thus assigned the hydraulic properties of the Hanford H2 unit as appropriate for the locally sandier texture of the H1 unit within the model domain.

[d] Based on the central tendency of the gravel content for the 25 samples used to represent the gravel-dominated HSUs (RPP-20621; PNNL-23711, *Physical, Hydraulic, and Transport Properties of Sediments and Engineered Materials Associated with Hanford Immobilized Low-Activity Waste*): range 43 to 89% with a central tendency of 66% (by weight).

[e] The e superscript indicates that θ_s^e, θ_r^e, α^e, and n^e are "effective" parameters, as discussed in Section 3.1.4.3 and Appendix B, Section B.3.

[f] Based on the average gravel content, rounded to zero, for the 10 samples used to represent the fine-textured HSUs (WHC-EP-0645, *Performance Assessment for the Disposal of Low-Level Waste in the 200 West Area Burial Grounds*; WHC-EP-0883, *Variability and Scaling of Hydraulic Properties for 200 Area Soils, Hanford Site*); average 0.6% (by weight), range 0-4% (by weight).

Using a combined power-averaging and tensorial connectivity-tortuosity (PA-TCT) model, Zhang and Khaleel (2010) developed a practical method to estimate the 3-D effective unsaturated hydraulic conductivity. Further details on the development of the PA-TCT model and its application are presented in Appendix B and PNNL-23711. Briefly, following the PA-TCT model, the effective unsaturated hydraulic conductivity in the ith principal direction,

$K_i^e(h)$, for each of the anisotropic EHM, as a function of pressure head, h, is first estimated with a power-averaging model (Zhang and Khaleel 2010)

$$K_i^e(h) = \left\{\frac{1}{N}\sum_{j=1}^{N}[K_j(h)]^{p_i}\right\}^{1/p_i} \quad i = 1, 2, or\ 3 \tag{3-3}$$

where j denotes the sediment sample index, N is the number of samples, $K_j(h)$ is the hydraulic conductivity of the jth sample as a function of h, and the power p varies between -1 (i.e., harmonic average) and 1 (i.e., arithmetic average); it approaches the geometric mean when p approaches zero. The use of a larger p yields a larger $K^e(h)$ for a given data set.

For an unsaturated anisotropic EHM, the directional hydraulic conductivity is defined for each of three principal directions, i = 1, 2, 3. The unsaturated conductivity $\mathbf{K}(S_e)$ is considered as a symmetric second-order tensor, which for a coordinate system coinciding with the three principal directions can be represented as:

$$\boldsymbol{K}(S_e) = A(S_e, \beta, \gamma)\begin{pmatrix} K_{s1} & 0 & 0 \\ 0 & K_{s2} & 0 \\ 0 & 0 & K_{s3} \end{pmatrix}\begin{pmatrix} S_e^{L_1} & 0 & 0 \\ 0 & S_e^{L_2} & 0 \\ 0 & 0 & S_e^{L_3} \end{pmatrix} \tag{3-4}$$

where β and γ are empirical constants. The above equation is an extension of Appendix B Equation B-7. For the combination of Mualem (1976) model (β = 2 and γ = 1) and van Genuchten model (1980), the coefficient A in Equation 3-4 is

$$A = \left[1 - \left(1 - S_e^{1/m}\right)^m\right]^2 \tag{3-5}$$

A comparison of Equations 3-4 and 3-2 shows that both saturated hydraulic conductivity and pore-connectivity are tensors in Equation 3-4; the two parameters are scalar in Equation 3-2. The symbol l in Equation 3-2 is replaced by L in Equation 3-4 to signify the upscaled estimate for the pore-connectivity parameter. Appendix B, Section B.4.6 includes details about the application of the PA-TCT model to develop hydraulic properties for the HSUs at WMA A-AX. Table 3-3 summarizes the four sets of optimized K_s^e and L^e values corresponding to the four p values used for power averaging. As discussed in Appendix B, Section 4.6, the low anisotropy values in Table 3-3 (p=1 in the horizontal directions and p =1/3 in the vertical direction) represent the derived PA-TCT parameters applicable to the different HSUs for the WMA A-AX PA modeling.

Table 3-3. Optimized Saturated Hydraulic Conductivity and the Pore Connectivity-Tortuosity Coefficient for Different Averaging Schemes for Waste Management Area A-AX Hydrostratigraphic Units.

Hydrostratigraphic Unit	p = 1 (horizontal directions x and y)		p = 1/3 (vertical direction z)		p = 0		p = -1	
	K_s^e (cm/s)	L^e	K_s^e (cm/s)	L^e	K_s^e (cm/s)	L^e	K_s^e (cm/s)	L^e
Sand-Dominated Units: (241-AX farm backfill, Eolian sand, H1, and H2)	6.196E-03	-0.683	6.157E-03	0.375	6.575E-03	0.916	7.741E-03	2.386
Gravel-Dominated Units: (241-A farm backfill, H3, CCUg, Ringold E, and Ringold A)	4.671E-02	0.637	7.714E-03	-0.225	3.790E-03	-0.111	1.959E-04	1.471
Fine-Textured Units: (CCUz and Ringold mud)	8.37E-05	0.167	6.68E-05	0.407	5.42E-05	0.765	1.22E-05	1.7056

p = power averaging factor
K_s^e = effective saturated hydraulic conductivity
L^e = directionally dependent pore-connectivity tortuosity parameter

CCU = Cold Creek Unit
CCUg = Cold Creek Unit gravel
CCUz = Cold Creek Unit silt

H1 = Hanford formation unit 1
H2 = Hanford formation unit 2
H3 = Hanford formation unit 3

Ringold A = Ringold Formation Unit A
Ringold E = Ringold Formation Unit E
Ringold mud = Ringold Formation Lower Mud Unit

Using the combined PA-TCT model, Zhang and Khaleel (2010) estimated the 3-D effective unsaturated hydraulic conductivity tensor for the Sisson and Lu field injection site in 200 East Area. The simulation results best matched the observed moisture plume behavior when the power values of p = 1 and p = 1/3 (Appendix B, Section B.4.6) were used for determining the effective unsaturated conductivity in the horizontal and vertical directions, respectively, i.e., a case of low macroscopic anisotropy (Zhang and Khaleel 2010). Based on the documented field-testing results for the Sisson and Lu site, the low anisotropy case (p = 1 for the x- and y-directions and p = 1/3 for the z-direction) is the recommendation for the WMA A-AX PA simulations. The other cases of intermediate and high anisotropy that are presented in Appendix B are included only for reference and completeness.

3.1.4.5 Effective Transport Parameters. The effective transport parameters include dispersivity estimates applicable to the field scale (referred to as macrodispersivity **A**, as opposed to **α** for laboratory-scale measurement; see Section 3.1.4.5.1), bulk density (Section 3.1.4.5.2), and diffusivity (Section 3.1.4.5.3). The transport parameters are all spatially variable.

3.1.4.5.1 Macrodispersivity. Dispersivities are a function of matric potential (or soil moisture content) in unsaturated media ("Stochastic Modeling of Large-Scale Transient Unsaturated Flow Systems," [Mantoglou and Gelhar 1987]). As with saturated media, heterogeneities that exist at various length scales result also in a scale dependence of macrodispersivities in unsaturated media ("A Critical Review of Data on Field-Scale Dispersion in Aquifers" [Gelhar et al. 1992]). Dispersivities increase with time, or equivalently with distance, until they tend to converge on their unique asymptotic (large-time) values. However, it can take a long time (e.g., years or decades) for the asymptotic Fickian approximation to take hold. This well-known asymptotic behavior is usually attributed to heterogeneity-induced spreading and mixing until the point at which the heterogeneity has effectively been "sampled" by the contaminant plume such that dispersion becomes constant. As described in Appendix B, Section B.6.3, the WMA A-AX PA transport simulations involve a constant (asymptotic) macrodispersivity estimate.

Table 3-4 summarizes the macrodispersivity estimates, discussed in Appendix B, Section B.6.3, based on results of (a) numerical simulation ("Upscaled flow and transport properties for heterogeneous unsaturated media" [Khaleel et al. 2002]), (b) stochastic solutions ("Stochastic Analysis of Simulated Vadose Zone Solute Transport in a Vertical Cross Section of Heterogeneous Soil During Nonsteady Water Flow" [Russo 1991]; Large-Scale Models of Transient Unsaturated Flow and Contaminant Transport Using Stochastic Methods [Mantoglou 1984]), and (c) 200 Areas experimental data (RPP-20621 Appendix E). For the WMA A-AX PA, the recommendation is to use the minimum of the range of values presented in Table 3-4 to estimate the longitudinal macrodispersivity: 25 cm for sand-dominated units, from the range of values between 25 cm to 100 cm; 15 cm for gravel-dominated units, from the range of values between 15 cm to 30 cm, and 5 cm for the fine-textured units, from the range of values between 5 cm to 10 cm.

The transverse macrodispersivity is typically much lower; in saturated media, it typically ranges from 1 to 10% of the longitudinal macrodispersivity ("Three-dimensional stochastic analysis of macrodispersion in aquifers" [Gelhar and Axness 1983]). As shown in Table 3-4, in the absence of unsaturated media experimental data, the recommendation is to use a transverse

macrodispersivity 1/10th of the longitudinal macrodispersivity (PNNL-23711, PNNL-25146, *Scale-Dependent Solute Dispersion in Variably Saturated Porous Media*).

Table 3-4. Macrodispersivity and Particle Density Estimates for the Hydrostratigraphic Units at Waste Management Area A-AX.

Hydrostratigraphic Unit	Estimated Range (cm)	Longitudinal Dispersivity α_L (cm)	Transverse Dispersivity α_T (cm)	Bulk Density (ρ_d) (g/cm^3)	Particle Density (ρ_s) (g/cm^3)*
Sand-Dominated Units: (241-AX farm backfill, Eolian sand, H1, and H2)	~25 – 100	25	2.5	1.67	2.71
Gravel-Dominated Units: (241-A farm backfill, H3, CCUg, Ringold E, and Ringold A)	~15 – 30	15	1.5	2.15	2.60
Fine Textured Units: (CCUz and Ringold mud)	~5 – 10	5	0.5	1.60	2.83

*Particle density is calculated for each hydrostratigraphic unit using the bulk density data and the particle density equation presented in Section B.6.1.

CCUg = Cold Creek Unit gravel
CCUz = Cold Creek Unit silt
H1 = Hanford formation unit 1
H2 = Hanford formation unit 2
H3 = Hanford formation unit 3
Ringold A = Ringold Formation Unit A
Ringold E = Ringold Formation Unit E
Ringold mud = Ringold Formation Lower Mud Unit

3.1.4.5.2 Bulk Density and Particle Density. Following Stochastic Subsurface Hydrology (Gelhar 1993), the effective, large-scale estimates for bulk density are the averages of small-scale laboratory measurements as discussed in Section B.6.1 of Appendix B. Table 3-4 includes the particle density calculated for each HSU using the bulk density data and particle density equation presented in Section B.6.1. Although the effective transport parameters include bulk density, STOMP input requires the particle density, and the program calculates the bulk density internally.

3.1.4.5.3 Diffusivity. It is assumed that the effective, large-scale diffusion coefficients for all strata in the vadose zone at the WMA A-AX site are a function of volumetric moisture content, θ, and can be expressed using the Millington-Quirk empirical relation described in PNNL-12030, *STOMP Subsurface Transport Over Multiple Phases Version 2.0 Theory Guide*:

$$D_e(\theta) = D_0 \frac{\theta^{10/3}}{\theta_s^2} \tag{3-6}$$

where:

$D_e(\theta)$ = effective diffusion coefficient of an ionic species
D_0 = effective diffusion coefficient in free water
θ = volumetric moisture content.

The molecular diffusion coefficient for all species in pore water is assumed to be 2.5×10^{-5} cm^2/s (WHC-SD-WM-EE-004, *Performance Assessment of Grouted Double-Shell Tank Waste Disposal at Hanford*), which is consistent with and representative of values used in other Hanford PAs.

3.1.5 Infiltration and Recharge

The data and information contained in RPP-RPT-58693 serve as the basis for model recharge estimates. The magnitude of the recharge estimates for soils at the Hanford Site varies as a function of the soil type, condition of the vegetation cover, and soil integrity (e.g., disturbed versus undisturbed). The range of recharge values reported in RPP-RPT-58693 represents distinct sets of data applicable to different surface conditions based on lysimetry, isotopic measurements, and interpretation and extrapolation (in some instances) by Hanford Site subject matter experts. The natural background recharge rates represent a set of estimates for natural vegetated conditions. The range of values for operational conditions represents a set of estimates of recharge rates for vegetation-free disturbed soil. Table 3-5 presents a summary of model recharge rates applied to the different surface types shown in Figure 3-1. The area within the solid yellow lines on Figure 3-1 is assumed to be covered by a surface barrier at the time of closure, consistent with the conceptual barrier extent in Figure E-31 of Appendix E of DOE/EIS-0391. The areas subdivided by the dashed yellow lines on Figure 3-1 are used to implement changes in surface conditions that occurred at different times outside each tank farm during the operational history.

The recharge rate estimate applicable to WMA tank farm surfaces with no vegetation is estimated to be 100 mm/yr (3.9 in./yr). This estimate is consistent with the value estimated in DOE/EIS-0391, and includes as its basis data collected from gravel-covered small tube lysimeters, gravel mulch lysimeters, and sandy gravel and gravel pit lysimeters at the Field Lysimeter Test Facility (FLTF), as well as drainage rates observed through the prototype barrier gravel side slope during the first few years when there was little or no vegetation ("Variations in Recharge at the Hanford Site" [Gee et al. 1992]; PNNL-19945, *Soil Water Balance and Recharge Monitoring at the Hanford Site – FY 2010 Status Report*, and PNNL-14744, *Recharge Data Package for the 2005 Integrated Disposal Facility Performance Assessment*). The lysimeter and barrier side slope data include the effects of late fall and winter precipitation on water accumulation in the soil, and water received from that precipitation tends to remain in the soil until the soil drains or the temperatures warm and the water evaporates ("Long-Term Drainage from the Riprap Side Slope of a Surface Barrier" [Zhang 2017]).

The design for the WMA A-AX surface barrier at closure has not been finalized but it is expected to function comparably to a Modified RCRA Subtitle C Barrier, which PNNL-16688, *Recharge Data Package for Hanford Single-Shell Tank Waste Management Areas* indicates should function similarly to the Prototype Hanford Barrier (DOE/RL-93-33, *Focused Feasibility Study of Engineered Barriers for Waste Management Units in the 200 Areas*). Summary of data collected over nearly two decades at the Prototype Hanford Barrier (DOE/RL-2016-37, *Prototype Hanford Barrier 1994 to 2015*) indicates that infiltration through the prototype is much less than 0.1 mm/yr, and evaluations of the design using lysimeter data indicate that the barrier is capable of limiting recharge to this amount even with a complete lack of vegetation

("Design and Performance Evaluation of a 1000-year Evapotranspiration-Capillary Surface Barrier" [Zhang et al., 2017]; "Performance of a Surface Barrier for Waste Isolation and Flux Reduction at the Hanford Site" [Zhang et al. 2016]; "Evaluating the long-term hydrology of an evapotranspiration-capillary barrier with a 1000 year design life" [Zhang 2016]; "Multiple-Year Water Balance of Soil Covers in a Semiarid Setting" [Fayer and Gee 2006]). However, for PA simulations involving WMA A-AX with a functioning surface barrier, a recharge rate of 0.5 mm/yr is assumed, which is consistent with the drainage design specification in DOE/RL-93-33.

At the end of 500 years, the surface barrier performance is assumed to degrade instantaneously to an infiltration rate of 3.5 mm/yr and maintain that infiltration rate for the remainder of the sensitivity and uncertainty analysis timeframe. This assumption is consistent with the assumption regarding barrier performance in DOE/EIS-0391. No quantifying data are available for specifying the performance of the barrier after its design life. According to PNNL-13033, *Recharge Data Package for the Immobilized Low-Activity Waste 2001 Performance Assessment*, the erosion of the silt loam layer and deposition of dune sand on the barrier is not likely to alter the barrier performance significantly, and Zhang et al. (2017) and Zhang (2016) indicate that the barrier is very likely to perform for its 1,000-year design life, even after a fire. The value of 3.5 mm/yr (0.14 in./yr) corresponds to the recharge in an undisturbed area, which indicates that native vegetation is assumed to reclaim the land.

Although the side slopes and berms associated with the barrier are likely to function and perform differently than the surface of the barrier, they are included as part of the barrier surface. The impact of the side slopes on the overall recharge rate is expected to be relatively minor. The sandy gravel/gravelly sand barrier side slope and berm are assumed eventually to resemble a Burbank loamy sand, and if that assumption is valid, then PNNL-16688 indicates that the long-term recharge rate for that soil type is 1.9 mm/yr, which is less than the value of 3.5 mm/yr used in the analysis for the degraded barrier surface.

RPP-RPT-58693 does not include information about recharge occurring in areas outside of WMA A-AX apart from those assumed to remain undisturbed. As indicated in Figure 3-1, much of the area outside of WMA A-AX and double-shell tank farms but within the model domain has been impacted by Hanford operations. Construction and operations outside the tank farms removed the surface soil, broke up any near-surface layering, and exposed Hanford formation sands at land surface. These sediments tend to be coarser than the original soil. As indicated in photographs of the area around WMA A-AX, plants have difficulty growing on this soil, although some, such as the surface of burial grounds, appear to allow some vegetation regrowth.

Very few recharge rate data are available for these types of disturbed conditions at Hanford. PNNL-14702, *Vadose Zone Hydrogeology Data Package for Hanford Assessments* recommends a recharge rate of 63 mm/yr for this type of surface condition that is void of vegetation. This value is supported by drainage data collected from the 300 North Lysimeter, which contains coarse Hanford formation material screened to less than 1% gravel (material > 2 mm); the long-term recharge rate averaged 62 mm/yr from 1981 to 2005 (PNNL-16688). DOE/RL-2007-27, *Feasibility Study for the Plutonium/Organic-Rich Process Condensate/Process Waste Group Operable Unit: Includes the 200-PW-1, 200-PW-3, and*

200-PW-6 Operable Units applies the recharge estimate of 63 mm/yr to represent ground conditions during the operational period of the cribs where Hanford Sand remains disturbed with no vegetation. For the purpose of the WMA A-AX PA model, it is assumed that the recharge is 63 mm/yr in all areas outside of WMA A-AX and double-shell tank farms until revegetation is assumed to occur at closure.

The transition period from the young revegetated shrub steppe to the mature shrub steppe community is assumed to require 30 years, which is the assumption included in PNNL-14702. Net infiltration during this time is assumed to decrease linearly from the disturbed value to the value representing completed revegetation. DOE/RL-2011-116, 2013, *Hanford Site Revegetation Manual* indicates that restoration of a functional shrub-steppe plant community in graded backfill or bare soil may require decades. Results of revegetated waste site monitoring at Hanford indicate that sagebrush and other native plant species often reclaim the land within five years of planting or seeding (BHI-01745, *2004 Environmental Restoration Contractor Revegetation Monitoring Report*; WCH-223, *2007 River Corridor Closure Contractor Revegetation and Mitigation Monitoring Report*). Big sagebrush (Artemisia tridentata) normally requires three to four years to establish, mature, and flower ("Management of Restored and Revegetated Sites" [Stevens 2004]). Additional time, as much as a decade may be necessary where poor seedbed conditions exist, the ground has burned or broadcast seeding has occurred, seeding occurs in surface soils occupied by cheatgrass or red brome, or seeding is attempted in soils with exposed and disturbed subsoil (Stevens 2004). All of these conditions appear to exist in the ground around and outside of WMA A-AX.

3.1.6 Geochemistry Conceptual Model

The geochemistry conceptual model component involves the partitioning behavior or sorption characteristics regarding release, retardation, and attenuation mechanisms and any simplifying assumptions for specific radionuclides and non-radiological contaminants. Reactions such as radioactive decay also affect transport, but radionuclide half-lives depend only on the radionuclide rather than media (half-lives may be found in "ICRP Publication 107: Nuclear Decay Data for Dosimetric Calculations" [ICRP 2008]). DOE/RL-2011-50 provides rationale and explanation for the following elements of the geochemistry conceptual model and its applicability to the Hanford Site 200 Areas:

- The simplifying assumption that the use of a linear distribution coefficient (K_d) isotherm is a reasonable conservative description for the release and attenuation of radionuclides in the context of providing a bounding condition for contaminant migration[4]

- The source(s) of the data used in the selection of radionuclide K_d values

- The use of single K_d values in individual vadose zone HSUs.

[4] Note that the underlying assumption of dilute aqueous concentrations of contaminants that is considered valid for the analysis of future releases from waste residuals is not necessarily valid for the analysis of potential past releases of liquid wastes handled at WMA A-AX. Analysis of these past releases may require development of alternative sorption models or further evaluation of the K_d model, which is outside the scope of this MPR.

Table 3-5. Model Recharge Rate (Net Infiltration) Estimates for Surface Conditions during the Pre-Construction, Operational, and Post-Closure Periods.

Period	Waste Management Area (WMA) A-AX Region and Surface Condition	Model Value of Recharge Rate (mm/yr)
Pre-construction (before 1953)	Undisturbed region (Rupert Sand with vegetation)	3.5
Operational period (1953 to 2050)	Undisturbed region (Rupert Sand with vegetation)	3.5
	WMA A-AX: 241-AX Tank Farm Surface region starting 1963 (Sand without vegetation)	100
	WMA A-AX: 241-A Tank Farm Surface region starting 1954 (Gravel without vegetation)	100
	Disturbed and resurfaced unrevegetated region (Rupert Sand with no vegetation); start dates are 1953 (241-AW Tank Farm and areas west and south of tank farms), 1954 (241-AX Tank Farm, 241-AZ Tank Farm, and area north of 241-A Tank Farm and northeast of tank farms), 1963 (241-AN Tank Farm), 1977 (area east of 241-A Tank Farm), and 1982 (area east of 241-AP Tank Farm)	63*
	Double-shell tank farms surface regions (gravel or sand without vegetation); start dates are 1970 (241-AZ Tank Farm), 1976 (241-AW Tank Farm), 1977 (241-AN Tank Farm), and 1982 (241-AP Tank Farm)	100
Early post-closure (2050 to 2550)	Undisturbed region (Rupert Sand with vegetation)	3.5
	WMA A-AX Surface region (Surface barrier with vegetation)	0.5
	WMA A Surface region (Surface barrier with vegetation beginning in 2050)	0.5
	Disturbed revegetated region (Rupert Sand with vegetation beginning in 2050 with vegetation recovery completed in 2080)	3.5
	Disturbed unrevegetated region (Rupert Sand with no vegetation until vegetation recovery begins in 2050 and completes in 2080)	3.5
Late post-closure (2550 to 3050 and beyond)	Undisturbed region (Rupert Sand with vegetation)	3.5
	WMA A-AX Surface region (Surface barrier with vegetation)	3.5
	WMA A Surface region (Degraded surface barrier with vegetation begins in 2550)	3.5
	Disturbed revegetated region (Rupert Sand with vegetation recovery completed in 2080)	3.5
	Disturbed unrevegetated region (Rupert Sand with vegetation recovery completed in 2080)	3.5

* PNNL-14702, *Vadose Zone Hydrogeology Data Package for Hanford Assessments*; DOE/RL-2007-27, *Feasibility Study for the Plutonium/Organic-Rich Process Condensate/Process Waste Group Operable Unit: Includes the 200-PW-1, 200-PW-3, and 200-PW-6 Operable Units*; and PNNL-16688, *Recharge Data Package for Hanford Single-Shell Tank Waste Management Areas.*

General source: RPP-RPT-58693, *Engineered System Data Package for Waste Management Area A-AX.*

Geochemistry conceptual models involving linear K_d isotherms and developed for the Hanford Site include consideration of the dominant sediment textures, the percentage of gravel, the mineral character of the natural sediments, the chemical character of the released waste, and the extent of interaction between waste releases and the natural sediments (DOE/RL-2011-50; PNNL-17154, *Geochemical Characterization Data Package for the Vadose Zone in the Single-Shell Tank Waste Management Areas at the Hanford Site*). Representative and bounding distribution coefficients (K_d values) recommended for vadose zone modeling are based on extensive laboratory studies, testing, and measurements of adsorption and desorption coefficients under saturated and unsaturated conditions involving Hanford Site-specific sediments, contaminants, and conditions (PNNL-13037, *Geochemical Data Package for the 2005 Hanford Integrated Disposal Facility Performance Assessment*; PNNL-13895, *Hanford Contaminant Distribution Coefficient Database and Users Guide*; PNNL-16663, *Geochemical Processes Data Package for the Vadose Zone in the Single-Shell Tank Waste Management Areas at the Hanford Site*; and PNNL-17154). The distribution coefficient (K_d) conceptual model describing contaminant partitioning holds that for a given volume of sediment, the surface area with reactive mineral phases, organic carbon, or both is less for coarse-textured sediments than for fine-textured sediments (PNNL-13895). Therefore, coarse-textured sediments typically exhibit weaker sorption characteristics than fine-textured sediments, which leads to lower K_d values for HSUs representing coarse-textured sediments than for HSUs representing fine-textured sediments. In most cases, empirical K_d values are determined using sediment samples sieved finer than 2 mm in size (PNNL-13895). Corrections for gravel-size and larger sediments physically excluded by sampling and laboratory techniques are necessary to make the K_d values measured for the fine fraction applicable to a particular HSU.

3.1.6.1 Distribution Coefficient (K_d) Estimates for Waste Management Area A-AX Hydrostratigraphic Units. PNNL-17154 provides recommendations for K_d values applicable to the waste and sediments present at WMA A-AX based on the broader Hanford Site database. K_d values presented in PNNL-17154 include values for sorption of key radiological and non-radiological contaminants to sand-size and silt-size sediments[5] where waste-sediment interactions are considered to have had no impact, intermediate impact, or high impact on sorption processes. The key characteristics relevant to sorption of the WMA A-AX wastes are high salinity and alkaline pH, which are expected for past releases of waste liquids and to a lesser degree for future releases from solid waste residuals leached into natural porewater by alkaline grout pore fluids (PNNL-17154, RPP-RPT-58693). As conceived in PNNL-17154 for WMAs with tank waste releases, the high impact zone is assumed to have elevated salinity and pH, whereas the intermediate impact zone is assumed to have pH largely neutralized by reaction with the natural sediments, but the salinity remains elevated. For the analysis of future releases from waste residuals, it is assumed that most of the vadose zone and saturated zone below each release location is characterized by intermediate impact. Intermediate impact represents zones where reactions between the natural sediment and the waste releases have largely neutralized the acidic or basic nature of the wastes likely to cause changes in the K_d values. Overall, the assumption of intermediate impact throughout the transport pathway leads to similar or faster contaminant transport than if the impacted sediments give way to an unimpacted zone at some distance from

[5] PNNL-17154 also provides values for "carbonate-dominated sediments" at WMA A-AX. Although carbonate minerals appear to exist in much of the vadose zone at WMA A-AX, none of the HSUs are interpreted in RPP-RPT-60171 to be carbonate dominated.

the releases. Table 3-6 gives the complete list of sand K_d values with their references for the WMA A-AX PA, including the minimum and maximum values applicable to an uncertainty analysis distribution.

Table 3-6. K_d Value Estimates (mL/g) for Sand in the Waste Management Area A-AX Performance Assessment Models. (2 sheets)

Contaminant	Most Likely	Minimum	Maximum	Basis
Ac	350	100	1,500	PNNL-16663 Table C.5
Al	1,500	1,500	1,500	RPP-RPT-46088
Am	600	200	2,000	PNNL-17154 Table A.4
B	3	3	3	RPP-RPT-46088
C-14	1	0	100	PNNL-17154 Table A.4
Cd	6.7	6.7	6.7	CLARC
Cm	350	100	1,500	PNNL-16663 Table C.5
CN	0	0	0	RPP-RPT-46088
Co	0	0	10	PNNL-17154 Table A.4
Cr(VI)	0	0	3	PNNL-17154 Table A.4
Cs	100	10	1,000	PNNL-17154 Table A.4
Eu	10	3	100	PNNL-17154 Table A.4
F	0	0	1	PNNL-17154 Table A.4
Fe	25	25	25	RPP-RPT-46088
H-3	0	0	0	PNNL-17154 Table A.4
Hg	52	52	100	CLARC; RPP-ENV-58782 Table 8-6
I	0.2	0	2	PNNL-17154 Table A.4
Mn	65	65	65	RPP-RPT-46088
Nb	0	0	0.1	PNNL-16663 Table C.5
Ni	3	1	20	PNNL-17154 Table A.4
NO_2	0	0	0.1	PNNL-17154 Table A.4
NO_3	0	0	0.1	PNNL-17154 Table A.4
Np	10	2	30	PNNL-17154 Table A.4
Pa	10	2	30	Assume analogue to Np
Pb	10	3	100	PNNL-17154 Table A.4
Pu	600	200	2,000	PNNL-17154 Table A.4
Ra	10	5	20	PNNL-17154 Table A.4

Table 3-6. K_d Value Estimates (mL/g) for Sand in the Waste Management Area A-AX Performance Assessment Models. (2 sheets)

Contaminant	Most Likely	Minimum	Maximum	Basis
Rn	0	0	0	No relevant information; RPP-ENV-58782 Table 8-6
Se	0.1	0	3	PNNL-17154 Table A.4
Sm	10	3	100	RPP-ENV-58782 Table 8-6
Sn	0.5	0	20	PNNL-17154 Table A.4
Sr	10	5	20	PNNL-17154 Table A.4
Tri-butyl Phosphate	1.89	1.89	1.89	RPP-RPT-46088
Tc	0	0	0.1	PNNL-16663 Table C.5
Th	300	40	500	PNNL-16663 Table C.5
U	0.6	0.2	2	RPP-RPT-46088
Zr	300	40	500	PNNL-16663 Table C.5

References:
CLARC 2017, Cleanup Levels and Risk Calculation (CLARC), Queried 02/28/2017, [CLARC Master Table], https://fortress.wa.gov/ecy/clarc/FocusSheets/CLARC%20Master%20Spreadsheet.xlsx..
PNNL-16663, *Geochemical Processes Data Package for the Vadose Zone in the Single-Shell Tank Waste Management Areas at the Hanford Site*.
PNNL-17154, *Geochemical Characterization Data Package for the Vadose Zone in the Single-Shell Tank Waste Management Areas at the Hanford Site*.
RPP-ENV-58782, *Performance Assessment of Waste Management Area C, Hanford Site, Washington*.
RPP-RPT-46088, *Flow and Transport in the Natural System at Waste Management Area C*.

Unlike nearby WMA C, WMA A-AX has a silt-dominated HSU of significant areal extent below the footprint of the SSTs, i.e., the CCUz unit of the Cold Creek Formation (RPP-RPT-60171). As previously stated, PNNL-17154 provides recommended K_d values for silt-sized sediments with varying degrees of chemical impact. The values therein associated with intermediate impact form the basis of the list of silt K_d values in Table 3-7. Radiological and non-radiological contaminants with no data for silt default to the sand values, which are generally expected to underestimate sorption on silt. Values for ^{99}Tc and uranium sorption on silt likewise default to the sand values with the intention of conservatism, given the existing uncertainty in how to interpret empirical data from other facilities and sites. Table 3-7 also includes the minimum and maximum values applicable to an uncertainty analysis distribution.

Table 3-6 and Table 3-7 present estimates of the K_d values prior to gravel correction, which is discussed in Section 3.1.6.2. Sand K_d values are applicable to sediments <2 mm in size, which excludes gravel and may include any combination of sand, silt, and clay. The silt K_d values listed in Table 3-7 are applicable to silt- and clay-sized sediments with little or no sand or gravel. K_d values listed for an element are used for all its isotopes. For example, uranium K_d values may be applied to any uranium isotope and to total uranium. In lieu of more information, chromium is assumed to be transported as Cr(VI), which is less strongly sorbing and migrates faster through the subsurface than Cr(III).

Table 3-7. K_d Value Estimates (mL/g) for Silt in the Waste Management Area A-AX Performance Assessment Models. (2 sheets)

Contaminant	Most Likely	Minimum	Maximum	Basis
Ac	350	100	1,500	Assumes sand fraction values apply
Al	1,500	1,500	1,500	Assumes sand fraction values apply
Am	600	200	2,000	PNNL-17154 Table A.5
B	3	3	3	Assumes sand fraction values apply
C-14	1	0	100	PNNL-17154 Table A.5
Cd	6.7	6.7	6.7	Assumes sand fraction values apply
Cm	350	100	1,500	Assumes sand fraction values apply
CN	0	0	0	Assumes sand fraction values apply
Co	0	0	30	PNNL-17154 Table A.5
Cr(VI)	0	0	10	PNNL-17154 Table A.5
Cs	100	30	3,000	PNNL-17154 Table A.5
Eu	30	10	300	PNNL-17154 Table A.5
F	0.05	0	1	PNNL-17154 Table A.5
Fe	25	25	25	Assumes sand fraction values apply
H-3	0	0	0	Assumes sand fraction values apply
Hg	52	52	100	Assumes sand fraction values apply
I	0.2	0	2	PNNL-17154 Table A.5
Mn	65	65	65	Assumes sand fraction values apply
Nb	0	0	0.1	Assumes sand fraction values apply
Ni	10	3	60	PNNL-17154 Table A.5
NO_2	0	0	0.1	PNNL-17154 Table A.5
NO_3	0	0	0.1	PNNL-17154 Table A.5
Np	10	2	50	PNNL-17154 Table A.5
Pa	10	2	50	Assume analogue to Np
Pb	30	10	300	PNNL-17154 Table A.5
Pu	600	200	2,000	PNNL-17154 Table A.5
Ra	10	5	60	PNNL-17154 Table A.5
Rn	0	0	0	Assumes sand fraction values apply
Se	0.3	0	10	PNNL-17154 Table A.5
Sm	10	3	100	Assumes sand fraction values apply

Table 3-7. K_d Value Estimates (mL/g) for Silt in the Waste Management Area A-AX Performance Assessment Models. (2 sheets)

Contaminant	Most Likely	Minimum	Maximum	Basis
Sn	1.5	0	60	PNNL-17154 Table A.5
Sr	10	5	60	PNNL-17154 Table A.5
Tri-butyl Phosphate	1.89	1.89	1.89	Assumes sand fraction values apply
Tc	0	0	0.1	Assumes sand fraction values apply
Th	300	40	500	Assumes sand fraction values apply
U	0.6	0.2	2	Assumes sand fraction values apply
Zr	300	40	500	Assumes sand fraction values apply

Reference: PNNL-17154, *Geochemical Characterization Data Package for the Vadose Zone in the Single-Shell Tank Waste Management Areas at the Hanford Site.*

3.1.6.2 Distribution Coefficient (K_d) Gravel Correction. Gravel corrections may either be empirical or use simplifying assumptions. Empirical estimates of gravel correction are available for only a few radiological and non-radiological contaminants; therefore, it is generally assumed that gravel and larger sediments have no capacity for sorption, leading to Equation 3-7 (Equation 2.4 in PNNL-17154):

$$K_d(gc) = (1 - f) \times K_d(< 2mm) \tag{3-7}$$

where K_d(gc) is the gravel-corrected K_d, f is the fraction of gravel by weight, and K_d(<2 mm) is the K_d measured for the fine fraction. A K_d value for the coarser fraction of sediments, K_d(>2 mm), was measured for strontium in a ratio of 0.23 to K_d(<2 mm), and an even higher ratio was measured for cesium (PNNL-13037 Appendix A). For "high K_d contaminants" (strontium, cesium, and plutonium are given as specific examples in PNNL-17154), PNNL-17154 recommends the use of Equation 3-8 (Equation 2.3 in PNNL-17154) for gravel corrections:

$$K_d(gc) = (1 - 0.77f) \times K_d(< 2mm) \tag{3-8}$$

Table 3-6 and Table 3-7 present estimates of the K_d values prior to gravel correction for radionuclides and non-radiological contaminants in the sand- and silt-dominated HSUs, respectively, with an accompanying basis for the estimates. K_d values for each sand- or gravel-dominated HSU may be obtained from the sand K_d values by correcting for gravel content. Gravel-corrected K_d values for contaminants with relatively high mobility are presented in Table 3-8 for the set of gravel contents estimated for the various HSUs of ACM 1.

3.1.6.3 Summary of Distribution Coefficients (K_d) Estimate Basis. In general, the selected vadose zone K_d values for the WMA A-AX PA in this MPR are consistent with past Hanford Site PAs. Site-specific research into contaminant mobility at Hanford has tended to emphasize the key tank waste radiological and non-radiological constituents expected to impact

groundwater. For other constituents, it is necessary to survey other sources of information and parameter values such as research from other sites or Ecology's Cleanup Levels and Risk Calculation (CLARC) tables [CLARC 2015, Cleanup Levels and Risk Calculations (CLARC), Queried 02/28/2017, [CLARC Data Tables – July 2015], https://fortress.wa.gov/ecy/clarc/CLARCDataTables.aspx].

Table 3-8. Gravel-Corrected K_d (mL/g) Values for Mobile Contaminants Included in the Waste Management Area A-AX Residual Inventory Estimates.

Contaminant	Gravel Content				
	CCUz, Ringold mud 0%	Eolian Sand, H1, H2 5%	AX Tank Farm Backfill 7%	A Tank Farm Backfill 58%	H3, CCUg, Ringold E, Ringold A 66%
Carbon-14	1	0.950	0.930	0.420	0.340
Iodine-129	0.2	0.190	0.186	0.0840	0.0680
Selenium/Selenium-79	0.1	0.0950	0.0930	0.0420	0.0340
Tin/Tin-126	0.5	0.475	0.465	0.210	0.170
Tri-butyl Phosphate	1.89	1.80	1.76	0.794	0.643
Total Uranium/Uranium-238	0.6	0.570	0.558	0.252	0.204
Cyanide; Cobalt/Cobalt-60; Chromium, Hexavalent [Cr(VI)]; Fluoride; Tritium (H-3); Niobium-93m; Nitrite (NO_2); Nitrate (NO_3); Radon-222; Technetium-99	0	0	0	0	0

CCUg = Cold Creek Unit gravel
CCUz = Cold Creek Unit silt
H1 = Hanford formation unit 1
H2 = Hanford formation unit 2
H3 = Hanford formation unit 3
Ringold A = Ringold Formation Wooded Island Unit A
Ringold E = Ringold Formation Wooded Island Unit E
Ringold mud = Ringold Formation Wooded Island Lower Mud Unit

RPP-RPT-46088, *Flow and Transport in the Natural System at Waste Management Area C* includes a collection of proposed K_d values applicable to the WMA C PA, and final determinations are documented in RPP-ENV-58782. The representative and bounding K_d values recommended in PNNL-17154 for sand with intermediate impact at WMA A-AX are mostly the same as the values used in the WMA C PA (RPP-ENV-58782). Two notable exceptions are values for ^{99}Tc and uranium. The WMA C PA adopted slightly lower K_d values for sand than those recommended by PNNL-17154 for the most likely and maximum estimates of uranium K_d in sand and silt, and for the maximum estimate of ^{99}Tc K_d in silt. The WMA C PA adopted the lower K_d estimates in response to regulator concerns regarding uncertainty (RPP-RPT-46088). The WMA A-AX PA intends to adopt these same lower K_d estimates for ^{99}Tc and uranium. The references used in the WMA C PA also provide an appropriate basis for contaminant K_d values for sand-size sediments that lack recommended values developed specifically for WMA A-AX.

WCH-520 Table 3-37 contains K_d values for radionuclides in the CCUz that were used in the Environmental Restoration Disposal Facility (ERDF) PA, nearly all of which match the

recommended values for WMA A-AX in PNNL-17154 for silt with no bulk chemistry impacts. ERDF differs from WMA A-AX in that ERDF is a newer facility without any prior history of impacts in its vicinity, and the assumption of no bulk chemistry impacts in the vadose zone appears to be applicable there. The WMA A-AX PA includes evaluations of vadose zone material known to have been impacted by waste leaked from tanks and ancillary equipment, but the extent of that impact is not known. For this reason, the assumption of intermediate impact throughout the vadose zone, including the silt near the water table, is reasonable for the WMA A-AX PA analysis. Although radionuclide K_d values in the WMA A-AX and ERDF PAs may differ because of the assumed degree of chemical impact in the CCUz, the methodology the two PAs followed to determine the CCUz K_d values is not inconsistent.

The radionuclides listed in Table 3-8 are limited to those with K_d values less than or equal to 2 mL/g (prior to any adjustments because of gravel content) because the results of the WMA C PA screening analysis indicated that radionuclides with K_d values greater than 2 mL/g did not impact groundwater within the 10,000-year sensitivity-uncertainty timeframe (e.g., RPP-ENV-58782). In the event that results of the WMA A-AX screening analysis that is expected to be included as part of the system model development (RPP-RPT-60885) indicate that the K_d thresholds are different than those determined for WMA C, then the list of constituents considered relatively mobile could be shorter or longer than that shown in Table 3-8.

3.1.7 Groundwater Domain

The integrated, saturated-unsaturated, 3-D WMA A-AX model calculates groundwater contaminant concentrations at selected distances, including approximately 100 m downgradient from the WMA A-AX fence line, estimated to occur several hundred to several thousand years into the future. The unconfined aquifer flow and transport parameters play a critical role in WMA A-AX PA modeling because of the dilution and dispersion that occur as recharge containing contaminants enters the aquifer. Additional dispersion and dilution of concentration in groundwater occurs as the contaminants travel through the aquifer. The dilution and dispersion are strongly dependent on the groundwater flux, which is a rate measure defined as the flow volumetric rate through a defined surface area. Historically, groundwater flux beneath WMA A-AX has been difficult to measure because the hydraulic gradient is very small and the hydraulic conductivity is very large in this region of the Hanford Site (SGW-54165, *Evaluation of the Unconfined Aquifer Hydraulic Gradient Beneath the 200 East Area, Hanford Site*).

The groundwater in the aquifer system near WMA A-AX has been studied extensively as part of the site characterization as discussed in Appendix C. The HSUs comprising the saturated zone are illustrated in Section C.4. The groundwater conceptual model for WMA A-AX includes the unconfined aquifer system units that exist primarily within a channel eroded by the cataclysmic floods of the Pleistocene age, and the older/underlying Ringold Unit A. The aquifer also includes some small areas of Ringold Unit E and the Ringold lower mud units. The base of the aquifer is the underlying basalt surface. The undifferentiated lower sands and gravels associated with the Hanford formation, Cold Creek unit, and the Ringold Formation (Unit A) comprise most of the aquifer sediments in the channel. The Ringold Unit A also occurs outside of the flood channel.

For the WMA A-AX PA modeling, the unconfined aquifer consists of multiple HSUs that have varying hydraulic properties, which require individual parameterization for the appropriate scale. Effective parameterization for saturated hydraulic conductivity for the multiple HSUs within the aquifer has been achieved via a field-scale calibrated regional groundwater model which accounts for appropriate local-scale boundary conditions, flow configuration, and history matching of well head data (Appendix C). The CPGWM (CP-47631) provides a set of calibrated hydraulic conductivity estimates for the model layers and HSUs present within the aquifer near WMA A-AX. The CPGWM provides effective parameterization for WMA A-AX saturated hydraulic conductivity applicable to the overall dimensions of the WMA A-AX PA model domain.

When an HSU includes portions above and below the water table, those portions are designated as separate zones with parameters specified independently (see Table 3-9 for aquifer parameters and Table 3-2 and Table 3-3 for vadose zone parameters). Certain hydraulic parameters differ between portions of the same HSU above and below the water table, because different methods from those described for unsaturated zone parameters in Section 3.1.4 are used to determine the hydraulic parameters for the saturated portion of these HSUs. Parameterization of the unsaturated portion of the HSUs involves the evaluation of constitutive model parameters using laboratory measurements of hydraulic properties at the core scale (~order of 0.01 to 0.1 m, often in a vertical test configuration) under unsaturated conditions, and upscaling the parameters to make them applicable to macroscopic vadose zone flow and transport at the field scale (~order of 0.1 to 10 m horizontally and 0.1 to 100 m vertically). Hydraulic parameters applicable to the saturated portion of the HSUs are derived from the calibration of the CPGWM to saturated zone flow and transport observed at site scales to regional scales across the Central Plateau (~order of 100 to 10,000 m horizontally and 1 to 100 m vertically). The different scales, methods, and moisture conditions of parameterization produce different values for saturated hydraulic conductivity, dispersivity, and porosity that account for the characteristics of the unsaturated hydraulic conductivity constitutive models near the dry end of the moisture regime and the characteristics of saturated flow that occur in the aquifer. Similar differences are reported in other research; for example, PNNL-14284, *Laboratory Measurements of the Unsaturated Hydraulic Properties at the Vadose Zone Transport Field Study Site* and "Improved Prediction of Unsaturated Hydraulic Conductivity with the Mualem-van Genuchten Model" (Schaap and Leij 2000) indicate that saturated hydraulic conductivity determined as one of multiple fitting parameters in constitutive models is often much smaller than measured saturated hydraulic conductivity.

The two major aquifer HSUs identified in the Geologic Framework Model (RPP-RPT-60171) are the Plio-Pleistocene CCUg and the Mio-Pliocene Rwia gravel. Other saturated HSUs include small regions of Rwie gravel and Rlm in the southeastern portion of the WMA A-AX PA model domain. Table C-2 indicates the hydraulic conductivity and specific yield values for these HSUs as determined by the CPGWM Version 8.4.5 calibration. The use of these values in the WMA A-AX PA STOMP model (with specific yield used as a proxy for porosity) and their representativeness of the WMA A-AX sediments is discussed in Appendix C. The WMA A-AX PA model uses the CPGWM estimates of 0.076 and 0.1 (CP-47631) for the assumed anisotropy ratio, defined as the ratio of vertical to horizontal hydraulic conductivity, of the Cold Creek channel gravel and Ringold HSU, respectively.

Table 3-9. Waste Management Area A-AX Performance Assessment Unconfined Aquifer Flow and Transport Properties.

Property		Waste Management Area A-AX
Water table elevation (m NAVD88)[a,b,c]		119.5
Hydraulic gradient (m/m)[c]	Assumed steady-state average	-5.0×10^{-6}
	Upgradient, inflow boundary	-7.64×10^{-6}
Longitudinal macrodispersivity (m)[d]		10.5
Transverse macrodispersivity (m)[d]		1.05
Pore compressibility (1/Pa)[e]		1.0×10^{-7}

Aquifer Unit	Horizontal Saturated Hydraulic Conductivity (m/day)	Vertical Saturated Hydraulic Conductivity (m/day)	Effective Porosity (dimensionless)
Cold Creek gravel[f]	18,200	1,381	0.25
Ringold E[f]	35.6	3.56	0.08
Ringold mud[f]	0.008	0.0008	0.08
Ringold A[f]	1	0.1	0.08

[a] NAVD88 = North American Vertical Datum of 1988, National Geodetic Survey, U.S. Department of Commerce.
[b] Water table elevation derived from Central Plateau Groundwater Model-based estimate of post-closure steady-state conditions; see Figure 3-6.
[c] Water table elevation and assumed steady state average: Section C.3; Upgradient, inflow boundary: Section C.7.
[d] Section C.8.
[e] Groundwater, Table 2.5 (Freeze and Cherry 1979).
[f] Section C.5.

In the future, the groundwater gradient is expected to be generally from northwest to southeast. The water table in the unconfined aquifer is expected to continue its declining trend because the large discharges of operational liquid to the ground at the 216-B-3 Pond system and other large discharge sites in 200 East Area have ceased. After all Hanford Site discharges cease, hydraulic heads at WMA A-AX are expected to slowly continue declining (Figure 3-6, adapted from CP-47631, Rev. 4) until they stabilize around year 2100 around 119.9 m. This value is approximated as 119.5 m in the WMA A-AX PA model to be consistent with the WMA C PA model that used a previous estimate of the steady-state water table from the CPGWM (CP-47631, *Model Package Report: Central Plateau Groundwater Model Version 6.3.3*, Rev. 2), and is within the range of uncertainty associated with the long-term estimate (see Appendix C for further discussion). Small changes in hydraulic gradient are expected to occur only within the first 10 to 50 years of the post-closure simulation period, which, according to the WMA C evaluation (RPP-ENV-58782), is before the mobile radionuclides reach the water table. Thus, the hydraulic gradient is assumed to remain unchanged during the period of this analysis.

The longitudinal and transverse macrodispersivity estimates in the saturated zone are based on: 1) a review of three widely-cited general relationships ("Universal Scaling of Hydraulic Conductivities and Dispersivities in Geologic Media" [Neuman 1990]; "Longitudinal Dispersivity Data and Implications for Scaling Behavior" [Schulze-Makuch 2005]; and "Use of Weighted Least-Squares Method in Evaluation of the Relationship between Dispersivity and Field Scale" [Xu and Eckstein 1995]) that quantify the dependence of this parameter on measurement scale (L_s), and 2) the range of empirical data from other sites (Gelhar et al. 1992). For L_s near 100 m, which is the approximate distance of travel to the points of calculation where contaminant concentrations are evaluated in the saturated zone, most of the observed values and all the calculated values fall within the range of 1 to 20 m (see Section C.8). Thus, a value of 10.5 m is chosen for longitudinal macrodispersivity in the base calculation, consistent with the basis and selected value in WMA C PA (RPP-ENV-58782). This value is much larger than the longitudinal dispersivity of the same HSUs in the vadose zone because of the distinctly different saturation conditions. The ratio of longitudinal to transverse macrodispersivity is chosen to be 10 based on recommendations in RPP-20621 and PNNL-23711. The pore compressibility is assumed to equal the default value in STOMP for the bulk compressibility (1.0×10^{-7} 1/Pa, PNNL-12030), which is consistent with the range of compressibility values indicated for sand and gravel aquifers in Table 2.5 in Groundwater (Freeze and Cherry 1979).

3.1.8 Points of Calculation, Protectiveness Metric, and Timeframe Considerations

In accordance with risk and performance assessment guidelines, the determination of impacts to groundwater also requires the definition and rationale for (1) points of calculation, i.e., the place and points in the groundwater domain where modeled groundwater concentrations are to be assessed for potential impacts and protectiveness; (2) the protectiveness metric, i.e., the groundwater metric(s) to be used in the assessment of protectiveness at the points of calculation; and (3) the timeframe considered applicable for the calculation of impacts to groundwater. The points of calculation are intended to effectively serve as the point where exposure point groundwater concentrations are evaluated in the model to evaluate the achievement of the groundwater protection performance measures. The point of calculation for the protection of groundwater is related to "Point of Compliance" (i.e., location where impacts are evaluated and compared to performance objectives and measures) in DOE PA requirements (DOE M 435.1-1, Chapter IV Section P) and described as follows:

> "The point of compliance shall correspond to the point of highest projected dose or concentration beyond a 100 meter buffer zone surrounding the disposed waste. A larger or smaller buffer zone may be used if adequate justification is provided."

Thus, the points of calculation for the groundwater impact analysis are selected to be ~100 m downgradient from the WMA A-AX fence line. While the DOE Manual and Guide state that point of compliance is the point of highest calculated dose (groundwater concentration), neither indicates how that groundwater concentration should be calculated, i.e., within what volume is the concentration calculated, apart from indicating that the aquifer mixing must be consistent with State or local laws, regulations, or agreements.

Figure 3-6. Central Plateau Groundwater Model Calibration Results near Waste Management Area A-AX.

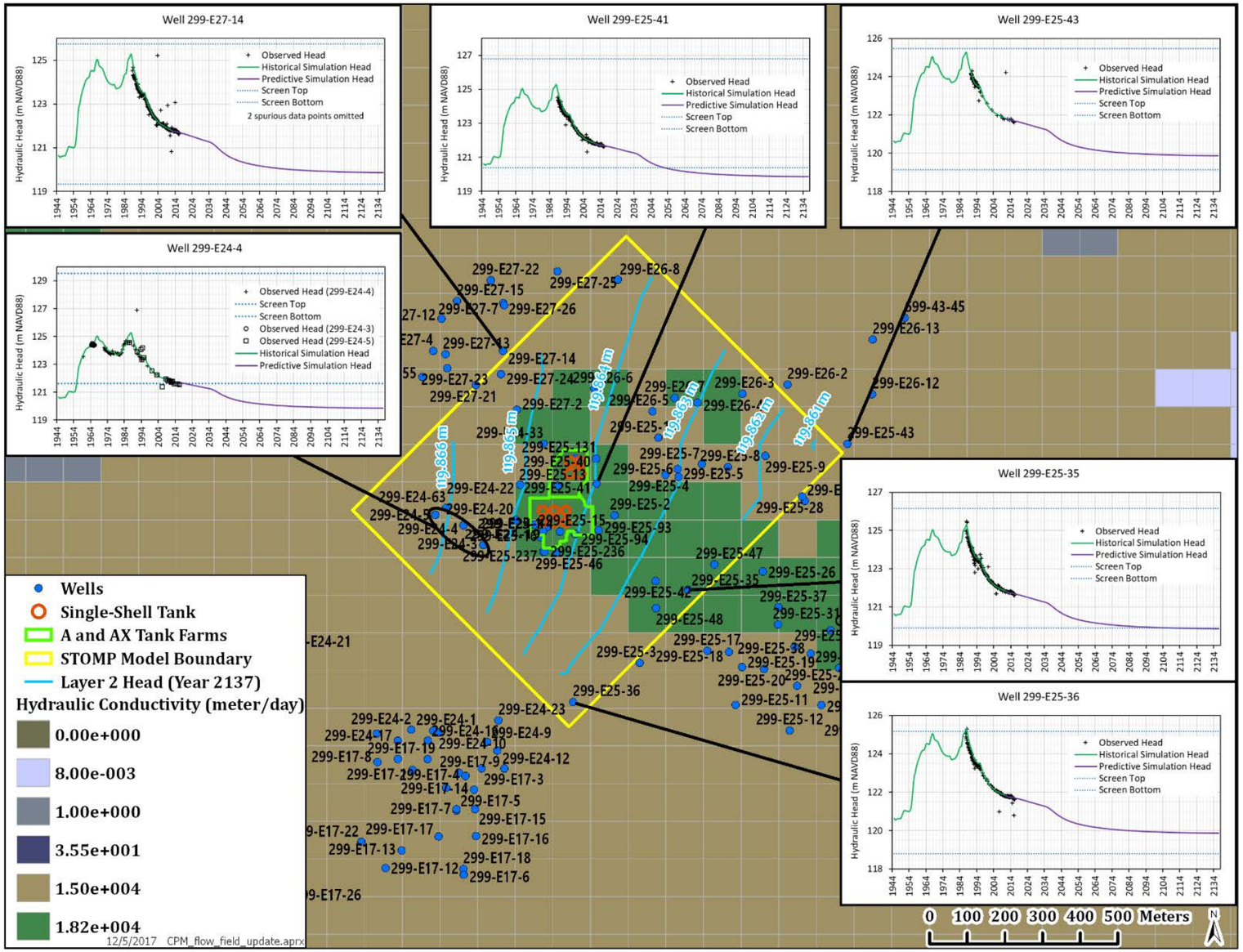

Sources:
CP-47631, *Model Package Report: Central Plateau Groundwater Model Version 8.4.5*, Rev. 4.
ECF-200W-17-0043, *Capture-Zone and Particle-Tracking Analysis for the 200-UP-1/200-ZP-1 Areas using the 2017 Updated Central Plateau Model.*
Environmental Dashboard Application, Queried 07/17/2017, [redacted].
HGIS Hanford Geographic Information System, Queried 06/26/2017, [HMAPS Interactive Maps], [redacted]
Subsurface Transport Over Multiple Phases (STOMP) is developed and distributed by Battelle Memorial Institute.

The approach identified in USEPA Soil Screening Level (SSL) document (EPA/540/R-95/128, *Soil Screening Guidance: Technical Background Document*) and WAC 173-340-747, "Deriving Soil Concentrations for Groundwater Protection" indicates that the cross-section of the aquifer volume is usually prescribed to be a unit width of 1 m (3.28 ft) because the equations are developed on unit width. This implies that the cross-section width is equal to the width of contamination entering the aquifer. Consistent with this reasoning, other performance assessments conducted at Hanford and other DOE facilities have used an aquifer mixing width equal to the width of the facility (e.g., WCH-520; WSRC-MS-2003-00582, *Performance Assessment/Composite Analysis Modeling to Support a Holistic Strategy for the Closure of F Area, a Large Nuclear Complex at the Savannah River Site*). The WMA C PA evaluates the concentration in groundwater within segments that are approximately 30 m in width (Table D-11 in RPP-ENV-58782). The 100-series C Farm tanks are approximately 23 m (75 ft) in diameter and the rows of four 100-series tanks are spaced approximately 8 m (25 ft) apart. Similarly, at WMA A-AX, the tanks are approximately 23 m (75 ft) in diameter and spaced approximately 8 m (25 ft) apart.

To calculate the highest groundwater concentration, the WMA A-AX model evaluates the average concentration in the aquifer within a series of nine hypothetical planes or segments oriented along lines parallel to the WMA A-AX fence line (Figure 3-7). Concentrations calculated in the nine segments of the aquifer are assumed to be comparable to concentrations that would be measured by sampling a monitoring well at those locations. STOMP input includes the ability to specify flux planes and have the output provide the rate and integrated total of mass, either contaminant or water, through the specified plane. The calculation planes or segments are ~30 m (98 ft) wide (Table 3-10) normal to the WMA A-AX fence line. The concentration represents both a spatial and temporal average, the mass of contaminant divided by the mass of water through each plane for each time step. The model results provided represent concentrations in the upper 5 m (16.4 ft) of the aquifer, which corresponds to an assumed well screen length of a hypothetical groundwater monitoring well, as discussed later in this section.

The point of calculation lines are aligned such that the centerline(s) of the plumes in the groundwater resulting from all of the sources intersect the lines toward their center. The flux planes in the WMA A-AX model alternate in orientation in the x- and y-directions. The segments zigzag northward from the south because the orientation of the model grid, rotated 45 degrees from the azimuth, is intended to parallel the direction of incoming flow, but the flow direction in the aquifer includes some curvature in the vicinity of WMA A-AX (Section C.6). Figure 3-8 provides an illustration of the geometry of the HSUs along transect A-A', as diagramed in Figure 3-7, and the orientation of the point of calculation segments along the line 100 m from WMA A-AX. Each segment consists of two subsegments (Table 3-10). Table 3-10 includes the segments located at the WMA A-AX fence line, which are offset from the segments in point of calculation lines located farther from WMA A-AX because the groundwater flow direction and plume centerlines change as the flow moves downgradient of WMA A-AX.

Figure 3-7. Points of Calculation at the Fence Line and 100 meters from Waste Management Area A-AX.

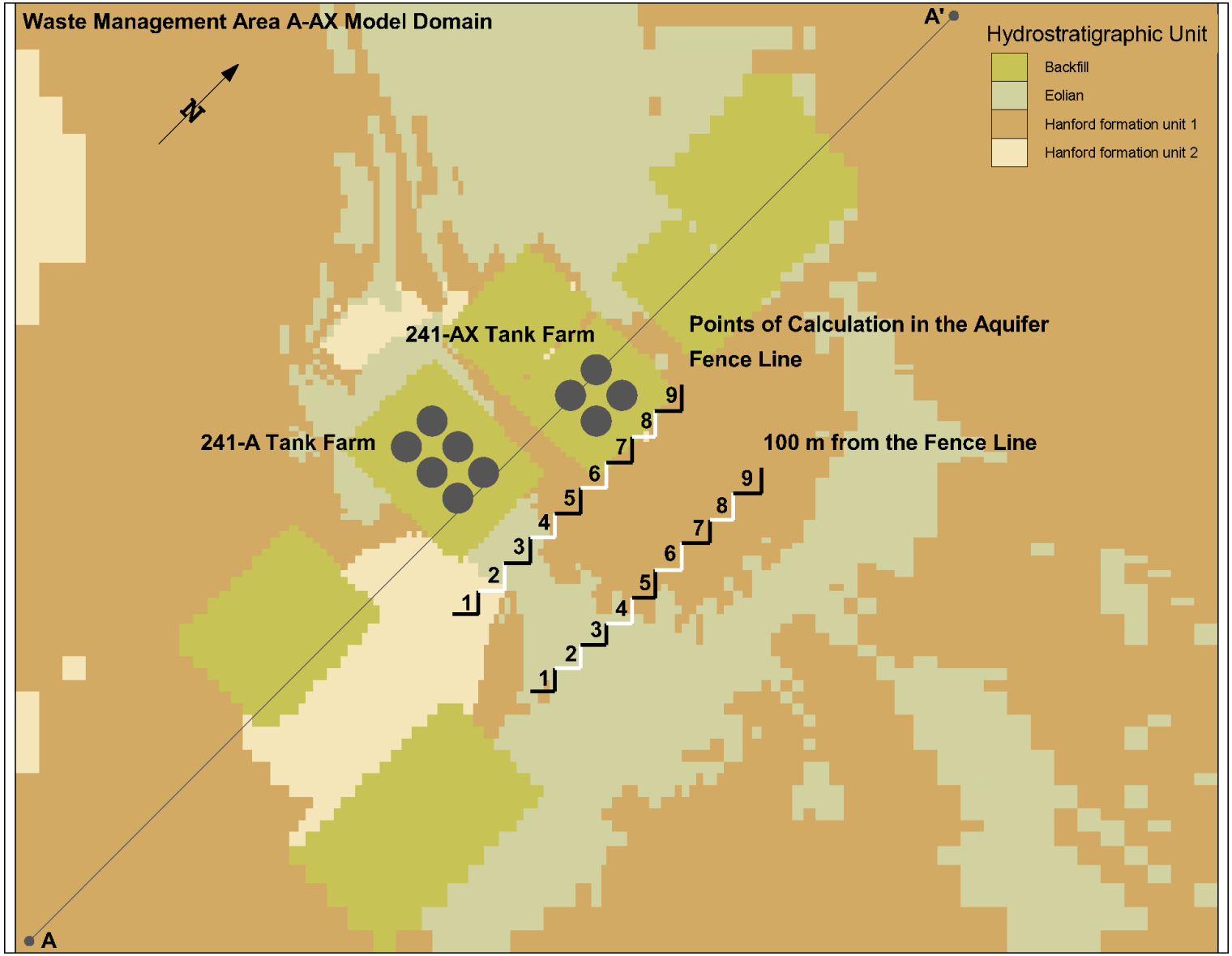

Table 3-10. Dimension of Widths for Point of Calculation Segments at the Fence Line and 100 meters from Waste Management Area A-AX. (2 sheets)

Point of Calculation Segment	Cell Face Direction	Beginning I Index	Ending I Index	Beginning J Index	Ending J Index	Subsegment Width (m) At WMA A-AX Fence Line	Segment Normal Width (m) At WMA A-AX Fence Line
1	east	75	75	46	50	21.982	29.7
	north	73	75	50	50	20	
2	east	72	72	51	55	22.227	32.7
	north	69	72	55	55	24	
3	east	68	68	56	59	22.297	31.3
	north	65	68	59	59	22	
4	east	64	64	60	63	20.85	28.9
	north	61	64	63	63	20	
5	east	60	60	64	68	21.982	31.1
	north	56	60	68	68	21.982	
6	east	55	55	69	73	21.982	31.1
	north	51	55	73	73	21.982	
7	north	50	50	74	78	21.982	31.1
	east	46	50	78	78	21.982	
8	north	45	45	79	82	19.562	29.4
	east	41	45	82	82	21.982	
9	north	40	40	83	86	23	31.8
	east	36	40	86	86	21.982	
Point of Calculation Segment	Cell Face Direction	Beginning I Index	Ending I Index	Beginning J Index	Ending J Index	Subsegment Width (m) 100 m from WMA A-AX	Segment Normal Width (m) 100 m from WMA A-AX
1	east	82	82	60	63	20.85	28.9
	north	81	82	63	63	20	
2	east	80	80	64	68	21.982	29.7
	north	79	80	68	68	20	
3	east	78	78	69	73	21.982	28.4
	north	77	78	73	73	18	
4	east	76	76	74	78	21.982	31.1
	north	74	76	78	78	22	

Table 3-10. Dimension of Widths for Point of Calculation Segments at the Fence Line and 100 meters from Waste Management Area A-AX. (2 sheets)

Point of Calculation Segment (continued)	Cell Face Direction	Beginning I Index	Ending I Index	Beginning J Index	Ending J Index	Subsegment Width (m) 100 m from WMA A-AX	Segment Normal Width (m) 100 m from WMA A-AX
5	east	73	73	79	82	19.562	31
	north	70	73	82	82	24	
6	east	69	69	83	86	23	32.5
	north	66	69	86	86	23	
7	north	65	65	87	90	24	31.2
	east	62	65	90	90	20	
8	north	61	61	91	93	20	30.2
	east	57	61	93	93	22.627	
9	north	56	56	94	96	24	32.5
	east	52	56	96	96	21.982	

WMA = Waste Management Area

For the purpose of the evaluations, the aquifer mixing zone is assumed to extend into the upper 5 m of the aquifer (Figure 3-8). DOE M 435.1-1 does not specify the level of protection required for water resources and there are no applicable parameterization requirements or guidelines indicated in DOE G 435.1-1, Chapter IV. Equation 747-4 in WAC 173-340-747 specifies a 5-m mixing zone in groundwater, which would be consistent with a 5-m vertical interval corresponding to a theoretical groundwater monitoring well with a 5-m (i.e., 15-ft) well screen length. *Ground Water Monitoring Guidance for Solid Waste Facilities* (Ecology 1990) indicates that monitoring well screens are typically 10 ft in length, but may be shorter or longer depending on site-specific conditions. SESDGUID-101-R1, *Design and Installation of Monitoring Wells* indicates only that the length of a well screen in permanent monitoring wells should normally not be less than 5 ft (1.5 m) in length.

For a DOE 435.1 PA (see DOE G 435.1-1, Chapter IV Section P), the period of the analysis, identified for which comparison of impacts with performance objectives and measures are made (i.e., the compliance timeframe), is defined as 1,000 years following closure of the facility. A second period of analysis, identified as the sensitivity-uncertainty analysis period in the U.S. Nuclear Regulatory Commission (NRC) draft guidance (NUREG-1854, *NRC Staff Guidance for Activities Related to U.S. Department of Energy Waste Determinations – Draft Final Report for Interim Use*), extends the evaluation from 1,000 years to 10,000 years. This period is deemed sufficient for evaluation of the peak impacts from all the radiological constituents that the screening analysis indicates may not impact groundwater within the first 1,000-year post-closure period. DOE G 435.1-1, Chapter IV Section P states that the sensitivity-uncertainty analysis timeframe should include calculation of the maximum impacts

(i.e., dose) regardless of the time at which the maximum occurs, as a means of increasing confidence in the outcome of the modeling and increasing the understanding of the models used. However, EPA-SAB-RAC-ADV-99-006, *An SAB Advisory: Modeling of Radionuclide Releases from Disposal of Low Activity Mixed Waste* warns that extending the modeling timeframe beyond 10,000 years could make the results irrelevant and hinder public acceptance of the results because of the inherent scientific and social uncertainties associated with such an extended timeframe. The 10,000-year timeframe is sufficient to address uncertainty associated with radionuclides that impact groundwater during the compliance period (NUREG-1573, *A Performance Assessment Methodology for Low-Level Radioactive Waste Disposal Facilities: Recommendations of NRC's Performance Assessment Working Group*).

DOE G 435.1-1, Chapter IV states that DOE low-level waste disposal facilities must comply with legally-applicable requirements for water resource protection. The protectiveness metrics determined to be most appropriate for the evaluation of impacts to groundwater during the compliance period from the radionuclide and contaminant inventory in WMA A-AX are the MCLs. MCLs represent the "allowable concentrations" and/or "acceptable limits" of a radionuclide for limiting further degradation of groundwater in accordance with the conditions identified in State and Federal anti-degradation goals [e.g., EPA/540/R-92/003, *Guidance for Data Useability in Risk Assessment (Part A) Final*; EPA/530-SW-87-017, *Alternate Concentration Limit Guidance Part I ACL Policy and Information Requirements Interim Final*; DOE/RL-2002-59, *Hanford Site Groundwater Strategy Protection, Monitoring, and Remediation*].

Defining the protection of groundwater in the context of vadose zone fate and transport models requires consideration of the soil and groundwater media as a coupled pathway. This coupled pathway involves the determination of future concentrations in the groundwater medium that result from the transport of the radionuclide and contaminant inventory existing in the WMA A-AX tank residuals through the soil (or vadose zone) medium. The working definition of protectiveness for the protection of groundwater pathway is considered achieved if the radionuclide and contaminant levels in the WMA A-AX tank residuals do not cause groundwater concentrations to exceed MCLs at the points of calculation within 1,000 years after the closure date assumed in the evaluation.

3.2 NATURE AND EXTENT OF CONTAMINATION

The WMA A-AX PA addresses the radionuclide and non-radiological contaminant inventory contained in waste residuals left in tanks and ancillary equipment in WMA A-AX at the assumed time of closure. Tank waste can be grouped into three types based on physical properties: supernate, salt, and sludge (RPP-RPT-58293). WMA A-AX contains primarily salt type waste, because most supernate was pumped out as part of interim stabilization (RPP-RPT-58293). As of the summer of 2018, retrieval has not begun in any tank (HNF-EP-0182, *Waste Tank Summary Report for Month Ending June 30, 2018*, Rev. 366).

Figure 3-8. Geologic Cross-Section A-A' through Waste Management Area A-AX.

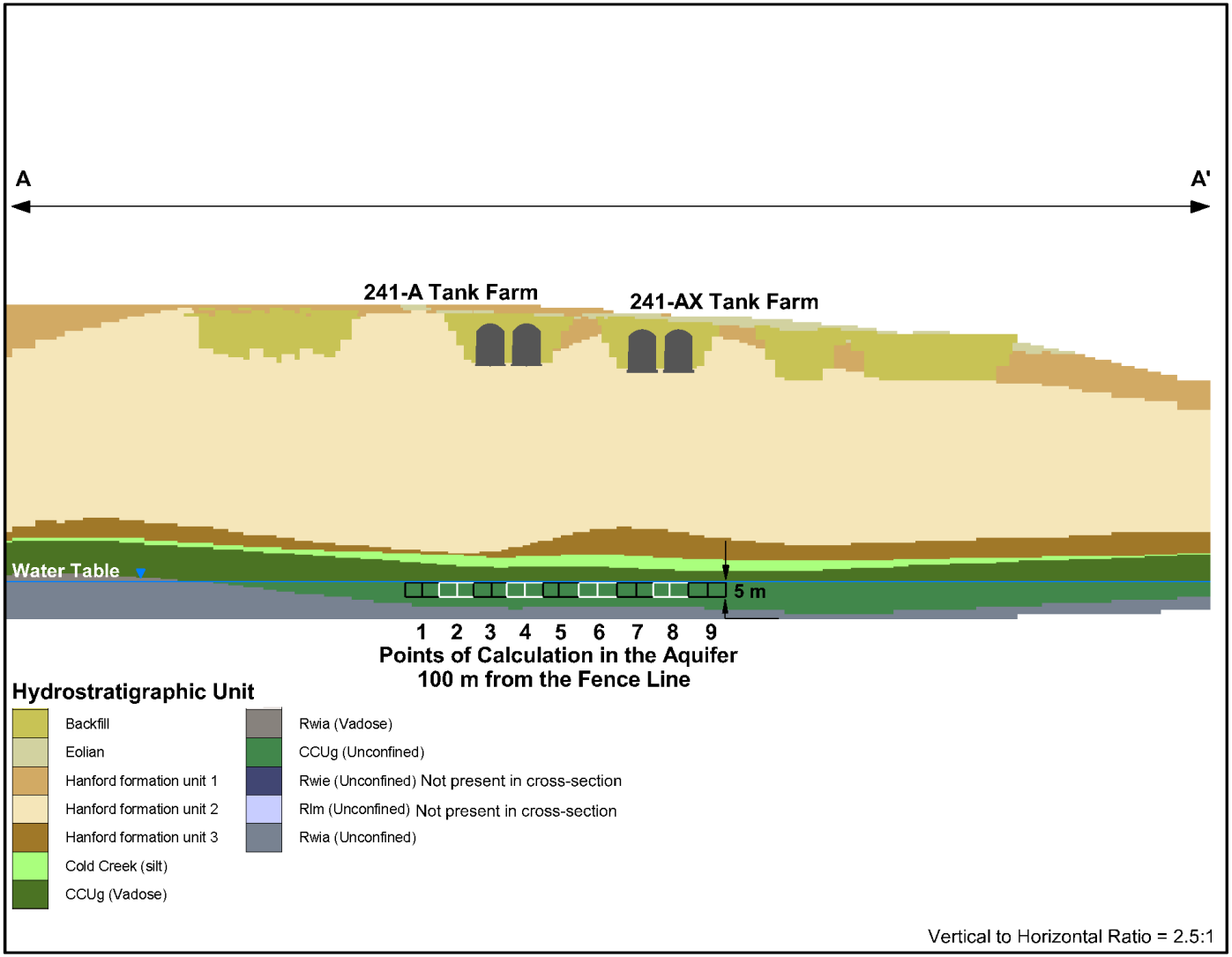

Notes: The location of cross-section A-A' is shown on Figure 3-7.

CCUg = Cold Creek Unit gravel Rlm = Ringold Formation Lower Mud Unit Rwia = Ringold Formation Unit A Rwie = Ringold Formation Unit E

The residual waste volume for tanks not yet retrieved is unknown; therefore, assumptions about the inventory have been made based on current threshold requirements. Constituents' inventory uncertainties may vary by as much as a factor of 10 for certain constituents in tanks not yet retrieved. Specific information about the residual inventory and the release of the radionuclide and non-radiological contaminant inventory from the tanks and ancillary equipment that includes the pipelines is presented in RPP-RPT-58293, RPP-RPT-60885, and RPP-CALC-62319.

4.0 MODEL IMPLEMENTATION

The 3-D construction of the model incorporates spatial distributions of major hydrogeologic units and the spatial and temporal changes in recharge conditions. The model provides the ability to evaluate the effect of assumed parameter and changes, including recharge, on potential lateral spreading and comingling of plumes from the different sources being considered. The gridding scheme and extent of the domain are intended to reduce the numerical error and impact that the boundary conditions have on the model calculations in the areas of interest, i.e., the points of calculation. The discretization scheme allows the distinct representation of the different sources within WMA A-AX such that no sources, except the ancillary equipment area, overlap one another.

This MPR only includes discussion of the results of certain simulations conducted to assist development of the system model (RPP-RPT-60885). The results of the selected simulations provide a check that the model domain is sufficient to prevent the boundary conditions from inappropriately affecting the solution in the area of interest. A comparison of results obtained using different Courant numbers provides a check on numerical dispersion caused by time-step size, and a comparison of results using different dispersivity values provides a check that numerical dispersion is not obscuring the solution. The results of these simulations and evaluations will be presented in a subsequent EMCF.

4.1 DISCRETIZATION

The horizontal node spacing used in the model domain varies between ~4.4 and 20 m to increase the resolution in the areas attempting to approximate the slopes associated with construction of WMA A-AX and the 100-series tanks without exceeding the capacity of the available computational resources. Within the confines of WMA A-AX, the horizontal grid cell dimensions ranged between ~4.4 and ~4.6 m to align the nodes with the tanks, vault, and other ancillary equipment (Figure 4-1). Outside of WMA A-AX, the grid cells expanded in size such that no adjoining grids differed in length by more than a factor of 1.5. Appendix D presents the pattern of the spacing of the finite difference cells. Vertical spacing in the vadose zone ranged between 0.5 and 1.0 m, with the finer resolution occurring around the water table where the more highly-resolved spacing attempts to capture the impacts of the silt layer and the fringe above the water table (Figure 4-2).

The total number of nodes in the modeled rectangular prism equals 1,500,000. During the pre-operational phase, WMA A-AX does not exist and the number of active and inactive nodes are 1,340,923 and 159,077, respectively. The inactive nodes account for the irregular shape of the underlying basalt and the ground surface. During the operational and post-closure phases, WMA A-AX backfill replaces part of the H1 top, and the number of active and inactive nodes are 1,337,683 and 162,317, respectively. The increase in inactive nodes is attributed to the inactivation of the tank and ancillary equipment nodes within the WMA A-AX excavation.

Figure 4-1. Horizontal Alignment of Three-Dimensional Model Computational Nodes with Waste Management Area A-AX Single-Shell Tanks.

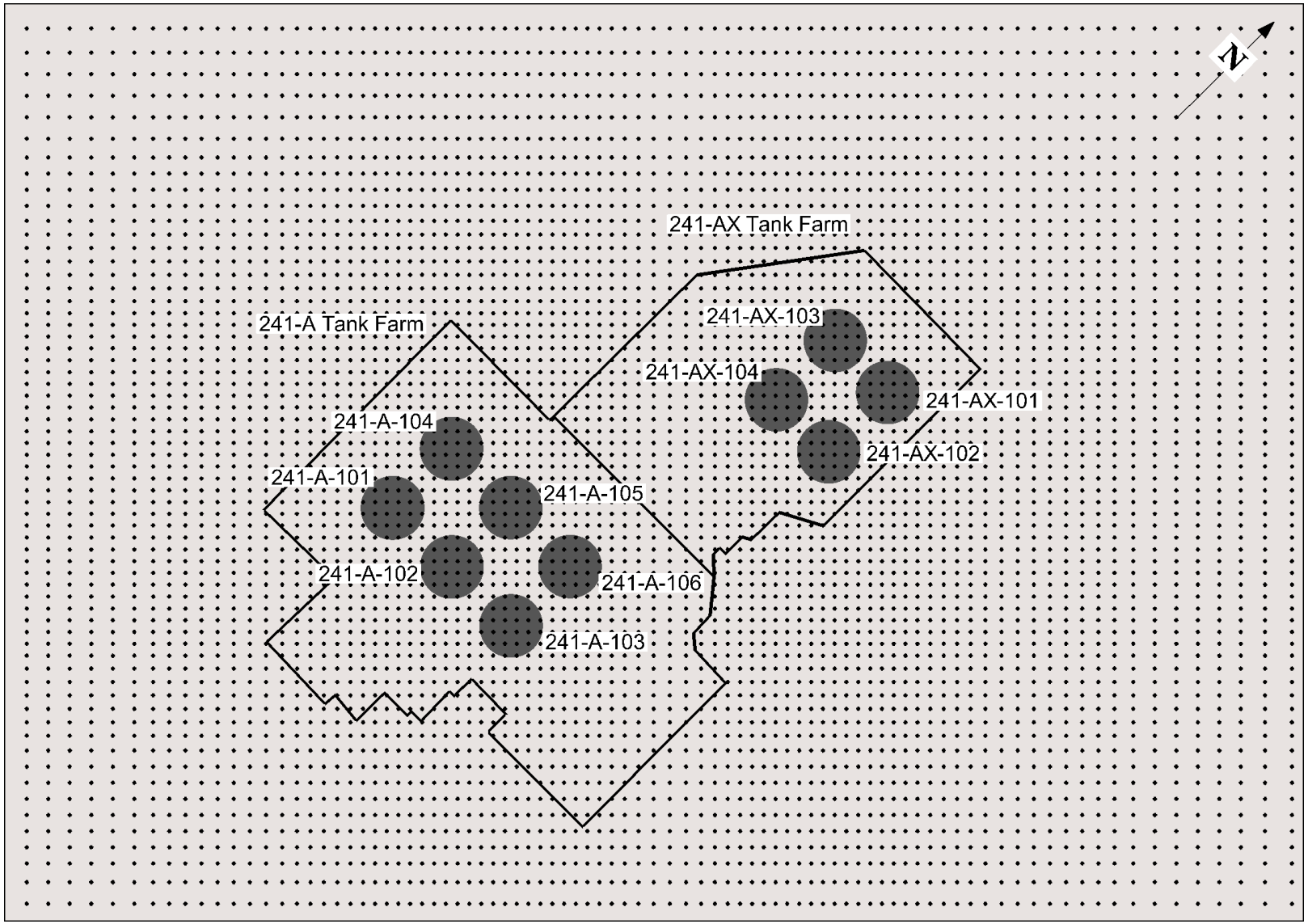

Figure 4-2. Horizontal and Vertical Alignment and Distribution of Waste Management Area A-AX Performance Assessment Alternative Conceptual Model 1 Three-Dimensional Model Computational Nodes.

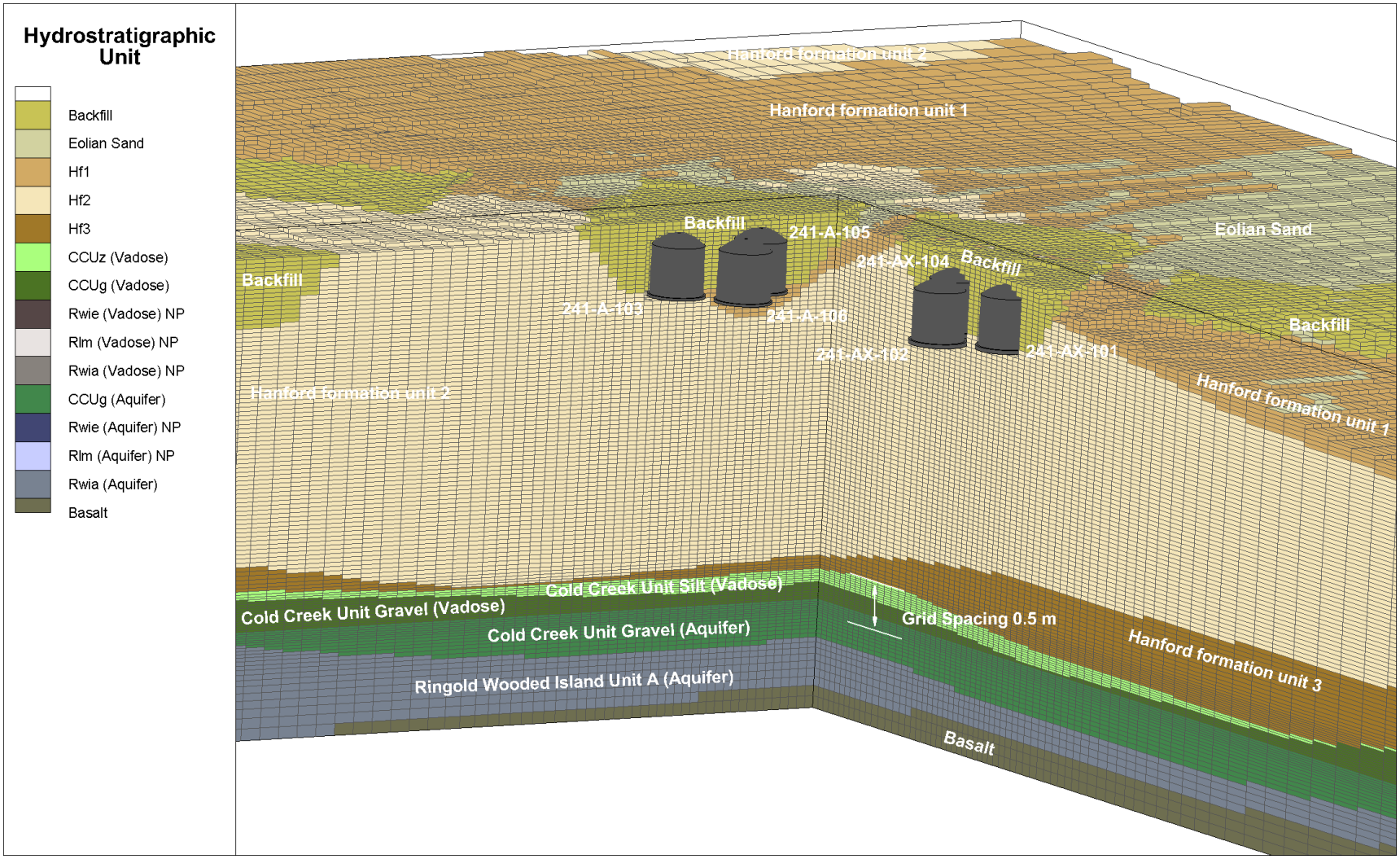

CCUg = Cold Creek Unit gravels
CCUz = Cold Creek Unit silt
Hf1 = Hanford formation unit 1
Hf2 = Hanford formation unit 2
Hf3 = Hanford formation unit 3
NP = Not Present in View
Rlm = Ringold Formation Wooded Island Lower Mud Unit
Rwia = Ringold Formation Wooded Island Unit A
Rwie = Ringold Formation Wooded Island Unit E

The evaluation of the model includes an evaluation of unintended impacts of the boundary conditions in the areas of interest around WMA A-AX. In this evaluation, recharge within WMA A-AX follows the timeline summarized in Table 3-5, but recharge in all areas outside of A Farm and AX Farm was assumed to remain at 3.5 mm/yr indefinitely. This recharge scheme provides contrast between the areas inside and outside of A Farm and AX Farm. According to the assumptions inherent in the boundary conditions, the moisture content at the boundaries should remain unchanged; therefore, the magnitude of any change at the boundaries provides an indication of possible numerical error. Figure 4-3 shows the relative change in moisture content from the pre-Hanford steady-state condition at the four vertical boundaries of the model at three times of interest: at Year 2050 at the end of the WMA A-AX operational period, at Year 2550 at the end of the design life of the WMA A-AX surface barrier, and at Year 3050, which is the end of the 1,000-year post-closure timeframe and when the system has reacquired or nearly reacquired steady-state conditions. In general, the effects are contained within a relatively small segment along the boundaries near the water table and appear to be minor. The changes in moisture content along the vadose zone boundary faces are relatively small in magnitude and occur primarily in areas where the soil type changes from the pre-Hanford unit(s) to the tank farm backfill. The small changes indicate that the boundaries are far enough removed from the tank farm area of interest to avoid unintentional impacts to the model solution. Consequently, the location of the boundaries is not considered to adversely affect the evaluation of radionuclide transport and groundwater impacts associated with the radionuclide and non-radiological contaminant inventory in WMA A-AX.

Solute transport, radioactive decay, and first-order chemical reactions are solved in STOMP using Patankar's power-law formulation (PNNL-12030). The power-law formulation is unconditionally bounded, which means that the solutions are free from oscillations that can cause numerical instability in regions of steep gradients. However, the power-law formulation does tend to misrepresent the diffusion transport process through the addition of numerical or "false" diffusion arising from flow-to-grid skewness, which is the offset of the direction of flow from the coordinate directions ("A higher-order bounded discretization scheme," [Song and Amano 2010]). As the time step of the simulation increases, the flow and skewness increase, and with that increase comes the possible introduction of numerical dispersion and solution inaccuracy. The benefit and sometimes necessity of increasing the time step is that it allows the simulations that are supposed to extend to 10,000 years to complete in a practical amount of time (e.g., less than one week on the existing workstations).

The Courant control feature in STOMP provides a means to limit numerical dispersion by limiting the allowable size of the time step used in the contaminant transport calculations. The Courant number (C_r) represents the ratio of the movement of a contaminant during a single time step and the distance between adjacent grid cells, i.e.,

$$C_r = \frac{v\Delta t}{\Delta x} \tag{4-1}$$

where v is the magnitude of the velocity of the water or contaminant (L/T), Δt is the time step (T), and Δx is the distance between adjacent model nodes (L). The Courant control in STOMP allows the user to impose a limit on the allowable Courant number, which in turn imposes a limit on the time step. The impacts of numerical dispersion introduced into the results because of

increases in the allowed time step size are then evaluated by comparing the results of simulations conducted with different degrees of Courant control. The Courant evaluation that is to be included in a subsequent EMCF intends to evaluate a range of Courant limits to determine the sufficient degree of Courant control that balances solution accuracy with computational practicality.

The Peclet number (Pe) represents the ratio of advective transport to diffusive-dispersive transport. A large Peclet number indicates that contaminant transport is dominated by advection, and a small number indicates that transport is dominated by diffusion. In numerical models, the grid Peclet number (Pe) depends on both the velocity of the fluid and a characteristic length associated with the grid, and can be approximated using the equation ("Review of the use of Péclet numbers to determine the relative importance of advection and diffusion in low permeability environments" [Huysmans and Dassargues 2005]):

$$Pe = \frac{v * \Delta x}{(\alpha_L v + D^*)} \tag{4-2}$$

where v and Δx are defined as before, α_L is the dispersivity (L), and D^* is the coefficient of diffusion (L^2/T). The denominator is known as the hydrodynamic dispersion tensor or coefficient of dispersion (L^2/T) and combines the effects of dispersion and diffusion. The grid Peclet number is cited in literature as a basis for stability criteria or accuracy criteria depending on the solution scheme, often with an upper limit of about 2 (e.g., Computational Techniques for Fluid Dynamics [Fletcher 1991]; PNNL-11216, *STOMP Subsurface Transport Over Multiple Phases: Application Guide*, Section 3.0). Models with high Peclet numbers are prone to numerical dispersion errors because of the large concentration gradients produced by the computation of the advective transport of the contaminant. The numerical dispersion can be limited by decreasing the grid spacing, but at the cost of computational practicality and increased computational times. Other comparably-scaled models indicate that the WMA A-AX PA grid size and spacing is sufficient for the PA analysis. DOE/EIS-0391 Appendix N indicates that the horizontal grid size and spacing of 5 m within WMA A-AX, and vertical spacing of 2 m, are small enough for a 3-D model to provide accurate simulations of flow and transport. The impacts of numerical dispersion associated with the grid Peclet number will be addressed in the subsequent EMCFs that this MPR supports. In general, the impacts of numerical dispersion on the differential equation solutions are not typically large enough to negate the use of the model, but need to be recognized and managed to promote confidence in the overall value and usefulness of the results ("The Secret to Successful Solute-Transport Modeling" [Konikow 2011]).

PETSc is currently the only approved solver option in CH2M HILL Plateau Remediation Company (CHPRC) Build 6 of eSTOMP, and eSTOMP includes the option to specify values other than the defaults for the PETSc convergence tolerances. Depending on input details for a given eSTOMP application, solute mass balance may not be maintained with the default PETSc settings for the convergence tolerance. Therefore, any EMCFs developed for the WMA A-AX PA and involving the PETSc solver must demonstrate that the convergence tolerances yield acceptable accuracy by showing that the results of some sample test cases identified in the EMCF are consistent with results obtained in serial STOMP.

Figure 4-3. Relative Change in Moisture Content (Volume %) from the Pre-Hanford Steady-State Condition at the Four Vertical Boundaries of the Model at Three Times of Interest: Year 2050, Year 2550, and Year 3050.

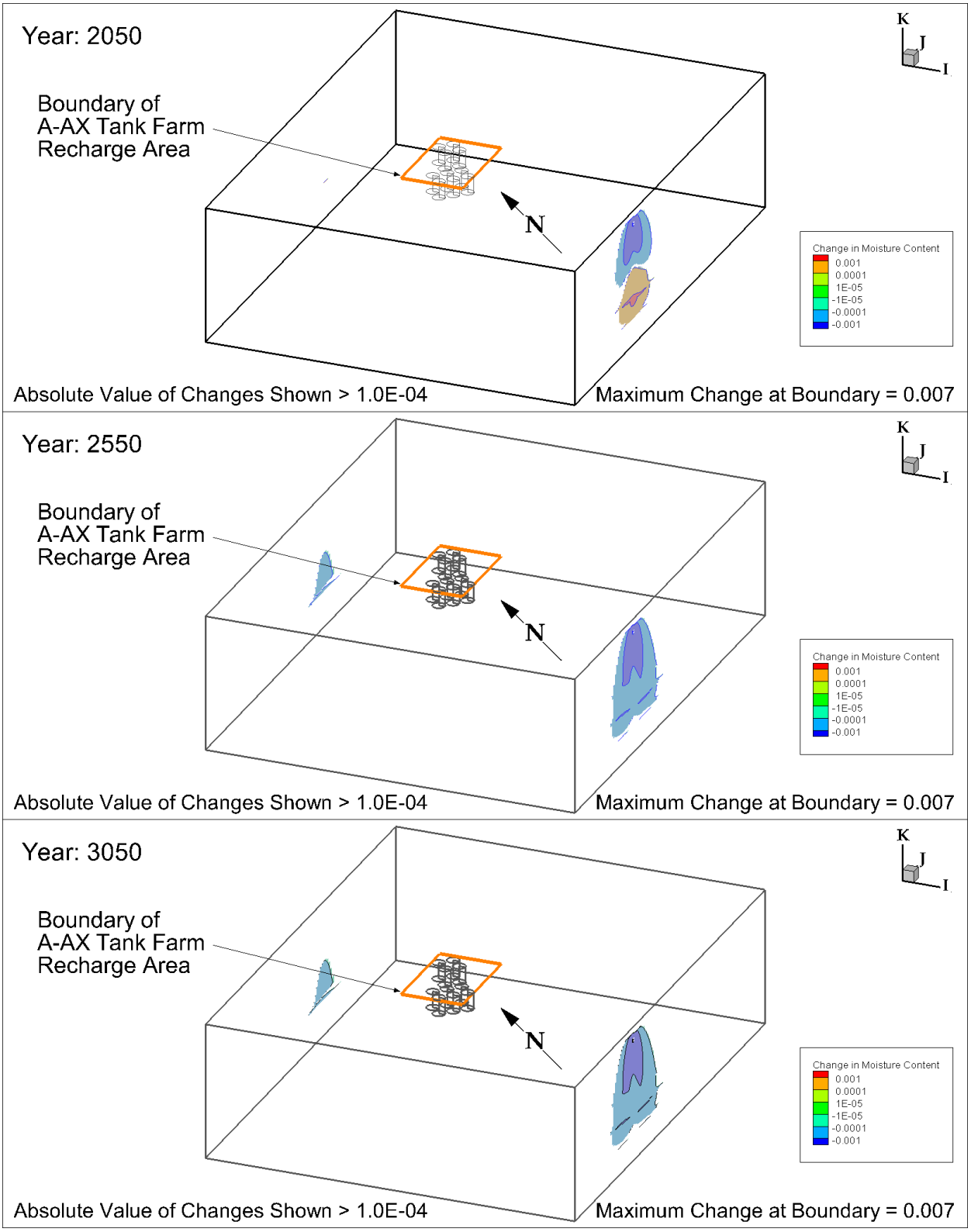

4.2 PARAMETERIZATION

Table 4- presents a summary of the model parameters and values assigned to nodes throughout the domain, including the identification of model boundary and initial conditions, and identifies the section where the data sources and data quality are discussed. Parameters and values that are already tabularized in the subsections of Section 3.1 are simply referenced by the applicable table number.

Table 4-1. Summary of Key Elements and Parameters Associated with Site-Specific Model Components for Waste Management Area A-AX. (2 sheets)

Model Domain and Boundary Conditions	Rectangular Prism: 812.6 m (2,666 ft) × 1,027.5 m (3,371 ft) × 119.5 m (392 ft) (Model Grid) Prescribed flux across the top (Recharge); no-flow along vertical side boundaries in the vadose zone; prescribed flux along the upgradient side and prescribed head along the other three vertical side boundaries in the aquifer; no-flow along the bottom of the model (aquifer).

Geologic Setting	The Waste Management Area (WMA) A-AX cross-section includes the following anthropogenic or natural units that occur from surface to groundwater (RPP-RPT-60171):
	• WMA A-AX Backfill (~16 m)
	• Hanford formation unit 1 (generally identified as gravel or very coarse sand, at WMA A-AX appears to be sand-dominated; ~0-10 m)
	• Hanford formation unit 2 (sand-dominated facies generally identified as fining upward sequences of gravel, sandy/gravel to sand to very fine sand; ~40-50 m)
	• Hanford formation unit 3 (coarse-grained open framework gravel to sandy gravel; ~0-20 m)
	• Cold Creek fine unit;
	  • in alternative conceptual model (ACM) 1, consists of Cold Creek silt (~0-15 m)
	  • in ACM 2, consists of two subunits:
	  ▪ Cold Creek silt (~0-15 m)
	  ▪ Cold Creek sand (~0-15 m)
	• Cold Creek gravel unit
	• Ringold Formation unit A (small regions of other Ringold units occur downgradient from WMA A-AX in the model domain)

Groundwater Domain and Characteristics	WMA A-AX post-closure water table elevation ~119.5 m NAVD88 (Section C.3) and estimate of flow through the domain 1,052 m^3/day (CP-47631, Rev. 4; Section C.6)
	Aquifer Horizontal Hydraulic Conductivity (Section C.5):
	  Cold Creek gravel = 18,200 m/day
	  Ringold E = 35.6 m/day
	  Ringold mud = 0.008 m/day
	  Ringold A = 1 m/day
	Prescribed flux along northwest cross-section boundary (Section C.7):
	  Flux in Cold Creek gravel along northwest cross-section boundary = 0.139 m/day
	  Flux in Ringold A along northwest cross-section boundary = 7.64E-06 m/day
	Prescribed head along southeast cross-section boundary = 119.4959 m (Section C.7)
	Aquifer Hydraulic Conductivity Horizontal to Vertical Anisotropy:
	  Cold Creek gravel = **13:1**
	  All other aquifer units = **10:1**
	Aquifer Dispersivity (all aquifer units) = 10.5 m
	  Aquifer Dispersivity Horizontal to Vertical Anisotropy **10:1**

Source Term/ Inventory	WMA A-AX ACM 1 inventory presented in Table 3-1. Diffusion controlled release from the grouted tanks and advection controlled release from the ancillary equipment that includes pipelines along with equilibrium sorption-desorption processes (i.e., K_d control).

Table 4-1. Summary of Key Elements and Parameters Associated with Site-Specific Model Components for Waste Management Area A-AX. (2 sheets)

Vadose Zone Hydrogeology and Fluid Transport	WMA A-AX ACM 1 hydrogeologic properties presented in Tables 3-2 through 3-4. Vadose Zone Hydraulic Conductivity and Anisotropy allowed to vary as a function of the moisture content in accordance with the TCT model (PNNL-23711 and Zhang et al. 2003). Vadose Zone Dispersion Horizontal to Vertical Anisotropy **10:1**
Recharge	WMA A-AX ACM 1 recharge estimates for various soil types, condition of the vegetation cover, and soil integrity during the pre-construction, operational, and post-closure periods are presented in Table 3-5.
Sorption Characteristics	K_d-control for radionuclide transport in the vadose zone and groundwater. WMA A-AX ACM 1 gravel-corrected K_d values (partition coefficients) presented in Table 3-8.

References:
CP-47631, *Model Package Report: Central Plateau Groundwater Model Version 8.4.5*, Rev. 4.
"A Tensorial Connectivity–Tortuosity Concept to Describe the Unsaturated Hydraulic Properties of Anisotropic Soils" (Zhang et al. 2003).
PNNL-23711, *Physical, Hydraulic, and Transport Properties of Sediments and Engineered Materials Associated with Hanford Immobilized Low-Activity Waste*.
RPP-RPT-60171, *Model Package Report: Geologic Framework Model used in WMA A-AX Performance Assessment and RCRA Closure Analysis*.
NAVD88 = North American Vertical Datum of 1988, National Geodetic Survey, U.S. Department of Commerce.
TCT = tensorial connectivity-tortuosity

4.3 MODELING STAGES

The WMA A-AX tank residual simulations using STOMP require running three separate stages in sequence. The first stage is a long-term transient simulation of only water flow resulting from historic recharge conditions. This stage is required to obtain steady-state soil moisture conditions throughout the model domain at the start time for the second stage. The second stage begins with the initial moisture distribution provided from the first stage and simulates water flow during the operational period of WMA A-AX, which is the time between the construction of WMA A-AX (A Farm in 1954 and AX Farm in 1963) and their assumed closure in 2050. The STOMP nomenclature refers to this as a "restart." To accommodate different timing of changes in surface condition for different subareas, the second stage restarts in calendar year 1943 at steady-state conditions, and infiltration rates are then changed for each subarea at the appropriate times as described in Section 3.1.5. The contaminant transport stage (stage 3) begins with the moisture distribution provided from the second stage, and simulates flow and transport for 10,000 years, from 2050 to 12050. Each tank and ancillary equipment residual source is simulated individually. The groundwater concentrations resulting from each source are summed according to the principle of superposition to produce time series concentration breakthrough curves at the points of calculation identified in Section 3.1.8. The principle of superposition also applies to the spatial distribution of the pore water concentrations in the vadose zone resulting from each source. The superposition and summing of the concentration results occurs outside of STOMP and is not addressed in this section.

4.4 CALIBRATION

DOE G 435.1-1 and Federal risk assessment guidelines [e.g., EPA/540/1-89/002, *Risk Assessment Guidance for Superfund Volume I Human Health Evaluation Manual (Part A) Interim Final*] acknowledge that the assessment of uncertainties associated with how well models approximate actual relationships and conditions in the field (i.e., field validation) is desirable, but that field data for model calibration is generally not available or attainable for vadose zone models.

No specific effort to calibrate the WMA A-AX PA flow and transport model has been made. Model hydraulic properties used to simulate the vadose zone flow field and ACM 1 simulation results will be cross-checked against WMA A-AX field-measured moisture contents in a subsequent EMCF. WMA A-AX site characterization has included the collection of an extensive database of moisture content measurements of the various HSUs present. RPP-ENV-58578 includes a summary of these measurements for the WMA A-AX area and associated statistics. The calibrated CPGWM provides the basis for parameterization of the multiple HSUs within the aquifer, and Figure 3-6 provides an indication of the degree to which the CPGWM matches observed hydraulic head measurements in the unconfined aquifer.

4.5 SCREENING

The system modeling (RPP-RPT-60885) is expected to include and describe the screening methods used to determine the maximum K_d value of contaminants in the WMA A-AX tank residuals that reach the water table in 1,000 and 10,000 years. The purpose of this screening phase is to streamline the PA modeling by identifying those contaminants sufficiently mobile to impact groundwater during the timeframes of analysis. The screening analysis is performed to limit the number of key radionuclides evaluated in the 3-D process model and therefore reduce the computation time required to conduct the PA modeling simulations. According to the facility performance requirements in DOE O 435.1, impacts are evaluated against performance objectives and measures during the initial 1,000 years following closure, and post-closure evaluations must extend out to 10,000 years to clarify long-term impacts. Given the combination of low infiltration rates and a deep vadose zone below the facility, contaminants that are highly sorbed onto the soils beneath the facility may not reach the water table within 10,000 years,[6] even for combinations of input parameters that are highly conservative. If the travel time exceeds 10,000 years, even for conservative combinations of input parameters, the contaminant or daughter products resulting from ingrowth will not affect any of the calculated results in the PA and can reasonably be screened from the analysis.

Parameter distributions for the WMA A-AX uncertainty analysis have not yet been developed. Until the system model screening analysis is complete, the WMA A-AX PA makes use of the analysis and results for WMA C (RPP-CALC-60448, *WMA C Performance Assessment Contaminant Fate and Transport Model to Evaluate Impacts to Groundwater*) as a guide until

[6] In this analysis, the travel time to the aquifer is defined as the time to first arrival of the contaminant at the aquifer, taking into account advection, diffusion, and dispersion. This metric will tend to screen fewer contaminants than using the arrival of the peak concentration.

screening results from RPP-RPT-60885 become available. The screening values are not expected to change substantially at WMA A-AX because the two WMAs are located close together.

The results of the WMA C screening analysis (RPP-CALC-60448) indicate that even when using parameter estimates biased to produce the greatest pore water velocity in the vadose zone, contaminants with a $K_d > 0.15$ mL/g for the fine fraction (<2 mm) do not reach groundwater within the 1,000-year compliance timeframe, and radionuclides with a $K_d > 2$ mL/g do not reach groundwater within the 10,000-year post-compliance period. The screening evaluation helps in reducing the number of radionuclides to be evaluated using 3-D modeling analysis. When parameter distributions are developed for WMA A-AX, the screening analysis in RPP-RPT-60885 will provide WMA A-AX-specific K_d screening values.

4.6 ALTERNATIVE CONCEPTUAL MODEL 1 ANALYSIS

As discussed in Section 2 and Section 3.1.3, model analysis of ACM 1 evaluates the contribution of individual sources on the peak concentration in groundwater and identifies at which point of calculation that peak concentration occurs. This approach was taken specifically to address the need to compare model results with groundwater MCLs. The use of the model to perform ACM 1 calculations for the PA evaluation will be documented in separate EMCFs after that analysis is conducted. Thus, specific PA-related ACM 1 results are not included in this MPR, except the evaluations that are necessary to support development of the system model (RPP-RPT-60885).

4.7 SENSITIVITY AND UNCERTAINTY ANALYSIS

This MPR focuses on the WMA A-AX 3-D numerical flow and transport model, the development of ACM 1, and the model's applicability to meeting the DOE M 435.1-1 evaluation requirements. The use of the model to perform sensitivity and uncertainty calculations and the sensitivity and uncertainty results that will be a part of the PA evaluation are not included in this MPR, but will be documented in separate EMCFs after those analyses have been conducted. The input parameters that will be implemented to evaluate ACM 2 are not yet available, but the WMA A-AX PA is expected eventually to include evaluation of ACM 2. ACM 2 represents an alternative conceptualization of the entire WMA A-AX geologic model, with certain HSUs divided into subunits, different estimated thicknesses of certain HSUs, and different parameterization of certain HSUs relative to ACM 1.

5.0 MODEL APPLICATION

The WMA A-AX PA 3-D VSZ model described in this report is to be utilized to estimate the impact to groundwater from radiological and non-radiological contaminants released from tank waste left in tanks and ancillary equipment in WMA A-AX at closure. The model results will not account for possible interaction with waste or discharges from waste sites outside WMA A-AX, or cumulative impacts from earlier UPRs from WMA A-AX sources. The results are limited to calculations consistent with the assumption of a porous media continuum and approximate the bulk-flow processes through the vadose zone to estimate the arrival time and concentration of contaminants in groundwater.

5.1 WASTE MANAGEMENT AREA A-AX PERFORMANCE ASSESSMENT MODEL LIMITATIONS

DOE/RL-2011-50 identifies generalized model and code limitations associated with the relevant FEPs for the 200 Areas vadose zone. Other limitations specific to WMA A-AX are comparable to those considered during working sessions conducted in 2015 and 2017 for WMA C (e.g., see section 1.1.1 in RPP-ENV-58782). The description of the limitations involves a summary of those FEPs considered and not considered in the model along with possible consequences of their omission on the model results. The limitations also address or involve uncertainties in the model results.

For the purposes of establishing that the requirements of DOE O 435.1 are being met, these limitations appear to be acceptable because the results represent reasonable (upper) bounding or limiting conditions. The implications of the results are not sensitive to the limitations apart from those identified through the sensitivity analysis. The limitations are considered acceptable because they do not affect the conclusions pertinent to DOE O 435.1 regarding protecting the public and environment from exposure to radiation from radioactive materials.

5.2 WASTE MANAGEMENT AREA A-AX PERFORMANCE ASSESSMENT MODEL RECOMMENDATIONS

None at this time.

This page intentionally left blank.

6.0 SUBSURFACE TRANSPORT OVER MULTIPLE PHASES SOFTWARE

The STOMP and eSTOMP software is licensed by CHPRC for use under the terms of a limited government license from Pacific Northwest National Laboratory (PNNL), which developed the code to meet American Society of Mechanical Engineers (ASME) NQA-1-2000, *Quality Assurance Requirements for Nuclear Facility Applications* and DOE O 414.1C, *Quality Assurance* software requirements when those were applicable orders and standards. Currently, PNNL manages STOMP and eSTOMP under Configuration Management Plans [PNNL-SA-92584, *Subsurface Transport Over Multiple Phases (STOMP) Software Configuration Management Plan* and PNNL-24121, *eSTOMP Configuration Management Plan*, respectively] in conjunction with Software Test Plans (PNNL-SA-92579, *STOMP Software Test Plan* and PNNL-24120, *eSTOMP Software Test Plan*, respectively) that detail the procedures used to test, document and archive modifications to the source code. PNNL maintains specific operational modes of STOMP and eSTOMP as qualified Safety Software, Level C, per the DOE O 414.1D, *Quality Assurance* definition for safety software and ASME NQA-1-2008 *Quality Assurance Requirements for Nuclear Facility Applications* with NQA-1a-2009 addenda (PNNL-24118, *STOMP/eSTOMP Software Quality Assurance Plan*).

STOMP and eSTOMP are used to solve the Richards equation (the water mass conservation equation in PNNL-12030) and the Advection-Dispersion equation (the solute mass conservation equation in PNNL-12030) that govern water flow and solute transport, respectively, under variably saturated conditions in the vadose zone and groundwater. STOMP and eSTOMP (PNNL-11216; PNNL-12030; PNNL-15782, *STOMP Subsurface Transport Over Multiple Phases Version 4.0 User's Guide*) have been selected to simulate the transport of contaminants in the vadose zone of the 200 Area in and around WMA A-AX because STOMP and eSTOMP fulfill the following specifications (in the following list STOMP refers to both STOMP and eSTOMP):

- The STOMP simulator operational modes needed for implementation of this model are available free for government use under a limited government-use agreement

- The STOMP simulator solves the necessary governing equations (i.e., Richards' equation and conservation of mass)

- It is capable of directly simulating the principal FEPs that are relevant (see Section 3.1)

- The STOMP simulator is well documented (PNNL-11216, PNNL-12030, PNNL-15782)

- The STOMP simulator development meets ASME NQA-1-2008 with NQA-1a-2009 addenda software requirements and is compliant with DOE O 414.1D requirements for Safety Software (PNNL-SA-92579; PNNL-24120; PNNL-SA-92584; PNNL-24121; PNNL-24122, *Software Requirements Document for STOMP and eSTOMP*)

- The STOMP simulator is distributed with source code, enhancing transparency

- The modeling team implementing this model has expertise in use of this simulator

- There is an extensive history of application of STOMP at Hanford and elsewhere including verification, benchmarking, and data comparisons (DOE/RL-2011-50)

- Use of STOMP is in keeping with DOE direction for simulation of integrated vadose and saturated zone flow and transport at the Hanford Site (Letter 06-AMCP-0132, "Contract No. DE-AC06-96RL13200 – Hanford Groundwater Modeling Integration").

6.1 SUBSURFACE TRANSPORT OVER MULTIPLE PHASES SOFTWARE QUALITY ASSURANCE

The use of STOMP and eSTOMP to implement the WMA A-AX PA model and perform calculations is performed in a manner that satisfies and complies with environmental quality assurance requirements indicated by Title 10, *Code of Federal Regulations* (CFR), Part 830, "Nuclear Safety Management," and Subpart A—Quality Assurance Requirements (10 CFR 830); DOE O 414.1D; and State and Federal environmental regulations. EM-QA-001, *EM Quality Assurance Program (QAP)*, Attachment G – "Software Quality Requirements" and Attachment H – "Model Development, Use, and Validation" list DOE management expectations for compliance, including configuration control, evaluation, implementation, verification and validation, and operation and maintenance.

Quality assurance project planning for STOMP and eSTOMP modeling follows the guidance in EPA/240/R-02/007, *Guidance for Quality Assurance Project Plans for Modeling, EPA QA/G-5M*. Model project planning includes documenting specific model development efforts and applications. It addresses as relevant and important all nine "Group A" elements presented in EPA/240/B-01/003, *EPA Requirements for Quality Assurance Project Plans, EPA QA/R-5*. The nine elements include problem definition and background, quality objectives and criteria for measurements and data acquisition leading to model inputs and outputs, data validation and usability, references, documentation and records management, special training requirements and certifications for modelers, and assessments and reports to management.

6.2 SUBSURFACE TRANSPORT OVER MULTIPLE PHASES CONTROLLED CALCULATION SOFTWARE

The following describes the STOMP and eSTOMP controlled calculation software and its computational platform.

- Software Title: STOMP-W and eSTOMP (a scientific tool for analyzing single- and multiple-phase subsurface flow and transport using the integrated finite volume discretization technique with Newton-Raphson iteration).

- Software Version: STOMP-W was provided by PNNL on January 30, 2013, and was tested and approved for use by CHPRC as "CHPRC Build 4." eSTOMP was provided by PNNL on May 30, 2017, and was tested and approved for use by CHPRC as "CHPRC

Build 6." For STOMP-W, CHPRC Build 4 is identical to CHPRC Build 5 and CHPRC Build 6; the latter were issued in response to development of eSTOMP.

- Hanford Information System Inventory Identification Number: 2471 (Safety Software S3, graded Level C).

- Computational Platforms:

  - Tellus Subsurface Modeling Platform (Tellus) hosted by Mission Support Alliance for CHPRC

    - Server Chassis: Dell PowerEdge®[7] M1000e Blade Enclosure

    - Compute Nodes: 16 Dell PowerEdge® M610 Blade Servers

      - Intel Xeon®[8] X5670 CPU (x2), 6 Cores/CPU, 2.93 GHz, 12MB Cache
      - 96 GB RAM; DDR3; 1,333 MHz
      - 10 Gbps Ethernet Mezzanine Card – Dual Port – X520DA2 x 2

    - Storage: internal hard drives on management (frontend) server includes 4 SAMSUNG 830 Series MZ-7PC512D/AM 2.5" SATAIII MLC Internal Solid State Drives

    - Operating System and Version

      - Red Hat Enterprise Linux®[9] 5 (Tikanga), Release 5.8
      - Rocks Cluster/Ganglia open source software operating system

  - GREEN hosted by INTERA Incorporated for CHPRC

    - Server Chassis: Dell PowerEdge R510 in Standard 2U Rack

      - Two Intel Xeon® X5660 6-core processors @ 2.80GHz
      - 48 GB (1,333 MHz Dual Ranked RDIMMs)

    - Storage: Two 300 GB 10K RPM SAS 6 Gbps hard-drives (RAID-1) for O/S and 12 2TB 7.2K RPM Near-Line SAS 6 Gbps hard-drives (RAID-6,5) for data and backup

[7] Dell® and PowerEdge® are registered trademarks of Dell Products, Inc.

[8] Intel® and Xeon® are trademarks of Intel Corporation or its subsidiaries in the U.S. and/or other countries.

[9] Linux® is the registered trademark of Linus Torvalds in the U.S. and other countries.

- Operating System and Version
  - Linux 4.4.0-62-generic #83~14.04.1-Ubuntu SMP Wed Jan 18 18:10:30 UTC 2017 x86_64x86_64 x86_64 GNU/Linux.

- Olive hosted by INTERA Incorporated for CHPRC
  - Server Chassis: Dell PowerEdge R530
    - Two Intel Xeon® E5-2680 v3 12-core processors @ 2.50GHz
    - 128 GB RAM; RDIMM, 2133 MT/s Dual Rank
  - Storage: 26 TB RAID-5 disk array
  - Operating System and Version
    - Linux 4.4.0-38-generic #57~14.04.1-Ubuntu SMP Tue Sep 6 17:20:43 UTC 2016 x86_64 x86_64 x86_64 GNU/Linux.

- Approved Users: W. J. (Bill) McMahon and A. Wahi.

6.3 SOFTWARE INSTALLATION AND CHECKOUT

After receipt of the STOMP and eSTOMP source code from PNNL, CHPRC commits the code to the MKS Integrity™[10] configuration management system that ensures traceability and precludes loss of information. Successful acceptance and installation include confirming that the software is operating correctly by benchmarking results produced on the local computer system to those presented for selected problems from the STOMP Application Guide (PNNL-11216). The CHPRC software owner maintains the configuration-managed copies in MKS Integrity™ and grants access to the executable files to users upon request in accordance with the approved software installation and checkout forms.

Receipt of the current STOMP and eSTOMP source code occurred January 2013 and May 2017, respectively; testing of CHPRC Build 4 of STOMP on Tellus and GREEN (hosted by INTERA) successfully concluded April 2013. No updates to the STOMP code received from PNNL have occurred since Build 4, so Build 5 and Build 6 of STOMP are identical to Build 4. Updates to eSTOMP have been received and implemented since then. Installation testing of CHPRC Build 6 of eSTOMP on Tellus successfully concluded September 2018, and successful acceptance and installation of eSTOMP on GREEN concluded in September 2017. Approved users are registered in the Hanford Information System Inventory for safety software, which identifies W. J. (Bill) McMahon as an authorized user of STOMP, which includes use of

[10] MKS Integrity, Integrity, and all other PTC product names and logos are trademarks or registered trademarks of Parametric Technology Corporation or its subsidiaries in the United States and in other countries.

eSTOMP, on the Tellus Platform as of May 6, 2013, and Arun Wahi as an authorized user of STOMP, which includes use of eSTOMP, on the GREEN Platform as of June 1, 2015.

6.4 STATEMENT OF VALID SOFTWARE APPLICATION

The WMA A-AX PA requires calculations of the potential long-term impact on groundwater of post-retrieval SST waste residuals and waste left in ancillary equipment, including pipelines. STOMP and eSTOMP have been developed for these types of applications, among others, and are used to solve the Richards equation and the Advection-Dispersion equation that govern water flow and solute transport, respectively, under variably saturated conditions in the vadose zone and groundwater. The WMA A-AX PA implementation of STOMP and eSTOMP to perform calculations satisfies and complies with environmental quality assurance requirements indicated by 10 CFR 830, Subpart A—Quality Assurance; DOE O 414.1D; and State and Federal environmental regulations. Successful acceptance and installation of STOMP Build 4 and eSTOMP Build 6 on Tellus concluded in April 2013 and September 2018, respectively, and the Hanford Information System Inventory for safety software lists W. J. (Bill) McMahon as an authorized user of STOMP, including use of eSTOMP, on the Tellus Platform. Successful acceptance and installation of STOMP Build 4 and eSTOMP Build 6 on GREEN concluded in April 2013 and September 2017, respectively, and the Hanford Information System Inventory for safety software lists Arun Wahi as an authorized user of STOMP, including use of eSTOMP, on the GREEN Platform.

The quality assurance project planning for STOMP and eSTOMP modeling follows the guidance in EPA/240/R-02/007, and the conduct of implementation is shown to comply with DOE management expectations for compliance. Calculations with the WMA A-AX PA model use only NQA-1 qualified options and code within the STOMP-W or eSTOMP-W executables, and are thus within the intended range of applications. Therefore, for this application, STOMP and eSTOMP are appropriate software code to use. Using it to implement the WMA A-AX PA model described in this report is consistent with STOMP's intended use, and its use is shown to comply with applicable quality assurance requirements.

6.5 MODFLOW AND RELATED CODES SUPPORT SOFTWARE

MODFLOW-2000 is documented in Open-File Report 00-92, *MODFLOW-2000, The U.S. Geological Survey Modular Ground-Water Model—User Guide to Modularization Concepts and the Ground-Water Flow Process*. Appendix C presents results of previously reported simulations of the saturated zone flow field from the CPGWM Version 8.4.5 (a MODFLOW-2000-MST application documented in CP-47631 Rev. 4 and ECF-200W-17-0043, *Capture-Zone and Particle-Tracking Analysis for the 200-UP-1/200-ZP-1 Areas using the 2017 Updated Central Plateau Model*) with new graphics focusing on the region of the aquifer in and around the WMA A-AX PA STOMP model domain. Model properties, simulated hydraulic heads, and simulated groundwater fluxes were visualized using Groundwater Vistas[11] and

[11] Groundwater Vistas is a product of Environmental Simulations, Inc., Reinholds, Pennsylvania.

ArcGIS®[12]. Steady-state fluxes for selected regions were extracted from the CPGWM output using ZONEBUDGET[13] (Open-File Report 90-392, *A Computer Program for Calculating Subregional Water Budgets Using Results from the U.S. Geological Survey Modular Three-dimensional Finite-difference Ground-Water Flow Model*).

CHPRC-00257, *MODFLOW and Related Codes Functional Requirements Document* distinguishes calculational software from supporting software because these two groups of software are classified and graded differently. The basis for the difference is that calculational software, including MODFLOW-2000-MST and MT3DMS-MST, calculate results that will be used to support decision making and as such, constitute safety software graded to level C. In contrast, supporting software includes graphical interfaces, visualization, and input preparation support but not calculation of results that directly support decision making, and are therefore not rated as safety software. The support software items identified in CHPRC-00258, *MODFLOW and Related Codes Software Management Plan* and used in this calculation were as follows.

- Groundwater Vistas ("Guide to Using Groundwater Vistas" [Rumbaugh and Rumbaugh 2007]): Graphical tools in Groundwater Vistas were used in post-processing some output files from previously-documented CPGWM runs to plot simulated heads at specified well locations and to export cell-by-cell flow field results for mapping.

- ArcGIS® (<u>The ESRI Guide to GIS Analysis, Volume 1: Geographic Patterns and Relationships</u> [Mitchell 1999]): Provided visualization tool for assessing and mapping CPGWM cell locations relative to WMA A-AX PA model domain and facility coordinates. ArcGIS® was used in post-processing previously-documented CPGWM simulation results.

- ZONEBUDGET (Open-File Report 90-392): Steady-state fluxes for selected regions were extracted from the previously-documented CPGWM output using ZONEBUDGET.

[12] ArcGIS® is a registered trademark of Environmental Systems Research Institute, Inc., Redlands, California.
[13] ZONEBUDGET software has been developed and distributed by the U.S. Geological Survey, Washington, D.C.

7.0 MODEL CONFIGURATION MANAGEMENT

All inputs and outputs for the development of WMA A-AX PA models are archived to the Washington River Protection Solutions (WRPS) Environmental Model Management Archive (EMMA) to maintain and preserve models, input files and select output files under configuration management. Inputs include the input files used in the STOMP simulations and the files called by the input files such as the zonation and boundary node list files. Basis information (that information collected to form the basis for model input parameterization) is also stored in the EMMA for traceability purposes. Use of the STOMP software for implementing the model described in this report is consistent with its intended use for CHPRC, as indicated in Section 6.4 "Statement of Valid Software Application."

This page intentionally left blank.

8.0 REFERENCES

06-AMCP-0132, 2006, "Contract No. DE-AC06-96RL13200 – Hanford Groundwater Modeling Integration" (letter from K. A. Klein to R. G. Gallagher, Fluor Hanford, Inc., March 9), U.S. Department of Energy, Richland Operations Office, Richland, Washington.

10 CFR 830, "Nuclear Safety Management," *Code of Federal Regulations*, as amended.

10 CFR 830, "Nuclear Safety Management," Subpart A—Quality Assurance Requirements, *Code of Federal Regulations*, as amended.

ARH-374, 1968, *244-AR Vault Information Manual*, Atlantic Richfield Hanford Company, Richland, Washington.

ARH-LD-127, 1976, *Geology of the 241-A Tank Farm*, Atlantic Richfield Hanford Company, Richland, Washington.

ARH-LD-128, 1976, *Geology of the 241-AX Tank Farm*, Atlantic Richfield Hanford Company, Richland, Washington.

ASME NQA-1, 2000, *Quality Assurance Requirements for Nuclear Facility Applications*, American National Standards Institute/American Society of Mechanical Engineers, New York, New York.

ASME NQA-1-2008, 2009, *Quality Assurance Requirements for Nuclear Facility Applications*, with the NQA-1a-2009 addenda, American National Standards Institute/American Society of Mechanical Engineers, New York New York.

BHI-01745, 2004, *Environmental Restoration Contractor Revegetation Monitoring Report*, Rev. 0, Bechtel Hanford Inc., Richland, Washington.

CHPRC-00257, 2010, *MODFLOW and Related Codes Functional Requirements Document*, Rev. 1, CH2M HILL Plateau Remediation Company, Richland, Washington.

CHPRC-00258, 2015, *MODFLOW and Related Codes Software Management Plan*, Rev. 4, CH2M HILL Plateau Remediation Company, Richland, Washington.

CLARC 2015, Cleanup Levels and Risk Calculation (CLARC), Queried 02/28/2017, [CLARC Data Tables – July 2015], https://fortress.wa.gov/ecy/clarc/CLARCDataTables.aspx.

CLARC 2017, Cleanup Levels and Risk Calculation (CLARC), Queried 02/28/2017, [CLARC Master Table], https://fortress.wa.gov/ecy/clarc/FocusSheets/CLARC%20Master%20Spreadsheet.xlsx.

CP-47631, 2015, *Model Package Report: Central Plateau Groundwater Model Version 6.3.3*, Rev. 2, INTERA, Inc., Richland, Washington.

CP-47631, 2017, *Model Package Report: Central Plateau Groundwater Model Version 8.4.5*, Rev. 4, CH2M HILL Plateau Remediation Company, Richland, Washington.

DOE/EIS-0391, 2012, *Final Tank Closure and Waste Management Environmental Impact Statement for the Hanford Site, Richland, Washington*, U.S. Department of Energy, Office of River Protection, Richland, Washington.

DOE G 435.1-1, 1999, *Implementation Guide for Use with DOE M 435.1-1, Radioactive Waste Management Manual*, U.S. Department of Energy, Washington, D.C.

DOE M 435.1-1, 1999, *Radioactive Waste Management Manual*, U.S. Department of Energy, Washington, D.C.

DOE O 414.1C, 2005, *Quality Assurance*, U.S. Department of Energy, Washington, D.C.

DOE O 414.1D, 2011, *Quality Assurance*, U.S. Department of Energy, Washington, D.C.

DOE O 435.1, 2001, *Radioactive Waste Management*, U.S. Department of Energy, Washington, D.C.

DOE/ORP-2005-01, 2006, *Initial Single-Shell Tank System Performance Assessment for the Hanford Site*, Rev. 0, U.S. Department of Energy, Office of River Protection, Richland, Washington.

DOE/RL-92-04, 1993, *PUREX Source Aggregate Area Management Study Report*, Rev. 0, U.S. Department of Energy, Richland Operations Office, Richland, Washington.

DOE/RL-93-33, 1996, *Focused Feasibility Study of Engineered Barriers for Waste Management Units in the 200 Areas*, Rev. 1, U.S. Department of Energy, Richland Operations Office, Richland, Washington.

DOE/RL-2002-59, 2004, *Hanford Site Groundwater Strategy Protection, Monitoring, and Remediation*, Rev. 0, U.S. Department of Energy, Richland Operations Office, Richland, Washington.

DOE/RL-2007-27, 2011, *Feasibility Study for the Plutonium/Organic-Rich Process Condensate/Process Waste Group Operable Unit: Includes the 200-PW-1, 200-PW-3, and 200-PW-6 Operable Units*, Rev. 0, U.S. Department of Energy, Richland Operations Office, Richland, Washington.

DOE/RL-2011-50, 2012, *Regulatory Basis and Implementation of a Graded Approach to Evaluation of Groundwater Protection*, Rev. 1, U.S. Department of Energy, Richland Operations Office, Richland, Washington.

DOE/RL-2011-116, 2013, *Hanford Site Revegetation Manual*, Rev. 1, U.S. Department of Energy, Richland Operations Office, Richland, Washington.

DOE/RL-2016-37, 2016, *Prototype Hanford Barrier 1994 to 2015*, Rev. 0, U.S. Department of Energy, Richland Operations Office, Richland, Washington.

ECF-200W-17-0043, 2018, *Capture-Zone and Particle-Tracking Analysis for the 200-UP-1/200-ZP-1 Areas using the 2017 Updated Central Plateau Model*, Rev. 0, INTERA, Inc. for CH2M HILL Plateau Remediation Company, Richland, Washington.

Ecology, 1990, *Ground Water Monitoring Guidance for Solid Waste Facilities*, Washington State Department of Ecology, Solid and Hazardous Waste Program, Olympia, Washington.

Ecology, EPA, and DOE, 1989, *Hanford Federal Facility Agreement and Consent Order – Tri-Party Agreement*, 2 vols., as amended, State of Washington Department of Ecology, U.S. Environmental Protection Agency, and U.S. Department of Energy, Olympia, Washington.

EM-QA-001, 2012, *EM Quality Assurance Program (QAP)*, Rev. 1, Office of Environmental Management, U.S. Department of Energy, Washington, D.C.

Environmental Dashboard Application, Queried 07/17/2017, [redacted]

EPA/240/B-01/003, 2001, *EPA Requirements for Quality Assurance Project Plans, EPA QA/R-5*, U.S. Environmental Protection Agency, Office of Environmental Information, Washington, D.C.

EPA/240/R-02/007, 2002, *Guidance for Quality Assurance Project Plans for Modeling, EPA QA/G-5M*, U.S. Environmental Protection Agency, Office of Environmental Information, Washington, D.C.

EPA 402-R-94-012, 1994, *A Technical Guide to Ground-Water Model Selection at Sites Contaminated with Radioactive Substances*, U.S. Environmental Protection Agency/ U.S. Department of Energy/Nuclear Regulatory Commission, Washington, D.C.

EPA/530-SW-87-017, 1987, *Alternate Concentration Limit Guidance Part I ACL Policy and Information Requirements Interim Final*, OSWER Directive 9481.00-6C, Office of Solid Waste, Waste Management Division, U.S. Environmental Protection Agency, Washington, D.C.

EPA/540/1-89/002, 1989, *Risk Assessment Guidance for Superfund Volume I Human Health Evaluation Manual (Part A) Interim Final*, Office of Emergency and Remedial Response, U.S. Environmental Protection Agency, Washington, D.C.

EPA/540/F-95/041, 1996, *Soil Screening Guidance: Fact Sheet*, Publication 9355.4-14FSA, U.S. Environmental Protection Agency, Office of Solid Waste and Emergency Response, Washington, D.C.

EPA/540/R-92/003, 1991, *Guidance for Data Useability in Risk Assessment (Part A) Final*, U.S. Environmental Protection Agency, Office of Emergency Response, Washington, D.C.

EPA/540/R-95/128, 1996, *Soil Screening Guidance: Technical Background Document*, Second Edition, U.S. Environmental Protection Agency, Washington, D.C.

EPA/600/2-91/065, 1991, *The RETC Code for Quantifying the Hydraulic Functions of Unsaturated Soils*, Office of Research and Development, U.S. Environmental Protection Agency, Washington, D.C.

EPA-SAB-RAC-ADV-99-006, 1999, *An SAB Advisory: Modeling of Radionuclide Releases from Disposal of Low Activity Mixed Waste*, U.S. Environmental Protection Agency, Science Advisory Board, Washington, D.C.

Fayer, M. J. and G. W. Gee, 2006, "Multiple-Year Water Balance of Soil Covers in a Semiarid Setting," *Journal of Environmental Quality*, Vol. 35, No. 2, pp. 366–377.

Fletcher, C. A. J., 1991, Computational Techniques for Fluid Dynamics, 2nd Edition, Springer-Verlag, Berlin, Germany.

Freeze, R. A., and Cherry, J. A., Groundwater, Prentice-Hall, Inc., Englewood Cliffs, New Jersey.

Gee, G. W., M. J. Fayer, M. L. Rockhold, and M. D. Campbell, 1992, "Variations in Recharge at the Hanford Site," *Northwest Science*, Vol. 66, No. 4, pp. 237–250.

Gelhar, L. W., 1993, Stochastic Subsurface Hydrology, Prentice Hall, New York, New York.

Gelhar, L. W. and C. L. Axness, 1983, "Three-dimensional stochastic analysis of macrodispersion in aquifers," *Water Resources Research*, Vol. 19, pp. 161–180.

Gelhar, L. W., C. Welty, and K. R. Rehfeldt, 1992, "A Critical Review of Data on Field-Scale Dispersion in Aquifers," *Water Resources Research*, Vol. 28, Issue 7, pp. 1955–1974.

Green, T. R., J. E. Constantz, and D. L. Freyberg, 1996, "Upscaled soil-water retention using van Genuchten's function," *Journal of Hydrologic Engineering*, Vol. 1, Issue 3, pp. 123–130.

GoldSim Technology Group, 2017, GoldSim Contaminant Transport Module User's Guide, Version 7.0, GoldSim Technology Group, LLC, Issaquah, Washington.

HGIS Hanford Geographic Information System, Queried 06/26/2017, [HMAPS Interactive Maps], [redacted]

HNF-5294, 1999, *Computer Code Selection Criteria for Flow and Transport Code(s) To Be Used in Vadose Zone Calculations for Environmental Analyses in the Hanford Site's Central Plateau*, Rev. 0, CH2M HILL Hanford Group, Inc., Richland, Washington.

HNF-EP-0182, 2016, *Waste Tank Summary Report for Month Ending November 30, 2016*, Rev. 347, Washington River Protection Solutions, LLC, Richland, Washington.

HNF-EP-0182, 2018, *Waste Tank Summary Report for Month Ending June 30, 2018*, Rev. 366, Washington River Protection Solutions, LLC, Richland, Washington.

HNF-SD-RE-TI-178, 2007, *Single-Shell Tank Interim Stabilization Record*, Rev. 9a, CH2M HILL Hanford Group, Inc., Richland, Washington.

Huysmans, M. and A. Dassargues, 2005, "Review of the use of Péclet numbers to determine the relative importance of advection and diffusion in low permeability environments," *Hydrogeology Journal*, Vol. 13, Issues 5-6, pp. 895–904.

ICRP, 2008, "ICRP Publication 107: Nuclear Decay Data for Dosimetric Calculations," *Annals of the ICRP*, International Commission on Radiation Protection, Vol. 38, No. 3, pp. 7–96.

Khaleel, R. and J. F. Relyea, 1997, "Correcting Laboratory-Measured Moisture Retention Data for Gravels," *Water Resources Research*, Vol. 33, Issue 8, pp. 1875–1878.

Khaleel, R., J. F. Relyea, and J. L. Conca, 1995, "Evaluation of van Genuchten-Mualem Relationships to Estimate Unsaturated Hydraulic Conductivity at Low Water Contents," *Water Resources Research*, Vol. 31, Issue 11, pp. 2659–2668.

Khaleel, R., T.-C. J. Yeh, and Z. Lu, 2002, "Upscaled flow and transport properties for heterogeneous unsaturated media," *Water Resources Research*, Vol. 38, Issue 5, pp. 11-1–11-12.

Konikow, L. F., 2011, "The Secret to Successful Solute-Transport Modeling," *Ground Water*, Vol. 49, Issue 2, pp. 144–159.

Mantoglou, A., 1984, Large-Scale Models of Transient Unsaturated Flow and Contaminant Transport Using Stochastic Methods, Ph.D. Thesis, Massachusetts Institute of Technology, Department of Civil Engineering, Cambridge, Massachusetts.

Mantoglou, A. and L. W. Gelhar, 1987, "Stochastic Modeling of Large-Scale Transient Unsaturated Flow Systems," *Water Resources Research*, Vol. 23, Issue 1, pp. 37–46.

Millington, R. J. and J. P. Quirk, 1961, "Permeability of Porous Solids," *Transactions of the Faraday Society*, Vol. 57, pp. 1200–1207.

Mitchell, A., 1999, The ESRI Guide to GIS Analysis, Volume 1: Geographic Patterns and Relationships, ESRI Press, Redlands, California.

Mualem, Y., 1976, "A New Model for Predicting the Hydraulic Conductivity of Unsaturated Porous Media," *Water Resources Research*, Vol. 12, Issue 3, pp. 513–522.

NAVD88, 1988, North American Vertical Datum of 1988, National Geodetic Survey, U.S. Department of Commerce, National Oceanic and Atmospheric Administration, Silver Spring, Maryland.

NCRP Report No. 152, 2005, Performance Assessment of Near-Surface Facilities for Disposal of Low-Level Radioactive Waste, National Council on Radiation Protection and Measurements, Bethesda, Maryland.

Neuman, S. P., 1990, "Universal Scaling of Hydraulic Conductivities and Dispersivities in Geologic Media," *Water Resources Research*, Vol. 26, Issue 8, pp. 1749–1758.

NOAA Manual NOS NGS 5, 1990, State Plane Coordinate System of 1983, *National Geodetic Survey*, U.S. Department of Commerce, National Oceanic and Atmospheric Administration, Rockville, Maryland.

NUREG-1573, 2000, *A Performance Assessment Methodology for Low-Level Radioactive Waste Disposal Facilities: Recommendations of NRC's Performance Assessment Working Group*, U.S. Nuclear Regulatory Commission, Office of Nuclear Material Safety and Safeguards, Washington, D.C.

NUREG-1854, 2007, *NRC Staff Guidance for Activities Related to U.S. Department of Energy Waste Determinations – Draft Final Report for Interim Use*, U.S. Nuclear Regulatory Commission, Office of Federal and State Materials and Environmental Management Programs, Washington, D.C.

Open-File Report 00-92, 2000, *MODFLOW-2000, The U.S. Geological Survey Modular Ground-Water Model—User Guide to Modularization Concepts and the Ground-Water Flow Process*, United States Geological Survey, Reston, Virginia.

Open-File Report 90-392, 1990, *A Computer Program for Calculating Subregional Water Budgets Using Results from the U.S. Geological Survey Modular Three-dimensional Finite-difference Ground-Water Flow Model*, U.S. Geological Survey, Reston, Virginia.

OSWER No. 9200.4-18, 1997, "Establishment of Cleanup Levels for CERCLA Sites with Radioactive Contamination" (memorandum from S. D. Luftig and L. Weinstock to Addressees, August 22), Office of Solid Waste and Emergency Response, U.S. Environmental Protection Agency, Washington, D.C.

PNNL-11216, 1997, *STOMP Subsurface Transport Over Multiple Phases: Application Guide*, Pacific Northwest National Laboratory, Richland, Washington.

PNNL-12030, 2000, *STOMP Subsurface Transport Over Multiple Phases Version 2.0 Theory Guide*, Pacific Northwest National Laboratory, Richland, Washington.

PNNL-13023, 2004, *RCRA Groundwater Monitoring Plan for Single-Shell Tank Waste Management Area A-AX at the Hanford Site*, Rev. 1, Pacific Northwest National Laboratory, Richland, Washington.

PNNL-13033, 1999, *Recharge Data Package for the Immobilized Low-Activity Waste 2001 Performance Assessment*, Pacific Northwest National Laboratory, Richland, Washington.

PNNL-13037, 2004, *Geochemical Data Package for the 2005 Hanford Integrated Disposal Facility Performance Assessment*, Rev. 2, Pacific Northwest National Laboratory, Richland, Washington.

PNNL-13895, 2003, *Hanford Contaminant Distribution Coefficient Database and Users Guide*, Rev. 1, Pacific Northwest National Laboratory, Richland, Washington.

PNNL-14284, 2003, *Laboratory Measurements of the Unsaturated Hydraulic Properties at the Vadose Zone Transport Field Study Site*, Pacific Northwest Laboratory, Richland, Washington.

PNNL-14702, 2006, *Vadose Zone Hydrogeology Data Package for Hanford Assessments*, Rev. 1, Pacific Northwest Laboratory, Richland, Washington.

PNNL-14744, 2004, *Recharge Data Package for the 2005 Integrated Disposal Facility Performance Assessment*, Pacific Northwest National Laboratory, Richland, Washington.

PNNL-15782, 2006, *STOMP Subsurface Transport Over Multiple Phases Version 4.0 User's Guide*, Pacific Northwest National Laboratory, Richland, Washington.

PNNL-16663, 2007, *Geochemical Processes Data Package for the Vadose Zone in the Single-Shell Tank Waste Management Areas at the Hanford Site*, Pacific Northwest National Laboratory, Richland, Washington.

PNNL-16688, 2007, *Recharge Data Package for Hanford Single-Shell Tank Waste Management Areas*, Pacific Northwest National Laboratory, Richland, Washington.

PNNL-17154, 2008, *Geochemical Characterization Data Package for the Vadose Zone in the Single-Shell Tank Waste Management Areas at the Hanford Site*, Pacific Northwest National Laboratory, Richland, Washington.

PNNL-19945, 2010, *Soil Water Balance and Recharge Monitoring at the Hanford Site – FY 2010 Status Report*, Pacific Northwest National Laboratory, Richland, Washington.

PNNL-23711, 2015, *Physical, Hydraulic, and Transport Properties of Sediments and Engineered Materials Associated with Hanford Immobilized Low-Activity Waste*, RPT-IGTP-004, Rev. 0, Pacific Northwest National Laboratory, Richland, Washington.

PNNL-24118, 2016, *STOMP/eSTOMP Software Quality Assurance Plan*, Rev. 2.2, Pacific Northwest National Laboratory, Richland, Washington.

PNNL-24120, 2017, *eSTOMP Software Test Plan*, Rev. 1.2, Pacific Northwest National Laboratory, Richland, Washington.

PNNL-24121, 2017, *eSTOMP Configuration Management Plan*, Rev. 1.1, Pacific Northwest National Laboratory, Richland, Washington.

PNNL-24122, 2018, *Software Requirements Document for STOMP and eSTOMP*, Rev. 3.5, Pacific Northwest National Laboratory, Richland, Washington.

PNNL-25146, 2016, *Scale-Dependent Solute Dispersion in Variably Saturated Porous Media*, RPT-IGTP-009, Rev. 0, Pacific Northwest National Laboratory, Richland, Washington.

PNNL-SA-92579, 2012, *STOMP Software Test Plan*, Rev. 2.0, Pacific Northwest National Laboratory, Richland, Washington.

PNNL-SA-92584, 2012, *Subsurface Transport Over Multiple Phases (STOMP) Software Configuration Management Plan*, Rev. 1.5, Pacific Northwest National Laboratory, Richland, Washington.

RCW 70.105D, "Hazardous Waste Cleanup—Model Toxics Control Act," *Revised Code of Washington*, as amended.

Resource Conservation and Recovery Act of 1976, 42 USC 6901, et seq.

RPP-7494, 2001, *Historical Vadose Zone Contamination from A, AX, and C Tank Farm Operations*, Rev. 0, Fluor Federal Services, Richland, Washington.

RPP-12051, 2003, *244-AR Vault Interim Stabilization Completion Report*, Rev. 0, CH2M HILL Hanford Group, Inc., Richland, Washington.

RPP-14430, 2003, *Subsurface Conditions Description of the C and A-AX Waste Management Area*, Rev. 0, CH2M HILL Hanford Group, Inc., Richland, Washington.

RPP-20621, 2004, *Far-Field Hydrology Data Package for the Integrated Disposal Facility Performance Assessment*, Rev. 0, CH2M HILL Hanford Group, Inc., Richland, Washington.

RPP-35484, 2008, *Field Investigation Report for Waste Management Areas C and A-AX*, Rev. 1, CH2M HILL Hanford Group, Inc., Richland, Washington.

RPP-CALC-60448, 2016, *WMA C Performance Assessment Contaminant Fate and Transport Model to Evaluate Impacts to Groundwater*, Rev. 0, CH2M HILL Plateau Remediation Company/Washington River Protection Solutions, LLC, Richland, Washington.

RPP-CALC-62319, (in preparation), *Residual Waste Source Inventory Term for the Waste Management Area A-AX Performance Assessment Inventory Case 1*, Rev. 0, Washington River Protection Solutions, LLC, Richland, Washington.

RPP-ENV-37956, 2017, *Hanford 241-A and 241-AX Tank Farms Leak Inventory Assessment Report*, Rev. 3, Washington River Protection Solutions, LLC, Richland, Washington.

RPP-ENV-58578, in process, *Summary of the Natural System at Waste Management Area A-AX*, Rev. 1, Washington River Protection Solutions, LLC, Richland, Washington.

RPP-ENV-58782, 2016, *Performance Assessment of Waste Management Area C, Hanford Site, Washington*, Rev. 0, Washington River Protection Solutions, LLC, Richland, Washington.

RPP-RPT-42231, 2011, *Summary of Twenty-Five Miscellaneous Tanks Associated with the Single-Shell Tank System*, Rev. 1, Washington River Protection Solutions, LLC, Richland, Washington.

RPP-RPT-46088, 2016, *Flow and Transport in the Natural System at Waste Management Area C*, Rev. 2, Washington River Protection Solutions, LLC/TecGeo, Inc./GSI Water Solutions, Inc., Richland, Washington.

RPP-RPT-58291, 2017, *Hanford Waste Management Area A-AX Soil Contamination Inventory Estimates*, Rev. 1, Washington River Protection Solutions, LLC, Richland, Washington.

RPP-RPT-58293, 2017, *Hanford 241-A and 241-AX Farm Tank and Ancillary Equipment Residual Waste Inventory Estimates*, Rev. 1, Washington River Protection Solutions, LLC, Richland, Washington.

RPP-RPT-58540, 2015, *Assessment Context for the WMA A-AX Closure Performance Assessment*, Rev. 0, Washington River Protection Solutions, LLC, Richland, Washington.

RPP-RPT-58693, 2020, *Engineered System Data Package for Waste Management Area A-AX*, Rev. 0, Washington River Protection Solutions, LLC, Richland, Washington.

RPP-RPT-60171, in process, *Model Package Report: Geologic Framework Model used in WMA A-AX Performance Assessment and RCRA Closure Analysis*, Rev. 0, Washington River Protection Solutions, LLC, Richland, Washington.

RPP-RPT-60885, 2020, *Model Package Report System Model for the WMA A-AX Performance Assessment*, Rev. 0, Washington River Protection Solutions, LLC, Richland, Washington.

Rumbaugh, J. O. and D. B. Rumbaugh, 2007, "Guide to Using Groundwater Vistas, Version 5," Environmental Simulations, Inc., Reinholds, Pennsylvania.

Russo, D., 1991, "Stochastic Analysis of Simulated Vadose Zone Solute Transport in a Vertical Cross Section of Heterogeneous Soil During Nonsteady Water Flow," *Water Resources Research*, Vol. 27, Issue 3, pp. 267–283.

Schaap, M. G. and F. J. Leij, 2000, "Improved prediction of unsaturated hydraulic conductivity with the Mualem-van Genuchten model," *Soil Science Society of America Journal*, Vol. 64, Issue 3, pp. 843–851.

Schulze-Makuch, D., 2005, "Longitudinal Dispersivity Data and Implications for Scaling Behavior," *Ground Water*, Vol. 43, Issue 3, pp. 443–456.

SESDGUID-101-R1, 2013, *Design and Installation of Monitoring Wells*, U.S. Environmental Protection Agency, Science and Ecosystem Support Division, Athens, Georgia.

SGW-54165, 2014, *Evaluation of the Unconfined Aquifer Hydraulic Gradient Beneath the 200 East Area, Hanford Site*, Rev. 0, CH2M HILL Plateau Remediation Company, Richland, Washington.

Song, B. and R. S. Amano, 2010, "A higher-order bounded discretization scheme," Chapter 1, Computational Fluid Dynamics and Heat Transfer, R. S. Amano and B. Sundén (eds.), pp. 3–18, WIT Press, Ashurst, Southampton, UK.

Stevens, R., 2004, "Management of Restored and Revegetated Sites" in General Technical Report RMRS-GTR-136-vol.-1, *Restoring Western Ranges and Wildlands*, Volume 1, compiled by S. B. Monsen, R. Stevens, and N. L. Shaw, U.S. Department of Agriculture, Forest Service, Rocky Mountain Research Station Fort Collins, Colorado.

van Genuchten, M. Th., 1980, "A Closed-form Equation for Predicting the Hydraulic Conductivity of Unsaturated Soils," *Soil Science Society of America Journal*, Vol. 44, No. 5, pp. 892–898.

WA7 89000 8967, 2007, *Hanford Facility Resource Conservation and Recovery Act Permit, Dangerous Waste Portion Revision 8C for the Treatment, Storage, and Disposal of Dangerous Waste*, State of Washington Department of Ecology, Richland, Washington.

WAC 173-340-747, "Deriving Soil Concentrations for Groundwater Protection," *Washington Administrative Code*, as amended.

WAC 246-290, "Group A Public Water Supplies," *Washington Administrative Code*, as amended.

WAC 246-290-310, "Maximum Contaminant Levels (MCLs) and Maximum Residual Disinfectant Levels (MRDLs)," *Washington Administrative Code*, as amended.

WCH-233, 2007, *2007 River Corridor Closure Contractor Revegetation and Mitigation Monitoring Report*, Rev. 0, Washington Closure Hanford, Richland, Washington.

WCH-520, 2013, *Performance Assessment for the Environmental Restoration Disposal Facility, Hanford Site, Washington*, Rev. 1, Washington Closure Hanford, Richland, Washington.

WHC-EP-0645, 1995, *Performance Assessment for the Disposal of Low-Level Waste in the 200 West Area Burial Grounds*, Westinghouse Hanford Company, Richland, Washington.

WHC-EP-0883, 1995, *Variability and Scaling of Hydraulic Properties for 200 Area Soils, Hanford Site*, Westinghouse Hanford Company, Richland, Washington.

WHC-SD-WM-EE-004, 1995, *Performance Assessment of Grouted Double-Shell Tank Waste Disposal at Hanford*, Rev. 1, Westinghouse Hanford Company, Richland, Washington.

WSRC-MS-2003-00582, 2003, *Performance Assessment/Composite Analysis Modeling to Support a Holistic Strategy for the Closure of F Area, a Large Nuclear Complex at the Savannah River Site*, Rev. 1, Savannah River Technology Center, Aiken, South Carolina.

Xu, M. and Y. Eckstein, 1995, "Use of Weighted Least-Squares Method in Evaluation of the Relationship between Dispersivity and Field Scale," *Ground Water*, Vol. 33, Issue 6, pp. 905–908.

Yeh, T.-C. J., M. Ye, and R. Khaleel, 2005, "Estimation of effective unsaturated hydraulic conductivity tensor using spatial moments of observed moisture plume," *Water Resources Research*, Vol. 41, Issue 3, W03014, pp. 1–12.

Zhang Z. F., 2016, "Evaluating the long-term hydrology of an evapotranspiration-capillary barrier with a 1000 year design life," *Water Resources Research*, Vol. 52, Issue 6, pp. 4883–4904.

Zhang Z. F., 2017, "Long-Term Drainage from the Riprap Side Slope of a Surface Barrier," *Water*, Vol. 8, pp. 156–164.

Zhang, Z. F., A. L. Ward, and G. W. Gee, 2003, "A Tensorial Connectivity–Tortuosity Concept to Describe the Unsaturated Hydraulic Properties of Anisotropic Soils," *Vadose Zone Journal*, Vol. 2, No. 3, pp. 313–321.

Zhang, Z. F., and R. Khaleel, 2010, "Simulating field-scale moisture flow using a combined power-averaging and tensorial connectivity-tortuosity approach," *Water Resources Research*, Vol. 46, Issue 9, W09505, pp. 1–14.

Zhang Z. F., C. E. Strickland, and S. O. Link, 2017, "Design and Performance Evaluation of a 1000-year Evapotranspiration-Capillary Surface Barrier," *Journal of Environmental Management*, Vol. 187, pp. 31–42.

Zhang Z. F., M. D. Freshley, D. M. Wellman, J. G. Morse, and K. D. Leary, 2016, "Performance of a Surface Barrier for Waste Isolation and Flux Reduction at the Hanford Site" in *Proceedings of the 42nd Annual Waste Management Conference (WM2016),* Paper No. 16099, Phoenix, Arizona.

APPENDIX A

KEY ASSUMPTIONS IN THE PERFORMANCE ASSESSMENT

This page intentionally left blank.

APPENDIX A KEY ASSUMPTIONS IN THE PERFORMANCE ASSESSMENT

A.1 LIST OF ASSUMPTIONS

- The time of closure of Waste Management Area (WMA) A-AX, related ancillary equipment, and adjacent double-shell tank farms is assumed to be January 1, 2050, consistent with the assumptions in the Tank Closure and Waste Management Environmental Impact Statement (DOE/EIS-0391, *Final Tank Closure and Waste Management Environmental Impact Statement for the Hanford Site, Richland, Washington*). The assumed closure date establishes the reference time for inventory of radionuclides in residual waste and the timing of changes in ground surface conditions that control infiltration rates. Additional details of the assumptions with respect to closure are provided in RPP-RPT-58693, *Engineered System Data Package for Waste Management Area A-AX*.

- The Central Plateau has been designated Industrial-Exclusive for the indefinite future, based on several Records of Decision [64 FR 61615, "Record of Decision: Hanford Comprehensive Land-Use Plan Environmental Impact Statement (HCP EIS)"; 73 FR 55824, "Amended Record of Decision for the Hanford Comprehensive Land-Use Plan Environmental Impact Statement"]. This area, which includes the 200 East and 200 West Areas, includes WMA A-AX. There is no stated intention to release the Central Plateau from this designation or from U.S. Department of Energy (DOE) control at any time in the future. Despite this designation, it is assumed in this analysis that institutional control and societal memory of the disposal activities are lost 100 years after site closure, for consistency with DOE O 435.1, *Radioactive Waste Management* requirements. This assumption is necessary to allow future hypothetical individuals to come onto the Central Plateau and engage in activities that might result in exposure.

- In initial model implementation using Alternative Conceptual Model 1, the land use and land cover, including the barrier, remain shrub steppe indefinitely after closure (RPP-RPT-58693). Alternative infiltration rates in the future are included in alternative analysis cases, which are intended to address a variety of potential future conditions, including progression to different land uses and land covers.

- The engineered cover for WMA A-AX is not yet designed but is assumed to be similar to the Modified *Resource Conservation and Recovery Act of 1976* (RCRA) Subtitle C Barrier that limits infiltration through the waste primarily by evapotranspiration processes (i.e., surface barrier) based on the work done for the Hanford Prototype barrier (DOE/ORP-2008-01, *RCRA Facility Investigation Report for Hanford Single-Shell Tank Waste Management Areas*, Appendix C). These processes are not modeled directly for this report, but those processes have been studied through field measurements, tracer studies, and numerical models to estimate net infiltration (PNNL-14744, *Recharge Data Package for the 2005 Integrated Disposal Facility Performance Assessment*; PNNL-14960, *200-BP-1 Prototype Hanford Barrier Annual Monitoring Report for Fiscal Year 2004*; "Multiple-Year Water Balance of Soil Covers in a Semiarid Setting" [Fayer

and Gee 2006]). Instead, the recommended net infiltration rates from those reports are applied to the area under the engineered cover and are varied spatially and temporally as appropriate according to the estimated or assumed time-dependent performance of a surface barrier.

- It is assumed the tanks will be filled with grout according to the basic assumptions outlined for landfill closure in DOE/EIS-0391 and the ensuing December 13, 2013 DOE Record of Decision (78 FR 75913, "Record of Decision: Final Tank Closure and Waste Management Environmental Impact Statement for the Hanford Site, Richland, Washington"). The specific formulation of the grout has not yet been established, but consistent with DOE/EIS-0391 (2012), it is assumed the fill material for the tanks will be similar to the cold-cap grout formulation developed by the U.S. Army Corps of Engineers for the Hanford Grout Vault Program.

- Radionuclide and chemical release mechanisms from the sources are assumed to occur by one of two mechanisms: (a) the entire inventory of the residual waste is assumed to be instantly available for release and transport out of the tanks, or (b) a semi-empirical release function is applied based on leach tests performed on residual waste from WMA C (RPP-RPT-58693).

- Transport of contamination from the tanks is assumed to be primarily controlled by diffusion from the grouted tanks through the base mat at the bottom of the tank (RPP-RPT-58693). This assumption provides the basis for the sensitivity cases included in the performance assessment that evaluate the consequences of earlier hydraulic failure (i.e., fracturing) of the grouted tanks that would include the base mat at the bottom of the tank. For the tanks in 241-AX Tank Farm, an implicit part of this assumption is that the 12-in. pipes connecting the leak detection wells to the drain slot network in the base of each single-shell tank (SST) will be grouted, whereas the drain slots themselves may or may not be completely grouted (see RPP-RPT-58693).

- The specific formulation of the grout has not yet been established, and site-specific measurements of the chemical influence of the grout have not been performed. The chemical effect of the presence of grout in the tank and the cementitious material that make the tank base mat is represented by contaminant-specific distributions of distribution coefficients (K_d), which have been developed from international literature on sorption of radionuclides on cementitious materials. These values are consistent with comparable values used for the facility-specific grout at the Savannah River F and H tank farm performance assessments [WSRC-STI-2007-00369, *Hydraulic and Physical Properties of Tank Grouts and Base Mat Surrogate Concrete for FTF Closure* and WSRC-STI-2007-00607, *Chemical Degradation Assessment of Cementitious Materials for the HLW Tank Closure Project (U)*].

- Release and migration of radionuclides and chemicals from each WMA A-AX source are independent of the other sources.

- The post-retrieval inventory of contaminants in WMA A-AX is assumed to be uniformly distributed throughout the waste residual volume. The residual volume in the tanks is assumed to be a uniform layer distributed at the bottom of the tanks. In ancillary equipment, which includes waste transfer pipelines, the residual waste is assumed to be distributed in a homogeneous layer across each SST farm at the approximate depth and over an approximate area where waste transfer pipelines and other ancillary equipment exist in the general vicinity of WMA A-AX.

- Tanks in WMA A-AX have yet to be retrieved, so inventories for tanks are based on a range of estimates of post-retrieval conditions that are available at time of publication. The approach and results of this estimation process are documented in RPP-CALC-62319, *Residual Waste Source Inventory Term for the Waste Management Area A-AX Performance Assessment Inventory Case 1* and RPP-RPT-58293, *Hanford 241-A and 241-AX Farm Tank and Ancillary Equipment Residual Waste Inventory Estimates*, which present the basis for chemical and radiological inventory estimates for residual waste remaining in WMA A-AX SSTs and associated transfer equipment after tank waste is retrieved. The radionuclide part of these inventories is decayed to January 1, 2050. Separate calculations are used to adjust these radionuclide inventories to the assumed time of closure.

- Transport of contamination from ancillary equipment is assumed to be primarily controlled by advection since much of the estimated inventory for ancillary equipment in RPP-RPT-58293 is attributed to the pipelines, and grouting the pipelines may not be practical. The effect of pipeline encasements is ignored. Although some of the other ancillary equipment may be grouted consistent with 78 FR 75913, it is assumed for the purpose of the analysis that none of the ancillary equipment will be grouted.

- The vadose zone is modeled as an aqueous-gas porous media system where flow and transport through the gas phase are assumed to be negligible.

- While geologic units typically exhibit some degree of heterogeneity, each geologic unit within the vadose zone is represented as a homogeneous material with upscaled, effective hydraulic properties.

- In specifying boundary conditions for the model domain, post-closure groundwater flow is assumed to be northwest to southeast (local flow directions vary within the domain). The justification for this assumption is found in Appendix C. Groundwater flow parameters have been derived from the Central Plateau groundwater model (CP-47631, *Model Package Report: Central Plateau Groundwater Model Version 8.4.5*).

- Distribution coefficients (K_d) are used to represent sediment-contaminant adsorptive-desorptive interaction that best represent plausible levels of reactivity, with a bias toward lower adsorption in cases where data are limited. Groups of radionuclides that show similar levels of chemical reactivity with Hanford soils and sediments were assigned the same K_d values. Justification for the selected parameter values is found in

PNNL-17154, *Geochemical Characterization Data Package for the Vadose Zone in the Single-Shell Tank Waste Management Areas at the Hanford Site*; PNNL-16663, *Geochemical Processes Data Package for the Vadose Zone in the Single-Shell Tank Waste Management Areas at the Hanford Site*; and RPP-ENV-58782, *Performance Assessment of Waste Management Area C, Hanford Site, Washington* and references therein. In addition, uncertainties in K_d values are assessed as part of the uncertainty analysis using the system model (RPP-RPT-60885, *Model Package Report System Model for the WMA A-AX Performance Assessment*).

- The points of calculation for evaluation of groundwater concentration correspond to the location about 100 m downgradient from the facility per DOE O 435.1. To calculate groundwater concentrations for comparison with groundwater protection requirements, it is necessary to identify the peak location in space at which the concentration occurs.

A.2 REFERENCES

64 FR 61615, 1999, "Record of Decision: Hanford Comprehensive Land-Use Plan Environmental Impact Statement (HCP EIS)," *Federal Register*, Vol. 64, pp. 61615–61625 (November 12).

73 FR 55824, 2008, "Amended Record of Decision for the Hanford Comprehensive Land-Use Plan Environmental Impact Statement," *Federal Register*, Vol. 73, pp. 55824–55826 (September 26).

78 FR 75913, 2013, "Record of Decision: Final Tank Closure and Waste Management Environmental Impact Statement for the Hanford Site, Richland, Washington," *Federal Register*, Vol. 78, pp. 75913–75919 (December 13).

CP-47631, 2017, *Model Package Report: Central Plateau Groundwater Model Version 8.4.5*, Rev. 4, CH2M HILL Plateau Remediation Company, Richland, Washington.

DOE/EIS-0391, 2012, *Final Tank Closure and Waste Management Environmental Impact Statement for the Hanford Site, Richland, Washington*, U.S. Department of Energy, Washington, D.C.

DOE O 435.1, 2001, *Radioactive Waste Management*, U.S. Department of Energy, Washington, D.C.

DOE/ORP-2008-01, 2010, *RCRA Facility Investigation Report for Hanford Single-Shell Tank Waste Management Areas*, Rev. 1, U.S. Department of Energy, Office of River Protection, Richland, Washington.

Fayer, M. J., and G. W. Gee, 2006, "Multiple-Year Water Balance of Soil Covers in a Semiarid Setting," *Journal of Environmental Quality*, Vol. 35, No. 2, pp. 366–377.

PNNL-14744, 2004, *Recharge Data Package for the 2005 Integrated Disposal Facility Performance Assessment*, Pacific Northwest National Laboratory, Richland, Washington.

PNNL-14960, 2005, *200-BP-1 Prototype Hanford Barrier Annual Monitoring Report for Fiscal Year 2004*, Pacific Northwest National Laboratory, Richland, Washington.

PNNL-16663, 2007, *Geochemical Processes Data Package for the Vadose Zone in the Single-Shell Tank Waste Management Areas at the Hanford Site*, Pacific Northwest National Laboratory, Richland, Washington.

PNNL-17154, 2008, *Geochemical Characterization Data Package for the Vadose Zone in the Single-Shell Tank Waste Management Areas at the Hanford Site*, Pacific Northwest National Laboratory, Richland, Washington.

Resource Conservation and Recovery Act of 1976, 42 USC 6901, et seq.

RPP-CALC-62319, (in preparation), *Residual Waste Source Inventory Term for the Waste Management Area A-AX Performance Assessment Inventory Case 1*, Rev. 0, Washington River Protection Solutions, LLC, Richland, Washington.

RPP-ENV-58782, 2016, *Performance Assessment of Waste Management Area C, Hanford Site, Washington*, Rev. 0, Washington River Protection Solutions, LLC, Richland, Washington.

RPP-RPT-58293, 2017, *Hanford 241-A and 241-AX Farm Tank and Ancillary Equipment Residual Waste Inventory Estimates*, Rev. 1, Washington River Protection Solutions, LLC, Richland, Washington.

RPP-RPT-58693, 2020, *Engineered System Data Package for Waste Management Area A-AX*, Rev. 0, Washington River Protection Solutions, LLC, Richland, Washington.

RPP-RPT-60885, 2020 *Model Package Report System Model for the WMA A-AX Performance Assessment*, Rev. 0, Washington River Protection Solutions, LLC, Richland, Washington.

WSRC-STI-2007-00369, 2007, *Hydraulic and Physical Properties of Tank Grouts and Base Mat Surrogate Concrete for FTF Closure*, Rev. 0, Savannah River National Laboratory, Aiken, South Carolina.

WSRC-STI-2007-00607, 2007, *Chemical Degradation Assessment of Cementitious Materials for the HLW Tank Closure Project (U)*, Rev. 0, Washington Savannah River Company/ Savannah River National Laboratory, Aiken, South Carolina.

This page intentionally left blank.

APPENDIX B

DEVELOPMENT OF VADOSE ZONE HYDRAULIC AND TRANSPORT PROPERTIES FOR WASTE MANAGEMENT AREA A-AX PERFORMANCE ASSESSMENT

This page intentionally left blank.

CONTENTS

APPENDIX B – DEVELOPMENT OF VADOSE ZONE HYDRAULIC AND TRANSPORT PROPERTIES FOR WASTE MANAGEMENT AREA A-AX PERFORMANCE ASSESSMENT B-1

B.1 MODELING APPROACH FOR VADOSE ZONE FLOW AND TRANSPORT B-1

B.2 CONSTITUTIVE RELATIONSHIPS FOR DETERMINING MOISTURE CONTENT AND UNSATURATED HYDRAULIC CONDUCTIVITY B-4

B.3 MOISTURE-DEPENDENT ANISOTROPY B-5

B.3.1 Variable Anisotropy Model B-6

B.4 ESTIMATION OF HYDRAULIC PROPERTIES B-9

B.4.1 Particle Size Distribution Data and Grouping of Hydrostratigraphic Units B-10

B.4.2 Sand-Dominated Units B-14

B.4.3 Gravel-Dominated Units B-21

B.4.4 Fine-Grained Units B-23

B.4.5 Effective Soil-Moisture Retention B-25

B.4.6 Effective Unsaturated Hydraulic Conductivity and Variable Anisotropy B-27

B.5 MOISTURE CONTENT MEASUREMENTS B-32

B.6 EFFECTIVE TRANSPORT PROPERTIES B-39

B.6.1 Bulk Density B-39

B.6.2 Diffusivity B-40

B.6.3 Vadose Zone Macrodispersivities B-40

B.7 REFERENCES B-44

FIGURES

Figure B-1. Illustration of Modeling Approaches for a Heterogeneous Geologic Outcrop (a) using an Anisotropic Equivalent Homogeneous Medium Representation with Each Unit Having its Own Uniform Average Properties (b), and using Different Hydraulic Properties for Each Grid Block in the Model Grid Representing the Outcrop (c).....B-2

Figure B-2. Schematic Illustrating Pressure Head Distributions during an Infiltration Experiment to Explain Moisture-Dependent Anisotropy (blue curves).....B-6

Figure B-3. Schematic Illustrating Contrast in Macroscopic Anisotropy Behavior for Saturated Media (left) versus Unsaturated Media (right). B-7

Figure B-4. Location of Waste Management Area A-AX Boreholes with ROCSAN Sieve Data.....B-13

Figure B-5. Waste Management Area C Hanford H2 Sand-Dominated Core. B-15

Figure B-6. Moisture Retention Data (44 Samples) (a) and Unsaturated Hydraulic Conductivity Data (44 Samples) (b) for the Sand-Dominated Units at Waste Management Area A-AX. B-19

Figure B-7. Typical Backfill (a) and Hanford H1 Unit Samples (b) from Borehole C4297....B-20

Figure B-8. Typical Gravel-Dominated CCUg Unit Sample from Waste Management Area B-BX-BY Borehole 299-E33-45. .....B-22

Figure B-9. Unsaturated Hydraulic Conductivity Measurements for Sand-Dominated and Gravel-Dominated Samples. B-23

Figure B-10. Typical Silt-Dominated Cold Creek Unit Sample from Waste Management Area B-BX-BY Borehole 299-E33-45. .....B-25

Figure B-11. Effective Moisture Retention Curves for the (a) Sand-Dominated, (b) Gravel-Dominated and (c) Fine-Textured Units at Waste Management Area A-AX.....B-28

Figure B-12. Effective Unsaturated Hydraulic Conductivities for the (a) Sand-Dominated, (b) Gravel-Dominated, and (c) Fine-Textured Units at Waste Management Area A-AX.....B-33

Figure B-13. Variable Tension Dependent Anisotropy for the (a) Sand-Dominated, (b) Gravel-Dominated, and (c) Fine-Textured Units at Waste Management Area A-AX.....B-36

Figure B-14. Longitudinal Laboratory- and Field-Scale Dispersivities in Unsaturated Media as a Function of Overall Problem Scale.....B-43

TABLES

Table B-1. Gravel, Sand, and Mud (Silt and Clay) Fractions for Various Hydrostratigraphic Units at Waste Management Area A-AX.....B-10

Table B-2. Average Gravel Content for Waste Management Area A-AX Hydrostratigraphic Units Based on ROCSAN Sieve Data.....B-14

Table B-3. The van Genuchten Parameters and Saturated Hydraulic Conductivity Data for 44 Borehole Samples Used to Represent the Sand-Dominated Units at Waste Management Area A-AX. B-17

Table B-4. The van Genuchten Parameters and Saturated Hydraulic Conductivity Data for the 25 Samples Used to Represent the Gravel-Dominated Units at Waste Management Area A-AX. B-24

Table B-5. The van Genuchten Parameters and Saturated Hydraulic Conductivity Data for the Ten Samples Used to Represent the Fine-Textured Units at Waste Management Area A-AX. B-26

Table B-6. Typical Cases with Varying Degrees of Anisotropy. B-31

Table B-7. Summary Statistics for Waste Management Area A-AX Alternative Conceptual Model 1 Moisture Content (% Volume) Database.....B-39

Table B-8. Bulk Density Estimates for Hydrostratigraphic Units at Waste Management Area A-AX.....B-40

TERMS

3-D	three-dimensional
ACM	Alternative Conceptual Model
CCU	Cold Creek Unit
CCUg	Cold Creek Unit gravel
CCUs	Cold Creek Unit sand
CCUz	Cold Creek Unit silt
EHM	equivalent homogeneous medium
H1	Hanford formation unit 1
H2	Hanford formation unit 2
H3	Hanford formation unit 3
HSU	hydrostratigraphic unit
IDF	Integrated Disposal Facility
MRC	moisture retention curve
PA	performance assessment
PA-TCT	power-averaging and tensorial connectivity-tortuosity (model)
RCRA	*Resource Conservation and Recovery Act of 1976*
SST	Single-Shell Tank
STOMP	Subsurface Transport Over Multiple Phases
TCT	tensorial connectivity tortuosity
WMA	Waste Management Area

APPENDIX B DEVELOPMENT OF VADOSE ZONE HYDRAULIC AND TRANSPORT PROPERTIES FOR WASTE MANAGEMENT AREA A-AX PERFORMANCE ASSESSMENT

This appendix provides a detailed description of the development and implementation of a conceptual model for vadose zone flow and transport for the Waste Management Area (WMA) A-AX performance assessment (PA) groundwater pathway analysis. The appendix also describes the basis for the selection of hydraulic properties for the hydrostratigraphic units (HSUs) identified at WMA A-AX. No WMA A-AX site-specific data are available that can be used to directly develop estimates of hydraulic properties needed for the PA. Thus, a process has been developed for identifying surrogate hydraulic properties based on samples collected at other sites within the 200 Areas and nearby locations that are representative of sediments characteristic of the major HSUs identified at WMA A-AX. RPP-RPT-60171, *Model Package Report: Geologic Framework Model used in WMA A-AX Performance Assessment and RCRA Closure Analysis* and the HSUs identified therein serve as the basis for the development of this appendix.

The following information is included in this appendix:

- A detailed description and technical basis for the conceptual model selected to represent vadose zone flow and transport at WMA A-AX (see Sections B.1, B.2 and B.3)
- A discussion of the evaluation of laboratory measurements of samples collected near WMA A-AX and nearby locations for vadose zone soil moisture retention and saturated and unsaturated hydraulic conductivity, and how these data were used as the basis for the selection of hydraulic properties for the major HSUs identified at WMA A-AX (see Section B.4)
- A summary of effective (upscaled) moisture retention, saturated and unsaturated hydraulic conductivity, bulk density, diffusivity, and macrodispersivity estimates used for various HSUs identified at WMA A-AX (see Sections B.4, B.5, and B.6).

B.1 MODELING APPROACH FOR VADOSE ZONE FLOW AND TRANSPORT

Within the 200 Areas of the Hanford Site, vadose zone sediments are heterogenous at a variety of scales. For example, an outcrop, provided in Figure B-1(a), provides an illustrative example of the inherent variability in geologic media that can be observed in vadose zone sediments. Depending on the resolution needed in a modeling analysis of this outcrop, a variety of conceptual models can be developed and implemented to approximate flow through this example outcrop with heterogeneous media. With respect to predictive resolution, however, geologic conceptual models can be classified into two broad categories: (1) an equivalent homogeneous medium (EHM) model, and (2) a heterogeneous model.

Following the EHM modeling approach, the outcrop [Figure B-1(a)], for instance, may be mapped into three distinct large-scale geologic formations based on facies distribution [Figure B-1(c)]. Each HSU is then assumed to have representative but uniform values in terms

of vadose zone hydraulic properties, and each HSU is treated as an anisotropic EHM. On the contrary, [Figure B-1(b)], in effect, conceptualizes the heterogeneous geologic media as a collection of numerous small blocks with different hydraulic properties, mimicking the detailed spatial variability that is inherent in geologic deposits.

Figure B-1. Illustration of Modeling Approaches for a Heterogeneous Geologic Outcrop (a) using an Anisotropic Equivalent Homogeneous Medium Representation with Each Unit Having its Own Uniform Average Properties (b), and using Different Hydraulic Properties for Each Grid Block in the Model Grid Representing the Outcrop (c). (1 of 2 sheets)

(a)

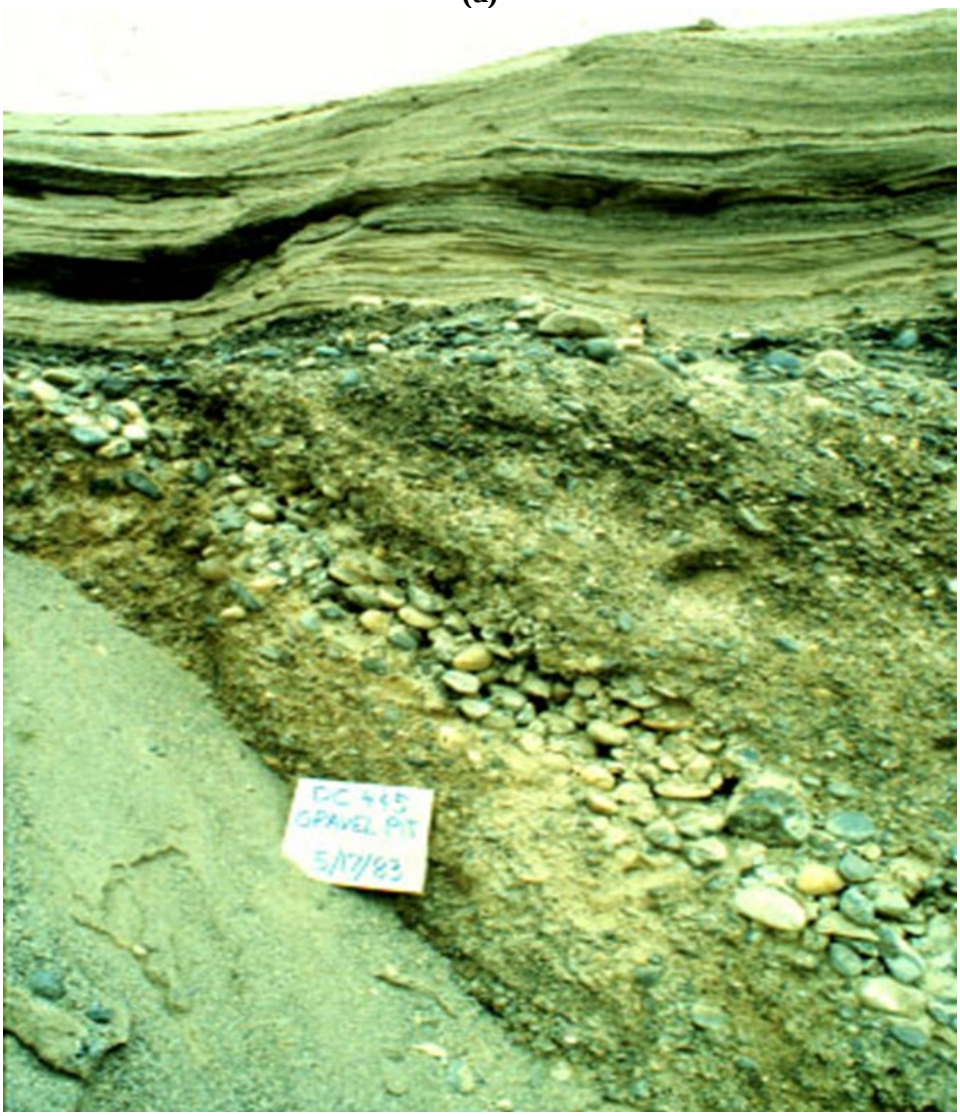

Figure B-1. Illustration of Modeling Approaches for a Heterogeneous Geologic Outcrop (a) using an Anisotropic Equivalent Homogeneous Medium Representation with Each Unit Having its Own Uniform Average Properties (b), and using Different Hydraulic Properties for Each Grid Block in the Model Grid Representing the Outcrop (c). (2 of 2 sheets)

(b)

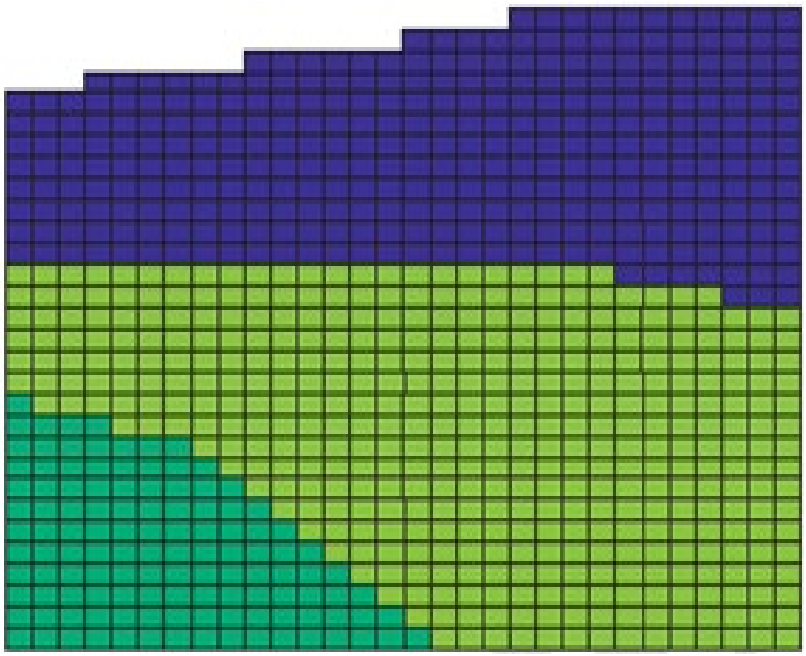

(c)

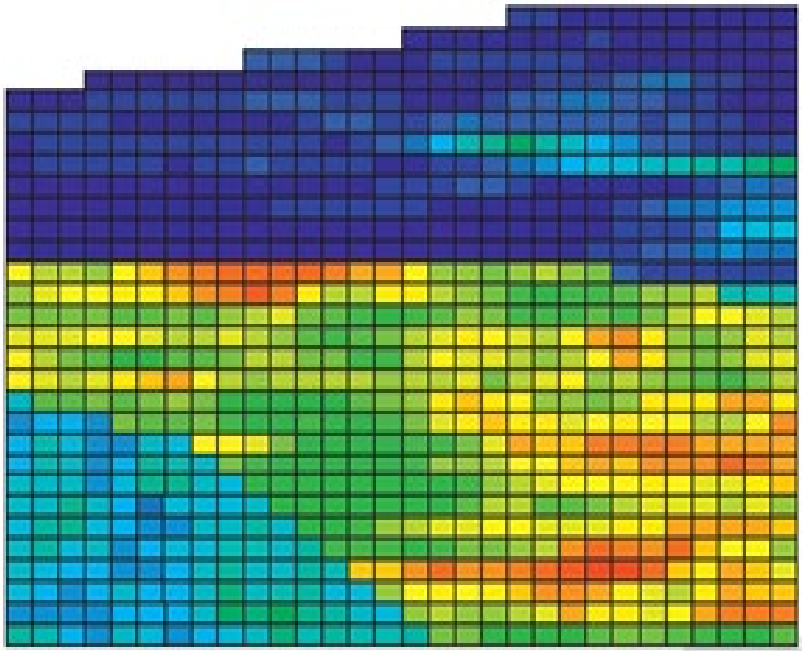

Adapted from "Estimation of effective unsaturated hydraulic conductivity tensor using spatial moments of observed moisture plume" (Yeh et al. 2005).

For this PA, the anisotropic EHM approximation [Figure B-1(b)] was selected for modeling flow and transport at WMA A-AX. This approach is deemed sufficient to meet the objectives of the PA and is consistent with the approach adopted by most modeling studies at Hanford. As discussed below, the equivalent homogeneous conceptual modeling approach uses small-scale laboratory measurements to predict the large, field-scale flow behavior.

B.2 CONSTITUTIVE RELATIONSHIPS FOR DETERMINING MOISTURE CONTENT AND UNSATURATED HYDRAULIC CONDUCTIVITY

The selected flow and transport codes for the WMA A-AX PA modeling are the Subsurface Transport Over Multiple Phases (STOMP[14]) simulator and the multi-processor capable extreme-scale STOMP (eSTOMP) simulator. Moisture content is a function of soil matric potential; the soil matric potential-moisture content relationships are described for each HSU using the following empirical relationship ("A Closed-form Equation for Predicting the Hydraulic Conductivity of Unsaturated Soils" [van Genuchten 1980]):

$$\theta(h) = \theta_r + (\theta_s - \theta_r)\{1 + [\alpha h]^n\}^{-m} \tag{B-1}$$

where $\theta(h)$ is the moisture content, here expressed explicitly as a function of the soil matric potential, and the other terms are defined as follows:

θ_r = residual moisture content (dimensionless)
θ_s = saturated moisture content (dimensionless)
α = a fitting parameter (cm^{-1})
n = a fitting parameter (dimensionless)
m = $1 - 1/n$.

Combining the van Genuchten model with Mualem's (1976) model ("A New Model for Predicting the Hydraulic Conductivity of Unsaturated Porous Media") for unsaturated conductivity produces the following relationship for unsaturated hydraulic conductivity:

$$K(S_e) = K_s S_e^l \left\{1 - \left(1 - S_e^{(1/m)}\right)^m\right\}^2 \tag{B-2}$$

where $K(S_e)$ is the hydraulic conductivity (cm/s), which is, as expressed, dependent on the effective saturation, S_e; K_s is the saturated hydraulic conductivity (cm/s); and l is a pore-connectivity parameter (dimensionless) that Mualem (1976) estimated as being about 0.5 based on an average of 45 samples. The effective saturation is determined from the equation:

$$S_e = \frac{(\theta(h) - \theta_r)}{(\theta_s - \theta_r)} \tag{B-3}$$

[14] Subsurface Transport Over Multiple Phases (STOMP) is developed and distributed by Battelle Memorial Institute.

For the WMA A-AX PA, l is treated as being directional and pore-interaction terms l_{xx}, l_{yy}, and l_{zz} are defined to characterize the large, field-scale variable, moisture-dependent anisotropy invoked as part of EHM modeling. While other constitutive relations are available and programmed in STOMP and eSTOMP, the van Genuchten-Mualem formulation is used because of the existence of an extensive database for Hanford sediments using this formulation (e.g., WHC-EP-0883, *Variability and Scaling of Hydraulic Properties for 200 Area Soils*).

B.3 MOISTURE-DEPENDENT ANISOTROPY

Earlier work in hydrology literature treated anisotropy of unsaturated hydraulic conductivity as an intrinsic property, the same as the anisotropy in saturated hydraulic conductivity. Thus, the unsaturated hydraulic conductivity anisotropy has often been modeled by scaling the unsaturated hydraulic conductivity—hydraulic head relationship in different directions as in saturated media. The anisotropy thus remains constant over the full range of saturation or pressure head – a constant anisotropy concept. However, such a simplistic approach is inappropriate due to the presence of highly nonlinear relationship that is prevalent between the unsaturated hydraulic conductivity and the pressure head or matric potential.

The anisotropy of the unsaturated effective hydraulic conductivity of an EHM can vary with pressure head or moisture content. This phenomenon is referred to as moisture- or pressure head-dependent anisotropy ("Stochastic Analysis of Unsaturated Flow in Heterogeneous Soils, 2. Statistically Anistropic Media with Variable α" [Yeh et al. 1985]). An interesting finding of the Yeh et al. (1985) analysis is that the macroscopic anisotropy of the effective unsaturated hydraulic conductivity for an EHM varies with the *mean* pressure head or the *mean* moisture content (i.e., moisture-dependent anisotropy). That is, the ratio of the effective unsaturated hydraulic conductivity in the direction parallel to bedding to that in the direction perpendicular to bedding increases as the medium becomes less saturated. Such a unique behavior provides explanation for the ubiquitous lateral spreading of observed moisture plumes in the stratified Hanford sediments (e.g., "Estimation of effective unsaturated hydraulic conductivity tensor using spatial moments of observed moisture plume" [Yeh et al. 2005]).

An illustrative sketch of the pressure head distribution during an infiltration event in a stratified heterogeneous media is shown in Figure B-2. Near the infiltration source where the degree of saturation is high, the pressure head contour is generally smooth and symmetrical (dark blue contour). Away from the infiltration source, the pressure head contours (light green and yellow contours) become more irregular and asymmetrical (i.e., large variability). Overall, the pressure head distributions spread out to greater distances horizontally because of media heterogeneities.

In the same Figure B-2, the pressure head distributions calculated from an equivalent homogeneous and isotropic conceptual model are depicted by the black dashed lines. They are smooth and symmetrical, and are elongated in the vertical direction, reflecting effects of gravity and hydraulic conductivity isotropy. Nonetheless, this homogeneous and isotropic conceptual model apparently overestimates the vertical migration and underestimates the horizontal spreading of the actual moisture plume in the field.

Figure B-2. Schematic Illustrating Pressure Head Distributions during an Infiltration Experiment to Explain Moisture-Dependent Anisotropy (blue curves).

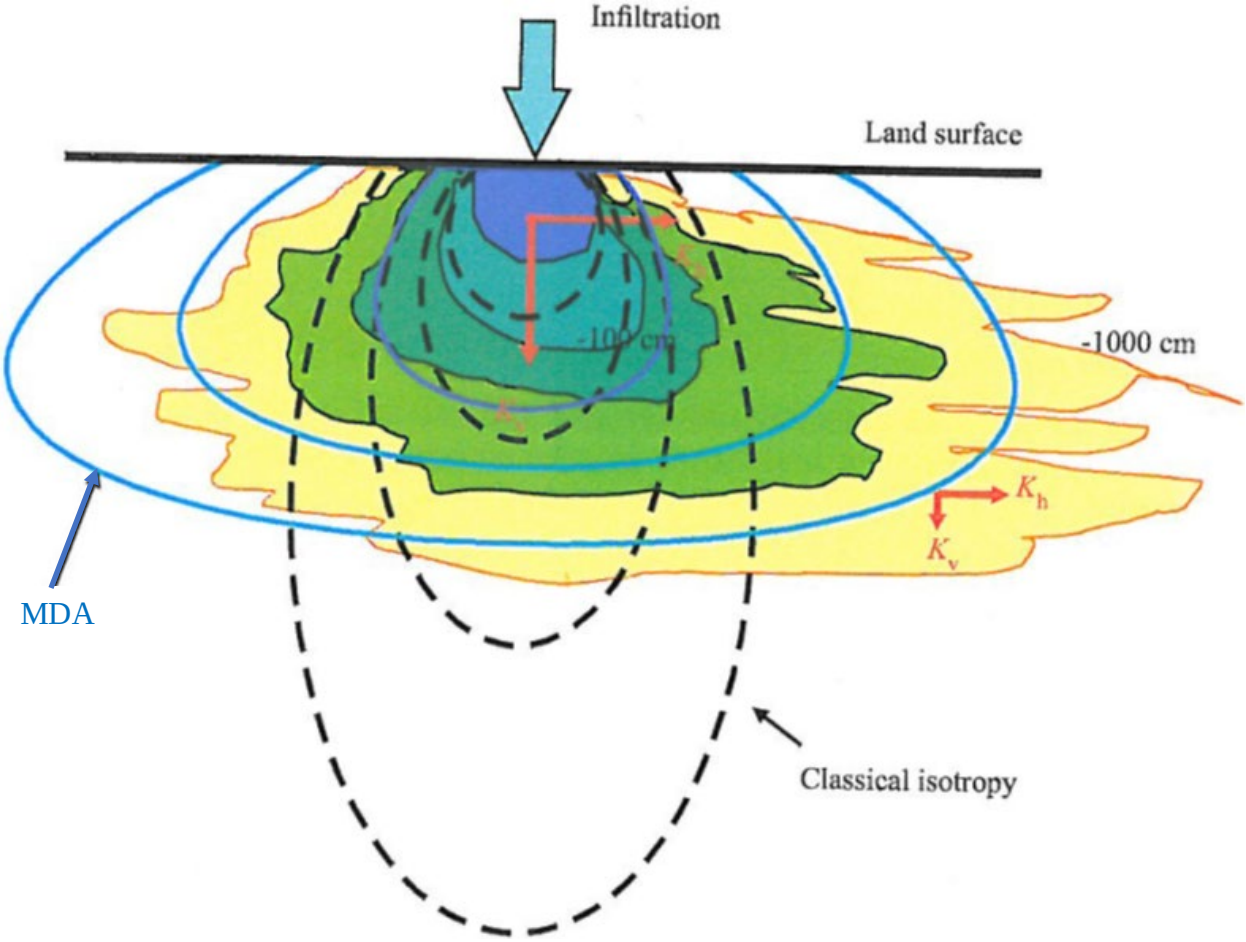

Note: The lengths of the red arrows denote the magnitudes of unsaturated hydraulic conductivity in the horizontal direction (K_h) and in the vertical direction (K_v) at the pressure head of the given location. MDA = moisture-dependent anisotropy.

Source: Flow Through Heterogeneous Geologic Media (Yeh et al. 2015).

The light blue solid lines (Figure B-2) are the simulated pressure head distributions for an EHM model with moisture-dependent anisotropy. That is, the hydraulic conductivity values in the horizontal and the vertical directions are almost the same near the infiltration source where the soil is wet. In the region where the soil is dry, both the horizontal and vertical hydraulic conductivities are smaller than those in the wet region, but the ratio of the horizontal hydraulic conductivity to the vertical is much greater than this ratio in the wet region (Figure B-3). Such a moisture-dependent anisotropy (Figure B-3) in the effective unsaturated hydraulic conductivity for an EHM model for the stratified Hanford sediments yields greater spreading in the lateral directions than in the vertical direction.

B.3.1 Variable Anisotropy Model

Based on the preceding discussion, moisture or tension-dependent anisotropy provides a framework for upscaling small-scale measurements to the effective (upscaled) properties for the

large-scale, macroscopic vadose zone (Figure B-2). For the WMA A-AX PA, a tensorial connectivity-tortuosity (TCT) model ("A Tensorial Connectivity–Tortuosity Concept to Describe the Unsaturated Hydraulic Properties of Anisotropic Soils" [Zhang et al. 2003]) is used to evaluate and apply tension-dependent anisotropy. Details about the development of the tension-dependent anisotropy model and its application are presented in PNNL-23711, *Physical, Hydraulic, and Transport Properties of Sediments and Engineered Materials Associated with Hanford Immobilized Low-Activity Waste*. A stochastic model (Application of Stochastic Methods to Transient Flow and Transport in Heterogeneous Unsaturated Soils [Polmann 1990]) can also be invoked to model tension-dependent anisotropy and develop the unscaled (effective) parameter estimates. Both Polmann and TCT models serve the same purpose, and both models are coded in STOMP. Unlike the Polmann model, the TCT model has the advantage that its data requirements are much less stringent, and has unrestricted application over the entire range of saturation from dry to wet.

Figure B-3. Schematic Illustrating Aspects of Constant (left) and Variable (right) Macroscopic Anisotropy.

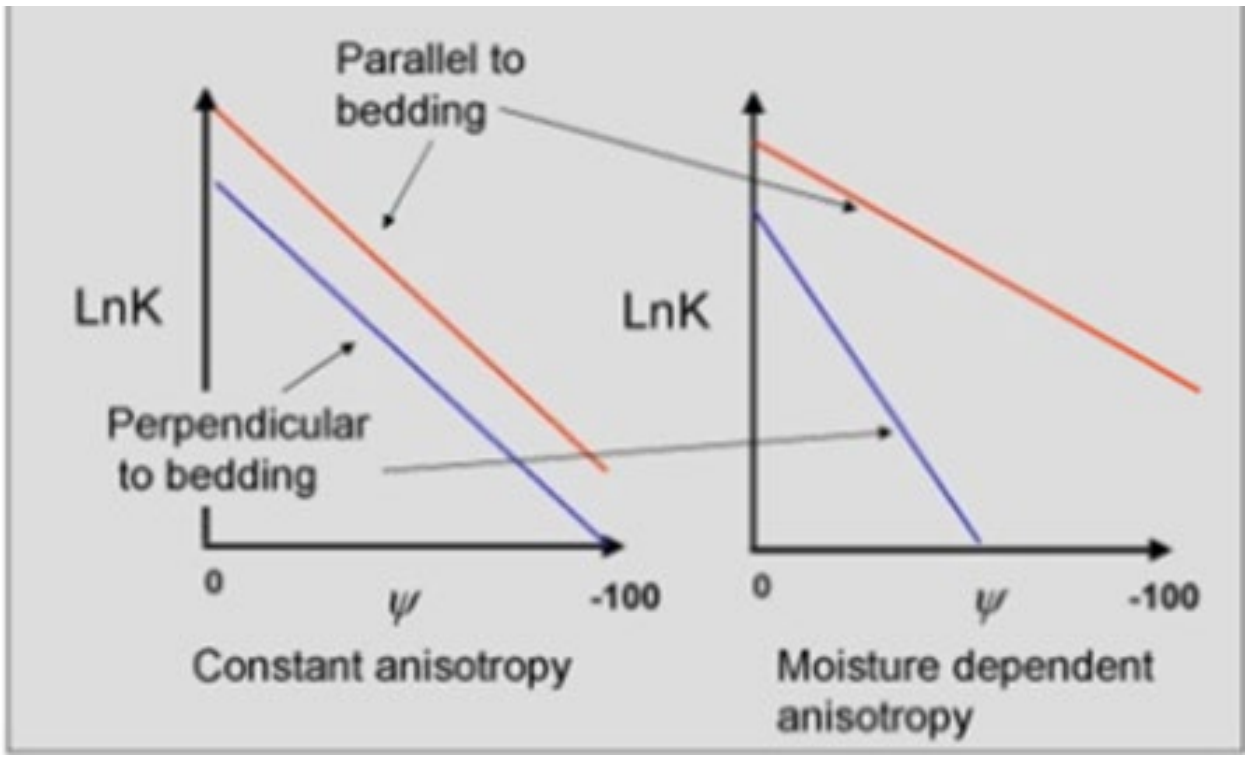

Note: ψ is the matric potential and LnK is the natural logarithm of either saturated or unsaturated hydraulic conductivity.

Using a combined power-averaging and tensorial connectivity-tortuosity (PA-TCT) model, a practical approach has recently been developed to estimate the three-dimensional (3-D) effective unsaturated hydraulic conductivity ("Simulating field-scale moisture flow using a combined power-averaging and tensorial connectivity-tortuosity approach" [Zhang and Khaleel 2010]). With the power averaging model, for each stratigraphic unit, the effective unsaturated hydraulic

conductivity in the ith principal direction, $K_i^e(h)$, for an anisotropic EHM, as a function of pressure head h, was estimated as

$$K_i^e(h) = \left\{\frac{1}{N}\sum_{j=1}^{N}[K_j(h)]^{p_i}\right\}^{1/p_i} \quad i = 1, 2, or\ 3 \tag{B-4}$$

where j denotes the sample index, N is the number of samples, $K_j(h)$ is the hydraulic conductivity of the jth sample as a function of h, and the power p varies between −1 and 1. The use of a larger p yields a larger $K^e(h)$ for a given data set. The averaging is equivalent to the arithmetic mean for $p = 1$ and the harmonic mean for $p = -1$; it approaches the geometric mean when p approaches zero. For $p_i = 1/3$, $K_1^e(h) = K_2^e(h) = K_3^e(h)$ and the power model is equivalent to the effective hydraulic conductivity of an isotropic EHM under 3-D flow (Eléments pour une Théorie des Milieux Poreux [Matheron 1967]; "Random Porous Media Flow on Large 3-D Grids: Numerics, Performance, and Application to Homogenization" [Ababou 1996]). However, for the combined PA-TCT approach, p_i is not necessarily equal to 1/3 for the isotropic media. For brevity, the subscript i in $K_i^e(h)$ is omitted if it represents the effective conductivity in any principal direction.

Using Equation B-4, the effective hydraulic conductivities of an EHM corresponding to different pressure heads are obtained as discrete K_i^e versus h data pairs. We describe the data pairs in the ith principal direction by the TCT model (Zhang et al. 2003):

$$K_i^e(h) = K_{si}^e[S^e(h)]^{L_i^e}B^e(h,\beta,\gamma) \quad i = 1, 2, or\ 3 \tag{B-5}$$

where K_s^e is the effective hydraulic conductivity of an EHM at full saturation, L^e is the effective connectivity-tortuosity coefficient; and $S^e(h) = [\theta(h)^e - \theta_r^e)]/(\theta_s^e - \theta_r^e)$ is the effective saturation; $\theta(h)^e$ is the effective soil water content as a function of matric potential, h; θ_s^e is the effective volumetric water content at full saturation; θ_r^e is the effective residual volumetric water content; and $B^e(h, \beta, \gamma)$ is the contribution of effective water retention to $K_i^e(h)$ and is defined by

$$B^e(h,\beta,\gamma) = \left[\int_0^{S^e}\left(h^{-\beta}dS^e\right) \Big/ \int_0^1\left(h^{-\beta}dS^e\right)\right]^{\gamma} \tag{B-6}$$

where β and γ are empirical constants. $B^e(h, \beta, \gamma)$ equals 1 when $S^e = 1$ and zero when $S^e = 0$ regardless of the values for β and γ and becomes smaller with decreasing saturation. Equation B-6 corresponds to the model from "Relative Permeability Calculations from Pore Size Distribution Data" (Burdine 1953) when $\beta = 2$ and $\gamma = 1$ and to Mualem's (1976) model when $\beta = 1$ and $\gamma = 2$. Equation B-5 implies that the directional unsaturated hydraulic conductivity is a symmetric second-order tensor, $\mathbf{K}^e(h)$, and is the product of a scalar variable, the symmetric connectivity-tortuosity tensor $\mathbf{T}(h, L_i^e)$, and the hydraulic conductivity tensor at saturation, $\mathbf{K}_s^e$ ("The Relative Connectivity-Tortuosity Tensor for Conduction of Water in Anisotropic Unsaturated Soils" [Raats et al. 2004]):

$$\boldsymbol{K}^e(h) = B^e(h,\beta,\gamma)\,\boldsymbol{T}(h, L_i^e)\ \boldsymbol{K}_s^e \tag{B-7}$$

Equation B-7 shows that the TCT model also applies to the field-scale effective hydraulic conductivity for anisotropic media. Note that, at full saturation, the relative connectivity-tortuosity tensor $\mathbf{T}(h, L_i^e)$ reduces to the unit second-order tensor $\mathbf{I}$, i.e., $\mathbf{T}(S_e = 1, L_i^e) = \mathbf{I}$.

To summarize, using an appropriate p_i in the ith principal direction and Equation B-4, the directional effective hydraulic conductivity, $K_i^e(h)$, is first obtained as a function of pressure head at discrete h values. Together with the effective retention curve, the Equation B-4-based $K_i^e(h)$ data pairs are described next with the TCT model, Equation B-5, by fitting the effective connectivity-tortuosity coefficient L_i^e.

Using the combined PA-TCT model, Zhang and Khaleel (2010) estimated the 3-D effective unsaturated hydraulic conductivity tensor for the Sisson and Lu field injection site in 200 East Area. Details of the Sisson and Lu site, field injections and the spatiotemporal distribution of the observed moisture plume are described in Zhang and Khaleel (2010). The PA-TCT-based numerical results compared well with the observed moisture plume at the Sisson and Lu site (Zhang and Khaleel 2010).

B.4 ESTIMATION OF HYDRAULIC PROPERTIES

For the heterogeneous unsaturated media, the small-scale laboratory measurements on hydraulic properties are used to simulate the large, field-scale behavior. Each heterogeneous geologic unit is replaced by an EHM with upscaled or effective (macroscopic) flow properties. The upscaling process, in addition to being a practical tool given the sparse supporting database for PA analyses, honors the underlying flow dynamics. For example, the upscaled or the effective unsaturated hydraulic conductivity is the hydraulic conductivity of an EHM that produces the same Darcy flux as the heterogeneous media under the same boundary conditions. Similarly, as described in Section B.4.5, the composite soil moisture retention curve (MRC) for an EHM is an effective MRC based on the laboratory-measured retention data of sediment samples.

The purpose of this section is to summarize data sources and laboratory measurements of core-scale sample properties for different HSUs; these are later upscaled for use in WMA A-AX PA modeling. Core-scale measurements, data sources, and their parameterization are described below for the following 11 HSUs that are identified in the WMA A-AX Geologic Framework Model (RPP-RPT-60171):

- Backfill
- Eolian sand
- Hanford formation unit 1 (H1)
- Hanford formation unit 2 (H2)
- Hanford formation unit 3 (H3)
- Cold Creek Unit silt (CCUz)
- Cold Creek sand (CCUs) ACM 2 only
- Cold Creek Unit gravel (CCUg)
- Ringold E gravel

- Ringold mud
- Ringold A gravel.

B.4.1 Particle Size Distribution Data and Grouping of Hydrostratigraphic Units

The particle size distribution controls the hydraulic property of bulk sediment sample in a fundamental manner. The determination of relative amounts of gravel, sand, and silt/mud content is therefore an important step in determination of hydraulic characteristics of an HSU. The relative fraction of gravel, sand, and silt/mud content along with their ranges is estimated based on grain size distribution data derived from sieve analysis. Table B-1(a) through B-1(g) list the summary statistics for different HSUs and for WMA A-AX Alternative Conceptual Model 1 (ACM 1) based on the ROCSAN sieve data (RHO-LD-11, *Granulometric Data 241-A Tank Farm Monitoring Well Sediments*; RHO-LD-12, *Granulometric Data 241-AX Tank Farm Monitoring Well Sediments*) from 74 boreholes located within a radius of 500 m from tank 241-A-106 (Figure B-4).

Table B-1. Gravel, Sand, and Mud (Silt and Clay) Fractions for Various Hydrostratigraphic Units at Waste Management Area A-AX. (3 sheets)

(a)			
Statistics for 241-A Tank Farm Backfill	**Gravel**	**Sand**	**Mud**
Count	63	63	63
Minimum (% weight)	0	33	0
Maximum (% weight)	67	94	19
Mean (% weight)	19.37	71.72	8.91
Median (% weight)	19.06	70.03	8.69
Standard Deviation (% weight)	11.28	9.95	4.44
Coefficient of variation	58.24	13.87	49.77
Sample variance (% weight)^2	127.22	98.97	19.68
Range (% weight)	67.22	61.21	19.25
(b)			
Statistics for 241-AX Tank Farm Backfill	**Gravel**	**Sand**	**Mud**
Count	102	102	102
Minimum (% weight)	0	59	5
Maximum (% weight)	36	92	26
Mean (% weight)	7.72	77.84	14.44
Median (% weight)	6.89	77.89	14.52
Standard Deviation (% weight)	4.66	4.34	3.89
Coefficient of variation	127.22	98.97	19.68

Table B-1. Gravel, Sand, and Mud (Silt and Clay) Fractions for Various Hydrostratigraphic Units at Waste Management Area A-AX. (3 sheets)

(b) (continued)			
Statistics for 241-AX Tank Farm Backfill	**Gravel**	**Sand**	**Mud**
Sample variance (% weight)^2	21.69	18.83	15.16
Range (% weight)	36.17	33.73	21.03
(c)			
Statistics for Hanford Formation Unit 1	**Gravel**	**Sand**	**Mud**
Count	152	152	152
Minimum (% weight)	0	31	0
Maximum (% weight)	67	95	48
Mean (% weight)	16.43	74.71	8.86
Median (% weight)	11.53	77.51	7.98
Standard Deviation (% weight)	14.03	12.90	6.78
Coefficient of variation	85.41	17.27	76.51
Sample variance (% weight)^2	196.95	166.39	45.91
Range (% weight)	66.97	63.92	47.74
(d)			
Statistics for Hanford Formation Unit 2	**Gravel**	**Sand**	**Mud**
Count	1,104	1,104	1,104
Minimum (% weight)	0	21	0
Maximum (% weight)	74	99	34
Mean (% weight)	13.58	79.61	6.81
Median (% weight)	9.20	83.00	6.67
Standard Deviation (% weight)	12.95	12.77	4.39
Coefficient of variation	95.35	16.05	64.55
Sample variance (% weight)^2	167.73	163.17	19.31
Range (% weight)	73.69	77.96	33.96
(e)			
Statistics for Hanford Formation Unit 3	**Gravel**	**Sand**	**Mud**
Count	93	93	93
Minimum (% weight)	0	0	0
Maximum (% weight)	100	98	49

Table B-1. Gravel, Sand, and Mud (Silt and Clay) Fractions for Various Hydrostratigraphic Units at Waste Management Area A-AX. (3 sheets)

(e) (continued)			
Statistics for Hanford Formation Unit 3	**Gravel**	**Sand**	**Mud**
Mean (% weight)	31.43	63.29	5.27
Median (% weight)	24.09	72.70	3.32
Standard Deviation (% weight)	30.68	28.99	6.49
Coefficient of variation	97.60	45.81	123.14
Sample variance (% weight)^2	941.16	840.68	42.18
Range (% weight)	99.65	97.98	49.04
(f)			
Statistics for Cold Creek Unit gravel	**Gravel**	**Sand**	**Mud**
Count	130	130	130
Minimum (% weight)	0	0	0
Maximum (% weight)	99	95	23
Mean (% weight)	44.36	51.05	3.82
Median (% weight)	40.14	50.99	1.60
Standard Deviation (% weight)	31.00	29.26	4.61
Coefficient of variation	69.89	57.31	120.60
Sample variance (% weight)^2	960.96	855.92	21.23
Range (% weight)	98.97	95.17	23.09
(g)			
Statistics for Ringold Formation Unit A	**Gravel**	**Sand**	**Mud**
Count	32	32	32
Minimum (% weight)	0	0	0
Maximum (% weight)	99	96	14
Mean (% weight)	47.05	46.20	3.62
Median (% weight)	48.78	44.35	2.16
Standard Deviation (% weight)	29.13	27.08	4.05
Coefficient of variation	61.92	58.61	111.82
Sample variance (% weight)^2	848.73	733.23	16.42
Range (% weight)	98.54	96.41	13.93

Note. Gravel: > 2 mm, Sand: 1/16 mm – 2 mm, Mud: <1/16 mm.

Figure B-4. Location of Waste Management Area A-AX Boreholes with ROCSAN Sieve Data.

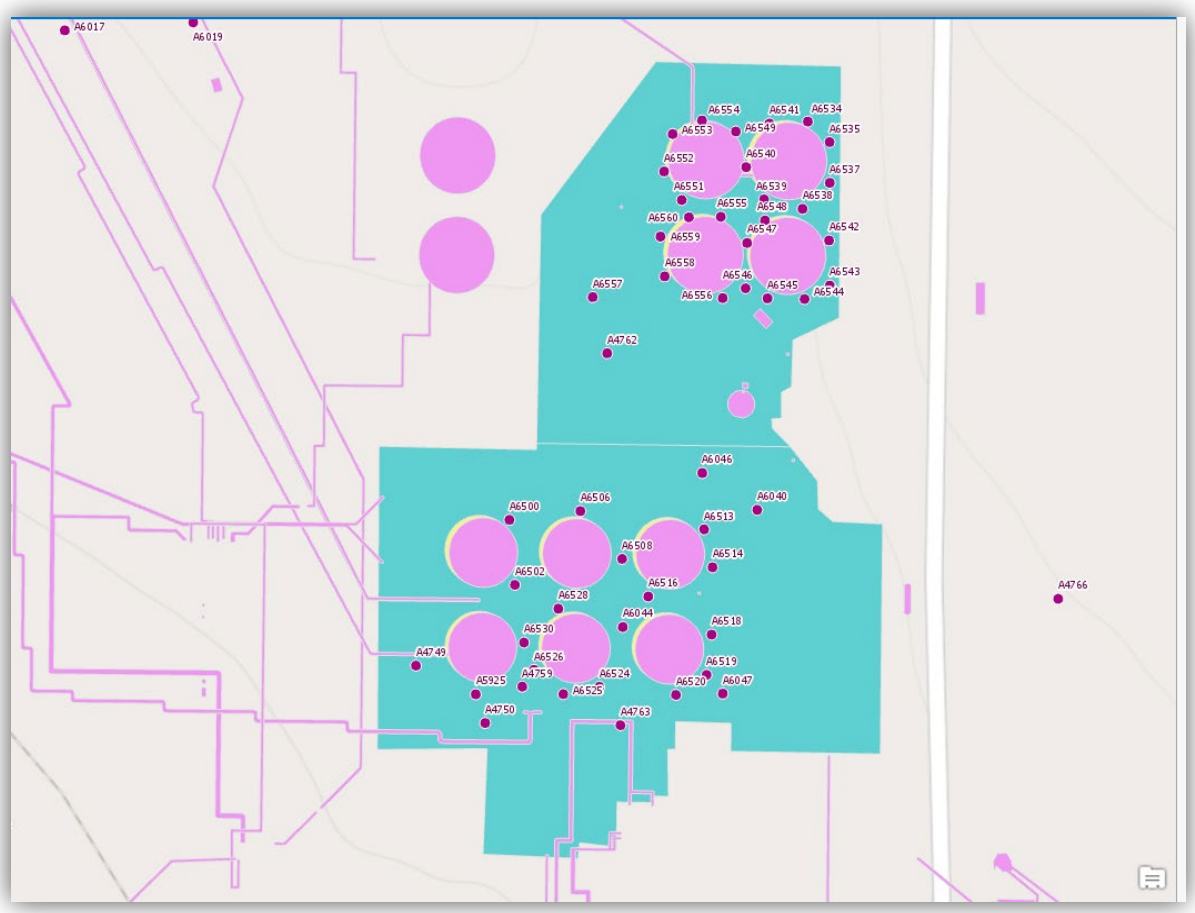

Based on the ROCSAN data and the particle-size distribution data for the sediment samples, as presented in Sections B.4.2 through B.4.4, the hydraulic properties for the preceding HSUs are presented below as three combined groupings of units (i.e., sand-dominated units, gravel-dominated units and fine-textured units):

- Sand-Dominated Units
  - Hanford formation unit 2 (H2)
  - Hanford formation unit 1 (H1)
  - Eolian sand
  - 241-AX Tank Farm Backfill
- Gravel-Dominated Units
  - Hanford formation unit 3 (H3)
  - Cold Creek Unit gravel (CCUg)
  - Ringold E
  - Ringold A
  - 241-A Tank Farm Backfill

- Fine-Grained Units
  - Cold Creek Unit silt (CCUz)
  - Cold Creek Unit sand (CCUs) ACM 2 only
  - Ringold mud.

Except for the backfill statistics, which are based on ARH-LD-127, *Geology of the 241-A Tank Farm* and ARH-LD-128,*Geology of the 241-AX Tank Farm* data, Table B-2 lists the average gravel content for various units based on the ROCSAN database for the 74 borehole samples [Table B-1(a) through B-1(g)]. Note the significant variability that exists with the reported averages [Table B-1(a) through B-1(g)]. For example, ARH-LD-127 and ARH-LD-128 state that the "typical" Ringold gravel contents are 77% weight – possibly so large because of a smaller number of borehole samples than the 74 samples noted above. Considerable variability in gravel content exists for different HSUs as evident by the calculated coefficient of variation. Although the ROCSAN database provides a basis for identifying similarities in the different HSUs and combining groups for the purpose of parameterization, the gravel content used in the contaminant transport simulations is based on the average gravel content of the samples used to develop the hydraulic property estimates.

Table B-2. Average Gravel Content for Waste Management Area A-AX Hydrostratigraphic Units Based on ROCSAN Sieve Data.

Hydrostratigraphic Unit	Average Gravel Content (% weight)	Source
Backfill	58 (241-A Tank Farm) 7 (241-AX Tank Farm)	ARH-LD-127, *Geology of the 241-A Tank Farm* ARH-LD-128, *Geology of the 241-AX Tank Farm*
Eolian sand	14	Table B-1(d) (same as H2)
Hanford formation unit 1	16	Table B-1(c)
Hanford formation unit 2	14	Table B-1(d)
Hanford formation unit 3	31	Table B-1(e)
Cold Creek Unit silt	0	No ROCSAN data available
Cold Creek Unit gravel	44	Table B-1(f)
Ringold Formation Unit E and Ringold Formation Unit A	47	Table B-1(g)
Ringold Formation Lower Mud Unit	0	No ROCSAN data available

B.4.2 Sand-Dominated Units

The Hanford formation unit 1 (H1), Hanford formation unit 2 (H2), the 241-AX Tank Farm (AX Farm) backfill unit, and Eolian sand units comprise the sand-dominated sequences for units at WMA A-AX in terms of thickness. Figure B-5 shows a representative sample of sediments associated with the sand-dominated H2 unit identified at nearby WMA C. Although tank farm backfill is usually gravel-dominated, the AX Farm backfill unit gravel content (>2-mm size

fraction) is only 7% (by weight), and the particle size distribution is similar to H2 sand (ARH-LD-127). Similarly, H1 is usually considered as gravel-dominated. However, the sediment data presented in Table B-2 indicate that the gravel content of the H1 unit at WMA A-AX is similar to the gravel content of the sand-dominated H2 unit, with the averages only differing by 2% (by weight). Because H2 hydraulic properties data specific to WMA A-AX are unavailable, the available hydraulic properties database for coarse sands in association with the WMA A-AX and WMA C moisture content distribution were used to identify and characterize hydraulic properties for the H2 unit identified at WMA A-AX. Soils used to characterize the WMA A-AX H2 unit properties are assumed to be similar to those pictured in Figure B-5.

Figure B-5. Waste Management Area C Hanford H2 Sand-Dominated Core.

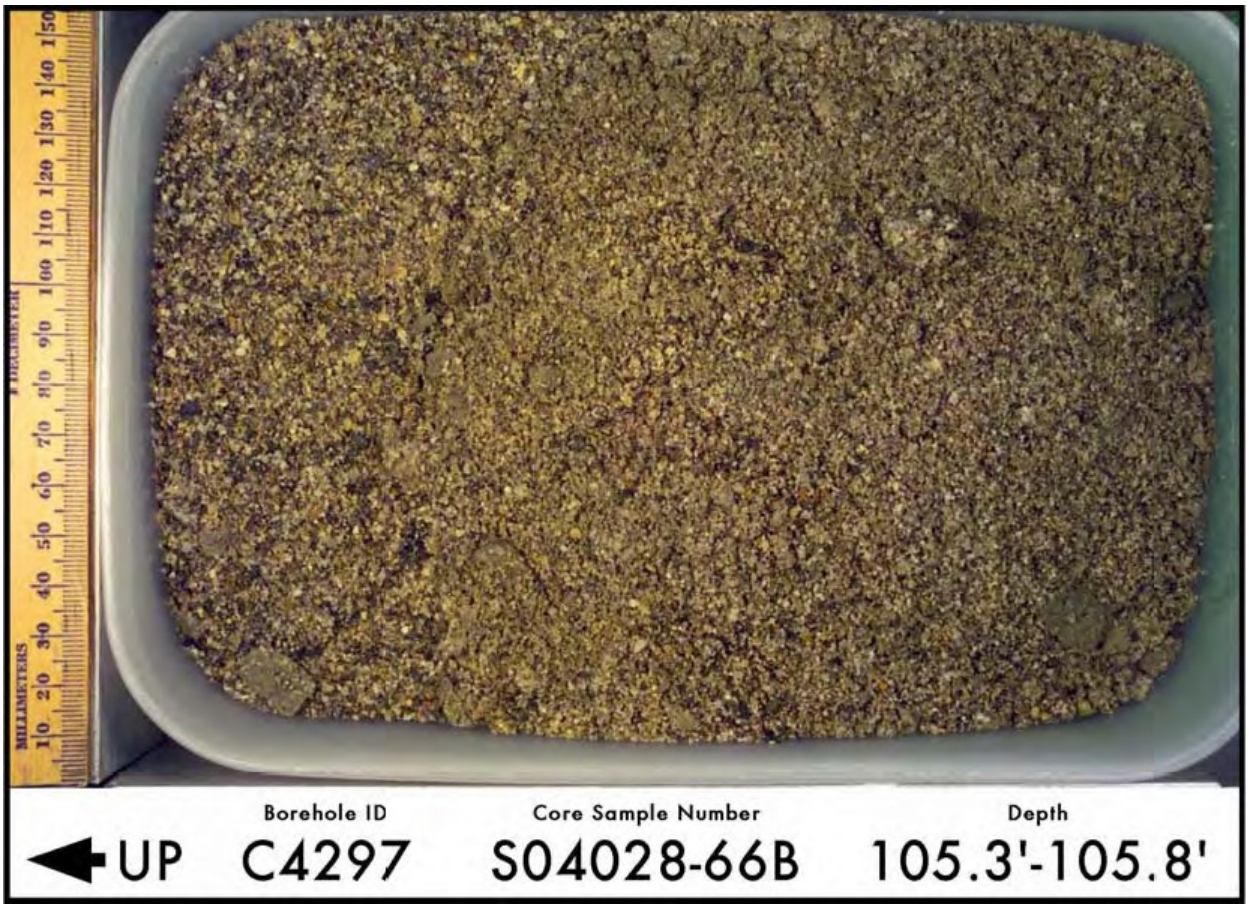

H2 = Hanford formation unit 2

Reference: PNNL-15503, *Characterization of Vadose Zone Sediments Below the C Tank Farm: Borehole C4297 and RCRA Borehole 299-E27-22*.

B.4.2.1 Hanford Formation Unit 2 Sand

Using moisture as a correlation parameter or proxy, the Hanford formation unit 2 sand identified at WMA A-AX and WMA C correlated well with a coarse sand unit identified at the nearby 200 East Area Integrated Disposal Facility (IDF) site. As part of site characterization used in the development of the IDF, sediment samples were obtained in fiscal years 1998, 2001 and 2002

via a borehole drilling and sampling program. The Hanford formation sandy H2 sequence identified at the IDF site is ~200 ft (~61 m) thick and, like WMA A-AX, is the dominant facies at the site. Because the units are similar, hydraulic properties that had been developed for the IDF coarse sands are thus used as surrogate for the WMA A-AX H2 sands.

The hydraulic properties for the IDF H2 unit were estimated for a total of 44 borehole samples. The laboratory procedures used to analyze the IDF H2 borehole samples and analysis of samples from the three boreholes are described in appendices found in RPP-20621, *Far-Field Hydrology Data Package for the Integrated Disposal Facility Performance Assessment*.

Briefly, the multistep and steady-state methods were used to obtain moisture retention and unsaturated conductivity data. The specific details for the two methods are described in RPP-20621 appendices. Both methods were performed on the same core using the same sensor locations. In addition to cumulative outflow, the multistep method provides water content-matric potential (θ-ψ) pairs. These data were used in conjunction with a numerical inversion procedure ("Optimization of Hydraulic Functions from Transient Outflow and Soil Water Pressure Data" [Eching and Hopmans 1993]) to determine the optimal set of van Genuchten model (van Genuchten 1980) parameters (RPP-20621). The steady-state method, described in "Hydraulic Conductivity and Diffusivity: Laboratory Methods" (Klute and Dirksen 1986), provides water content-matric potential-unsaturated conductivity (θ-ψ-K) triplets; the method was primarily used as a check on the multistep method.

RPP-20621 (Tables 1 through 3) provides the van Genuchten model parameters determined using the numerical inversion procedure and data from the multistep test. The pore-size distribution parameter ℓ (Mualem 1976) was kept fixed at 0.5. The fitted van Genuchten-Mualem parameters for the IDF H2 sandy sequence (44 samples) are reproduced in Table B-3. The fitted moisture retention curves and unsaturated conductivity curves for the H2 used in WMA A-AX PA modeling are shown in Figure B-6a and Figure B-6b, respectively. The average gravel content of the 44 samples is approximately 5%, which is applied as the gravel correction to the K_d values during the contaminant transport simulations.

B.4.2.2 Eolian Sand

WHC-EP-0883 includes particle size distribution data for several samples of Eolian sand (wind-blown deposits) from borehole 299-E25-234 situated just southeast of WMA A-AX. Because of its similarity in particle size distribution for H2 sands (WHC-EP-0883), the WMA A-AX Eolian sands are assigned the H2 properties.

B.4.2.3 241-AX Tank Farm Backfill and Hanford Formation Unit 1

Similar to the H2 sand-dominated unit, no data specific to WMA A-AX are available for the WMA A-AX backfill or Hanford formation unit 1 (H1). Typical examples of backfill and H1 sediments are provided in Figure B-7a and Figure B-7b, respectively.

As stated earlier, the AX Farm backfill unit gravel content (>2-mm size fraction) is 7% (weight) versus 58% (weight) for the 241-A Tank Farm (A Farm) backfill unit (ARH-LD-127 and ARH-LD-128). The H2 sand-dominated hydraulic properties are assumed to represent the hydraulic properties for the AX Farm backfill unit because of its relatively low (7%) gravel

content and similarity to H2 sands with respect to particle size distribution. Similarly, because of the relatively high (58%) gravel content, the A Farm backfill unit is characterized as a gravel-dominated unit (Section B.4.3). The gravel content values of 7% and 58% are applied as the gravel correction to the K_d values for the AX Farm and A Farm backfill units, respectively, during the contaminant transport simulations.

Table B-3. The van Genuchten Parameters and Saturated Hydraulic Conductivity Data for 44 Borehole Samples Used to Represent the Sand-Dominated Units at Waste Management Area A-AX. (2 sheets)

Sample	θ_s (cm^3/cm^3)	θ_r (cm^3/cm^3)	α (1/cm)	n	K_s (cm/s)	Gravel Content (% wt)
7A	0.377	0.0404	0.029	1.825	1.04E-03	0.2[a]
10A	0.413	0.0279	0.1161	1.784	2.95E-03	0[a]
12A	0.363	0.0309	0.065	1.755	2.15E-03	0.7[a]
14A	0.416	0.0324	0.0445	1.728	1.99E-03	0.2[a]
15A	0.38	0.0254	0.0487	1.844	2.09E-03	0.5[a]
16A	0.42	0.0228	0.0682	1.71	9.57E-03	1.5[a]
17A	0.423	0.0382	0.0689	1.899	1.99E-03	0.3[a]
19A	0.444	0.0279	0.201	1.542	4.31E-03	0[a]
20A	0.419	0.0321	0.0305	2.081	2.54E-03	0.2[a]
21A	0.403	0.0276	0.0545	1.926	2.94E-03	0.4[a]
22A	0.352	0.0252	0.1078	1.585	5.06E-03	1.6[a]
23A	0.371	0.0411	0.0079	1.553	2.65E-04	0[a]
24A	0.321	0.0413	0.013	1.684	5.69E-04	0.2[a]
25A	0.345	0.0267	0.0842	2.158	5.40E-03	0.3[a]
27A	0.377	0.0354	0.083	1.532	8.14E-03	1.7[a]
29A	0.359	0.0317	0.0784	1.732	3.75E-03	1.2[a]
31A	0.418	0.0444	0.0058	2.012	8.21E-04	0.2[a]
32A	0.359	0.0401	0.0931	1.703	6.71E-03	1.8[a]
34A	0.316	0.0324	0.0819	2.398	1.32E-02	13[a]
35A	0.299	0.0428	0.0897	2.16	1.06E-02	24.3[a]
45L	0.385	0.008	0.1039	1.737	3.24E-02	4.1[b]
45U	0.385	0.005	0.088	1.664	3.24E-02	4.1[b]
50L	0.42	0.025	0.073	1.71	1.75E-03	1.9[b]
50U	0.42	0.013	0.045	1.667	1.75E-03	1.9[b]

Table B-3. The van Genuchten Parameters and Saturated Hydraulic Conductivity Data for 44 Borehole Samples Used to Represent the Sand-Dominated Units at Waste Management Area A-AX. (2 sheets)

Sample	θ_s (cm^3/cm^3)	θ_r (cm^3/cm^3)	α (1/cm)	n	K_s (cm/s)	Gravel Content (% wt)
80L	0.359	0.031	0.0403	2.368	1.05E-03	13[b]
80U	0.359	0.033	0.0313	2.572	1.05E-03	13[b]
85L	0.406	0.023	0.1074	1.697	3.84E-02	3.6[b]
85U	0.406	0.027	0.0847	1.595	3.84E-02	3.6[b]
110L	0.412	0.039	0.0362	2.328	5.16E-04	0.4[b]
110U	0.412	0.046	0.0268	3.182	5.16E-04	0.4[b]
130L	0.358	0.032	0.094	2.003	1.97E-02	9.8[b]
130U	0.358	0.036	0.0674	1.934	1.97E-02	9.8[b]
150L	0.431	0.015	0.0992	1.547	7.48E-03	1.7[b]
150U	0.431	0.024	0.0703	1.514	7.48E-03	1.7[b]
200L	0.41	0.002	0.0995	2.162	4.93E-02	2.9[b]
215L	0.37	0.028	0.0448	1.918	2.24E-03	13.4[b]
215U	0.37	0.023	0.0333	1.815	2.24E-03	13.4[b]
230L	0.309	0.04	0.0472	1.658	3.56E-03	31.9[b]
230U	0.309	0.038	0.04	1.658	3.56E-03	31.9[b]
251L	0.427	0.032	0.084	1.845	1.43E-02	3[b]
261L	0.39	0.045	0.0191	2.485	5.54E-04	0.7[b]
C3826-171	0.382	0.0226	0.039	1.84	7.96E-03	0[c]
C3827-63.5	0.444	0	0.0914	1.5	2.23E-02	0[d]
C3827-221	0.361	0.022	0.066	1.77	7.30E-03	5[e]

[a]Gravel content equal to percentage of core with particle diameter greater than 2,000 µm, Table 4 in Appendix A of RPP-20621.

[b]Gravel content of cores applicable to the individual samples sectioned from the cores, Table 8 in Appendix B of RPP-20621.

[c]Gravel content inferred from comments in Table 1 in Appendix C of RPP-20621 that describe the sample as "Medium sand."

[d]Gravel content inferred from comments in Table 1 in Appendix C of RPP-20621 that describe the sample as "Medium sand; no evidence of anything that might indicate a paleosol."

[e]Gravel content inferred from comments in Table 1 in Appendix C of RPP-20621 that describe the sample as "Sandy; some fines and gravel (<5%)."

References:

PNNL-14029, *Geologic and Wireline Summaries from Fiscal Year 2002 ILAW Boreholes.*
PNNL-23711, *Physical, Hydraulic, and Transport Properties of Sediments and Engineered Materials Associated with Hanford Immobilized Low-Activity Waste.*
RPP-20621, *Far-Field Hydrology Data Package for the Integrated Disposal Facility Performance Assessment.*

Figure B-6. Moisture Retention Data (44 Samples) (a) and Unsaturated Hydraulic Conductivity Data (44 Samples) (b) for the Sand-Dominated Units at Waste Management Area A-AX.

(a)

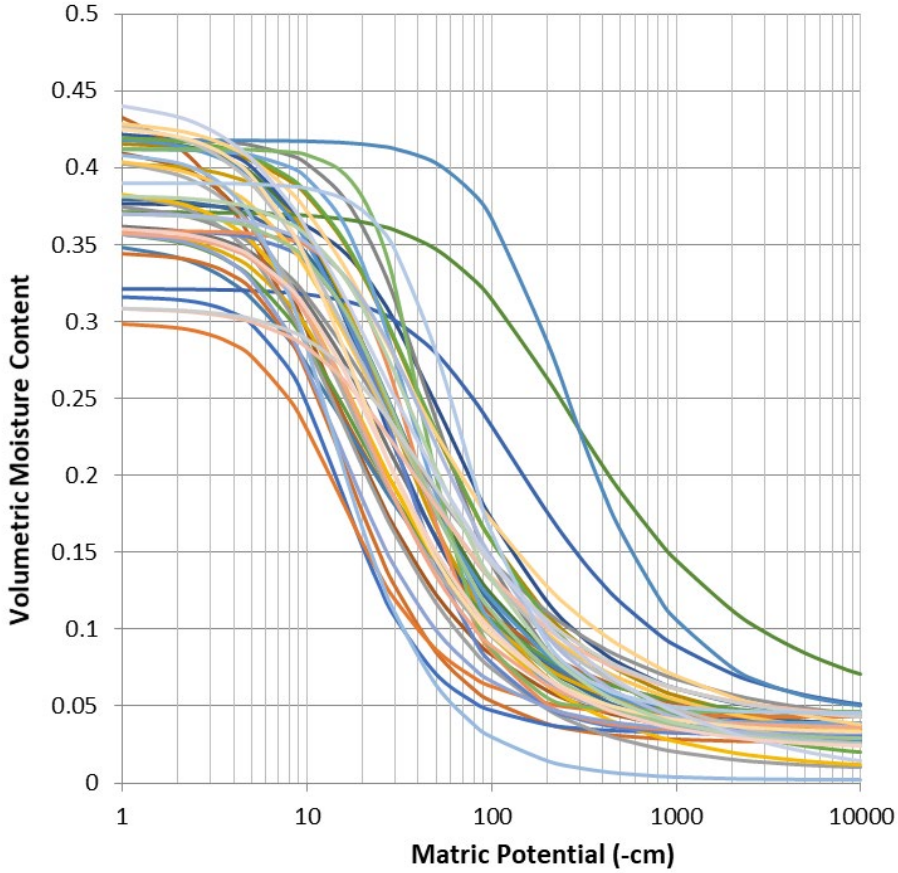

(b)

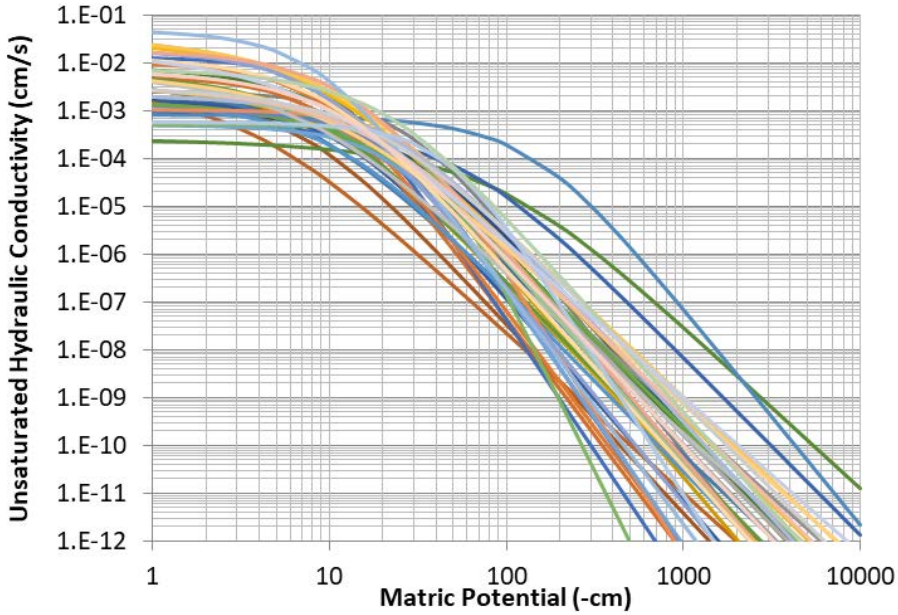

Reference: RPP-20621, *Far-Field Hydrology Data Package for the Integrated Disposal Facility Performance Assessment.*

Figure B-7. Typical Backfill (a) and Hanford H1 Unit Samples (b) from Borehole C4297.

(a)

(b)

H1 = Hanford formation unit 1

Source: PNNL-15503, *Characterization of Vadose Zone Sediments Below the C Tank Farm: Borehole C4297 and RCRA Borehole 299-E27-22*.

Unlike H2 sand-dominated sediments, H1 sediments typically are comprised of a significant gravel fraction and the unit is considered as "gravel-dominated." However, as the sediment data from ROCSAN (Table B-2) indicate with respect to gravel content, the H1 unit at WMA A-AX is similar to the sand-dominated H2 unit; the average gravel contents for H1 and H2 units are about 16 and 14% (by weight), respectively. The WMA A-AX H1 unit is therefore also assigned the hydraulic properties of the H2 unit, including the average gravel content of approximately 5%, which is applied as the gravel correction to the K_d values during the contaminant transport simulations.

B.4.3 Gravel-Dominated Units

The Hanford formation unit 3 (H3), Cold Creek Unit gravel (CCUg), Ringold E, Ringold A, and A Farm backfill units comprise the gravel-dominated sequences for WMA A-AX. A typical example of the CCUg gravel-dominated unit is shown in Figure B-8. Once again, no hydraulic data specific to WMA A-AX are available for the gravel sequences. To explore the impact of gravelly sediments for the drier moisture regime, a separate study was conducted ("Variability of Gardner's α for coarse-textured sediments" [Khaleel and Relyea 2001]); a total of 79 gravelly and sandy samples were analyzed in the laboratory. The gravel fraction for 41 samples ranged from 20 to 71% (by weight); the remaining 38 samples were sandy with very little gravel fraction (Figure B-9). A noteworthy feature of Figure B-9 is the fact that the variability in saturated conductivity is much greater than the variability in unsaturated conductivity near saturation. Furthermore, the measured unsaturated conductivities for the gravelly samples showed less variability for the drier moisture regime, fell within a narrower range, and were well within the range of measured unsaturated conductivities for the sandy samples (see Figure B-9). Such a generic behavior for the gravelly sediments for the drier moisture regime prompted assigning similar hydraulic properties for the WMA A-AX gravel-dominated units (i.e., H3, CCUg, Ringold E, Ringold A, and A Farm backfill units).

Twenty-five (25) borehole samples with high gravel contents from the 100 and 300 Areas were used as surrogate to represent the gravel-dominated units at WMA A-AX. The dataset is compiled for PA modeling from two sources (i.e., RPP-20621 for 100 Area [15 samples], and PNNL-22886, *System-Scale Model of Aquifer, Vadose Zone, and River Interactions for the Hanford 300 Area – Application to Uranium Reactive Transport* for 300 Area [10 samples]).

The average gravel content for the H3 unit, based on the ROCSAN database, is about 31% by weight; however, the variability is large, with the gravel content as high as 100% for some samples. The 15 samples from the 100 Area (RPP-20621) contain a gravel fraction from 43% to 75% with an average of 62% by weight. The moisture retention data for the fine fraction (<2 mm) were measured using the Tempe pressure cells or the pressure plate extraction method. The unsaturated hydraulic conductivity was measured using a variation of the unit gradient method (Klute and Dirksen 1986). All five unknown parameters—θr, θs, α, n, and Ks, with m = 1-1/n (van Genuchten 1980)—were fitted to the data and the tortuosity-connectivity coefficient ℓ was set as a constant 0.5. The hydraulic parameters for the 15 samples of the gravel sequence were summarized in Table 4 of RPP-20621 and are reproduced in Table B-4.

Figure B-8. Typical Gravel-Dominated CCUg Unit Sample from Waste Management Area B-BX-BY Borehole 299-E33-45.

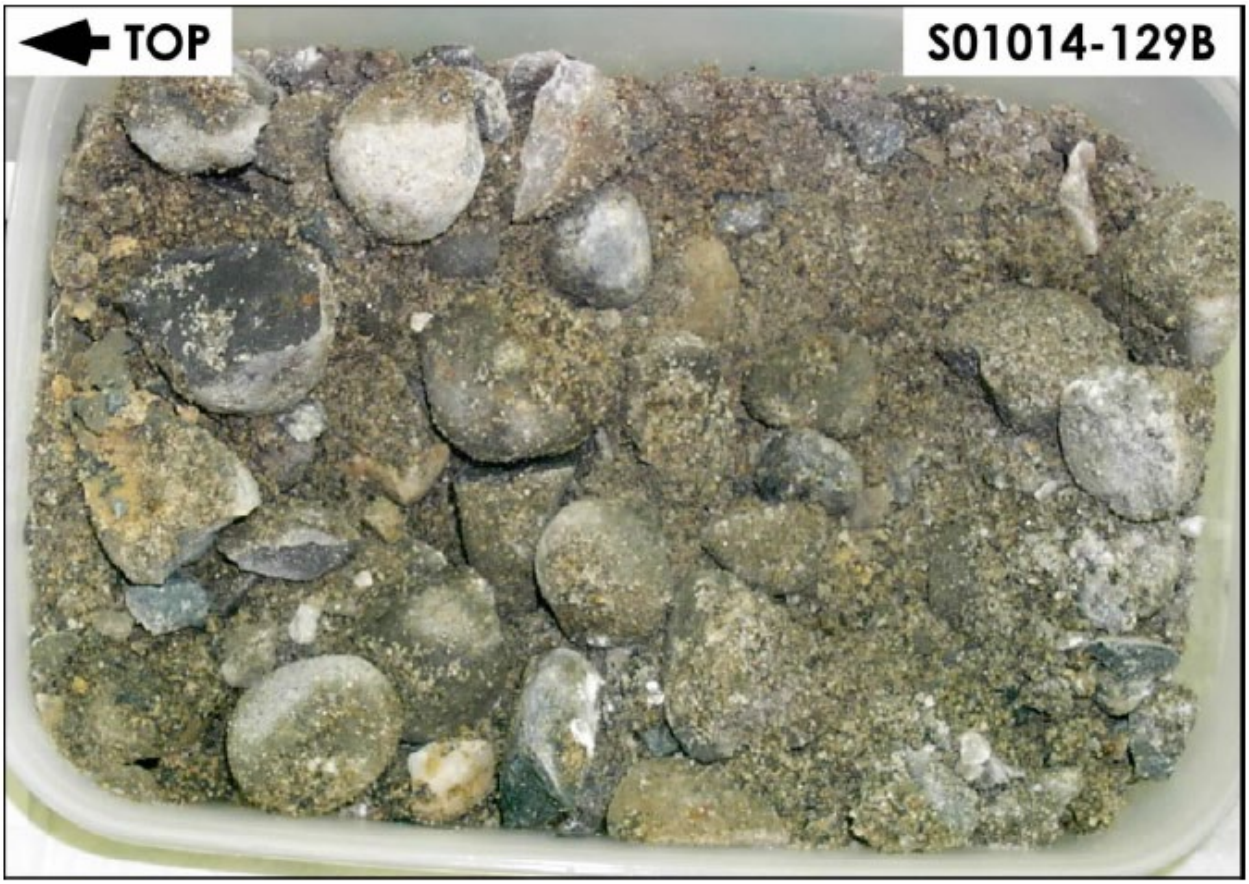

CCUg = Cold Creek Unit gravel

Source: PNNL-19277, *Conceptual Models for Migration of Key Groundwater Contaminants Through the Vadose Zone and Into the Unconfined Aquifer Below the B-Complex*.

The 10 samples from the 300 Area (PNNL-22886) contain a gravel fraction from 45% to 89% with an average of 71%. The hydraulic properties of the intact cores were measured using the multistep methods (see appendices of RPP-20621). Measured pressure data from two locations in each core and measured cumulative outflow data were used to calculate average capillary pressures and water contents. These data were used to fit the retention parameters θ_r, α, and n. The parameters Ks and θ_s were measured independently. The tortuosity-connectivity coefficient ℓ was set as a constant 0.5. These parameters were summarized in Table A-2 of PNNL-22886 and are replicated in this appendix in Table B-4 as a starting basis for estimating effective hydraulic properties for all gravel-dominated sequences identified near WMA A-AX. The average gravel content of the 25 samples is approximately 66%, which is applied as the gravel correction to the K_d values during the contaminant transport simulations.

Figure B-9. Unsaturated Hydraulic Conductivity Measurements for Sand-Dominated and Gravel-Dominated Samples.

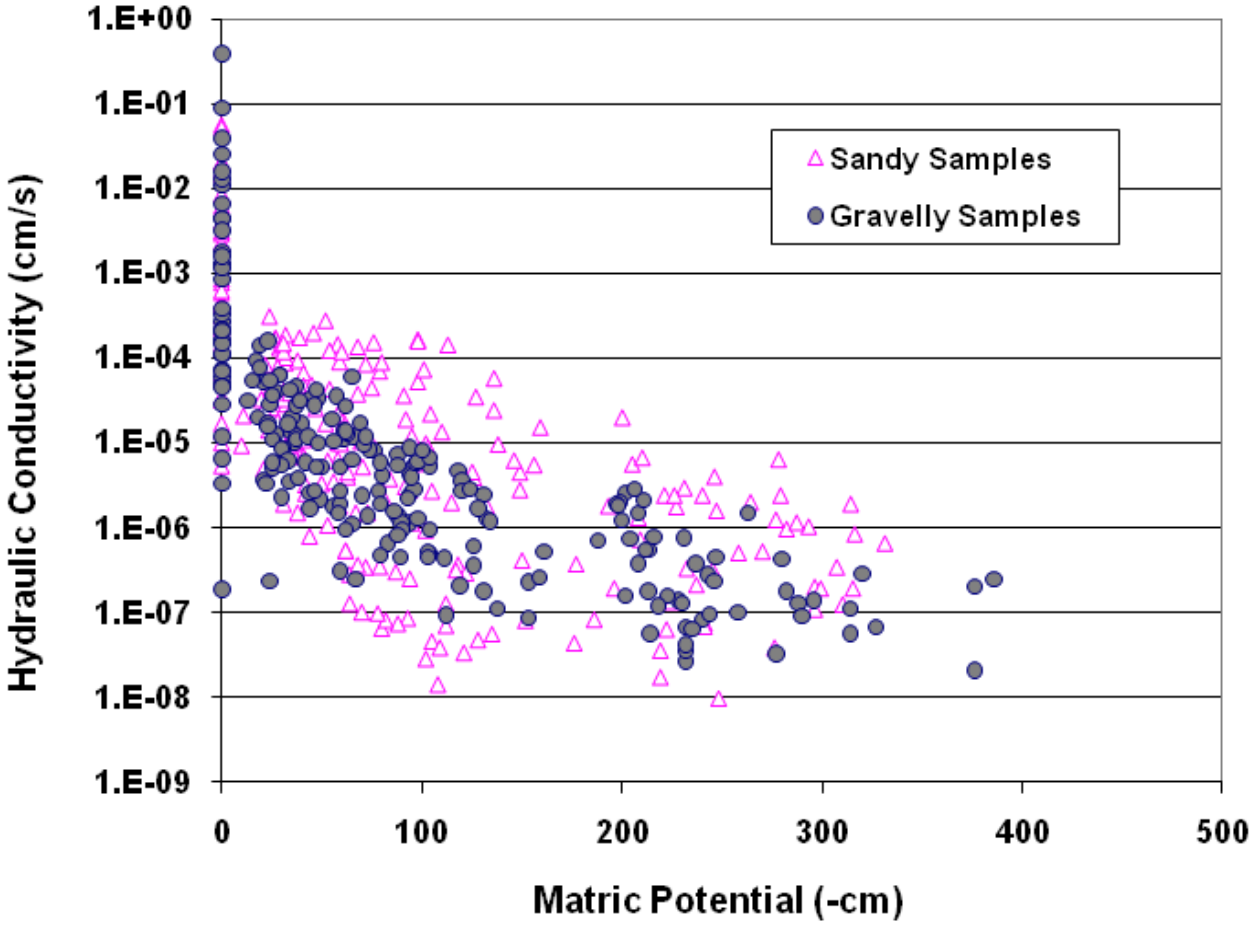

Reference: "Variability of Gardner's α for coarse-textured sediments" (Khaleel and Relyea 2001).

B.4.4 Fine-Grained Units

The Cold Creek Unit silt (CCUz), Ringold lower mud unit (Rlm), and, where it is differentiated from the CCUz, the Cold Creek Unit sand (CCUs) encompass the fine-textured units for WMA A-AX. A typical example of the Cold Creek Unit silt is shown in Figure B-10. The particle size distribution information for the WMA A-AX fine-textured units are not available in the ROCSAN database. The CCUs that has been locally identified in some borehole logs is not likely to be as permeable as H2 sand because of the cemented and compacted nature of the CCUs. Therefore, the hydraulic properties representative of a fine-textured sediment (e.g., CCUz), rather than those of a coarse-textured sediment (e.g., H2), are expected to represent the CCUs properties.

Table B-4. The van Genuchten Parameters and Saturated Hydraulic Conductivity Data for the 25 Samples Used to Represent the Gravel-Dominated Units at Waste Management Area A-AX.

Sample Locations	Sample	θ_s (cm^3/cm^3)	θ_r (cm^3/cm^3)	α (1/cm)	n	K_s (cm/s)	Gravel Content (% wt)
100 Area[(a)]	2-1307	0.236	0.0089	0.013	1.447	1.29E-04	43
	2-1308	0.12	0.0208	0.0126	1.628	6.97E-05	58
	2-1318	0.124	0.0108	0.0081	1.496	1.67E-04	60
	2-2663	0.135	0.0179	0.0067	1.527	6.73E-05	61
	2-2664	0.125	0.0136	0.0152	1.516	1.12E-04	73
	2-2666	0.138	0	0.0087	1.284	1.02E-04	71
	2-2667	0.094	0	0.0104	1.296	1.40E-04	75
	3-0570	0.141	0	0.0869	1.195	2.06E-02	60
	3-0577	0.107	0	0.0166	1.359	2.49E-04	66
	3-0686	0.184	0	0.0123	1.6	5.93E-04	55
	3-1702	0.103	0	0.0491	1.26	1.30E-03	68
	4-1086	0.137	0	0.1513	1.189	5.83E-02	65
	4-1090	0.152	0.0159	0.0159	1.619	4.05E-04	50
	4-1118	0.163	0	0.2481	1.183	3.89E-02	66
	4-1120	0.131	0.007	0.0138	1.501	2.85E-04	63
300 Area[(b)]	C6186,18.4-19.4	0.152	0	0.0388	1.378	2.83E-04	82
	C6197,27-28	0.176	0	0.115	1.324	4.33E-04	68
	C6197,42-43	0.178	0	0.0929	1.366	2.61E-02	67
	C6197,51-52	0.214	0	0.0435	1.272	5.43E-05	56
	C6200,21-22	0.219	0	0.0626	1.383	2.85E-01	89
	C6203,16-17	0.213	0	0.358	1.195	1.06E-01	81
	C6203,20-21	0.285	0	0.2286	1.269	3.72E-03	79
	C6203,35.8-36.8	0.302	0	2.4189	1.299	3.26E-02	72
	C6203,40-41	0.266	0	0.2733	1.509	1.30E-02	45
	C6208,23-24	0.246	0	0.1479	1.201	2.13E-02	77

(a) After Table 4 and Figure 3 of RPP-20621, *Far-Field Hydrology Data Package for the Integrated Disposal Facility Performance Assessment*.
(b) After Tables A-1 and A-2 of PNNL-22886, *System-Scale Model of Aquifer, Vadose Zone, and River Interactions for the Hanford 300 Area – Application to Uranium Reactive Transport*.

Figure B-10. Typical Silt-Dominated Cold Creek Unit Sample from Waste Management Area B-BX-BY Borehole 299-E33-45.

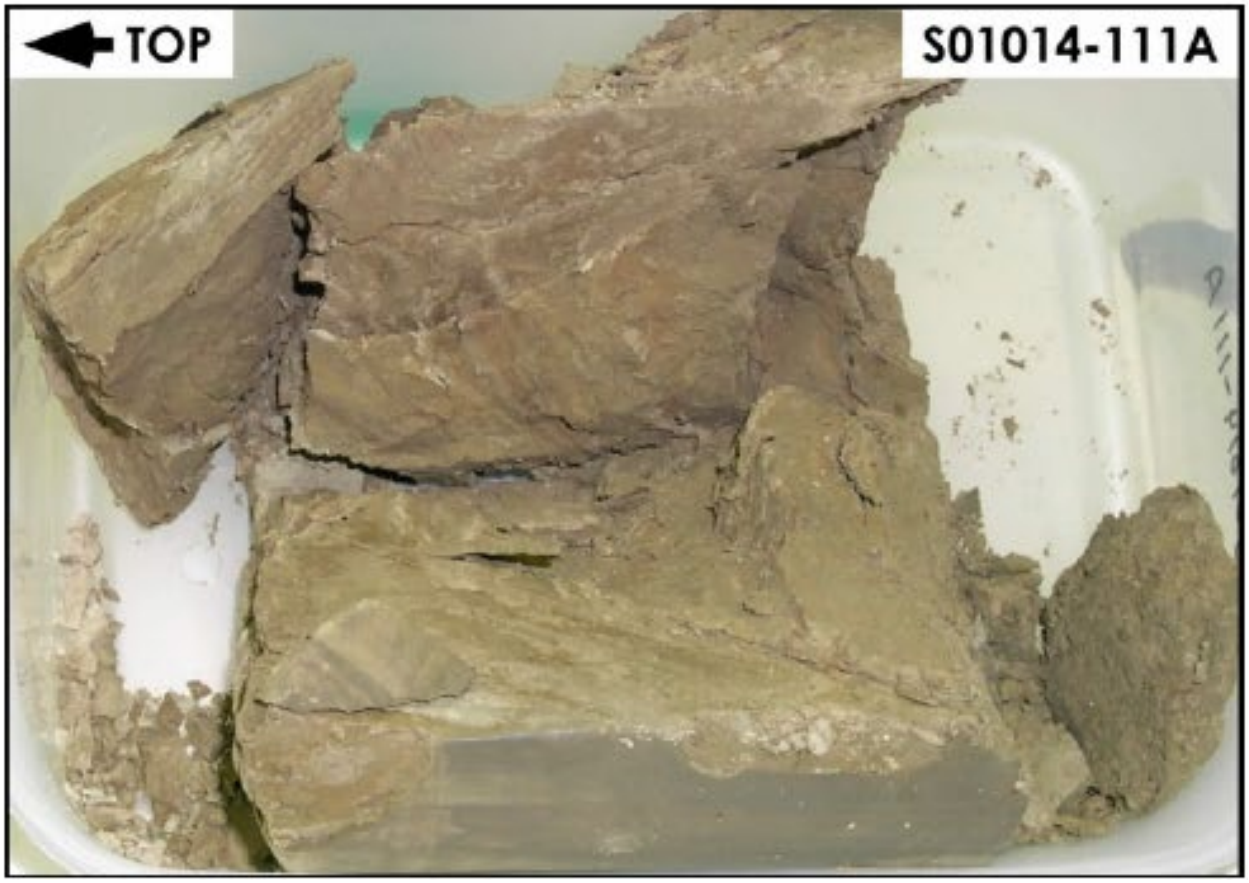

Source: PNNL-19277, *Conceptual Models for Migration of Key Groundwater Contaminants Through the Vadose Zone and Into the Unconfined Aquifer Below the B-Complex*.

Because of their fine-grained nature and the primary presence of fine sand and mud, ten gravel-free samples (WHC-EP-0645, *Performance Assessment for the Disposal of Low-Level Waste in the 200 West Area Burial Grounds*; WHC-EP-0883) were used to represent the other two fine-textured sediments at WMA A-AX. Table B-5 lists the van Genuchten parameters and saturated hydraulic conductivity data for the samples. All ten gravel-free samples are comprised of a high fine-grained fraction with the fine fraction (silt and clay) being as high as 46% (weight) (McGee Ranch silt loam sample D09-01; Table B-5).

B.4.5 Effective Soil-Moisture Retention

Simple averaging of data listed in Tables B-3, B-4, and B-5 was used to define the effective saturated and residual moisture contents for the sand-dominated, gravel-dominated, and fine-textured units, respectively. A linear averaging scheme ("Upscaled soil-water retention

using van Genuchten's function" [Green et al. 1996]) was used to calculate the effective soil-water saturation $S^e(h)$ at a given pressure head h:

$$S^e(h) = \frac{1}{N}\sum_{j=1}^{N} S_j(h) \tag{B-8}$$

Table B-5. The van Genuchten Parameters and Saturated Hydraulic Conductivity Data for the Ten Samples Used to Represent the Fine-Textured Units at Waste Management Area A-AX.

Sample	θ_s	θ_r	α (1/cm)	n	K_s (cm/s)
0-080[a]	0.4257	0.047	0.0061	3.4887	2.51E-05
0-073[a]	0.4124	0.089	0.0008	2.1917	4.01E-07
0-072[a]	0.3905	0.056	0.0090	2.0877	5.43E-05
0-079[a]	0.3881	0.076	0.0077	2.4196	1.43E-05
D08-15[b]	0.4543	0.085	0.0059	1.8533	1.20E-04
D09-01[b]	0.4544	0.08	0.0066	1.7677	1.20E-04
D13-08[b]	0.4513	0.082	0.0070	1.7877	1.20E-04
D02-10[b]	0.4531	0.0778	0.0049	1.9773	1.20E-04
D04-04[b]	0.4508	0.07	0.0072	1.6501	1.20E-04
D12-14[b]	0.4686	0.098	0.0063	1.7576	1.20E-04

References:
[a]WHC-EP-0645, *Performance Assessment for the Disposal of Low- Level Waste in the 200 West Area Burial Grounds* (Table A-1 and Figures A-24 through A-26 and A-28).
[b]WHC-EP-0883, *Variability and Scaling of Hydraulic Properties for 200 Area Soils, Hanford Site* (tabulated values on page A-5 and figures on pages B-22 through B-26).

The effective soil-water retention for the five different units was evaluated for 15 discrete pressure head values within the range of (−10, 0) m. The pressure head range was restricted to (−10, 0) m to replicate the simulated moisture regime for WMA A-AX PA modeling. The 15 pairs of $S^e(h)$ data constitute the effective soil-moisture retention curve (Equation B-8). The effective retention curves were next described by van Genuchten's (1980) soil moisture retention model:

$$S^e(h) = \left[1 + (\alpha^e|h|)^{n^e}\right]^{\left(1/n^e - 1\right)} \tag{B-9}$$

where α^e and n^e are the effective van Genuchten parameters. The values for n^e and α^e presented in Table 3-2 were estimated by fitting Equation B-9 to the $S^e(h)$ data pairs obtained from Equation B-8.

Figure B-12 (a) through (c) illustrates the fitted effective retention curve as well as the individual retention curves for the sand-dominated, gravel-dominated, and fine-textured units at WMA A-AX. The parameters presented in Table 3-2 for the sand-dominated, gravel-dominated, and fine-textured units represent the effective retention curve parameters for the WMA A-AX HSUs.

B.4.6 Effective Unsaturated Hydraulic Conductivity and Variable Anisotropy

As stated earlier, for stratified sediments such as those existing at WMA A-AX, the effective hydraulic conductivity tensor is anisotropic with a moisture-dependent (or tension-dependent) degree of anisotropy. The large-scale anisotropy, defined as the ratio of horizontal hydraulic conductivity to vertical hydraulic conductivity, increases with decreasing moisture content or more negative pressure head. Variable, moisture-dependent anisotropy in unsaturated soils is, however, an effective, large-scale (macroscopic) flow property which results from media heterogeneities at a smaller scale, and provides a framework for upscaling laboratory-scale measurements to delineate the effective or upscaled properties for the large-scale vadose zone.

As was described earlier, the PA-TCT model was used to derive variable moisture-dependent macroscopic anisotropy. At the field site, the degree of macroscopic anisotropy in hydraulic conductivity is not known a priori, except that horizontal stratification is visually observed in each of the stratigraphic units. The power p can take any value between −1 and 1; hence, $K^e(h)$ was determined with different combinations of (p_1, p_2, p_3) in the x, y, and z directions, where z aligns with the vertical direction. Table B-6 presents four typical cases, representing isotropy (ISO), low anisotropy (LA), intermediate anisotropy (IA), and high anisotropy (HA). For the ISO case, $p_1 = p_2 = p_3 = 0$, which corresponds to the geometric mean for $K(h)$. For the three anisotropy cases, $p_1 = p_2 = 1$ was used to determine the effective hydraulic conductivity $K_1^e(h)$ and $K_2^e(h)$ in the two horizontal directions; three different p_3 values (i.e., $p_3 = 1/3$, 0, and −1) were used to determine the effective hydraulic conductivity in the vertical direction, $K_3^e(h)$, for cases LA, IA, and HA, respectively (Table B-6). For all cases, identical procedures were repeated over the expected pressure head range of (−10, 0) m. By using four different p values (i.e., 1, 1/3, 0, and −1), four sets of effective $K^e(h)$ values were obtained.

The $K^e(h)$ data sets obtained by power averaging were described by the TCT model (Equation B-4) after incorporating the van Genuchten (1980) retention function (Equation B-9) and the Mualem (1976) hydraulic conductivity function ($\beta = 1$ and $\gamma = 2$) via Equations B-6 and B-5. As initial estimates, the effective hydraulic conductivities at full saturation were determined with the sample K_s values corresponding to $h = 0$ and Equation B-4. The effective tortuosity-connectivity coefficients L^e and K_s^e were then fitted using a least-squares method to the effective K^e versus h data pairs by fixing α^e and n^e.

Figure B-11. Effective Moisture Retention Curves for the (a) Sand-Dominated, (b) Gravel-Dominated and (c) Fine-Textured Units at Waste Management Area A-AX. (1 of 3 sheets)

(a)

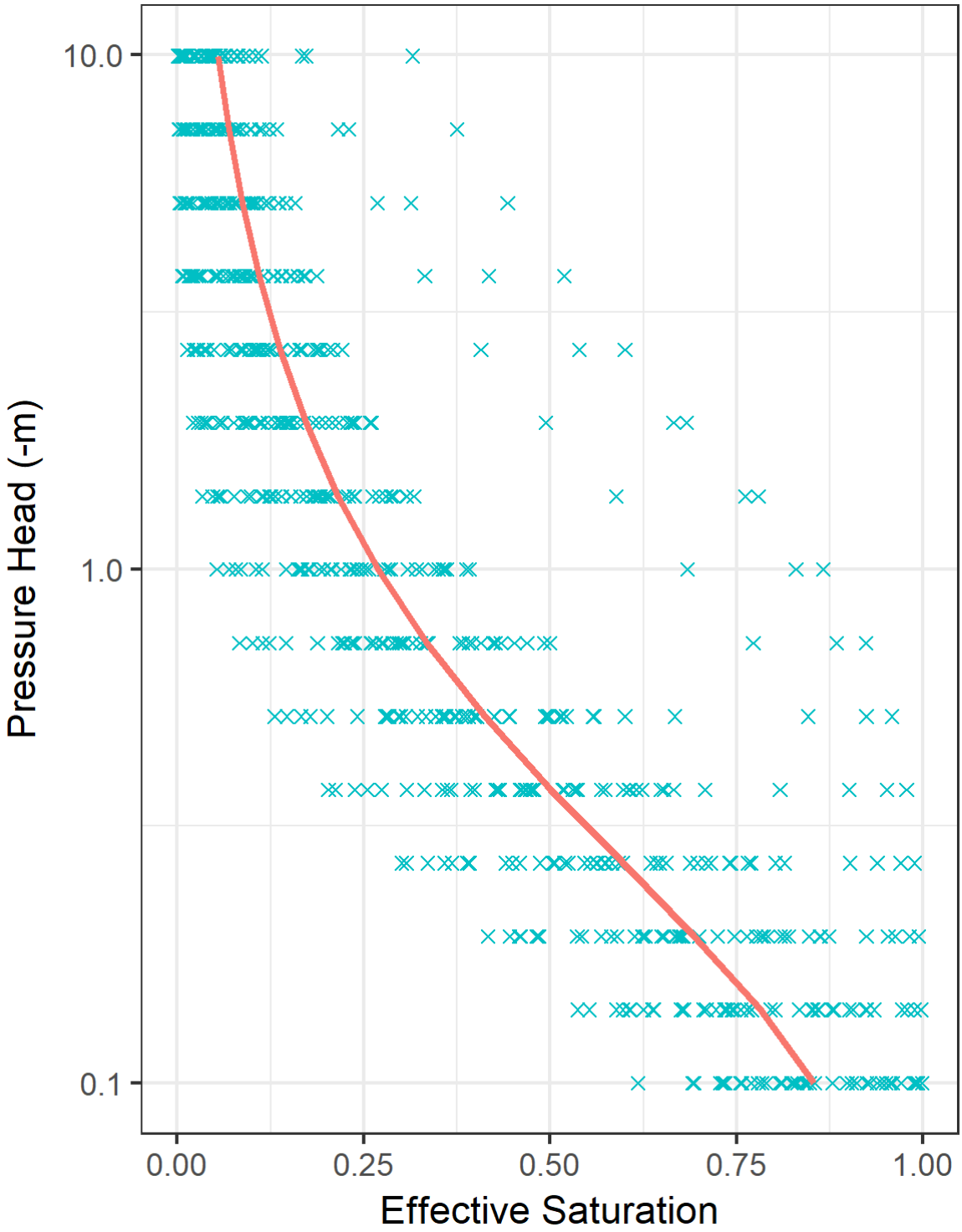

Note. The symbols represent data for the 44 samples and the solid curve is the effective retention curve.

Figure B-11. Effective Moisture Retention Curves for the (a) Sand-Dominated, (b) Gravel-Dominated and (c) Fine-Textured Units at Waste Management Area A-AX. (2 of 3 sheets)

(b)

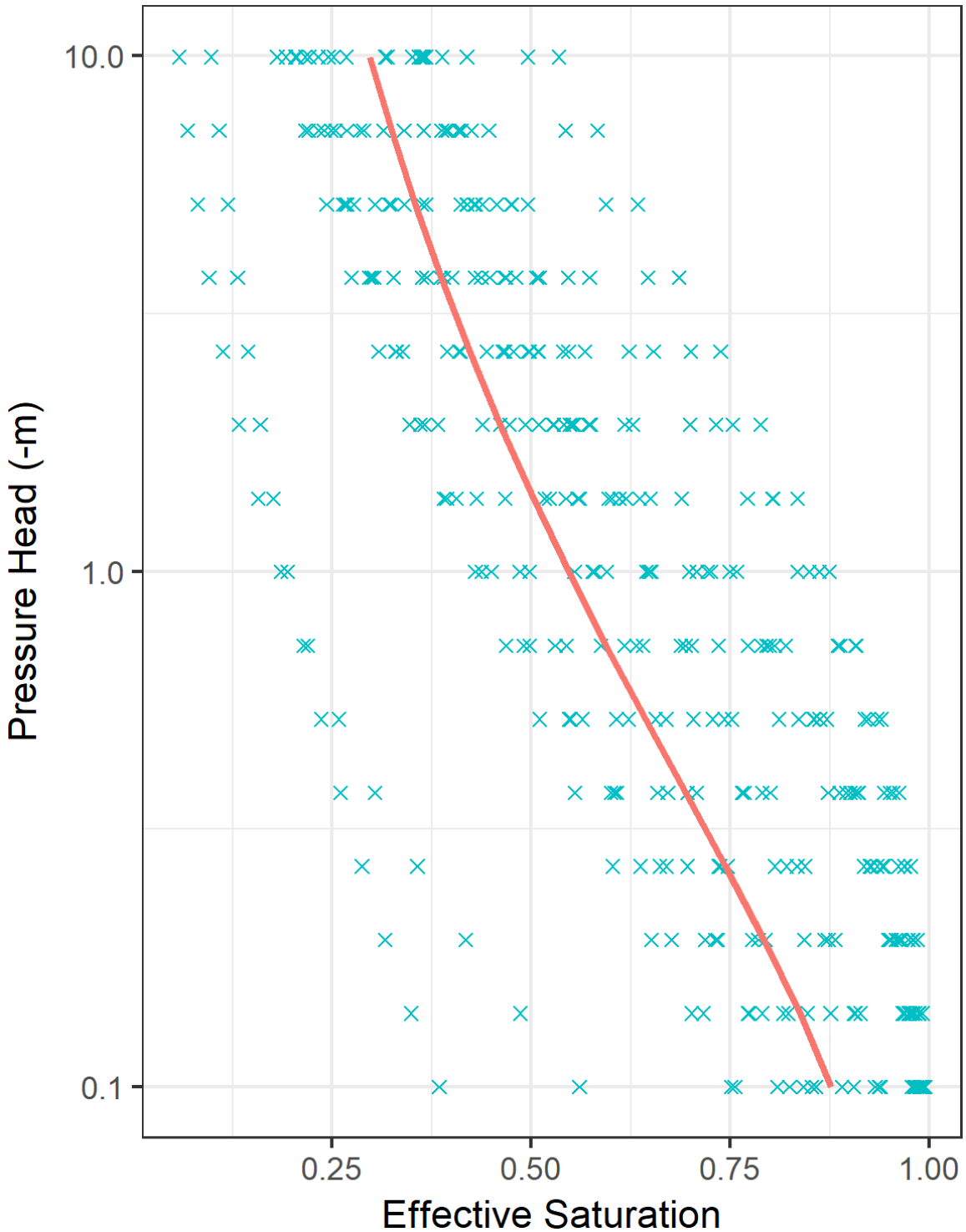

Note. The symbols represent data for the 25 samples and the solid curve is the effective retention curve.

Figure B-11. Effective Moisture Retention Curves for the (a) Sand-Dominated, (b) Gravel-Dominated and (c) Fine-Textured Units at Waste Management Area A-AX. (3 of 3 sheets)

(c)

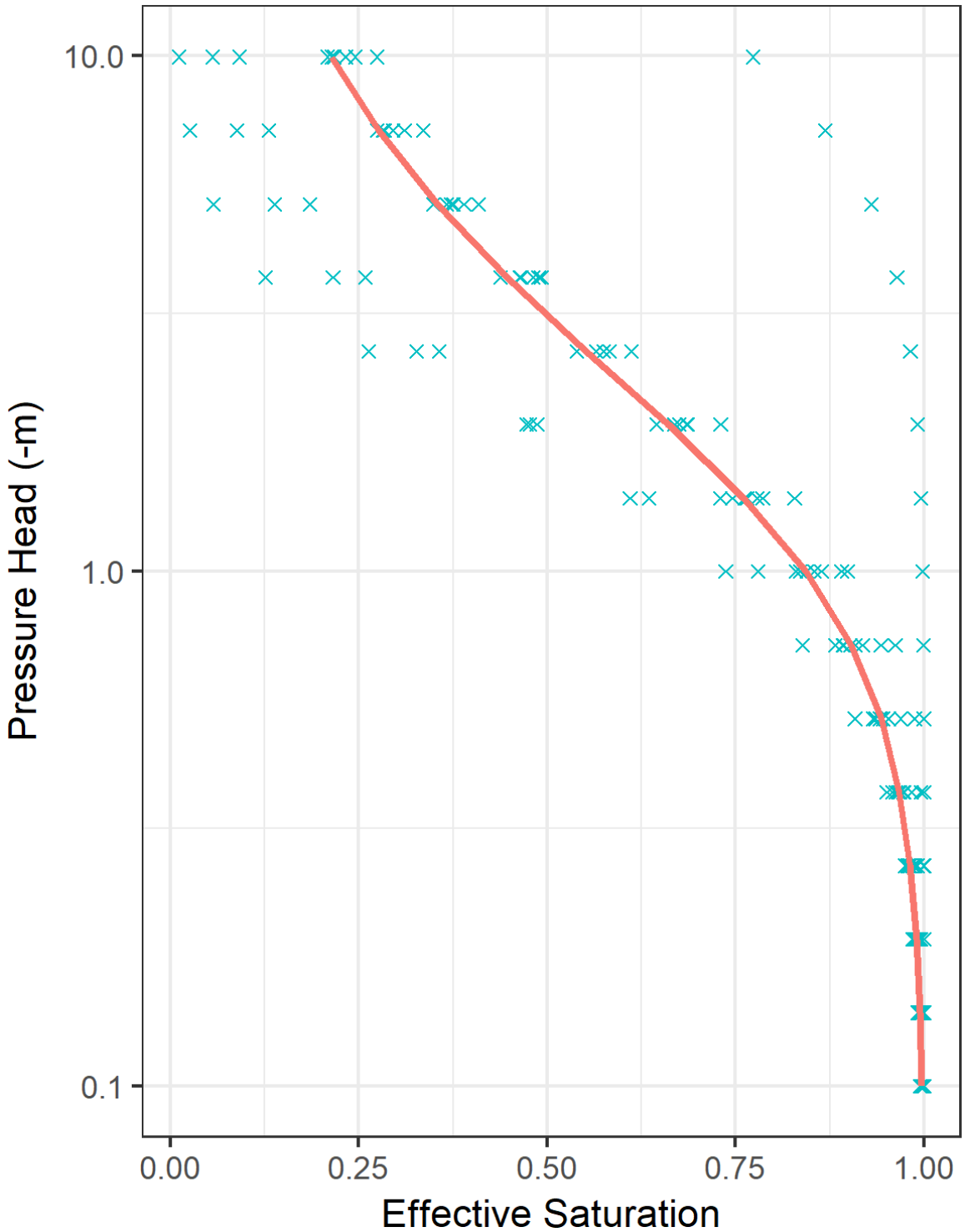

Note. The symbols represent data for the 10 samples and the solid curve is the effective retention curve.

Table B-6. Typical Cases with Varying Degrees of Anisotropy.

Case	Anisotropy Level	p Value for the Horizontal Direction (i = 1, 2)	p Value for the Vertical Direction (i = 3)
ISO	Isotropic	0	0
LA	Low Anisotropy	1	1/3
IA	Intermediate Anisotropy	1	0
HA	High Anisotropy	1	-1

Note. For the Sisson and Lu field injection site in 200 East Area ("Simulating field-scale moisture flow using a combined power-averaging and tensorial connectivity-tortuosity approach" [Zhang and Khaleel 2010]), the simulation results best matched the observed moisture plume behavior when the power values of 1 and 1/3 were used for determining the effective unsaturated conductivity $K^e(h)$ (h=matric potential) in the horizontal directions and vertical direction, respectively, i.e., a case of low macroscopic anisotropy (LA). Based on the documented field-testing results for Hanford sediments, the LA case (p = 1 for the x- and y-directions and p =1/3 for the z-direction) is the recommendation for the Waste Management Area A-AX Performance Assessment model simulations.

Table 3-3 in Section 3.1.4.4 summarizes the four sets of optimized K_s^e and L^e values corresponding to the four p values used for power averaging. For each stratigraphic unit, the magnitude for K_s^e follows the sequence for p, with K_s^e the largest for $p = 1$ and the smallest for $p = -1$, as expected. The sequence for L^e is just the opposite to that for p, with L^e the smallest for $p = 1$ and the largest for $p = -1$. A smaller L^e indicates less flow-path tortuosity and/or larger connectivity. Hence, the sequence of flow-path tortuosity or connectivity follows the sequence of magnitude for L^e. Parameter L^e for different textures, although referred to as the tortuosity-connectivity coefficient, appears to be mainly a reflection of flow-path connectivity under unsaturated conditions.

A larger L^e is indicative of more poorly-connected pore space or flow networks at a given saturation of less than 1. Textural differences for L^e suggest that coarse-textured soils tend to have a larger L^e than fine-textured soils.

Figure B-12 (a) through (c) illustrates the respective effective (upscaled) unsaturated hydraulic conductivity-pressure head relationship for the sand-dominated, gravel-dominated, and fine-textured units at WMA A-AX. Figure B-13 (a) through (c) illustrates the respective PA-TCT-based macroscopic variable anisotropy for the sand-dominated, gravel-dominated, and fine-textured units at WMA A-AX. In general, the macroscopic anisotropy increases with increases in pressure head (or with decreasing moisture content). The low and intermediate anisotropy plots for gravel show the opposite trend [Figure B-13(b)]. This is due to the mixed usage of two different sets of gravel-dominated sediment samples; one from the 100 Area and the other from the 300 Area. Nonetheless, for the simulated (expected) moisture regime of 2 to 4 m tension, the anisotropy for the gravelly sediments, as expected, is indeed low and, for all practical purposes, nearly constant for the low and intermediate anisotropy.

As stated earlier, no data specific to WMA A-AX are available that can be used to directly develop estimates of hydraulic properties needed for the WMA A-AX PA. Surrogate hydraulic properties have been identified based on samples collected at other sites within the 200 Areas

and nearby locations that are representative of sediments characteristic of the major HSUs identified at WMA A-AX.

B.5 MOISTURE CONTENT MEASUREMENTS

As part of WMA A-AX site characterization, a moisture content database is available for the uppermost HSUs. Most neutron moisture data were collected from drywells and direct push boreholes in WMA A-AX in 2014, long after the occurrence of past leaks and discharges at the tank farms. A summary of statistics of the moisture content measurements for WMA A-AX HSUs is provided in Table B-7 for ACM 1 (Table 4-1 in RPP-ENV-58578, *Summary of the Natural System at Waste Management Area A-AX*). Overall, for WMA A-AX, the moisture content data show considerable variability – the values range from close to zero to as high as 43.2 (% volume) (Table B-7). For H2, the average moisture content is ~5.2 (% volume) based on field data (Table B-7). For backfill, the measured average is ~9.5 (% volume), and for H1, the measured moisture content average is ~6.8 (% volume). Overall, the average moisture contents reflect the presence of a relatively dry moisture regime and are in general agreement with the averages of the moisture content measurements collected at nearby WMA C (RPP-CALC-60345, *Heterogeneous Media Model for Waste Management Area C Performance Assessment*; RPP-CALC-60450, *Process for Determining the Volumetric Moisture Content for the Vadose Zone Geologic Units Underlying Waste Management Area C*).

Table 3.3 in PNNL-15141, *Investigation of Accelerated Casing Corrosion in Two Wells at Waste Management Area A-AX* includes gravimetric moisture data from CCUz samples from two boreholes near WMA A-AX, well 299-E24-33 and well 299-E25-94. Excluding samples that are identified as not being representative of the silt unit as a whole (Section 3.1 in PNNL-15141), the moisture content of samples collected from depths of 255.5 ft to 259.5 ft below ground surface at well 299-E24-33 and from depths of 273.5 ft to 279.5 ft below ground surface at well 299-E25-94 ranged from 18.6% to 27.9% by weight, with a central value of about 24%. Assuming a bulk density of 1.8 g/cm^3, the estimated moisture range is about 33% to 50% by volume.

Compared to the saturated moisture contents of the silty samples used to parameterize the CCUz identified in Table B-5, the CCUz samples near WMA A-AX appear to be near saturation.

Figure B-12. Effective Unsaturated Hydraulic Conductivities for the (a) Sand-Dominated, (b) Gravel-Dominated, and (c) Fine-Textured Units at Waste Management Area A-AX. (1 of 3 sheets)

(a)

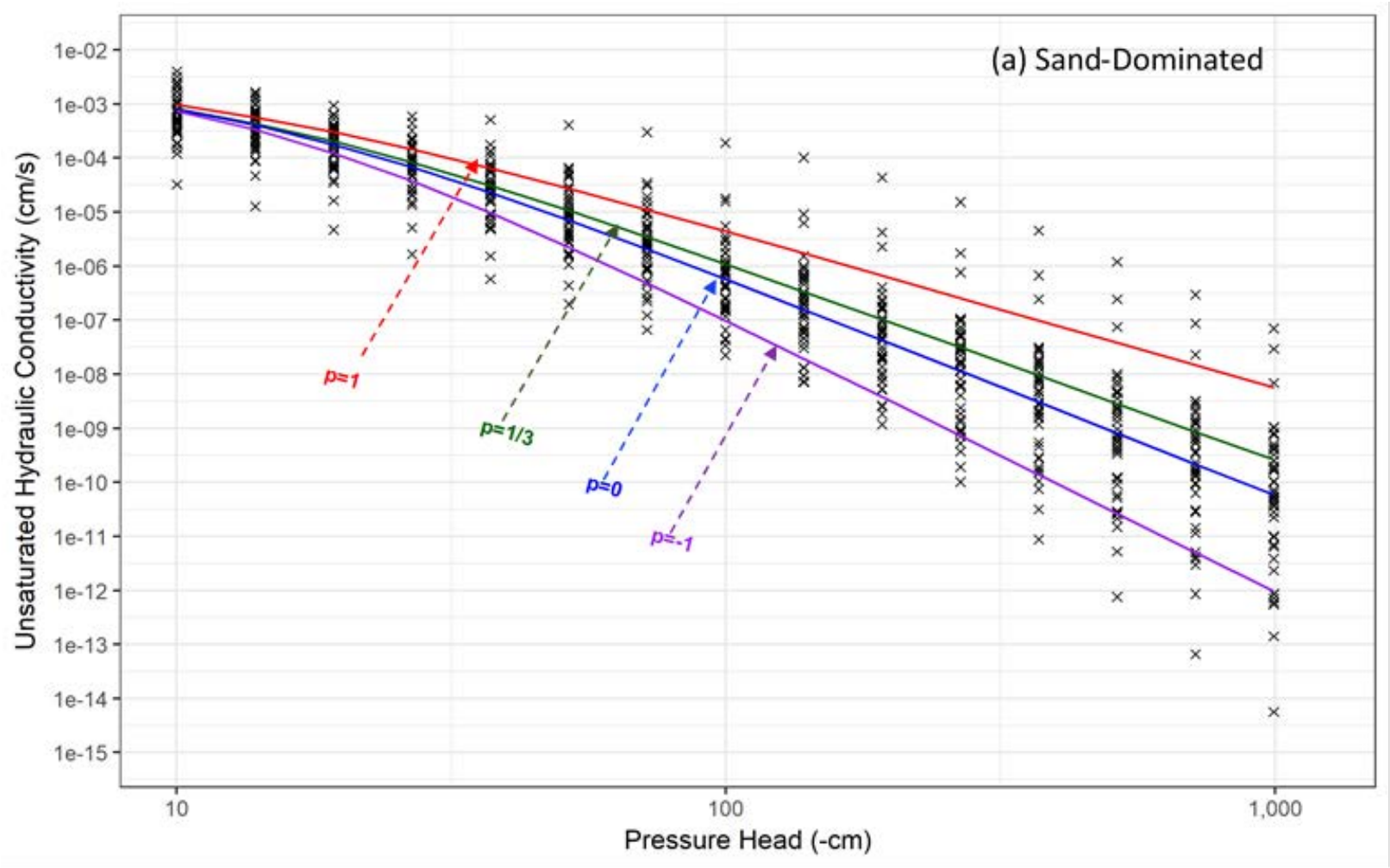

Figure B-12. Effective Unsaturated Hydraulic Conductivities for the (a) Sand-Dominated, (b) Gravel-Dominated, and (c) Fine-Textured Units at Waste Management Area A-AX. (2 of 3 sheets)

(b)

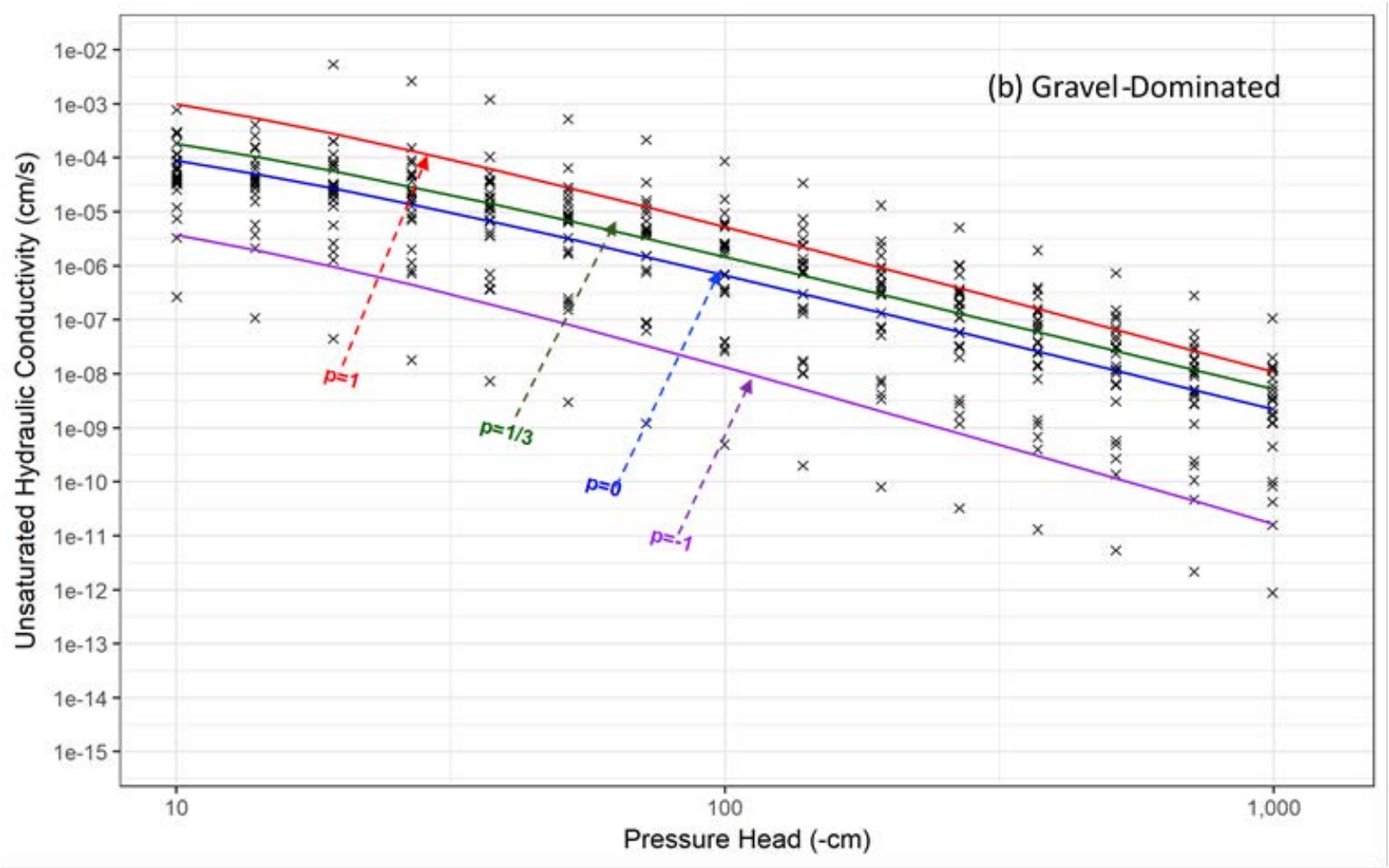

Figure B-12. Effective Unsaturated Hydraulic Conductivities for the (a) Sand-Dominated, (b) Gravel-Dominated, and (c) Fine-Textured Units at Waste Management Area A-AX. (3 of 3 sheets)

(c)

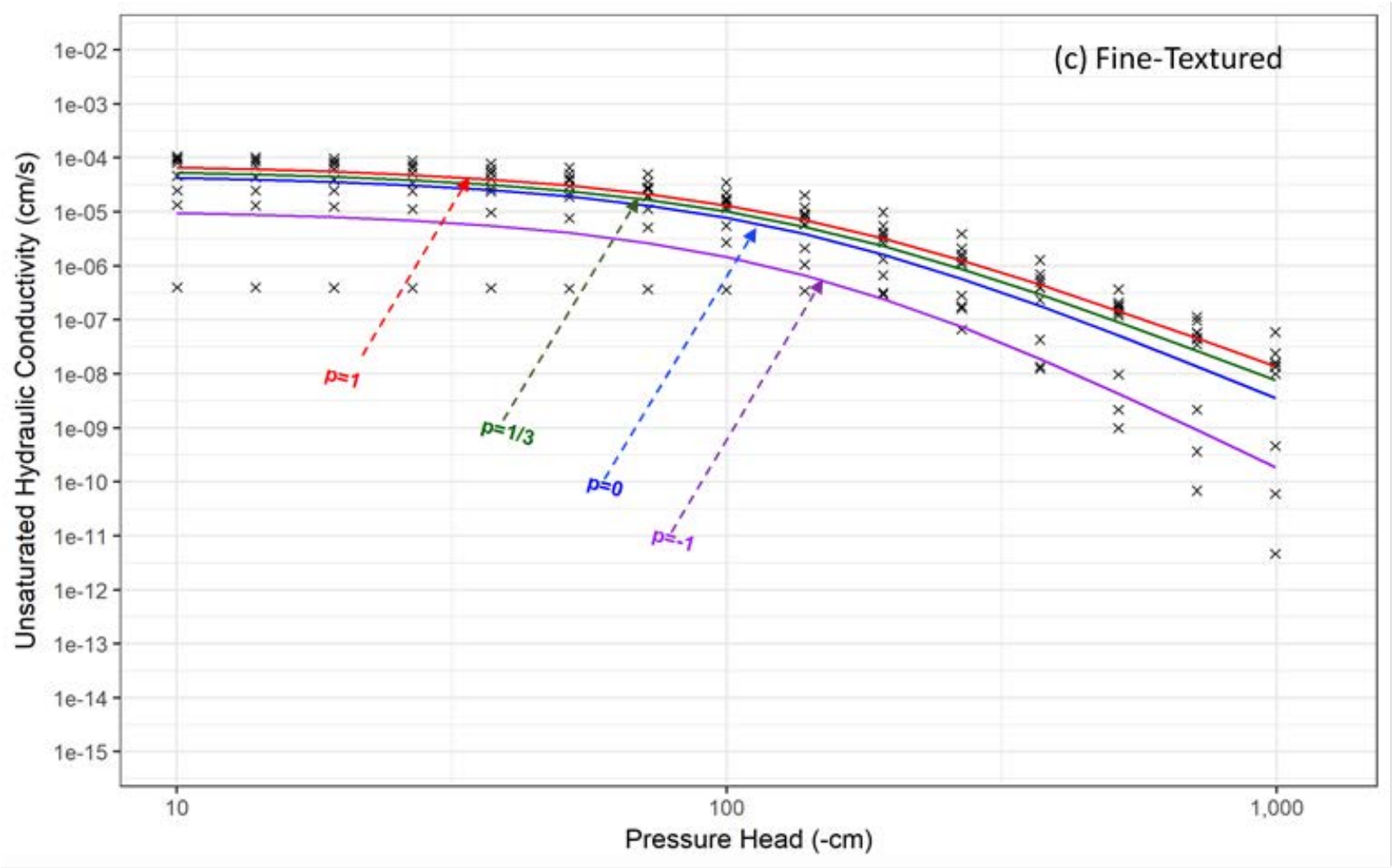

Figure B-13. Variable Tension Dependent Anisotropy for the (a) Sand-Dominated, (b) Gravel-Dominated, and (c) Fine-Textured Units at Waste Management Area A-AX. (1 of 3 sheets)

(a)

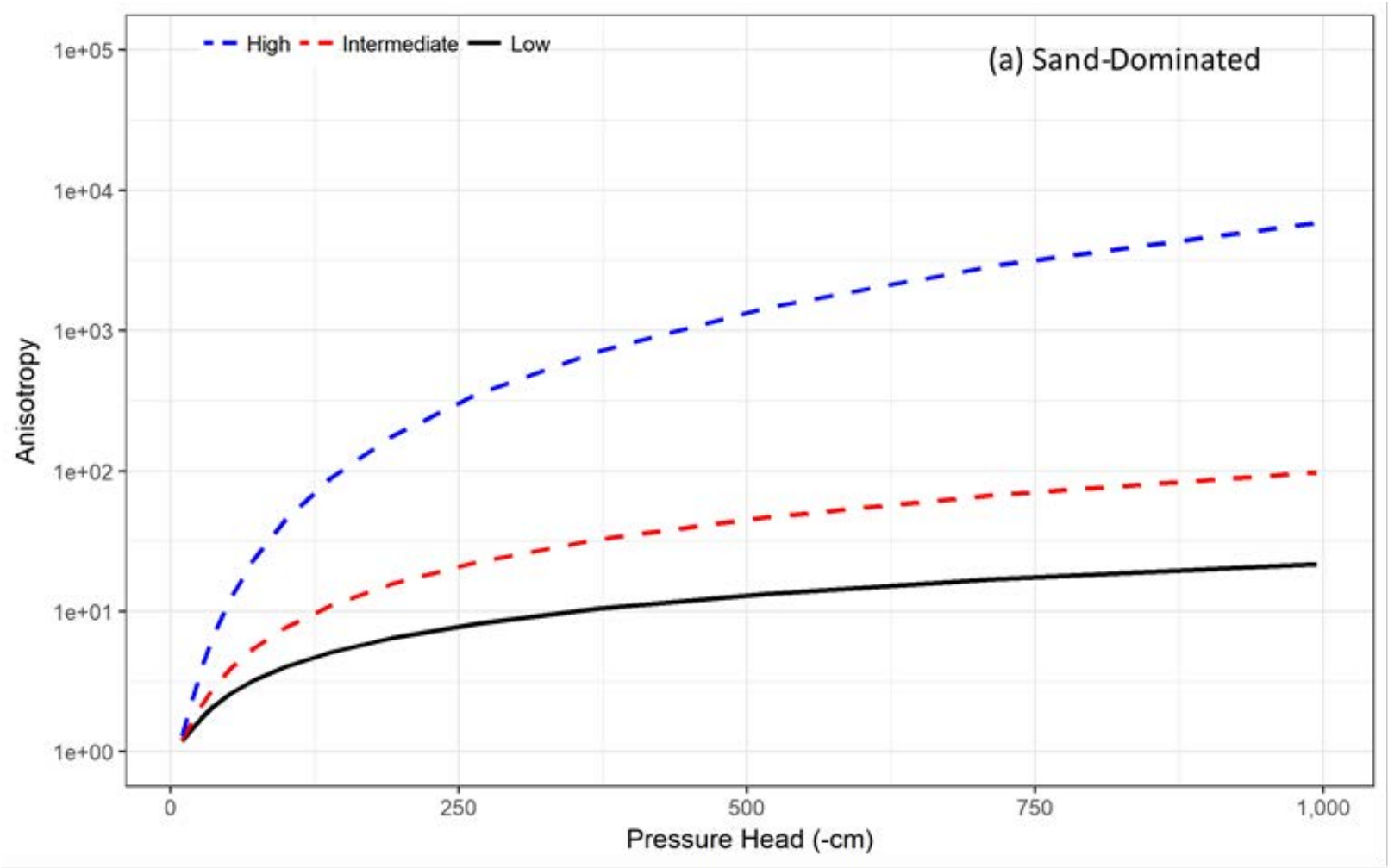

Figure B-13. Variable Tension Dependent Anisotropy for the for the (a) Sand-Dominated, (b) Gravel-Dominated, and (c) Fine-Textured Units at Waste Management Area A-AX. (2 of 3 sheets)

(b)

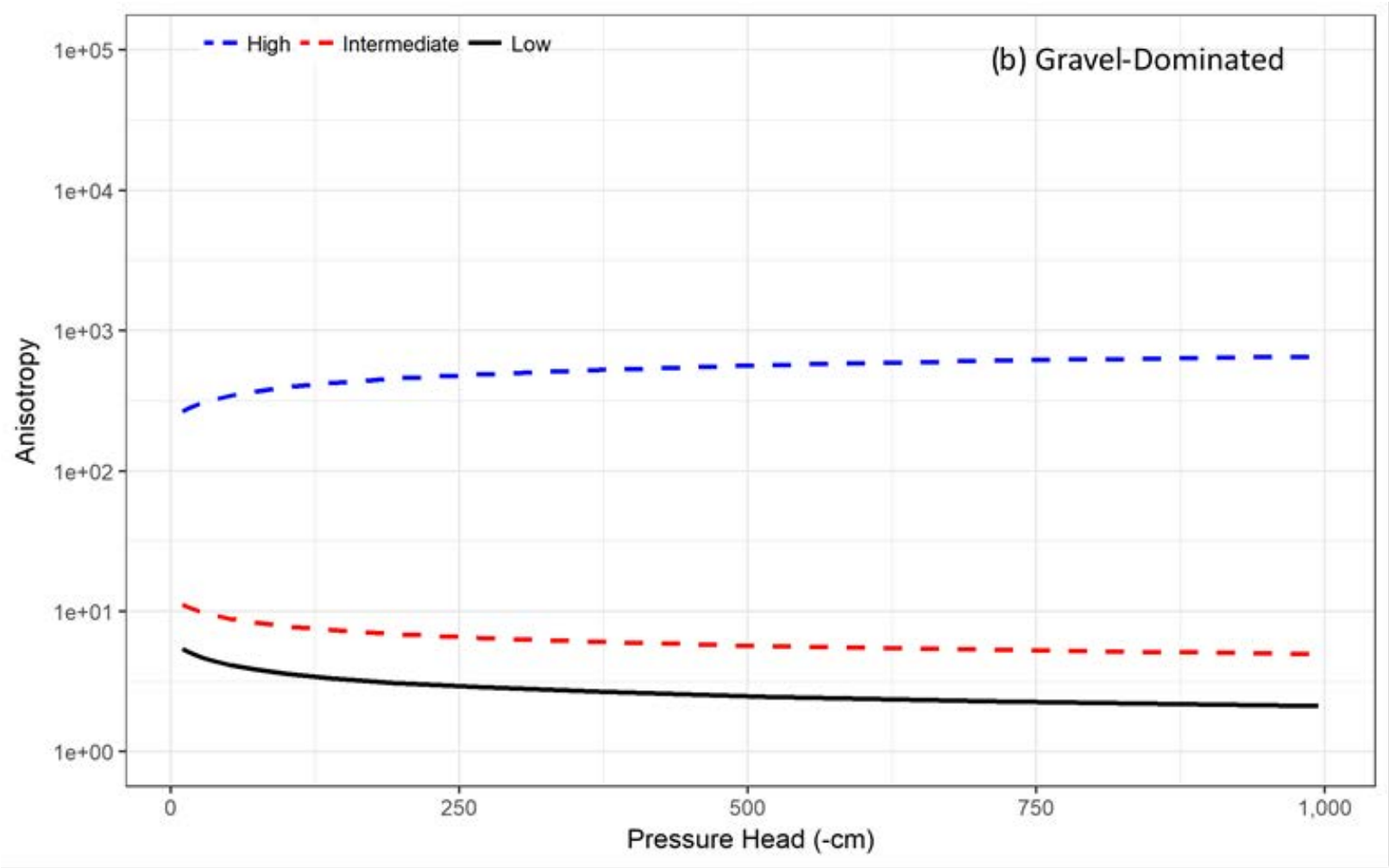

Figure B-13. Variable Tension Dependent Anisotropy for the for the (a) Sand-Dominated, (b) Gravel-Dominated, and (c) Fine-Textured Units at Waste Management Area A-AX. (3 of 3 sheets)

(c)

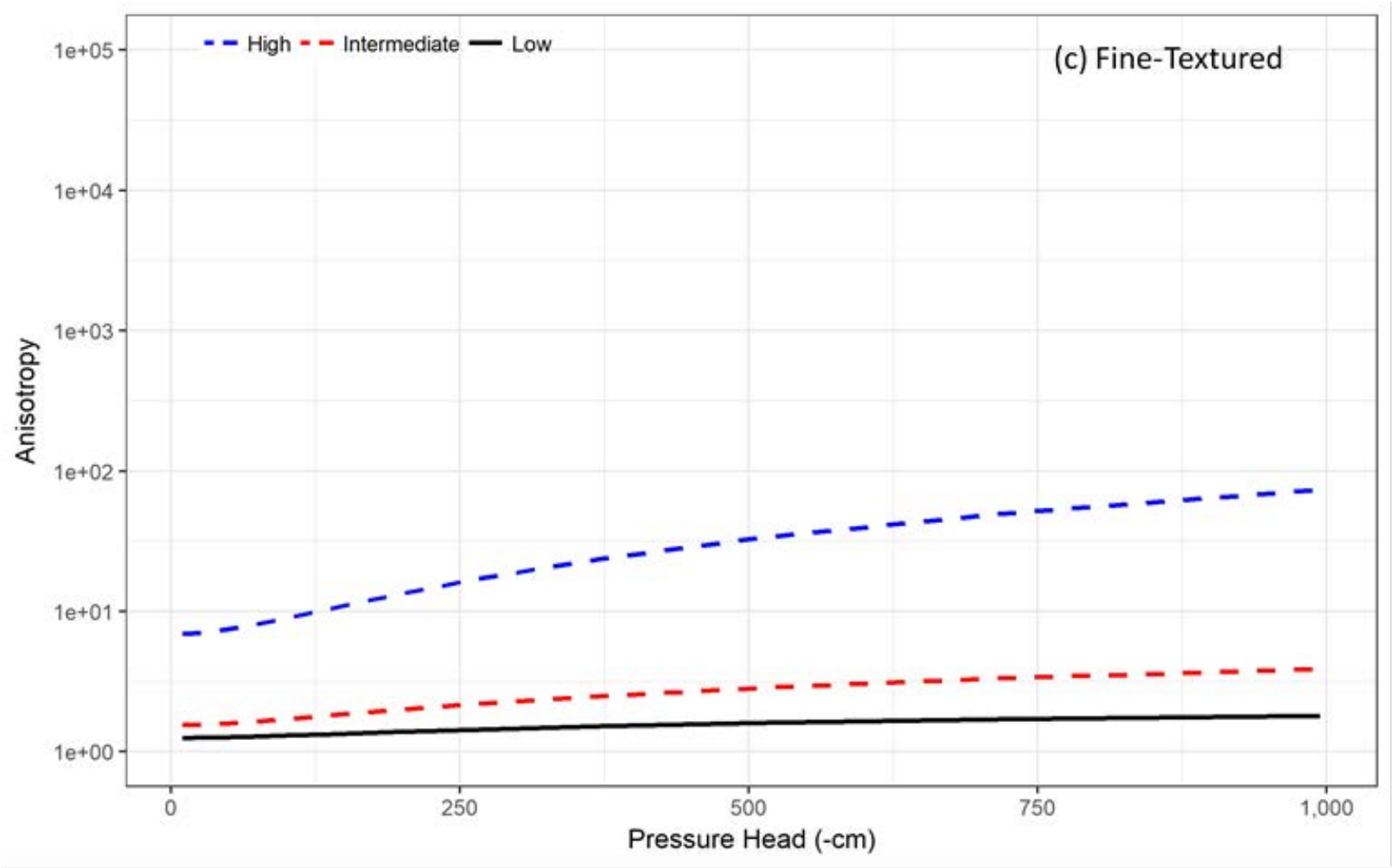

Table B-7. Summary Statistics for Waste Management Area A-AX Alternative Conceptual Model 1 Moisture Content (% Volume) Database.

Unit	Count	Minimum	Maximum	Average
Backfill	7,814	0.00023	43.24	9.50
Hanford formation unit 1 (H1)	146	3.99	17.45	6.80
Hanford formation unit 2 (H2)	10,705	0.52	43.01	5.23
All Units	18,665	0.00023	43.24	7.03

Reference: RPP-ENV-58578 Rev. 1 Draft, *Summary of the Natural System at Waste Management Area A-AX*, Table 4-1.

In addition, measurements of core samples from the CCUz and CCUg from the nearby WMA B-BX-BY borehole 299-E33-45 shown in Figure 2.6 of PNNL-19277, *Conceptual Models for Migration of Key Groundwater Contaminants through the Vadose Zone and into the Unconfined Aquifer Below the B-Complex* can be used as proxy for those units at WMA A-AX. Borehole 299-E33-45 is located near a large past release from tank 241-BX-102 and in an area where perched water has been observed above the CCUz (PNNL-19277), so the conditions differ from WMA A-AX, but the range of moisture content observed is still useful for comparison. The silt-dominated CCUz samples from borehole 299-E33-45 have moisture content measurements that range from about 12% to 26% by weight. Assuming a bulk density of 1.8 g/cm^3, the estimated moisture range for the CCUz at WMA B-BX-BY is about 22% to 47% by volume. Moisture content in samples from the gravel-dominated CCUg from borehole 299-E33-45 range from 2 to 4% by weight. Assuming a bulk density of 2.0 g/cm^3, the estimated range for the CCUg at WMA B-BX-BY is about 4 to 8% by volume.

B.6 EFFECTIVE TRANSPORT PROPERTIES

Base case effective transport parameter (bulk density, diffusivity, and dispersivity) estimates are presented in this section. Because of natural variability, the transport parameters are all spatially variable. The purpose is again, similar to the flow parameters, to evaluate the effect of such variability on the large-scale transport process.

B.6.1 Bulk Density and Particle Density

For transport calculations, bulk density (ρ_b) as well as K_d estimates are needed to calculate the retardation factors for different species. The effective, large-scale estimate for bulk density is the average of the small-scale laboratory measurements for bulk density (Stochastic Subsurface Hydrology [Gelhar 1993]). Table B-8 provides the effective, large-scale bulk density estimates for WMA A-AX HSUs. STOMP input requires particle density values, and the particle density values listed in Table 3-4 for WMA A-AX HSUs are estimated from the equation (Soil Physics [Jury et al. 1991]):

$$\rho_s = \frac{\rho_b}{(1-\theta_s)} \tag{B-9}$$

where ρ_s is the particle density and the porosity is assumed to equal the saturated moisture content. The estimated K_d values and the gravel corrections for different HSUs are discussed in Chapter 3.

Table B-8. Bulk Density Estimates for Hydrostratigraphic Units at Waste Management Area A-AX.

Hydrostratigraphic Unit	Bulk Density Range of Measurements (g/cm^3)	Effective Bulk Density (ρ_b) (g/cm^3)
Sand-Dominated Units: (241-AX farm backfill, Eolian sand, Hanford formation unit 1, and Hanford formation unit 2)	1.51 - 1.98	1.67
Gravel-Dominated Units: (241-A farm backfill, Hanford formation unit 3, Cold Creek Unit gravel, Ringold Formation Unit E, and Ringold Formation Unit A)	1.89 - 2.38	2.15
Fine Textured Units: (Cold Creek Unit silt and Ringold Formation Lower Mud Unit)	1.50 - 1.72	1.60

References:
PNNL-22886, *System-Scale Model of Aquifer, Vadose Zone, and River Interactions for the Hanford 300 Area – Application to Uranium Reactive Transport.*
RPP-20621, *Far-Field Hydrology Data Package for the Integrated Disposal Facility Performance Assessment.*
WHC-EP-0645, *Performance Assessment for the Disposal of Low-Level Waste in the 200 West Area Burial Grounds.*
WHC-EP-0883, *Variability and Scaling of Hydraulic Properties for 200 Area Soils, Hanford Site.*

B.6.2 Diffusivity

It is assumed that the effective, large-scale diffusion coefficients for all HSUs are a function of volumetric moisture content, θ, and can be estimated based on the Millington and Quirk empirical relation (presented as Equation 7-11 in Jury et al. [1991]):

$$D_e(\theta) = D_0 \frac{\theta^{10/3}}{\theta_s^2} \qquad \text{(B-10)}$$

where $D_e(\theta)$ is the effective diffusion coefficient of an ionic species, and D_0 is the effective diffusion coefficient for the same species in free water. The molecular diffusion coefficient for all species in pore water is assumed to be 2.5×10^{-5} cm^2/sec (WHC-SD-WM-EE-004, *Performance Assessment of Grouted Double-Shell Tank Waste Disposal at Hanford*).

B.6.3 Vadose Zone Macrodispersivities

Field-scale dispersivities are often referred to as macrodispersivities. The terms macrodispersivity and dispersivity are used interchangeably in this section. Details are provided in RPP-ENV-58782, *Performance Assessment of Waste Management Area C, Hanford Site,*

Washington (Appendix B) on how the macrosdispersivities are estimated using different methods.

Field observations indicate that the dispersion coefficients required to describe the large-scale transport processes, at field scales of tens or hundreds of meters, are much different from those observed in small-scale laboratory experiments (Gelhar 1993). In fact, field-scale dispersivities may often be orders of magnitude larger than those observed in the laboratory. Consequently, laboratory-scale dispersivities, which are typically ~1 cm or less, are of little use in estimating field-scale dispersivities.

There is general agreement in hydrology literature that hydraulic conductivity variations induced by field-scale heterogeneities play an important role in field-scale transport processes. However, there does not appear to be a clear consensus about how best to describe such processes quantitatively (Gelhar 1993). While well-designed, large-scale tracer experiments would provide useful information, limited field data are available at this time to quantify macrodispersivities in unsaturated media.

Dispersivities are a function of matric potential (or soil moisture content) in unsaturated media ("Stochastic Modeling of Large-Scale Transient Unsaturated Flow Systems" [Mantoglou and Gelhar 1987]). As with saturated media, heterogeneities that exist at various length scales result also in a scale dependence of macrodispersivities in unsaturated media ("A Critical Review of Data on Field-Scale Dispersion in Aquifers" [Gelhar et al. 1992]). Dispersivities increase with time, or equivalently with distance, until they tend to converge on their unique asymptotic (large-time) values. However, it can take a long time (e.g., years or decades) for the asymptotic Fickian approximation to take hold. This well-known asymptotic behavior is usually attributed to heterogeneity-induced spreading and mixing until the point at which the heterogeneity has effectively been "sampled" by the contaminant plume such that dispersion becomes constant. As with other numerical simulation work, the use of a constant (asymptotic) macrodispersivity for the WMA A-AX PA is considered appropriate (NUREG/CR-6114, *Auxiliary Analyses in Support of Performance Assessment of a Hypothetical Low-Level Waste Facility: Groundwater Flow and Transport Simulation*, Vol. 3; NUREG/CR-5965, *Modeling Field Scale Unsaturated Flow and Transport Processes*). The second-moment evolution or the time-dependent, pre-asymptotic dispersivities are of only marginal interest in simulations involving long times or large-mean travel distances such as those for the WMA A-AX PA modeling.

Note that, because of the relatively dry moisture regime, unsaturated media macrosdispersivity estimates are expected to be smaller, compared to saturated media estimates. Also note that, unlike saturated media, the vadose zone flow is typically perpendicular to geologic bedding. Numerical simulations of vadose zone transport for H2 sands demonstrated that the longitudinal macrodispersivities for flow perpendicular to bedding are smaller than those for flow parallel to bedding ("Upscaled flow and transport properties for heterogeneous unsaturated media" [Khaleel et al. 2002]). For both perpendicular and parallel flows to bedding, macrodispersivities increase as the mean matric potential becomes more negative. However, the Fickian regime is reached much earlier for cases with flow perpendicular to bedding than for flow parallel to bedding (Khaleel et al. 2002).

Section B.6.3.1 provides a range of estimates based on numerical simulations, stochastic theory and experimental observations. To obtain macrodispersivity, the local pore-scale dispersivities, which are typically small (<1 cm), are not included either in numerical simulations or stochastic solutions. This is consistent with the approach used by other investigators ("Stochastic analysis of adsorbing solute transport in three-dimensional, heterogeneous, unsaturated soils" [Yang et al. 1997]; Gelhar 1993; "Three-dimensional stochastic analysis of macrodispersion in aquifers" [Gelhar and Axness 1983]).

B.6.3.1 Recommended Macrodispersivities for Waste Management Area A-AX Performance Assessment

The macrodispersivity values presented in Table 3-4 (Section 3.1.4.5.1) represent estimates based on results of (a) numerical simulation (Khaleel et al. 2002), (b) stochastic solutions ("Stochastic Analysis of Simulated Vadose Zone Solute Transport in a Vertical Cross Section of Heterogeneous Soil During Nonsteady Water Flow" [Russo 1991]; Large-Scale Models of Transient Unsaturated Flow and Contaminant Transport Using Stochastic Methods [Mantoglou 1984]), and (c) 200 Areas experimental data (RPP-20621 Appendix E).

Overall, the recommended asymptotic macrodispersivity estimates (Table 3-4) are consistent with values reported in literature for relatively dry unsaturated media (e.g., Gelhar 1993; "The Second Las Cruces Trench Experiment: Experimental Results and Two-Dimensional Flow Predictions" [Hills et al. 1991]; "Chlorine 36 and Tritium from Nuclear Weapons Fallout as Tracers for Long-Term Liquid and Vapor Movement in Desert Soils" [Phillips et al. 1988]; RPP-20621 Appendix E).

For the sandy media, estimates are available by all three methods: numerical simulation, stochastic solutions, and field experiments. However, for the PA modeling for the sandy units, the recommendation is to use longitudinal macrodispersivity values ranging from 25 cm (based on numerical simulations [Khaleel et al. 2002]) to 100 cm (based on extrapolation of field data up to a length scale of 10 m (Figure B-14.).

The perturbation analysis for the stochastic solutions applies to small variance estimates. Stochastic theory-based estimates are often considerably larger than those based on numerical simulations and field experiments for the sandy media because of the large variance of unsaturated hydraulic conductivity estimate ($\sigma^2_{LnK_u}$) (Appendix B in RPP-ENV-58782). These values are not included within the estimated range of values presented in Table 3-4. The range of estimates for sandy sediments compares well with those reported elsewhere (e.g., PNNL-25146, *Scale-Dependent Solute Dispersion in Variably Saturated Porous Media*). Using different methods, PNNL-25146 notes that the longitudinal dispersivity estimates for the 200 Areas sandy sediments can range from tens of centimeters to as high as 100 cm.

Unlike the sandy media, the calculated variance ($\sigma^2_{LnK_u}$) for the gravelly and silty units is much lower. For the gravelly media, the recommendation is to use longitudinal macrodispersivity values based on stochastic theory that range from 15 cm to 30 cm, as reported in Appendix B of RPP-ENV-58782. This is again consistent with the estimates (i.e., 15 cm to 43 cm), based on other methods, for the 200 Areas gravelly media (PNNL-25146). The contrast in $\sigma^2_{LnK_u}$ estimates

for the Hanford sandy and gravelly media is illustrated in Figure B-9; the observed log unsaturated conductivity variance for the gravelly sediments is much lower than that for the sandy sediments. Consequently, the calculated dispersivities for the gravelly sediments are expected to be lower than those for the sandy sediments.

Figure B-14. Longitudinal Laboratory- and Field-Scale Dispersivities in Unsaturated Media as a Function of Overall Problem Scale.

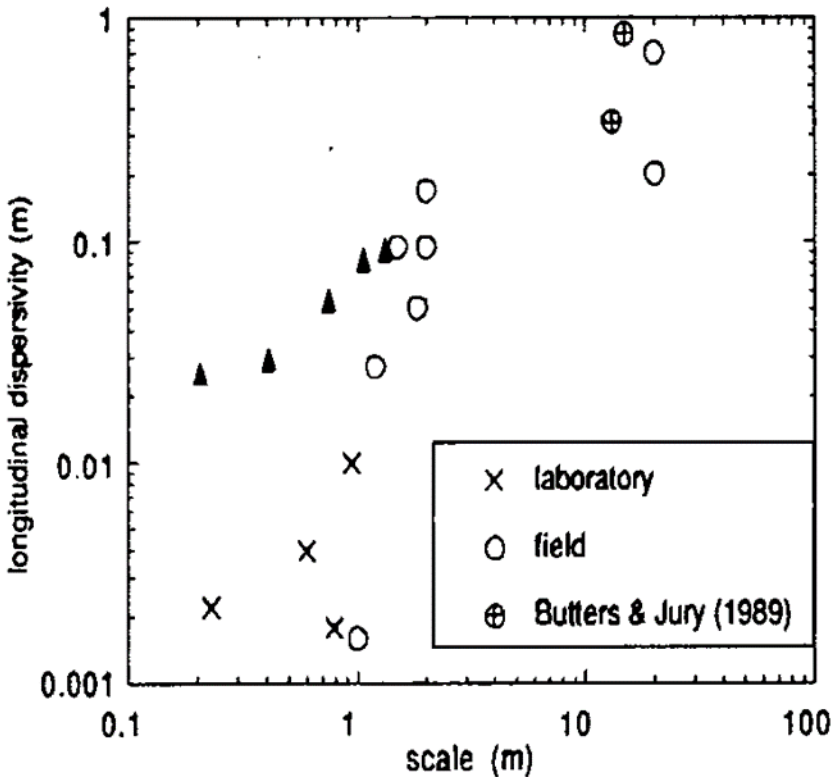

Note. The triangles shown above are based on field tracer experiments in 200 East Area Hanford sands (RPP-20621, *Far-Field Hydrology Data Package for the Integrated Disposal Facility Performance Assessment*, Appendix E, "Hanford Low-Activity Tank Waste Performance Assessment Activity: Determination of In Situ Hydraulic Parameters of the Upper Hanford Formation").

Also, as suggested by a comparison of Figures B-11 and B-12, the $\sigma^2_{LnK_u}$ estimates for the silty sediments are lower than those for the sandy and gravelly sediments. For the silty units, the recommendation is to use, based on stochastic theory, longitudinal macrodispersivity values ranging from 5 cm to 10 cm. Overall, the sequence of magnitudes for macrodispersivities follows the sequence of reduction in variance for the sandy, gravelly, and silty sediments. The asymptotic macrodispersivity estimates in Table 3-4 are for a relatively dry moisture regime (i.e., $\sigma^2_{LnK_u}$ estimated for mean tensions of 2 m for the sandy units, 4 m for the gravelly units, and 1 to 2 m for the silty units).

The transverse macrodispersivity is typically much lower; in saturated media, it may range from 1 to 10% of the longitudinal macrodispersivity (Gelhar and Axness 1983). In the absence of

unsaturated media experimental data, the recommendation is to use a transverse macrodispersivity 1/10th of the longitudinal macrodispersivity (PNNL-23711, PNNL-25146).

B.7 REFERENCES

Ababou, R., 1996, "Random Porous Media Flow on Large 3-D Grids: Numerics, Performance, and Application to Homogenization," in Environmental Studies Mathematical, Computational, and Statistical Analysis, edited by M. F. Wheeler, Springer-Verlag, New York, New York.

ARH-LD-127, 1976, *Geology of the 241-A Tank Farm*, Atlantic Richfield Hanford Company, Richland, Washington.

ARH-LD-128, 1976, *Geology of the 241-AX Tank Farm*, Atlantic Richfield Hanford Company, Richland, Washington.

Burdine, N. T., 1953, "Relative Permeability Calculation from Pore Size Distribution Data," *The American Institute of Mining, Metallurgical, and Petroleum Engineers*, Vol. 198, pp. 71–78.

Eching, S. O. and J. W. Hopmans, 1993, "Optimization of Hydraulic Functions from Transient Outflow and Soil Water Pressure Data," *Soil Science Society of America Journal*, Vol. 57, No. 5, pp. 1167–1175.

Gelhar, L.W., 1993, Stochastic Subsurface Hydrology, Prentice Hall, New York, New York.

Gelhar, L. W. and C. L. Axness, 1983, "Three-dimensional stochastic analysis of macrodispersion in aquifers," *Water Resources Research*, Vol. 19, Issue 1, pp. 161–180.

Gelhar, L. W., C. Welty, and K. R. Rehfeldt, 1992, "A Critical Review of Data on Field-Scale Dispersion in Aquifers," *Water Resources Research*, Vol. 28, Issue 7, pp. 1955–1974.

Green, T. R., J. E. Constantz, and D. L. Freyberg, 1996, "Upscaled soil-water retention using van Genuchten's function," *Journal of Hydrologic Engineering*, Vol. 1, Issue 3, pp. 123–130.

Hills, R. G., P. J. Wierenga, D. B. Hudson, and M. R. Kirkland, 1991, "The Second Las Cruces Trench Experiment: Experimental Results and Two-Dimensional Flow Predictions," *Water Resources Research*, Vol. 27, Issue 10, pp. 2707–2718.

Jury, W. A., W.R. Gardner, and W. H. Gardner, 1991, Soil Physics, 5th edition, John Wiley & Sons, Inc., New York, New York.

Khaleel, R. and J. F. Relyea, 2001, "Variability of Gardner's α for coarse-textured sediments," *Water Resources Research*, Vol. 37, Issue 6, pp. 1567–1575.

Khaleel, R., T.-C. J. Yeh, and Z. Lu, 2002, "Upscaled flow and transport properties for heterogeneous unsaturated media," *Water Resources Research*, Vol. 38, Issue 5, pp. 11-1–11-12.

Klute, A. and C. Dirksen, 1986, "Hydraulic Conductivity and Diffusivity: Laboratory Methods," in Methods of Soil Analysis, Part 1—Physical and Mineralogical Methods, Second Edition, American Society of Agronomy-Soil Science Society of America, Madison, Wisconsin, pp. 687–734.

Mantoglou, A., 1984, Large-Scale Models of Transient Unsaturated Flow and Contaminant Transport Using Stochastic Methods, Ph.D. Thesis, Massachusetts Institute of Technology, Department of Civil Engineering, Cambridge, Massachusetts.

Mantoglou, A. and L. W. Gelhar, 1987, "Stochastic Modeling of Large-Scale Transient Unsaturated Flow Systems," *Water Resources Research*, Vol. 23, Issue 1, pp. 37–46.

Matheron, G., 1967, Eléments pour une Théorie des Milieux Poreux, Masson et Cie, Paris, France.

Millington, R. J. and J. P. Quirk, 1961, "Permeability of Porous Solids," *Transactions of the Faraday Society*, Vol. 57, pp. 1200–1207.

Mualem, Y., 1976, "A New Model for Predicting the Hydraulic Conductivity of Unsaturated Porous Media," *Water Resources Research*, Vol. 12, Issue 3, pp. 513–522.

NUREG/CR-5965, 1994, *Modeling Field Scale Unsaturated Flow and Transport Processes*, Nuclear Regulatory Commission, Washington, D.C.

NUREG/CR-6114, 1994, *Auxiliary Analyses in Support of Performance Assessment of a Hypothetical Low-Level Waste Facility: Groundwater Flow and Transport Simulation*, Vol. 3, U.S. Nuclear Regulatory Commission, Washington, D.C.

Phillips, F. M., J. L. Mattick, T. A. Duval, D. Elmore, and P. W. Kubik, 1988, "Chlorine 36 and Tritium from Nuclear Weapons Fallout as Tracers for Long-Term Liquid and Vapor Movement in Desert Soils," *Water Resources Research*, Vol. 24, Issue 11, pp. 1877–1891.

PNNL-14029, 2002, *Geologic and Wireline Summaries from Fiscal Year 2002 ILAW Boreholes*, Pacific Northwest National Laboratory, Richland, Washington.

PNNL-15141, 2008, *Investigation of Accelerated Casing Corrosion in Two Wells at Waste Management Area A-AX*, Rev. 1, Pacific Northwest National Laboratory, Richland, Washington.

PNNL-15503, 2008, *Characterization of Vadose Zone Sediments Below the C Tank Farm: Borehole C4297 and RCRA Borehole 299-E27-22*, Rev. 1, Pacific Northwest National Laboratory, Richland, Washington.

PNNL-19277, 2010, *Conceptual Models for Migration of Key Groundwater Contaminants Through the Vadose Zone and Into the Unconfined Aquifer Below the B-Complex*, Pacific Northwest National Laboratory, Richland, Washington.

PNNL-22886, 2013, *System-Scale Model of Aquifer, Vadose Zone, and River Interactions for the Hanford 300 Area – Application to Uranium Reactive Transport*, RPT-DVZ-AFRI-019, Pacific Northwest National Laboratory, Richland, Washington.

PNNL-23711, 2015, *Physical, Hydraulic, and Transport Properties of Sediments and Engineered Materials Associated with Hanford Immobilized Low-Activity Waste*, RPT-IGTP-004, Rev. 0, Pacific Northwest National Laboratory, Richland, Washington.

PNNL-25146, 2016, *Scale-Dependent Solute Dispersion in Variably Saturated Porous Media*, RPT-IGTP-009, Rev. 0, Pacific Northwest National Laboratory, Richland, Washington.

Polmann, D. J., 1990, Application of Stochastic Methods to Transient Flow and Transport in Heterogeneous Unsaturated Soils, Ph.D. Thesis, Massachusetts Institute of Technology, Department of Civil Engineering, Cambridge, Massachusetts.

Raats, P. A. C., Z. F. Zhang, A. L. Ward, and G. W. Gee, 2004, "The Relative Connectivity-Tortuosity Tensor for Conduction of Water in Anisotropic Unsaturated Soils," *Vadose Zone Journal*, Vol. 3, No. 4, pp. 1471–1478.

Resource Conservation and Recovery Act of 1976, 42 USC 6901, et seq.

RHO-LD-11, 1997, *Granulometric Data 241-A Tank Farm Monitoring Well Sediments*, Rockwell Hanford Operations, Richland, Washington.

RHO-LD-12, 1997, *Granulometric Data 241-AX Tank Farm Monitoring Well Sediments*, Rockwell Hanford Operations, Richland, Washington.

RPP-20621, 2004, *Far-Field Hydrology Data Package for the Integrated Disposal Facility Performance Assessment*, Rev. 0, CH2M HILL Hanford Group, Inc., Richland, Washington.

RPP-CALC-60345, 2016, *Heterogeneous Media Model for Waste Management Area C Performance Assessment*, Washington River Protection Solutions, LLC, Richland, Washington.

RPP-CALC-60450, 2016, *Process for Determining the Volumetric Moisture Content for the Vadose Zone Geologic Units Underlying Waste Management Area C*, Washington River Protection Solutions, LLC, Richland, Washington.

RPP-ENV-58578, in process, *Summary of the Natural System at Waste Management Area A-AX*, Rev. 1, Washington River Protection Solutions, LLC, Richland, Washington.

RPP-ENV-58782, 2016, *Performance Assessment of Waste Management Area C, Hanford Site, Washington*, Rev. 0, Washington River Protection Solutions, LLC, Richland, Washington.

RPP-RPT-60171, in process, *Model Package Report: Geologic Framework Model used in WMA A-AX Performance Assessment and RCRA Closure Analysis*, Rev. 0, Washington River Protection Solutions, LLC, Richland, Washington.

Russo, D., 1991, "Stochastic Analysis of Simulated Vadose Zone Solute Transport in a Vertical Cross Section of Heterogeneous Soil During Nonsteady Water Flow," *Water Resources Research*, Vol. 27, Issue 3, pp. 267–283.

van Genuchten, M. Th., 1980, "A Closed-form Equation for Predicting the Hydraulic Conductivity of Unsaturated Soils," *Soil Science Society of America Journal*, Vol. 44, No. 5, pp. 892–898.

WHC-EP-0645, 1995, *Performance Assessment for the Disposal of Low-Level Waste in the 200 West Area Burial Grounds*, Westinghouse Hanford Company, Richland, Washington.

WHC-EP-0883, 1995, *Variability and Scaling of Hydraulic Properties for 200 Area Soils, Hanford Site*, Rev. 0, Westinghouse Hanford Company, Richland, Washington.

WHC-SD-WM-EE-004, 1995, *Performance Assessment of Grouted Double-Shell Tank Waste Disposal at Hanford*, Rev. 1, Westinghouse Hanford Company, Richland, Washington.

Yang, J., R. Zhang, J. Wu, and M. B. Allen, 1997, "Stochastic analysis of adsorbing solute transport in three-dimensional, heterogeneous, unsaturated soils," *Water Resources Research*, Vol. 33, Issue 8, pp. 1947–1956.

Yeh, T.-C. J., R. Khaleel, and K. C. Carroll, 2015, Flow Through Heterogeneous Geologic Media, Cambridge University Press, New York, New York.

Yeh, T.-C. J., L. W. Gelhar and A. L. Gutjahr, 1985, "Stochastic Analysis of Unsaturated Flow in Heterogeneous Soils, 2. Statistically Anisotropic Media with Variable α," *Water Resources Research*, Vol. 21, Issue 4, pp. 457–464.

Yeh, T.-C.J., M. Ye, and R. Khaleel, 2005, "Estimation of effective unsaturated hydraulic conductivity tensor using spatial moments of observed moisture plume," *Water Resources Research*, Vol. 41, Issue 3, W03014, pp. 1–12.

Zhang, Z. F., and R. Khaleel, 2010, "Simulating field-scale moisture flow using a combined power-averaging and tensorial connectivity-tortuosity approach," *Water Resources Research*, Vol. 46, Issue 9, W09505, pp. 1–14.

Zhang, Z. F., A. L. Ward, and G. W. Gee, 2003, "A Tensorial Connectivity–Tortuosity Concept to Describe the Unsaturated Hydraulic Properties of Anisotropic Soils," *Vadose Zone Journal*, Vol. 2, No. 3, pp. 313–321.

APPENDIX C

TECHNICAL BASIS FOR WASTE MANAGEMENT AREA A-AX UNCONFINED AQUIFER CONCEPTUAL MODEL

This page intentionally left blank.

CONTENTS

APPENDIX C – TECHNICAL BASIS FOR WASTE MANAGEMENT AREA A-AX UNCONFINED AQUIFER CONCEPTUAL MODEL C-1

C.1 INTRODUCTION C-1

C.2 DEFINITION OF THE SATURATED ZONE MODEL DOMAIN EXTENT C-2

C.3 WATER TABLE ELEVATION AND HYDRAULIC GRADIENT C-4

C.4 STOMP MODEL GRID AND DISCRETIZATION OF GEOLOGIC MATERIALS OF SATURATED ZONE AND LOWER VADOSE ZONE C-13

C.5 HYDRAULIC PROPERTIES OF SATURATED MATERIALS C-20

C.6 GROUNDWATER FLUX THROUGH THE MODEL DOMAIN C-23

C.7 METHOD OF CALCULATING SATURATED ZONE BOUNDARY CONDITIONS C-31

C.8 TRANSPORT PROPERTIES OF SIMULATED GROUNDWATER CONTAMINANTS C-35

C.9 SOLUTION CONTROL CRITERIA FOR NUMERICAL SOLUTIONS C-38

C.10 REFERENCES C-41

FIGURES

Figure C-1. Hydraulic Heads Near Waste Management Area A-AX Simulated by the Central Plateau Groundwater Model Version 8.4.5. ....C-5

Figure C-2. Water Table in 200 East Area in 2016 Estimated from Low-Gradient Monitoring Network. C-7

Figure C-3. Water Table at Waste Management Area A-AX in 2016 Estimated from Low-Gradient Monitoring Network. C-8

Figure C-4. Water Table in 200 East Area in 2015 Estimated from Low-Gradient Monitoring Network. C-10

Figure C-5. Water Table in 200 East Area in 2014 Estimated from Low-Gradient Monitoring Network. C-11

Figure C-6. Hydrostratigraphic Units in Alternative Conceptual Model 1 at Estimated Steady-State Water Table in Geologic Framework Model (Left) and STOMP Model (Right). C-14

Figure C-7. Saturated Hydrostratigraphic Units in Alternative Conceptual Model 1 at Northwest Boundary in Geologic Framework Model (Top) and STOMP Model (Bottom). C-15

Figure C-8. Saturated Hydrostratigraphic Units in Alternative Conceptual Model 1 at Northeast Boundary in Geologic Framework Model (Top) and STOMP Model (Bottom). C-16

Figure C-9. Saturated Hydrostratigraphic Units in Alternative Conceptual Model 1 at Southwest Boundary in Geologic Framework Model (Top) and STOMP Model (Bottom). C-17

Figure C-10. Saturated Hydrostratigraphic Units in Alternative Conceptual Model 1 at Southeast Boundary in Geologic Framework Model (Top) and STOMP Model (Bottom). C-18

Figure C-11. Photograph of Hanford Formation Gravel Exposed at North Richland Borrow Pit. C-22

Figure C-12. Photograph of Open Framework Structure of Hanford Formation Gravel Occurring in the Paleochannel Region. C-23

Figure C-13. Photograph of Cold Creek Gravel Unit Sediments from the Location of the Pumping Test in Paleochannel Region. C-25

Figure C-14. Photograph at Outcrop of Ringold Wooded Island Member Gravel-Dominated Sequence Suggested as Visual Analogue for Ringold Unit A. C-26

Figure C-15. Simulated Steady-State Flow Field Near Waste Management Area A-AX in Model Layer 2 of the Central Plateau Groundwater Model Version 8.4.5. ..... C-27

Figure C-16. Simulated Steady-State Flow Field Near Waste Management Area A-AX in Model Layer 3 of the Central Plateau Groundwater Model Version 8.4.5. ..... C-28

Figure C-17. Simulated Steady-State Flow Field Near Waste Management Area A-AX in Model Layer 4 of the Central Plateau Groundwater Model Version 8.4.5. ..... C-29

Figure C-18. Simulated Steady-State Flow Field Near Waste Management Area A-AX in Model Layer 5 of the Central Plateau Groundwater Model Version 8.4.5. ..... C-30

Figure C-19. Simulated Steady-State Flow Field Near Waste Management Area A-AX in Model Layer 6 of the Central Plateau Groundwater Model Version 8.4.5. ..... C-31

Figure C-20. Simulated Steady-State Flow Field Near Waste Management Area A-AX in Model Layer 7 of the Central Plateau Groundwater Model Version 8.4.5. ..... C-32

Figure C-21. Longitudinal Macrodispersivity in Saturated Media as a Function of Overall Problem Scale with Data Classified by Reliability. C-37

TABLES

Table C-1. Cross-Sectional Areas of Hydrostratigraphic Units in Saturated Zone Along Waste Management Area A-AX STOMP Performance Assessment Model Domain Boundaries for Geologic Alternative Conceptual Model 1. ..... C-19

Table C-2. Hydraulic Parameters for Hydrostratigraphic Units in Waste Management Area A-AX Saturated Zone from Central Plateau Model Version 8.4.5 Calibration. C-20

Table C-3. Relationship Between Saturated Longitudinal Macrodispersivity (α_L) and Scale of Measurement (L_s). C-38

TERMS

ACM	Alternative Conceptual Model
CCUg	Cold Creek Unit gravel
CCUs	Cold Creek Unit sand
CCUz	Cold Creek Unit silt
CHPRC	CH2M HILL Plateau Remediation Company
CPM/CPGWM	Central Plateau Groundwater Model
CRBG	Columbia River Basalt Group
CY	calendar year
eSTOMP	extreme-scale STOMP
GFM	Geologic Framework Model
HF1	Hanford formation unit 1
HF2	Hanford formation unit 2
HF3	Hanford formation unit 3
HSU	hydrostratigraphic unit
IDF	Integrated Disposal Facility
LERF	Liquid Effluent Retention Facility
LLWMA	Low-Level Waste Management Area
NAVD88	North American Vertical Datum of 1988
PA	performance assessment
RCRA	*Resource Conservation and Recovery Act of 1976*
Rlm	Ringold Formation Wooded Island Lower Mud Unit
Rwia	Ringold Formation Wooded Island Unit A
Rwie	Ringold Formation Wooded Island Unit E
SST	single-shell tank
STOMP	Subsurface Transport Over Multiple Phases
TEDF	Treated Effluent Disposal Facility
TVD	total variation diminishing
WMA	Waste Management Area

APPENDIX C TECHNICAL BASIS FOR WASTE MANAGEMENT AREA A-AX UNCONFINED AQUIFER CONCEPTUAL MODEL

C.1 INTRODUCTION

This appendix presents the technical basis for the Waste Management Area (WMA) A-AX performance assessment (PA) model saturated zone conceptual model and the parameterization of the saturated portion of the three-dimensional flow and transport model as organized by the following topics:

- Definition of the saturated zone model domain extent
- Water table elevation and hydraulic gradient
- STOMP[15] model grid and discretization of geologic materials of saturated zone and lower vadose zone
- Hydraulic properties of saturated materials
- Groundwater flux through the model domain
- Method of calculating boundary conditions
- Transport properties of simulated groundwater contaminants
- Solution control criteria for numerical solutions.

Parameterization of any groundwater flow and transport model is dependent on the horizontal and vertical extent of the model domain and on the model discretization of space and time. The definition of the domain extent is of fundamental importance because key flow and transport parameters are dependent on the scale of calculation. Representative values of aquifer properties typically vary depending on the specific volume in space for which they are determined. Spatial and temporal discretization exert control on the accuracy of calculations, with finer discretization offering potentially greater accuracy at a higher cost of computational resources. Using a process referred to as telescoping, more detailed or refined models of an area of interest are constructed using boundary conditions and model parameters determined in other larger-scale models that encompass the area of interest but involve coarser grids (Open-File Report 99-238, *Procedures and Computer Programs for Telescopic Mesh Refinement Using MODFLOW*).

The primary basis for the parameterization of the saturated zone portion of the WMA A-AX PA model is the most current calibration of the Central Plateau Groundwater Model (CPGWM), which is CPGWM Version 8.4.5 as documented in CP-47631, *Model Package Report: Central*

[15] Subsurface Transport Over Multiple Phases (STOMP) is developed and distributed by Battelle Memorial Institute.

Plateau Groundwater Model, Version 8.4.5, Rev. 4. The CPGWM provides the computational framework to simulate groundwater transport of contaminants in the 200-PO-1 and 200-BP-5 groundwater operable units, and identifies the development of scale-appropriate, telescopic-mesh refinement models as an intended use (CP-47631). The WMA A-AX PA model does not involve telescopic refinement of a specific portion of the CPGWM, but the CPGWM provides the basis for the aquifer boundary conditions and hydraulic properties for the aquifer HSUs in the WMA A-AX PA model. The long-term steady-state flow field relevant to the multi-millennial timescale of the WMA A-AX PA modeling, as simulated using CPGWM Version 8.4.5, is documented in ECF-200W-17-0043, *Capture-Zone and Particle-Tracking Analysis for the 200-UP-1/200-ZP-1 Areas using the 2017 Updated Central Plateau Model*. Whereas the CPGWM extends throughout the Central Plateau area of the Hanford Site and provides calibration appropriate to hydrostratigraphic units (HSUs) and subunits on a horizontal scale of kilometers to tens of kilometers, the WMA A-AX PA model is a smaller-scale model as appropriate for the PA objectives.

There is an inherent limit to the ability to compare any two models constructed with significantly different domains or discretization. Some interpretation is therefore necessary to translate information from the CPGWM to the domain of the WMA A-AX PA model, but CPGWM Version 8.4.5 is nevertheless the best available basis for developing the saturated zone portion of the local-scale PA model. CPGWM incorporates the most complete information available to date on groundwater flow in the region including WMA A-AX. Other available sources of information are briefly discussed in the relevant subsections and used to fill data gaps where appropriate.

C.2 DEFINITION OF THE SATURATED ZONE MODEL DOMAIN EXTENT

The WMA A-AX PA model domain (Figure 3-1 and Figure 3-6 in Section 3.1) has horizontal area of about 0.8 km^2 selected to satisfy the requirements of DOE O 435.1, *Radioactive Waste Management* and DOE M 435.1-1, *Radioactive Waste Management Manual*, which necessitate an ability to determine groundwater doses for hypothetical human exposures at “the point of highest projected dose or concentration beyond a 100 meter buffer zone surrounding the disposed waste” unless a different buffer zone is justified. The WMA A-AX PA adopts the standard 100-m buffer zone. The suprabasalt sediments that are saturated near WMA A-AX belong to the late Miocene to Pliocene Ringold formation, the late Pliocene Cold Creek Unit, and in places the lower portion of the Pleistocene Hanford formation (RPP-RPT-60171, *Model Package Report: Geologic Framework Model used in WMA A-AX Performance Assessment and RCRA Closure Analysis*; RPP-ENV-58578, *Summary of the Natural System at Waste Management Area A-AX*).

The aquifer of interest for calculations in the WMA A-AX PA is the suprabasalt aquifer of the Hanford Site Central Plateau, i.e., the uppermost aquifer comprising the unconsolidated sediments above the Miocene Columbia River Basalt Group (CRBG). The top surface of the CRBG basalt bedrock represents a lower boundary for the highly-transmissive unconfined aquifer; it can be modeled as either an impermeable boundary or as the lowermost HSU for

which the hydraulic conductivity is several orders of magnitude lower than for the unconsolidated sediments comprising the overlying HSUs.

The decision to include the suprabasalt aquifer as the aquifer of interest and exclude aquifers below the basalt surface from the WMA A-AX PA model domain is based on the objectives of DOE M 435.1-1 (including calculation of the highest projected groundwater concentration, given the expected decrease in concentrations with distance below the water table), and it is consistent with conceptual models adopted for other Hanford Site numerical models (including but not limited to those reported in CP-47631; RPP-ENV-58782, *Performance Assessment of Waste Management Area C, Hanford Site, Washington*; DOE/EIS-0391, *Final Tank Closure and Waste Management Environmental Impact Statement for the Hanford Site, Richland, Washington*; and PNNL-13641, *Uncertainty Analysis Framework - Hanford Site-Wide Groundwater Flow and Transport Model*).

The uppermost basalt of the CRBG is the Elephant Mountain Member of the Saddle Mountains Basalt Formation, which is intercalated with the sedimentary Ellensburg Formation such that sedimentary interbeds separate the basalt members (PNNL-16407, *Geology of the Waste Treatment Plant Seismic Boreholes*). The surface of the Elephant Mountain Member is eroded, and the member is 68-ft- (20.7-m-) to 118-ft- (36.0-m-) thick in the boreholes nearest to the 200 East Area that fully penetrate the member (Figure 4.4 in PNNL-16407). Estimates for the vertical hydraulic conductivity of this basalt member range from 10^{-8} m/day (RHO-RE-ST-12P, *An Assessment of Aquifer Intercommunication in the B Pond-Gable Mountain Pond Area of the Hanford Site*, pp. 44) to 2.6×10^{-4} m/day ("Task 4.2: Effects of Surface Waste Disposal Activity on Ground-Water Levels in the Saddle Mountain Basalt" [Nevulis et al. 1987], in PNNL-13641 Appendix B Exhibit 1). The contrast between this range for basalt and the hydraulic conductivities estimated for the suprabasalt sediments in Section C.5 is sufficient to justify an assumption of no flow at the top of basalt surface for purposes of the WMA A-AX PA model. A review of characterization of flow in the basalt fractures and sedimentary interbeds that may be relevant in other contexts is presented in Appendix B of PNNL-13641.

The lower extent of the active model domain can be further reduced by treating the deepest portions of suprabasalt sediments as inactive model layers. Flow is expected to be predominantly through the shallower layers because the deeper sediments have such low hydraulic conductivities by comparison. Doing so is an optional measure to improve computational efficiency for reasons explained in Section C.9, and the conditions in which it is considered reasonable are discussed in Section C.5. The model includes representation of sediments all the way to the top of basalt so that the decision to leave the deepest portions active or inactive for any given application rests with the modeler.

The water table is the top of the saturated zone and the location of the transition to unsaturated conditions, defining the upper extent to which saturated zone boundary conditions apply in the model. As explained in Section C.5, a thin model layer above the water table is assigned the same hydraulic properties as the saturated zone, but it is not part of the saturated zone by virtue of the prescribed boundary conditions (see Section C.7). Section C.3 discusses that the water table has historically risen and fallen in response to changes in Hanford Site discharges, and that

the long-term steady-state water table elevation in the absence of such discharges is estimated to be about 119.5 m on the North American Vertical Datum of 1988 (NAVD88).

C.3 WATER TABLE ELEVATION AND HYDRAULIC GRADIENT

Figure C-1 presents well hydrographs of selected wells near WMA A-AX with comparisons of CPGWM-simulated historical hydraulic heads (CP-47631 Rev. 4) to measured data (Environmental Dashboard Application, Queried 07/17/2017, https://ehs.hanford.gov/eda/) and CPGWM-simulated future hydraulic heads (ECF-200W-17-0043). The current calibration in Version 8.4.5 of the regional-scale CPGWM appears to provide a good fit to the historical variations in measured data at the local scale; therefore, the flow field simulated for future conditions is a reasonable basis for inputs to the WMA A-AX PA STOMP model. As discussed later in this section, the simulated steady-state elevation of about 119.9 m NAVD88 is considered to be within model uncertainty of the 119.5 m NAVD88 that was predicted by earlier calibrated versions of the CPGWM and used in other recent Hanford Site PAs (e.g., RPP-ENV-58782), so the latter value is retained as the estimate for the absolute water table elevation in the WMA A-AX PA model.

In response to historical liquid discharges across the Hanford Site, the water table elevation rose to a local maximum of about 125.9 m NAVD88 as measured at well 299-E25-4 in December 1985[16] (PNNL-15837, *Data Package for Past and Current Groundwater Flow and Contamination Beneath Single-Shell Tank Waste Management Areas*). With the cessation of most liquid discharges, the water table has steadily declined since the early 1990s to a local elevation of about 121.73 m NAVD88 as of 2016 (see Figure C-1 herein and Figures 2-14 and 3-1 from DOE/RL-2016-66, *Hanford Site RCRA Groundwater Monitoring Report for 2016*, reproduced in this section as Figure C-2 and Figure C-3, respectively). Given an adequate period of time after liquid discharges and groundwater pumping are assumed to eventually cease altogether by the future closure of the Hanford Site, the water table is expected to continue declining to a steady-state elevation of about 119.9 m NAVD88 near WMA A-AX as predicted by CPGWM Version 8.4.5 (Figure C-1; ECF-200W-17-0043). Simulations in ECF-200W-17-0043 assumed discharges and withdrawals cease in calendar year (CY) 2037, and thus achieved a reasonable approximation of steady-state conditions by the end of the simulation 100 years later in CY 2137, with most of the water table decline occurring within a few decades after discharges cease (Figure C-1).

Figure C-1 illustrates that the hydraulic gradient in the 200 East Area is extremely flat; the simulated steady-state hydraulic heads vary by only about 6 mm throughout the 0.8 km^2 domain of the WMA A-AX PA STOMP model. The direction of groundwater flow is generally southeastward. Along the groundwater flowpath from northwest to southeast through the central portion of the STOMP model domain where WMA A-AX is located, the CPGWM simulated steady-state hydraulic heads contoured in Figure C-1 decrease by approximately 4 mm over 800 m, indicating a hydraulic gradient magnitude of -5×10^{-6} m/m.

[16] The maximum water table elevation is stated to provide an upper bound for historical variations. Somewhat higher groundwater elevations have been recorded in wells closer to B Pond and somewhat lower maximum elevations have been recorded within WMA A-AX.

Figure C-1. Hydraulic Heads Near Waste Management Area A-AX Simulated by the Central Plateau Groundwater Model Version 8.4.5.

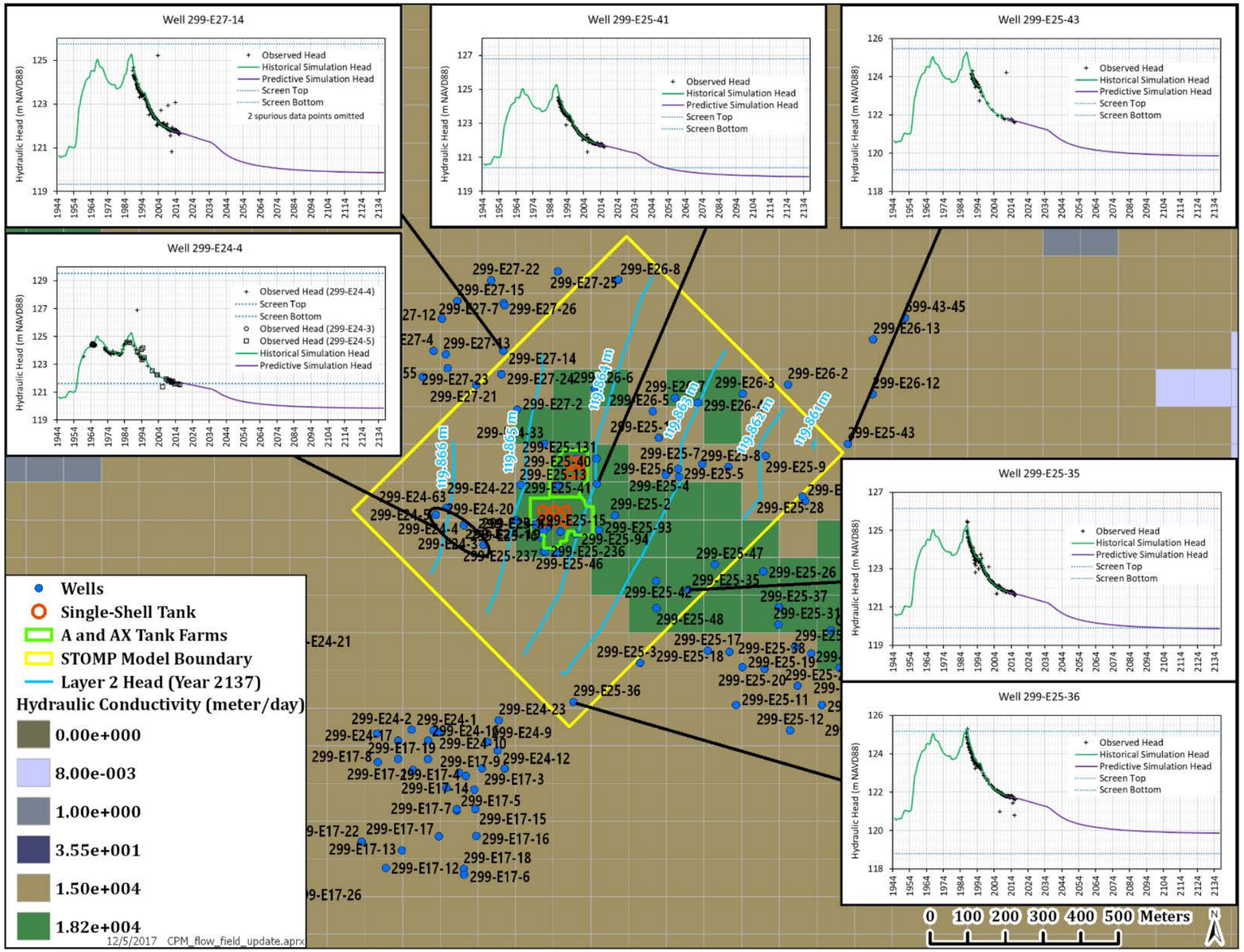

Sources:
CP-47631, *Model Package Report: Central Plateau Groundwater Model Version 8.4.5*, Rev. 4.
ECF-200W-17-0043, *Capture-Zone and Particle-Tracking Analysis for the 200-UP-1/200-ZP-1 Areas using the 2017 Updated Central Plateau Model*.
Environmental Dashboard Application, Queried 07/17/2017, https://ehs.hanford.gov/eda/.
HGIS Hanford Geographic Information System, Queried 06/26/2017, [HMAPS Interactive Maps], [redacted]
Subsurface Transport Over Multiple Phases (STOMP) is developed and distributed by Battelle Memorial Institute.

Figure C-2. Water Table in 200 East Area in 2016 Estimated from Low-Gradient Monitoring Network.

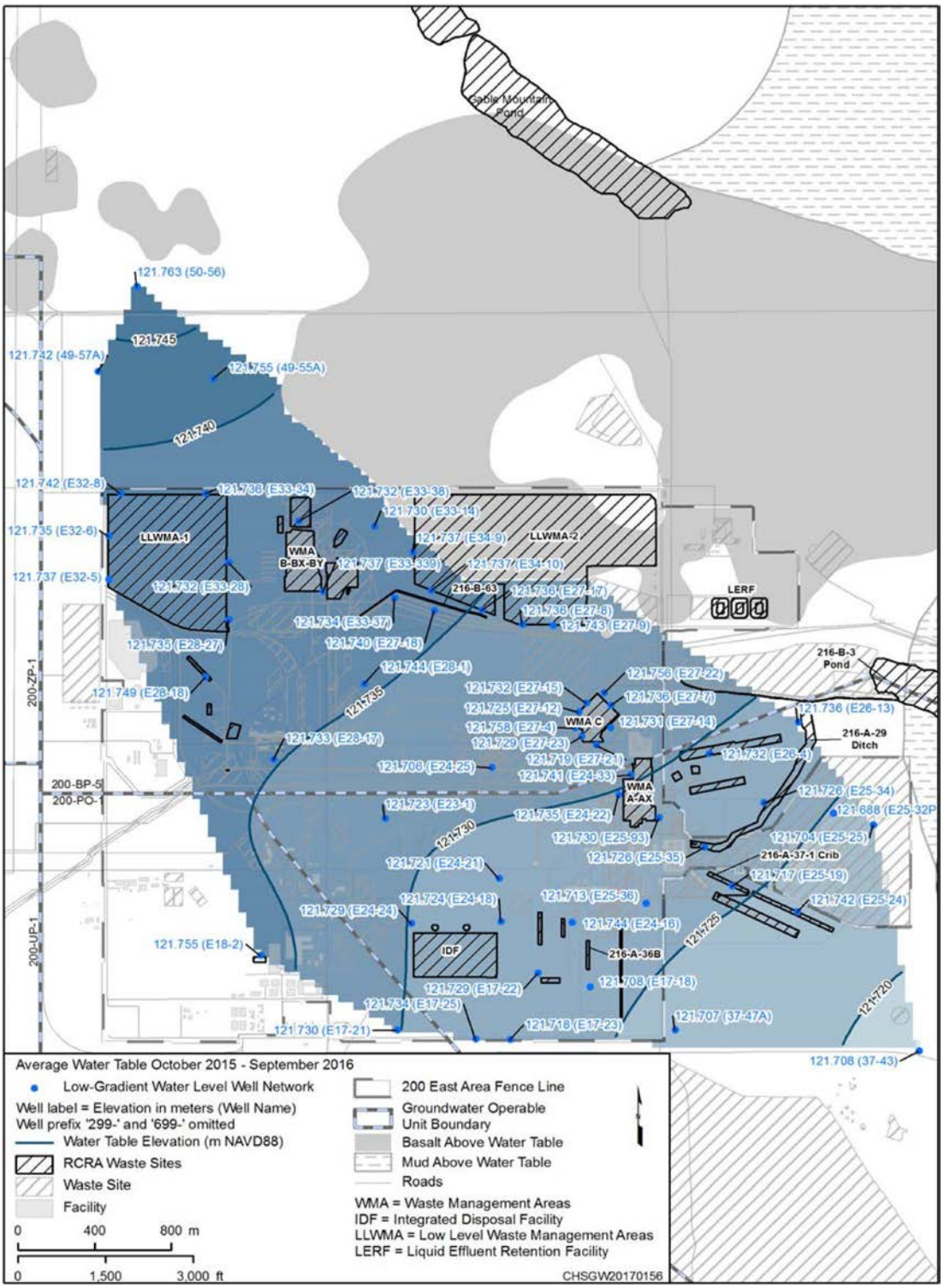

NAVD88 = North American Vertical Datum of 1988 RCRA = *Resource Conservation and Recovery Act of 1976*

Source: DOE/RL-2016-66, *Hanford Site RCRA Groundwater Monitoring Report for 2016*, Figure 2-14 (see source document for corrections to raw measurements).

Figure C-3. Water Table at Waste Management Area A-AX in 2016 Estimated from Low-Gradient Monitoring Network.

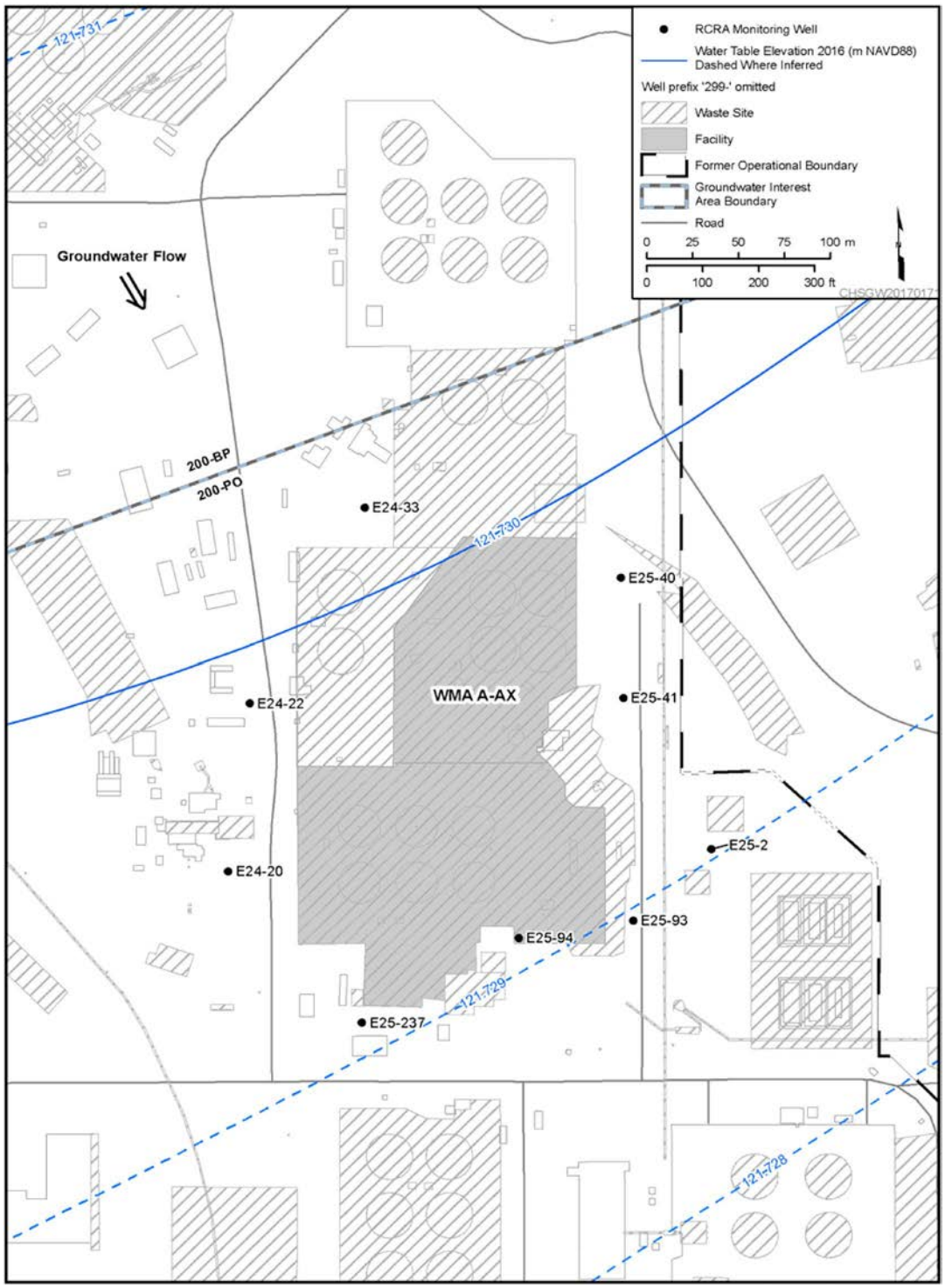

NAVD88 = North American Vertical Datum of 1988 WMA = Waste Management Area
RCRA = *Resource Conservation and Recovery Act of 1976*

Source: DOE/RL-2016-66, *Hanford Site RCRA Groundwater Monitoring Report for 2016*, Figure 3-1 (see source document for corrections to raw measurements).

The low gradient obtained from the CPGWM is consistent with large estimated values of the hydraulic conductivity of gravels in the paleochannel region of the Central Plateau (see Section C.5) and with past and current observations of hydraulic heads (Figure C-2 through Figure C-5) which require thorough data quality control measures to allow adequate accuracy for estimation of hydraulic gradients (SGW-54165, *Evaluation of the Unconfined Aquifer Hydraulic Gradient Beneath the 200 East Area, Hanford Site*)[17]. Quite similar to the simulated steady-state conditions, ECF-HANFORD-16-0139, *Hydraulic Gradients and Velocity Calculations for RCRA Sites in 2016* estimated the current hydraulic gradient at WMA A-AX as of 2016 to be 150 degrees east of north at a magnitude of 4.61×10^{-6} m/m (the figures beyond the first digit are reported in the original calculation but are not significant) using the methods of SGW-54165 and ECF-HANFORD-16-0013, *Hydraulic Gradients and Velocity Calculations for RCRA Sites in 2015*. Figure C-2 shows the corresponding 2016 water table in the 200 East Area and Figure C-3 shows the 2016 water table close to WMA A-AX. It should be noted that recently the magnitude and direction of the hydraulic gradient in the 200 East Area are overall similar from year to year, but are both sensitive to small measurement errors and to transient external stresses given the convergence of flow from upgradient areas and the relative flatness of the water table in 200 East (compare the 2016 water table in Figure C-2 to the 2015 water table in Figure C-4 and the 2014 water table in Figure C-5). Transient external stresses may include artificial discharges (e.g., historical discharges from B Pond or recent discharges from the Treated Effluent Disposal Facility [TEDF]), groundwater extraction wells, the stage of the Columbia River, and/or long-term changes to regional flow fields. For the same reasons that make the current hydraulic gradient intrinsically difficult to measure, model predictions of the steady-state gradient are regarded as accurate only to one or two digits for the magnitude and general direction (as in SGW-54165) rather than to the full precision output from the model.

In a previous version of the CPGWM, Version 6.3.3, the predicted steady-state water table elevation was about 119.5 m NAVD88 near WMA A-AX (see page A-3 of RPP-CALC-60497, *Peak Groundwater Concentrations for Tank Farm 241-AX TWRWP Risk Assessment* and CP-47631, *Model Package Report: Central Plateau Groundwater Model Version 6.3.3*, Rev. 2). The 40-cm difference in predictions between Versions 6.3.3 and 8.4.5 is within the model uncertainty implied for predicted conditions more than 100 years in the future. The recently-completed PA for the immediately upgradient WMA C (RPP-ENV-58782) based calculations on the previously predicted steady-state water table elevation of 119.5 m NAVD88.

[17] Measures recently implemented to increase accuracy of hydraulic gradient estimation in 200 East include the following (SGW-54165): correcting depth to water measurements for deviations of wells from perfect verticality; resurveying reference points to a common, high-accuracy survey; correcting measurements for barometric pressure variation; statistical tests for anomalous data; and relying on subsets of measurements obtained within short windows of time from the Low-Gradient Monitoring Network which comprises only the wells of highest-quality construction.

Figure C-4. Water Table in 200 East Area in 2015 Estimated from Low-Gradient Monitoring Network.

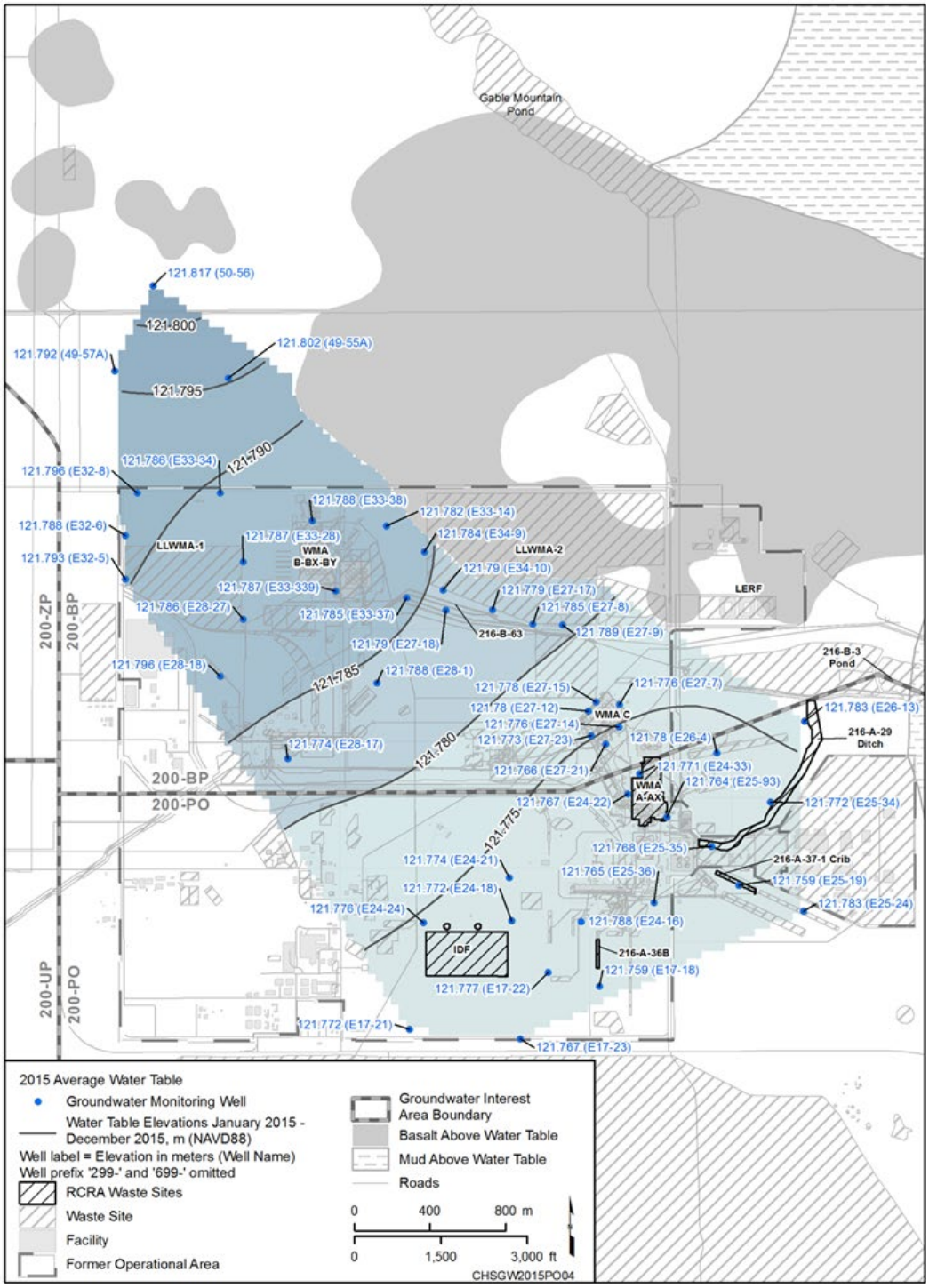

IDF = Integrated Disposal Facility
LERF = Liquid Effluent Retention Facility
LLWMA = Low-Level Waste Management Area
NAVD88 = North American Vertical Datum of 1988
RCRA = *Resource Conservation and Recovery Act of 1976*
WMA = Waste Management Area

Source: DOE/RL-2016-09, *Hanford Site Groundwater Monitoring Report for 2015*, Figure 10-4 (see source document for corrections to raw measurements).

Figure C-5. Water Table in 200 East Area in 2014 Estimated from Low-Gradient Monitoring Network.

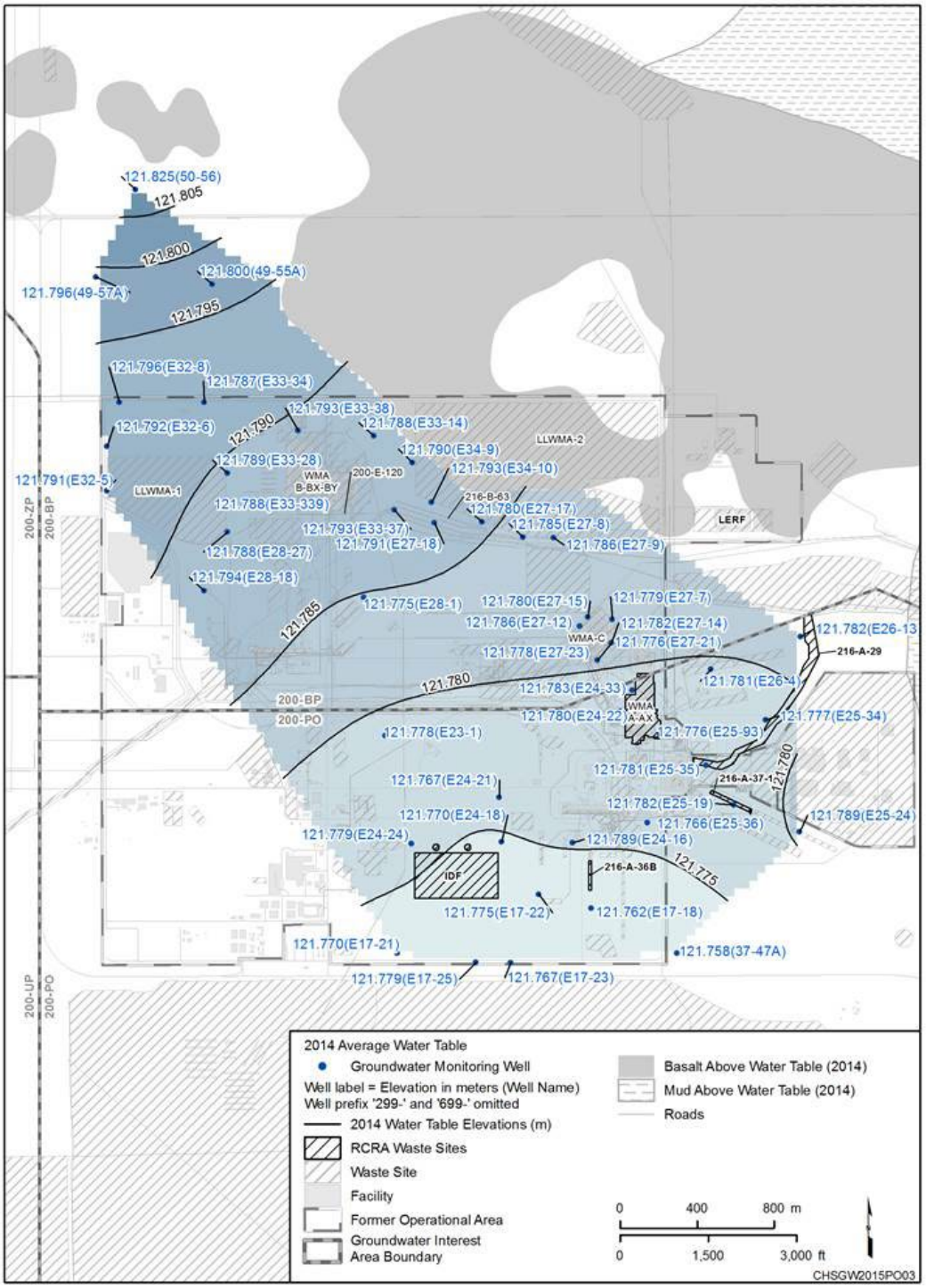

IDF = Integrated Disposal Facility
LERF = Liquid Effluent Retention Facility
LLWMA = Low-Level Waste Management Area
NAVD88 = North American Vertical Datum of 1988
RCRA = *Resource Conservation and Recovery Act of 1976*
WMA = Waste Management Area

Source: DOE/RL-2016-09, *Hanford Site Groundwater Monitoring Report for 2015*, Figure 10-3 (see source document for corrections to raw measurements).

With the bases of the deepest single-shell tanks (SSTs) in WMA A-AX at an elevation of about 192 m NAVD88 (RPP-RPT-58693, *Engineered System Data Package for Waste Management Area A-AX*, pp. 3-2), the vadose zone between the SSTs and the steady-state water table is 72.5 m thick. Given the low post-closure recharge rates discussed in Section 3.1.5, the time needed for a non-sorbing solute to be transported this distance is expected to be hundreds of years, even if recharge rates are somewhat higher or moisture contents are somewhat lower than anticipated. Vadose zone transport times on the order of centuries are supported by previous modeling of releases from waste residuals at WMA A-AX (Figure 7-1 in RPP-CALC-60497) and WMA C (Figure 7-15 and Table D-18 in RPP-ENV-58782). Therefore, for purposes of simulating future releases from waste residuals it is not necessary to represent past or current transient water table conditions expected to dissipate within several decades, so using the steady-state water table elevation throughout such simulations is sufficient to calculate transport times for the complete vadose zone and groundwater pathway.

Whereas the WMA A-AX PA model simulations of future releases from waste residuals use steady-state water table conditions, it is useful to understand that past discharges affected not only the historical water table elevation but also the historical hydraulic gradient and to be aware of potential differences between reported past conditions and simulated future conditions. After Hanford Site operations began in the mid-1940s, artificial recharge from wastewater disposal facilities caused an increase in the water table elevation over most of the Hanford Site, including a rise of as much as 5 m near WMA A-AX (RPP-ENV-58578, Section 5.1.4). The local water table elevation at WMA A-AX prior to Hanford Site operations is not well known because the rise began prior to construction of the 241-A and 241-AX Tank Farms and most of the nearby monitoring wells. Variability in the water table rise across the Hanford Site due to more distinct groundwater mounding near wastewater disposal facilities caused large changes to hydraulic gradients that influenced contaminant transport for existing groundwater plumes (CP-47631, Rev. 4, Section 3.2.1). Wastewater disposal facilities near WMA A-AX included ponds, cribs, trenches, ditches, French drains, and septic systems for which the timing and estimated magnitude of past discharges are discussed in RPP-RPT-58693 and RPP-RPT-58291, *Hanford Waste Management Area A-AX Soil Contamination Inventory Estimates*. Examples of large-scale discharges that have influenced the hydraulic gradient at WMA A-AX are past discharges at B Pond to the east (CP-47631 Rev. 4) and periodically-continuing discharges at TEDF to the east (SGW-54165). Possible effects on the local gradient depend not only on the magnitude of discharges but also on the role of underlying vadose zone and saturated zone HSUs in distributing the artificial recharge; so, for instance, the uncertain location of B Pond discharges relative to the upper surface topography of the Ringold Lower Mud unit results in an uncertain flow divide that may explain apparently much larger historical changes in groundwater flow direction at upgradient WMA C or the downgradient Waste Treatment and Immobilization Plant than at WMA A-AX (CP-47631 Rev. 4, pp. 4-56).

Finally, it should be noted that the magnitude of the simulated decline of the water table from the current elevation to the steady-state elevation directly affects the magnitude and direction of the steady-state flux, because the steady-state water table elevation determines which sediments are modeled as being saturated. If the decline is as simulated in the CPGWM, the saturated sediments near the water table are largely the same for current and future conditions; hence, the similar estimated hydraulic gradients. Historically, the water table has been higher and has

saturated a larger sequence of highly-transmissive gravel units in the Ringold, Cold Creek, and Hanford formations, under which conditions groundwater likely flowed in a similar direction (at the local scale where influence of B Pond is less obvious than at upgradient or downgradient areas) but with a higher magnitude of flux. If the decline were greater than simulated in the CPGWM and the HSUs have properties close to those reported in Section C.5, then the lower-transmissivity units deeper below the current water table would likely divert most groundwater flow around their upper surfaces and reduce the total magnitude of flux through the domain. Historical water level measurements from the Central Plateau do not suggest the future water table decline is likely to be much greater than as simulated in the CPGWM.

C.4 STOMP MODEL GRID AND DISCRETIZATION OF GEOLOGIC MATERIALS OF SATURATED ZONE AND LOWER VADOSE ZONE

Vertical grid spacing in the saturated zone portion of the WMA A-AX PA STOMP model increases from a minimum of 0.5 m at the estimated steady-state water table elevation of 119.5 m NAVD88 to a maximum of 3 m in the bottom layer with its base at 95.25 m NAVD88; horizontal grid spacing increases outward from a minimum of 4.355 m near the SSTs in x- (northwest-southeast) and y- (southwest-northeast) directions up to 20 m at the domain boundaries. Each model cell is assigned a material based on the applicable HSU using the STOMP “rock/soil zonation” variable. The STOMP model grid has 18 layers in the saturated zone between 95.25 m NAVD88 and 119.5 m NAVD88 (layers numbered from bottom to top with the k index). The boundary conditions discussed in Section C.7 maintain the steady-state water table at or just below the top of Layer 18. The calculation of groundwater concentrations to be reported for PA will use the 5-m interval below the water table comprising the k-indexed Layers 12 through 18, consistent with the length of a well screen assumed in state guidance (see Section 3.1.8). For reasons explained in Sections C.5, C.7, and C.9, Layers 1 through 5 (below 106.75 m NAVD88) are assumed to be overwritten with inactive cells for typical simulations used in the WMA A-AX PA. Layer 19, located from 119.5 m NAVD88 to 120.0 m NAVD88, is assigned the same rock/soil zones used to specify hydraulic properties in the saturated zone as opposed to those used for the vadose zone, because, as the layer immediately above the water table, Layer 19 is expected to be closer to saturation at steady state than overlying layers (with a hydraulic conductivity approaching the saturated value), and because portions of Layer 19 may become saturated if the model is used to simulate transient changes in recharge or perhaps liquid discharges.

The process by which geologic materials delineated at higher resolution in the Geologic Framework Model (GFM) for WMA A-AX PA are interpolated onto the STOMP model grid is described in RPP-RPT-60171. Figure C-6 through Figure C-10 provide comparisons of the interpolated geology in the GFM versus that in the STOMP model. The STOMP model geology shown in these figures is based on ACM 1 described in RPP-RPT-60171.

Figure C-6. Hydrostratigraphic Units in Alternative Conceptual Model 1 at Estimated Steady-State Water Table in Geologic Framework Model (Left) and STOMP Model (Right).

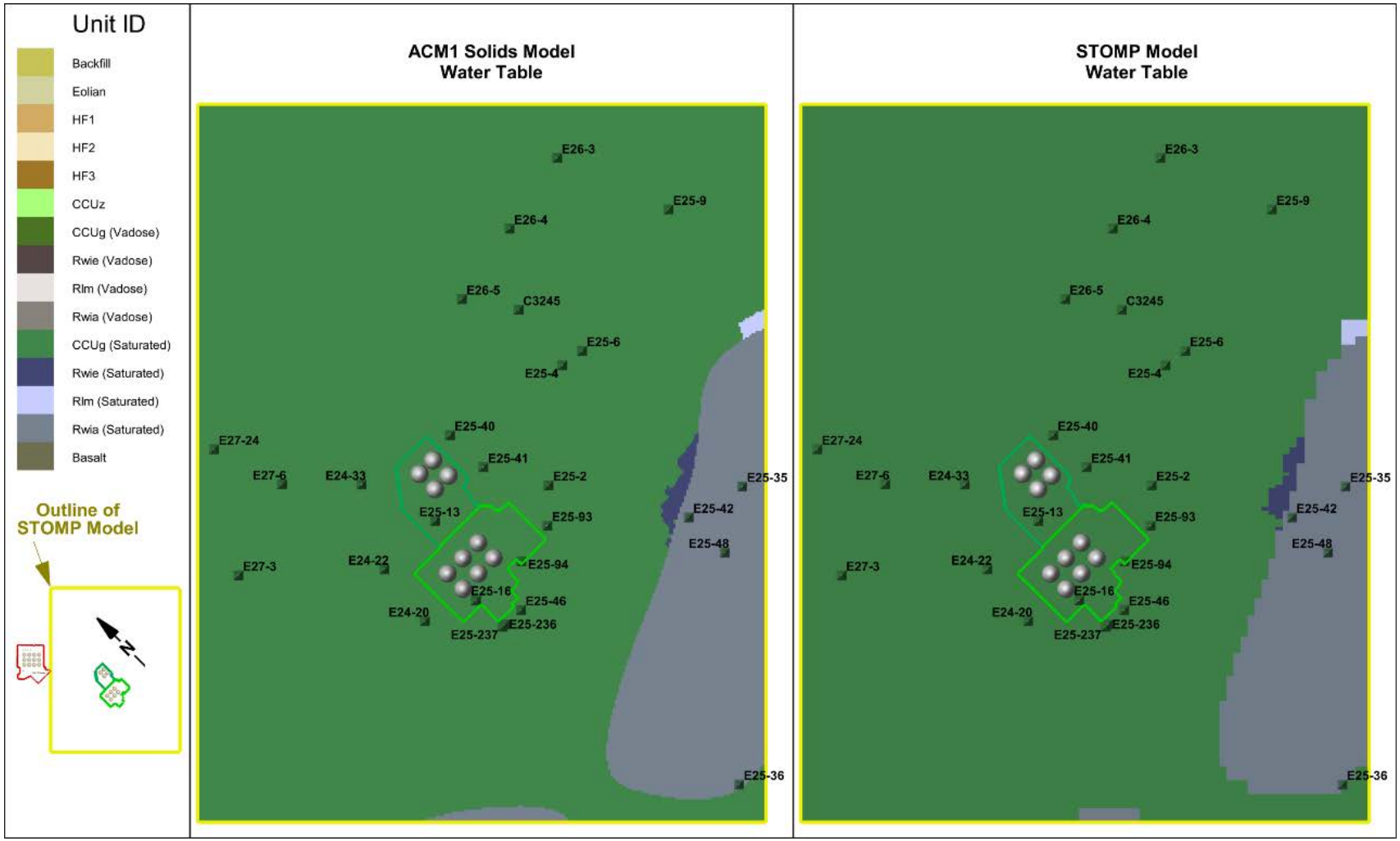

ACM = alternative conceptual model
CCUg = Cold Creek Unit gravels
CCUz = Cold Creek Unit silt
HF1 = Hanford formation unit 1
HF2 = Hanford formation unit 2
HF3 = Hanford formation unit 3
Rlm = Ringold Formation Wooded Island Lower Mud Unit
Rwia = Ringold Formation Wooded Island Unit A
Rwie = Ringold Formation Wooded Island Unit E
Subsurface Transport Over Multiple Phases (STOMP) is developed and distributed by Battelle Memorial Institute.

Figure C-7. Saturated Hydrostratigraphic Units in Alternative Conceptual Model 1 at Northwest Boundary in Geologic Framework Model (Top) and STOMP Model (Bottom).

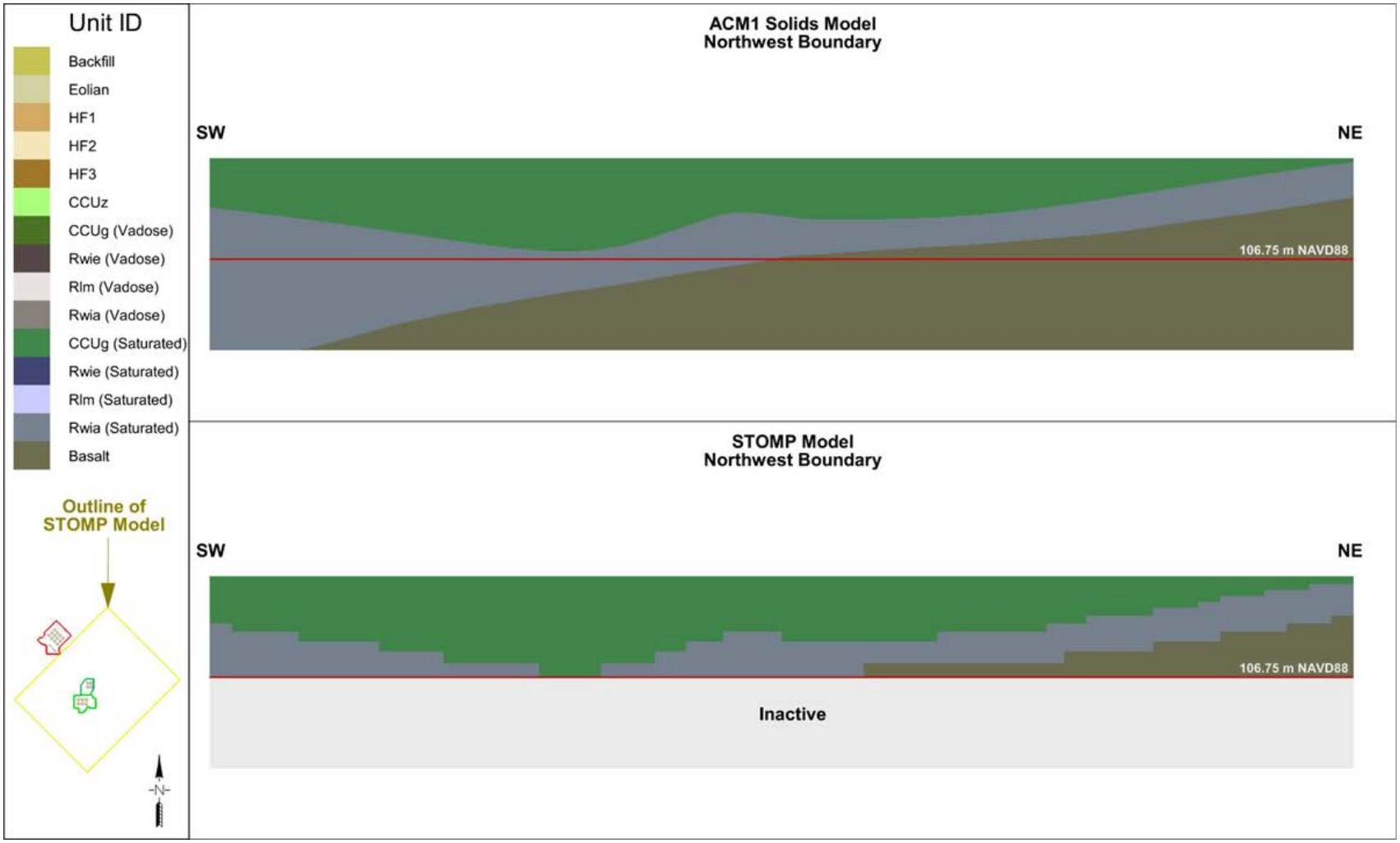

ACM = alternative conceptual model
CCUg = Cold Creek Unit gravels
CCUz = Cold Creek Unit silt
HF1 = Hanford formation unit 1
HF2 = Hanford formation unit 2
HF3 = Hanford formation unit 3
Rlm = Ringold Formation Wooded Island Lower Mud Unit
Rwia = Ringold Formation Wooded Island Unit A
Rwie = Ringold Formation Wooded Island Unit E
Subsurface Transport Over Multiple Phases (STOMP) is developed and distributed by Battelle Memorial Institute.

Figure C-8. Saturated Hydrostratigraphic Units in Alternative Conceptual Model 1 at Northeast Boundary in Geologic Framework Model (Top) and STOMP Model (Bottom).

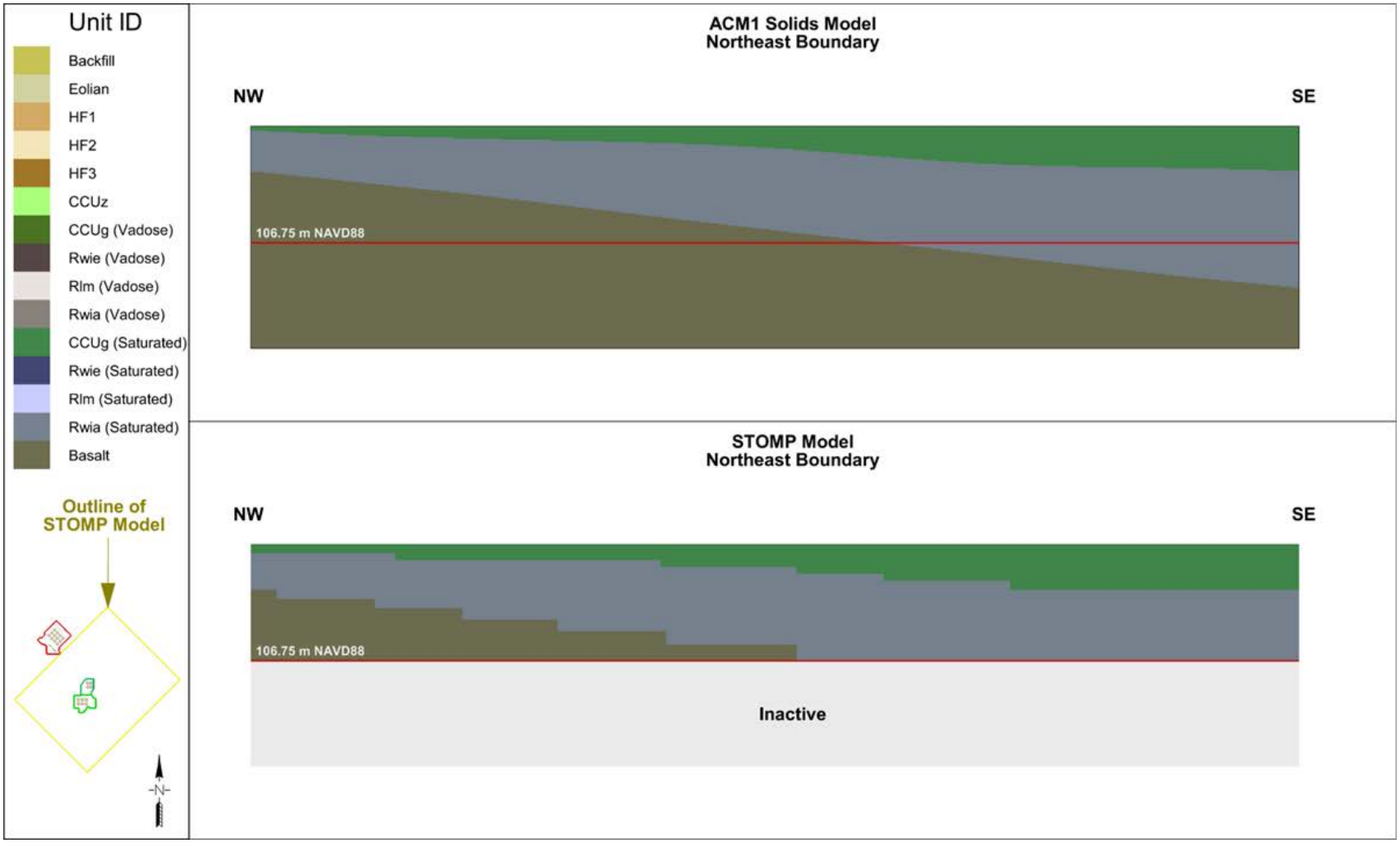

ACM = alternative conceptual model
CCUg = Cold Creek Unit gravels
CCUz = Cold Creek Unit silt
HF1 = Hanford formation unit 1
HF2 = Hanford formation unit 2
HF3 = Hanford formation unit 3
Rlm = Ringold Formation Wooded Island Lower Mud Unit
Rwia = Ringold Formation Wooded Island Unit A
Rwie = Ringold Formation Wooded Island Unit E
Subsurface Transport Over Multiple Phases (STOMP) is developed and distributed by Battelle Memorial Institute.

Figure C-9. Saturated Hydrostratigraphic Units in Alternative Conceptual Model 1 at Southwest Boundary in Geologic Framework Model (Top) and STOMP Model (Bottom).

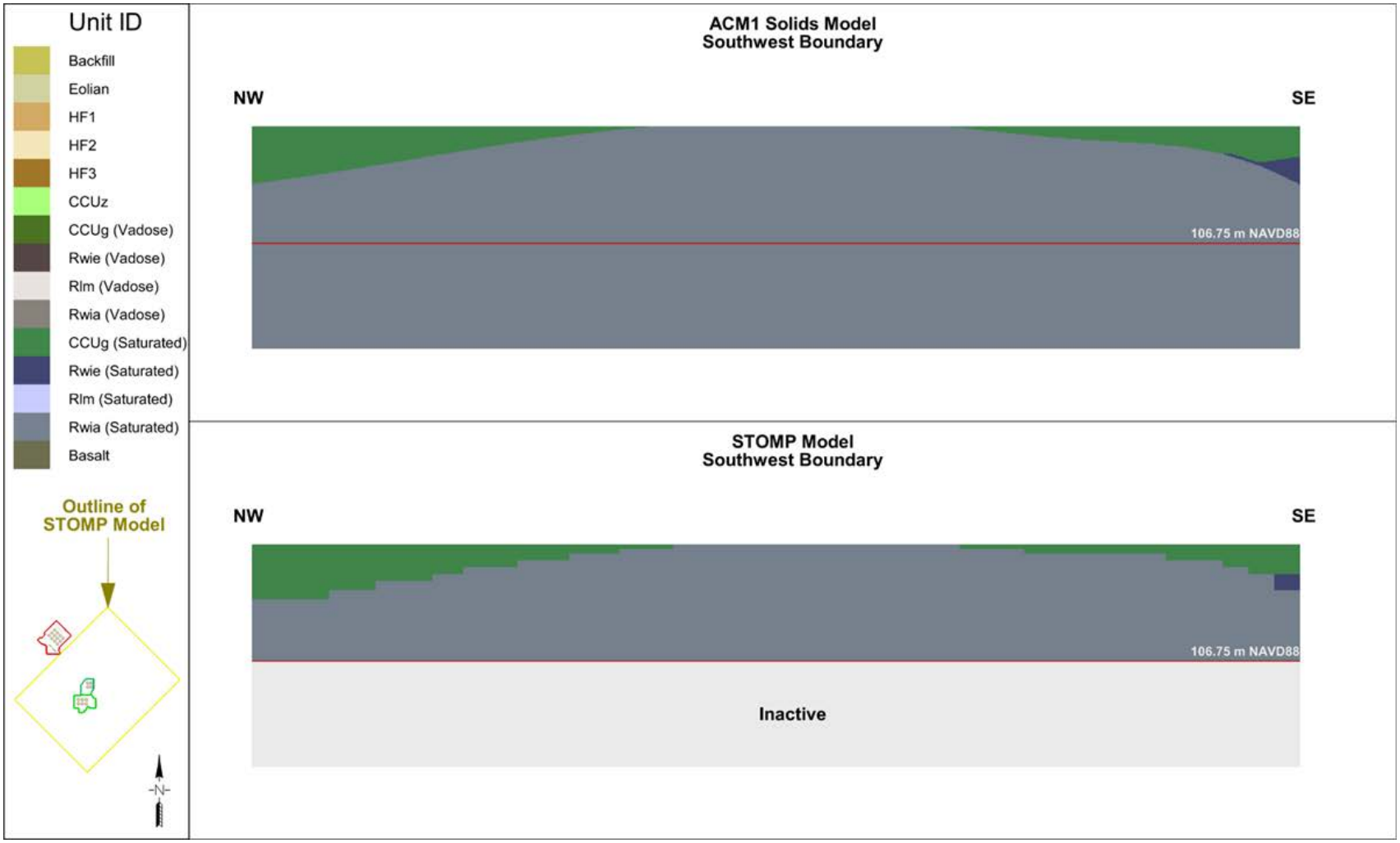

ACM = alternative conceptual model
CCUg = Cold Creek Unit gravels
CCUz = Cold Creek Unit silt
HF1 = Hanford formation unit 1
HF2 = Hanford formation unit 2
HF3 = Hanford formation unit 3
Rlm = Ringold Formation Wooded Island Lower Mud Unit
Rwia = Ringold Formation Wooded Island Unit A
Rwie = Ringold Formation Wooded Island Unit E
Subsurface Transport Over Multiple Phases (STOMP) is developed and distributed by Battelle Memorial Institute.

Figure C-10. Saturated Hydrostratigraphic Units in Alternative Conceptual Model 1 at Southeast Boundary in Geologic Framework Model (Top) and STOMP Model (Bottom).

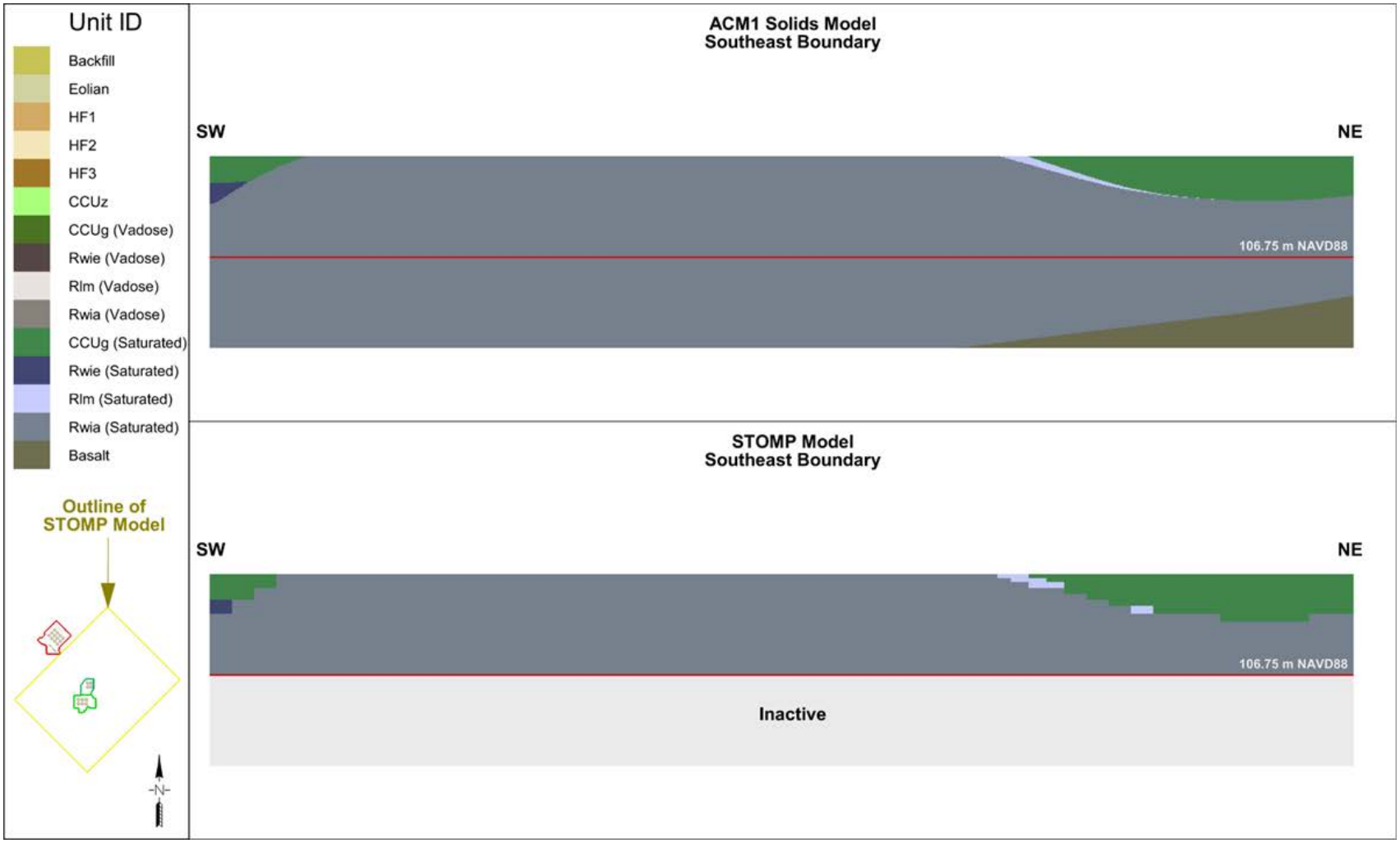

ACM = alternative conceptual model
CCUg = Cold Creek Unit gravels
CCUz = Cold Creek Unit silt
HF1 = Hanford formation unit 1
HF2 = Hanford formation unit 2
HF3 = Hanford formation unit 3
Rlm = Ringold Formation Wooded Island Lower Mud Unit
Rwia = Ringold Formation Wooded Island Unit A
Rwie = Ringold Formation Wooded Island Unit E
Subsurface Transport Over Multiple Phases (STOMP) is developed and distributed by Battelle Memorial Institute.

Given the STOMP model domain and estimated steady-state water table elevation, the HSUs comprising the saturated zone are the Ringold Unit A gravel-dominated unit (Rwia or Ringold A), the Ringold lower mud unit (Rlm or Ringold mud), the Ringold Unit E gravel-dominated unit (Rwie or Ringold E), and the Cold Creek gravel-dominated unit (CCUg). The distribution of these HSUs at the water table is shown in Figure C-6, with the STOMP model grid providing adequate resolution to specify rock/soil zonation that captures a similar level of detail as the GFM. The CCUg is the HSU underlying the 241-A and 241-AX Tank Farms at the water table elevation. The CCUg is the HSU at the water table across most of the model domain, with the Rwia underlying the CCUg down to basalt and rising above the water table over part of the domain in the south corner and along part of the southeast side (model east in STOMP syntax). Note that the uncertainty in the elevation of the CCUg/Rwia contact near the south corner arises from the relative sparsity of deep boreholes in that area, as seen from the locations of boreholes deeper than 119.5 m NAVD88 posted within the domain on Figure C-6 or the locations of wells below the current water table shown inside and outside the STOMP model domain in Figure C-1. The Rlm and Rwie occur at the water table in small regions of the southeast portion of the domain; these younger units of the Ringold Formation overlie the older Rwia further downgradient from WMA A-AX but have been removed by erosion through most of the model domain.

Figure C-7 shows vertical cross-sections along the geographic northwest domain boundary (model west boundary). The basalt bedrock dips significantly from north to south through the model domain. The areas of the HSUs from ACM 1 along each vertical domain boundary are given in Table C-1.

Table C-1. Cross-Sectional Areas of Hydrostratigraphic Units in Saturated Zone Along Waste Management Area A-AX STOMP Performance Assessment Model Domain Boundaries for Geologic Alternative Conceptual Model 1.

Hydrostratigraphic Unit	Area at Northwest (model west, i=1) Boundary (m^2)	Area at Southeast (model east, i=100) Boundary (m^2)	Area at Southwest (model south, j=1) Boundary (m^2)	Area at Northeast (model north, j=120) Boundary (m^2)
Cold Creek gravel-dominated unit (CCUg)	7,570	1,444	1,421	2,467
Ringold A (Rwia)	3,916 (k = 6 to 18)	11,548 (k = 6 to 18)	8,905 (k = 6 to 18)	6,052 (k = 6 to 18)
Ringold mud (Rlm)	0	74	0	0
Ringold E (Rwie)	0	35	35	0
Basalt and/or Inactive Layers	13,432	11,817	9,345	11,188
Total Saturated Area	24,918	24,918	19,706	19,706

Note: Hydrostratigraphic unit areas are totals of STOMP model cell areas to the nearest square meter.

Subsurface Transport Over Multiple Phases (STOMP) is developed and distributed by Battelle Memorial Institute.

Figure C-8 shows the vertical cross-section along the geographic northeast domain boundary (model north boundary). Along the northeast boundary, the Rwia and CCUg thicken to the southeast as they fill in above the southward-dipping basalt surface. Figure C-9 shows vertical cross-sections along the geographic southwest boundary (model south boundary). Basalt along the southwest boundary is below the 95.25 m NAVD88 elevation of the domain bottom. Most of the southwest boundary is occupied by Rwia, with smaller areas of CCUg and Rlm close to the water table. Figure C-10 shows vertical cross-sections along the geographic southeast boundary (model east boundary). Along the southeast boundary, there is a small region of basalt near the east corner, most of the boundary is occupied by Rwia, and there are small regions of CCUg, Rlm, and Rwie near the water table.

C.5 HYDRAULIC PROPERTIES OF SATURATED MATERIALS

The two major HSUs identified in the WMA A-AX PA model domain that are expected to control the flow field are the Plio-Pleistocene CCUg and the Mio-Pliocene Rwia due to their large spatial extent within the model domain. Other saturated HSUs include small regions of Rwie and Rlm in the southeastern portion of the domain. Table C-2 indicates the hydraulic conductivity and specific yield values for these HSUs in the CPGWM Version 8.4.5 calibration. The use of these values in the WMA A-AX PA STOMP model (with specific yield used as a proxy for porosity) and their representativeness of the WMA A-AX sediments is discussed in this section.

Table C-2. Hydraulic Parameters for Hydrostratigraphic Units in Waste Management Area A-AX Saturated Zone from Central Plateau Model Version 8.4.5 Calibration.

Hydrostratigraphic Unit as Defined in CPGWM Version 8.4.5	Horizontal Hydraulic Conductivity (m/day)	Vertical Hydraulic Conductivity (m/day)	Total Porosity from Specific Yield (cm^3/cm^3)
Cold Creek gravel (paleochannel region [CCUg])	18,200	1,381	0.25
Ringold E (Rwie) (east region)	35.6	3.56	0.08
Ringold mud (Rlm)	8.0×10^{-3}	8.0×10^{-4}	0.08
Ringold A (Rwia)	1.0	0.1	0.08

CPGWM = Central Plateau Groundwater Model

Source: CP-47631, *Model Package Report: Central Plateau Groundwater Model Version 8.4.5*, Rev. 4, Table 4-4.

The CCUg is a fluvial gravel deposit consisting of weakly- to moderately-cemented gravel in a sandy matrix (RPP-RPT-60171 Section 3.2.4.2). At WMA A-AX, the CCUg occurs within the paleochannel region of the Central Plateau in which cataclysmic flooding has influenced the deposition and reworking of Hanford formation and Cold Creek Formation sediments to such an extent that some of the gravels have an open framework matrix (e.g., Figure C-11 and Figure C-12), and in general the hydraulic conductivity reaches extremely high values (RPP-RPT-60171; CP-47631, Rev. 4; DOE/RL-2015-75, *Aquifer Treatability Test Report for the*

200-BP-5 Groundwater Operable Unit; RPP-ENV-58578). The horizontal hydraulic conductivity value of 18,200 m/day for the CCUg in the paleochannel estimated in the CPGWM Version 8.4.5 calibration is supported by the results of a pumping test[18] reported in DOE/RL-2015-75 and based on the reasonable match of the model calibration results to historic hydraulic heads. Figure C-13 is a photograph of Cold Creek gravel sampled from the pumping well at WMA B-BX-BY (see Figure C-2). Although the sample sediments are disturbed, it is apparent that the Cold Creek gravel at this location is clean and generically similar to Hanford formation gravels where they are also affected by the paleochannel.

In contrast, the Rwia is a fluvial conglomerate consisting of weakly- to well-cemented gravel in a sandy matrix (RPP-RPT-60171 Section 3.2.5), so the conglomeratic character used to distinguish Rwia from CCUg would be expected to correspond to much lower hydraulic conductivity as it does in CPGWM Version 8.4.5. In lieu of observations of undisturbed Rwia sediments, Figure C-14 is a photograph of Rwie sediments at an outcrop along the Columbia River about 15 miles (24 km) southeast of WMA A-AX; past Hanford Site geologists have similarly suggested that this outcrop can serve as a visual analogue for the Rwia (e.g., see PNNL-16407). The framework of the pore space created by the bimodal distribution of the gravel and the sandy matrix is markedly different than that of the paleochannel gravels and could reasonably be expected to have lower hydraulic conductivity and lower porosity.

If the presence of the CCUg/Rwia contact has been correctly identified and delineated in RPP-RPT-60171, and if the properties of the respective HSUs in Table C-2 are indeed representative, then the majority of the simulated groundwater flux will be through the CCUg, vertical gradients may be induced near the contact, and most groundwater will likely divert horizontally around the Rwia present at the water table through the surrounding CCUg. Therefore, uncertainty in the delineation of the contact may be sufficient to affect the direction of groundwater flow downgradient of WMA A-AX. Uncertainty in the local-model-scale values of hydraulic conductivity for the HSUs leads to uncertainty in the magnitude of the effects of the contact on the flow field. The morphology of existing groundwater contaminant plumes as narrow plumes with a southeastward trend unbroken by the interpreted contact of HSUs in the southeast corner of the 200 East Area (DOE/RL-2016-66) has been suggested as evidence that larger areas of sediments may have been reworked by cataclysmic flooding than suggested by the previously-interpreted extent of the paleochannel (CP-47631 Rev. 4 Section 4.5.4.3). The uncertainty in the delineation of the contact between paleochannel gravels and undisturbed Ringold gravel units and the uncertainty in their locally-representative hydraulic properties has been identified in other recent Hanford Site modeling, including the CPGWM itself, as an

[18] The pumping test was a 27-day constant-rate discharge test at 379 L/min with multiple observation wells, from which horizontal hydraulic conductivity estimates ranged from 15,100 to 21,100 m/day with an average of 18,200 m/day; a 3-day constant-rate discharge test at 473 L/min at the same pumping well produced a slightly higher average estimate of 18,800 m/day for the horizontal hydraulic conductivity (DOE/RL-2015-75). In the authors' estimation, these pumping tests are superior to all earlier hydraulic testing of Hanford Site paleochannel sediments due to the longer duration, higher discharge rate, use of more observation wells, and better documentation than earlier tests, all of which have clear importance given the difficulty of physically measuring such high hydraulic conductivities. Only by imposing a large stress on the aquifer and observing at multiple points at increasing distance can a hydraulic test determine values representative of scales approaching those modeled in PAs or the CPGWM.

unresolved topic of significance for contaminant transport which may potentially benefit from future data collection (CP-47631 Rev. 4 Section 8.4).

Figure C-11. Photograph of Hanford Formation Gravel Exposed at North Richland Borrow Pit.

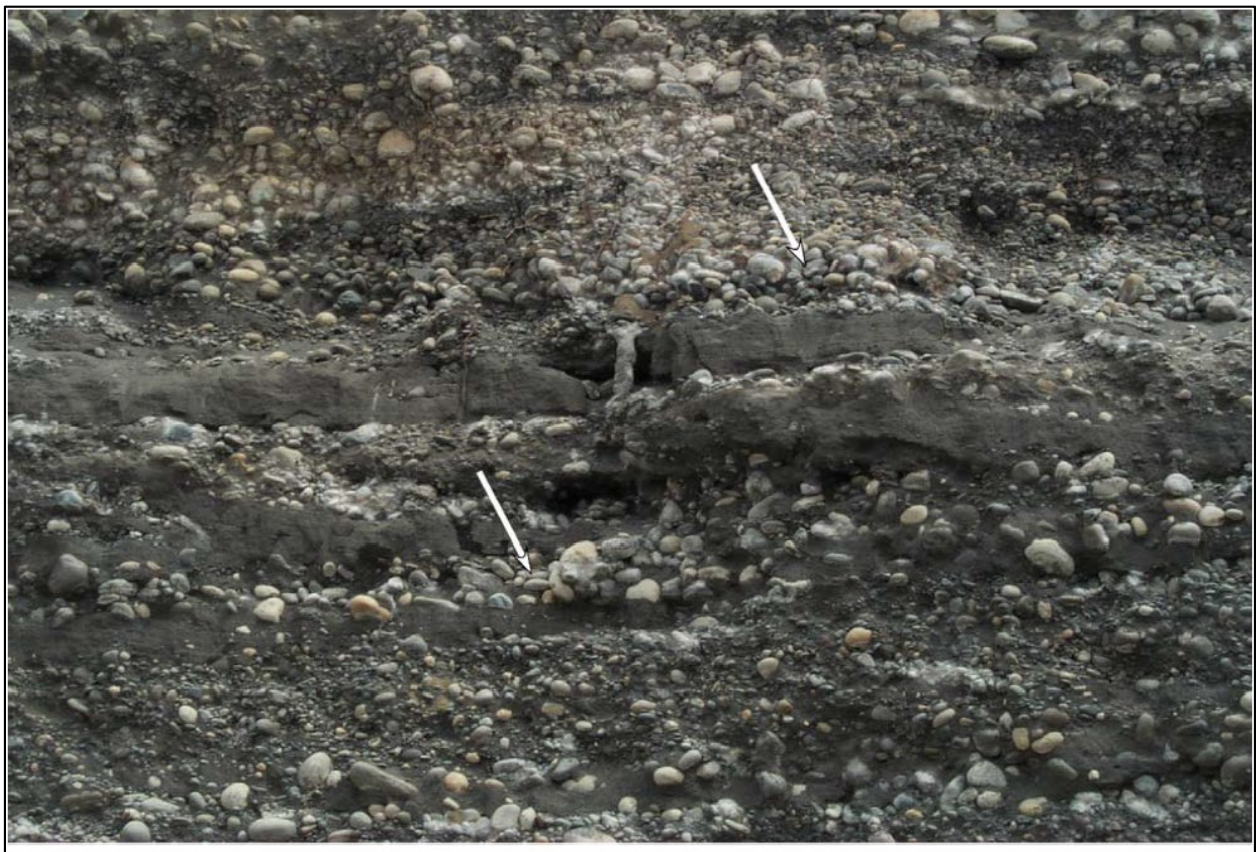

Figure 3.7. Example of Gravel-Dominated Hanford Formation from Borrow Pit in North Richland, Approximately 15 Miles Southeast of the Waste Treatment Plant. Note chaotic bedding of basalt-rich, clast-supported gravels interbedded with basaltic, matrix-supported, pebbly sands. Arrows point to areas with open-work fabric, a feature common to coarse-grained flood deposits of the Hanford formation.

Source: PNNL-16407, *Geology of the Waste Treatment Plant Seismic Boreholes*, Figure 3.7.

Bulk groundwater flux does not directly depend on the total porosity or specific yield, but effective porosity is a factor in the average linear groundwater velocity and thus could influence advective transport rates. If the effective porosity for transport is assumed equal to the specific yield, then a hydraulic gradient of 5×10^{-6} m/m applied to the CCUg horizontal hydraulic conductivity of 18,200 m/day and porosity of 0.25 cm^3/cm^3 would produce an average linear velocity of 133 m/yr in the CCUg. This value is inversely proportional to the effective porosity, so uncertainty in the porosity would easily propagate to uncertainty in the average linear groundwater velocity. However, the estimated value also indicates that advective transport along a 100-m-long groundwater pathway may take less than one year; therefore, any uncertainty in the average linear groundwater velocity is insignificant to transport of simulated releases from

WMA A-AX compared to uncertainties in the centuries-long vadose zone transport time discussed in Section C.3, so uncertainties in the porosities in Table C-2 are unlikely to affect the PA objectives.

Figure C-12. Photograph of Open Framework Structure of Hanford Formation Gravel Occurring in the Paleochannel Region.

Source: PNNL-13641, *Uncertainty Analysis Framework - Hanford Site-Wide Groundwater Flow and Transport Model*, Figure 4.4.

C.6 GROUNDWATER FLUX THROUGH THE MODEL DOMAIN

The groundwater flux in a given model cell in the CPGWM depends on boundary conditions distant from WMA A-AX and on the hydraulic properties of the HSUs assigned to the cell and its neighbors. Potential differences between the geologic models assumed by the CPGWM and by the WMA A-AX PA may prevent direct comparison of fluxes at a given point in space, and whether or not such differences exist, the difference in grid resolution of the CPGWM (with cell sizes of 100 m by 100 m horizontally and cell heights varying from about 0.6 m to 16 m near WMA A-AX) and the PA STOMP model (with cell sizes of 4.355 m by 4.355 m to 20 m by 20 m horizontally and saturated zone cell heights of 0.5 m to 3 m) will inevitably cause differences in the models' interpolations of the HSUs and effectively the same problem with

comparing fluxes at a point. On the other hand, the use of broadly similar underlying geologic models implies that the PA STOMP model should be able to match the groundwater flux over a larger region of more than just one or a few cells in the CPGWM. With this in mind, the total fluxes across the STOMP model domain boundaries estimated from the corresponding cells in the CPGWM were extracted from the CY 2137 results reported in ECF-200W-17-0043 to determine values appropriate for prescribed flux boundary conditions in the STOMP model.

Before presenting the flux estimation, this section presents details of the CPGWM flow field to better understand the model features contributing to the simulated bulk fluxes. The CPGWM is a seven-layer MODFLOW model (layers numbered from top to bottom), with Layer 1 near WMA A-AX containing the dry vadose zone and used only to convey recharge to the top of Layer 2, and the bottom of Layer 7 representing the top of the basalt bedrock surface (CP-47631). Local portions of the steady-state flow field near WMA A-AX for Layer 2 through Layer 7 are shown in Figure C-15 through Figure C-20, respectively. The MODFLOW model cells are indexed by row (north to south) and column (west to east) for reference.

Figure C-15 hows the flow field near the water table in Layer 2. Thicknesses and elevations vary from cell to cell, so the bottom of Layer 2 over the STOMP model domain area varies from about 107 m NAVD88 to 122 m NAVD88 with an average of about 117.6 m NAVD88. At the simulated steady-state water table elevation of about 119.9 m NAVD88, some cells in Layer 2 are dry, whereas most are partially saturated. Within the resolution of the CPGWM model grid, the entire extent of the STOMP model domain at the water table is represented by CCUg (green color with 18,200 m/day hydraulic conductivity) or by Hanford channel gravel (light brown color with 15,000 m/day hydraulic conductivity), which for the purpose of the PA modeling, comprise the same paleochannel-influenced gravel-dominated HSU. The flow field is generally southeastward with some minor internal variation.

Figure C-16 shows the flow field in Layer 3. The bottom of Layer 3 over the STOMP model domain area varies from about 100 m NAVD88 to 119 m NAVD88 with an average of about 110.6 m NAVD88. At the simulated steady-state water table elevation of about 119.9 m NAVD88, cells in Layer 3 are partially to fully saturated. The saturated thicknesses of Layers 2 and 3 together comprise almost all the 5-m interval below the water table. As in Layer 2, the entire extent of the STOMP model domain in Layer 3 of the CPGWM is represented by CCUg or by Hanford channel gravel. Hydraulic heads are virtually the same as in Layer 2, implying little if any vertical flow between the two layers.

Figure C-17 shows the flow field in Layer 4. In addition to the paleochannel gravels, Layer 4 contains the tops of the Rwie (dark blue color with 35.5 m/day conductivity) and the Rwia (grey color with 1.0 m/day conductivity). This interpolation differs from that of the STOMP model in that most of the Ringold Formation in the domain area is attributed to Rwie rather than Rwia with corresponding difference in the calibrated hydraulic conductivity. Another difference is that the Cold Creek/Ringold contact occurs at elevations closer to or above the water table in the STOMP model. Those differences would be expected to affect fluxes at the southwest and southeast boundaries, but not the northwest or northeast boundaries. It is also interesting to note that the Rwie material in the “east” region of the CPGWM was not distinguished from other

regions in the previous version of the CPGWM and that increasing its hydraulic conductivity improved the calibration in Version 8.4.5.

Figure C-13. Photograph of Cold Creek Gravel Unit Sediments from the Location of the Pumping Test in Paleochannel Region.

DOE/RL-2015-75, REV. 0

Figure 1-8. Extraction Well 299-E33-268 Sediment Sample from 76.2 m (250 ft) below ground surface or 0.76 m (2.5 ft) above Elephant Mountain Basalt

Source: DOE/RL-2015-75, *Aquifer Treatability Test Report for the 200-BP-5 Groundwater Operable Unit*, Figure 1-8.

Figure C-14. Photograph at Outcrop of Ringold Wooded Island Member Gravel-Dominated Sequence Suggested as Visual Analogue for Ringold Unit A.

Photo by Terry Tolan, INTERA, Inc.

Figure C-18 shows the flow field in Layer 5. The STOMP model domain area in Layer 5 is dominated by paleochannel gravels in the northern half and by Ringold Formation units in the southern half. One cell on the southeast boundary contains Rlm (light blue color with 8.0×10^{-3} m/day conductivity). Hydraulic head contours diffract relative to the overlying layers, but only by less than 1 mm in a given cell, suggesting a minor upward flux may be expected from the Ringold Formation to the overlying CCUg. Horizontal components of Darcy fluxes in Layer 5 more visibly divert and accelerate around the Ringold gravels through the CCUg, with much smaller fluxes through the Ringold gravels and little flux at all through the Rlm.

Figure C-19 shows the flow field in Layer 6, which extends the trends observed in Layer 5. The Rlm occupies several cells in CPGWM Layer 6 near the south corner of the STOMP model domain area and continues beyond it, such that the laterally-continuous fine-grained HSU stops fluxes out of the Ringold gravels and forces groundwater flow to divert horizontally and vertically. This effect of the low hydraulic conductivity values estimated for the Rlm in the CPGWM supports conceptual decisions that flow within the even lower-conductivity basalt may be ignored and that flow in the deeper portions of the Ringold gravels may similarly have little

effect on much greater flows through the shallower paleochannel gravels with much higher hydraulic conductivities.

Figure C-15. Simulated Steady-State Flow Field Near Waste Management Area A-AX in Model Layer 2 of the Central Plateau Groundwater Model Version 8.4.5.

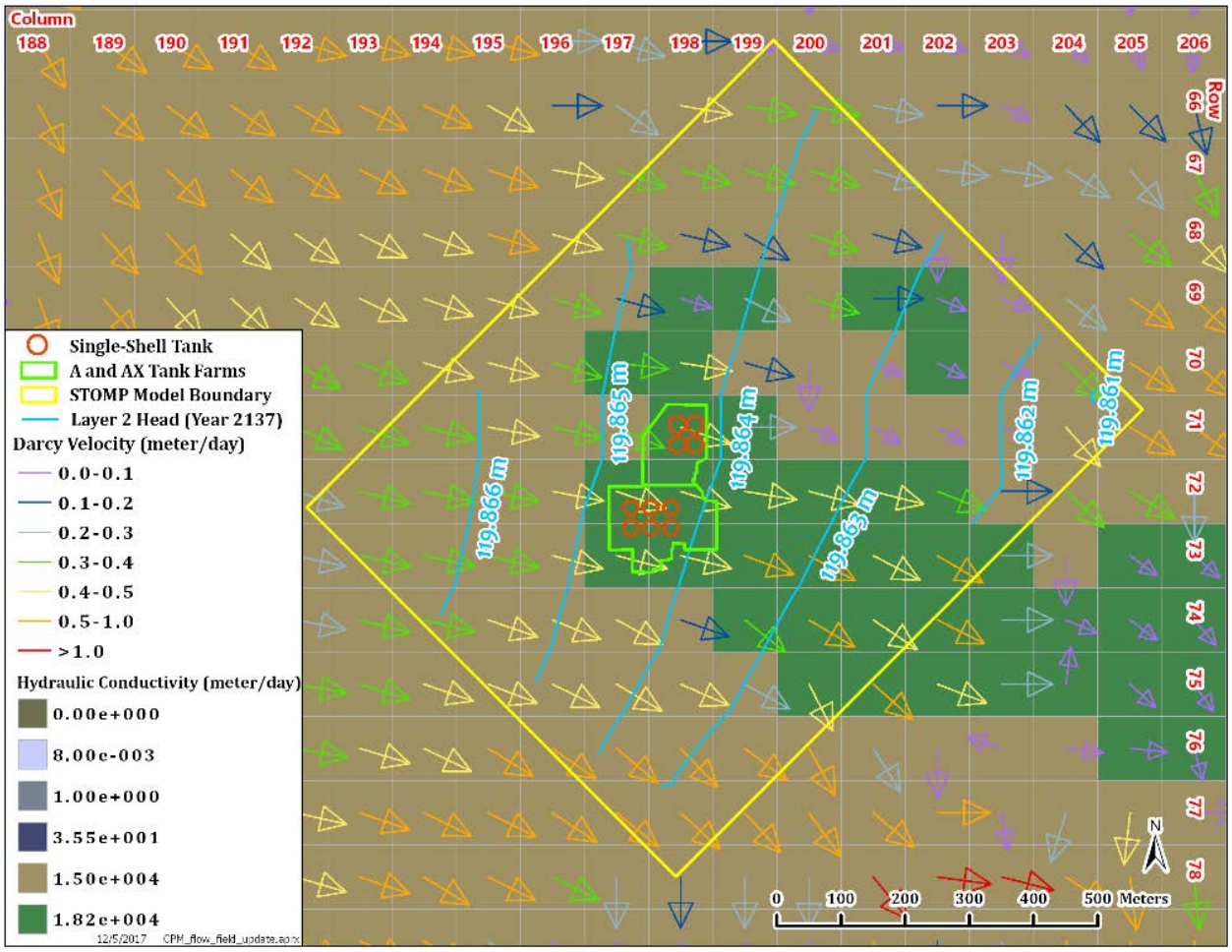

Source: Based on results in ECF-200W-17-0043, *Capture-Zone and Particle-Tracking Analysis for the 200-UP-1/200-ZP-1 Areas using the 2017 Updated Central Plateau Model.*

Subsurface Transport Over Multiple Phases (STOMP) is developed and distributed by Battelle Memorial Institute.

Figure C-20 shows the flow field in Layer 7, which is locally interrupted by the top of the basalt (inactive in the CPGWM) and which comprises relatively insignificant fluxes in the Rwia.

Along the northwest STOMP model boundary which is entirely basalt in Layer 7, the thick cells in Layer 6 are mostly represented by channel gravels, i.e., only a small cross-sectional area of the CPGWM contains Ringold gravel at this boundary.

Based on the observations of the STOMP model rock/soil zonation in Section C.4 and the simulated steady-state flow field in CPGWM Version 8.4.5 as depicted in Figure C-15 through Figure C-20, it was determined that the total flux across the northwest boundary of the STOMP

model domain area in CPGWM Layers 2 through 6 provides an analogous basis to prescribe flux for the same boundary in the STOMP model. Prescribed flux boundary conditions were chosen instead of prescribed head boundary conditions to ensure that the flow through the aquifer matched the flow estimated from the CPGWM. Prescribing heads instead of fluxes along the other vertical boundaries where flow directions are locally more variable is a more intuitive way to translate the interpreted flow conditions from one model to the other. The differences in the distributions of HSUs would be more complicated to reconcile in areas along those other boundaries. The total flux in all layers across the northwest boundary is likely the same total flux applicable to the upgradient boundary in the STOMP model, but the allocation of flux between HSUs needs to reflect the difference in their interpolations between the models, whereby the CPGWM does not represent the Rwia being present at the northwest boundary.

Figure C-16. Simulated Steady-State Flow Field Near Waste Management Area A-AX in Model Layer 3 of the Central Plateau Groundwater Model Version 8.4.5.

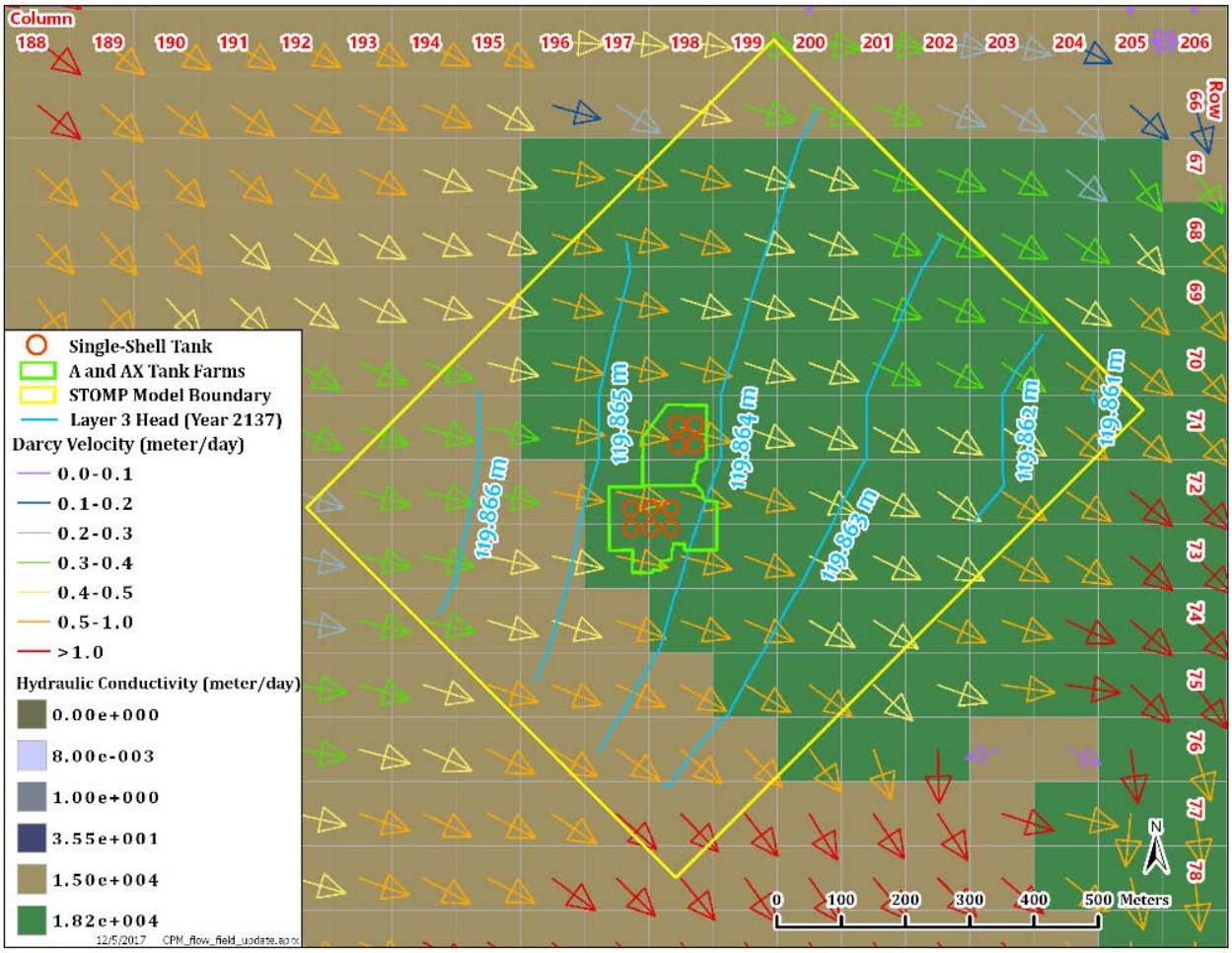

Source: Based on results in ECF-200W-17-0043, *Capture-Zone and Particle-Tracking Analysis for the 200-UP-1/200-ZP-1 Areas using the 2017 Updated Central Plateau Model*.

Subsurface Transport Over Multiple Phases (STOMP) is developed and distributed by Battelle Memorial Institute.

Figure C-17. Simulated Steady-State Flow Field Near Waste Management Area A-AX in Model Layer 4 of the Central Plateau Groundwater Model Version 8.4.5.

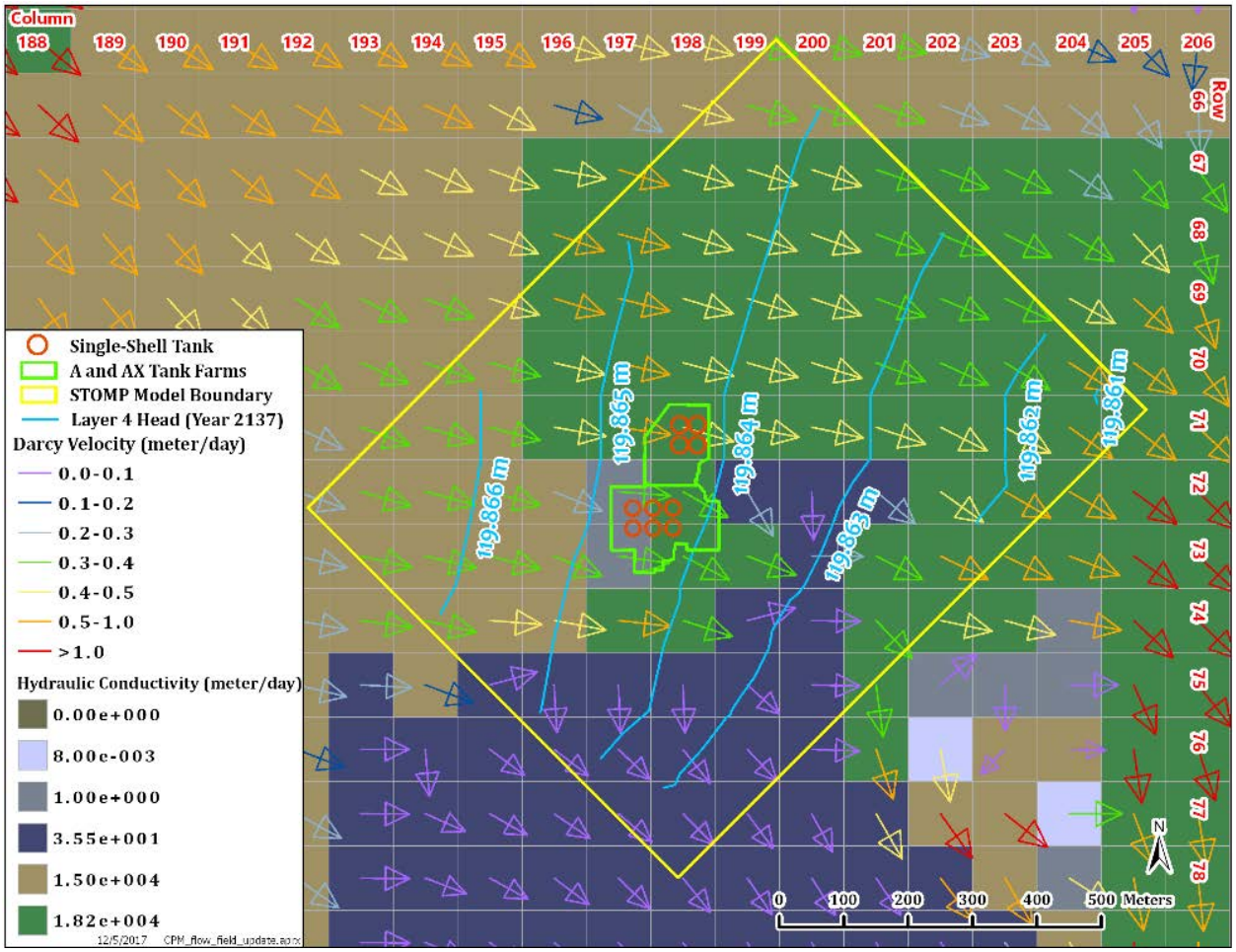

Source: Based on results in ECF-200W-17-0043, *Capture-Zone and Particle-Tracking Analysis for the 200-UP-1/200-ZP-1 Areas using the 2017 Updated Central Plateau Model.*

Subsurface Transport Over Multiple Phases (STOMP) is developed and distributed by Battelle Memorial Institute.

Fluxes into and out of the saturated region of the STOMP model domain area from the CPGWM results in the cell-by-cell budget file CPM_v845_2012-2137.cbb from the single-precision run from ECF-200W-17-0043 were determined by extracting sub-regional water budgets at Time Step 20 of Stress Period 97 (the final time step corresponding to the steady-state flow field in CY 2137) using the post-processing code ZONEBUDGET (Open-File Report 90-392, *A Computer Program for Calculating Subregional Water Budgets Using Results from the U.S. Geological Survey Modular Three-dimensional Finite-difference Ground-Water Flow Model*). Sub-regional zones were defined for the interior of the STOMP model domain and for the CPGWM cells along each edge of the domain for each CPGWM layer. Composite zones were defined to integrate fluxes in the same areas over model Layers 2 through 7. A zone covering the STOMP domain area in Layer 1 was also defined to calculate recharge.

Figure C-18. Simulated Steady-State Flow Field Near Waste Management Area A-AX in Model Layer 5 of the Central Plateau Groundwater Model Version 8.4.5.

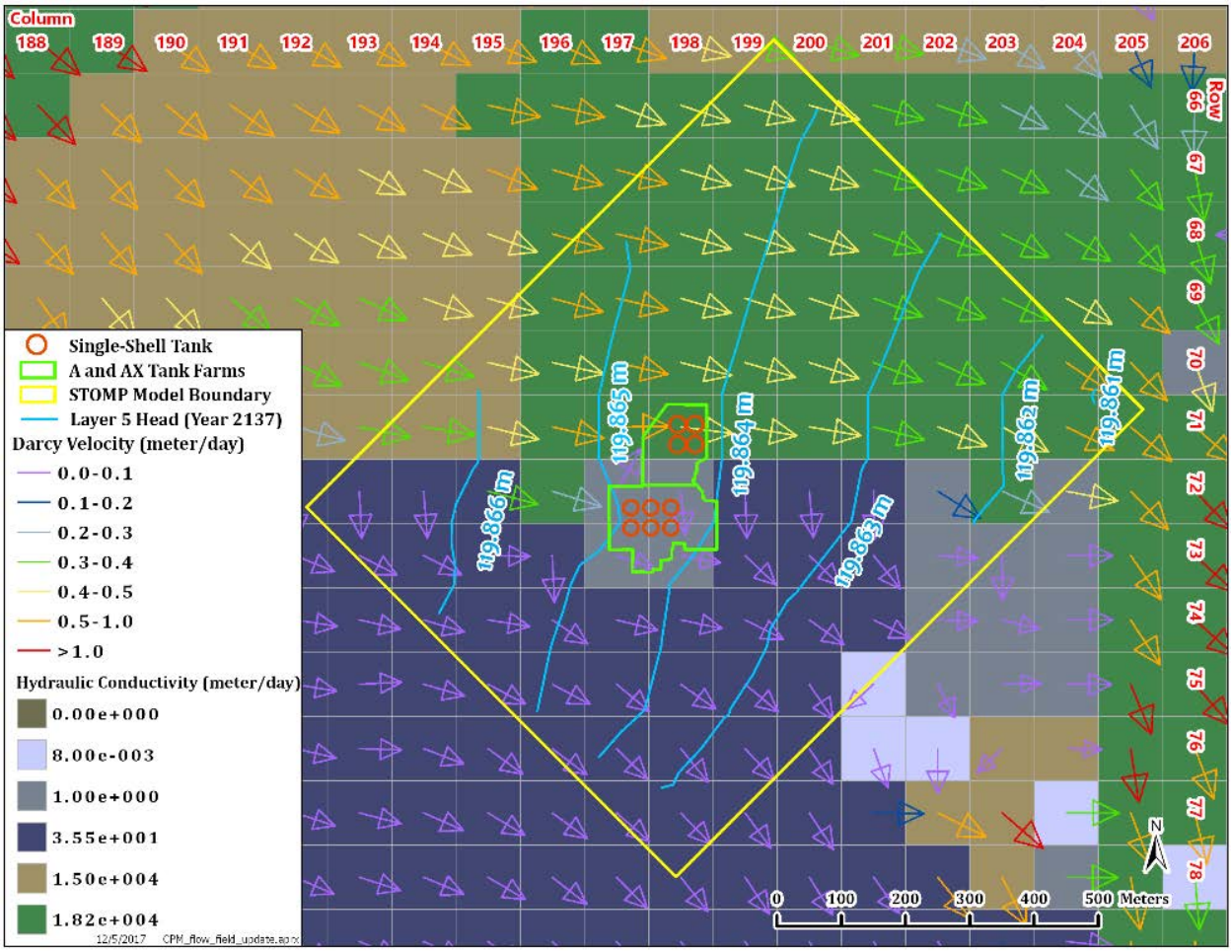

Source: Based on results in ECF-200W-17-0043, *Capture-Zone and Particle-Tracking Analysis for the 200-UP-1/200-ZP-1 Areas using the 2017 Updated Central Plateau Model*.

Subsurface Transport Over Multiple Phases (STOMP) is developed and distributed by Battelle Memorial Institute.

The total flux simulated by the CPGWM across the northwest boundary of the STOMP model domain area was 1,052 m^3/day, and the direction of flow was into the STOMP domain at every cell along that boundary. Smaller net fluxes occurred along the northeast and southwest boundaries, with cell-by-cell fluxes both into and out of the STOMP domain area along each of those cross-gradient boundaries. Flux out of the STOMP domain area across the southeast boundary approximately balanced the flux into the northwest boundary (there was a small difference due to recharge and net fluxes across the cross-gradient boundaries), with the direction of flow mostly outward across the southeast boundary except at some cells near the basalt contact in Layer 7 and some cells modeled as Rlm in the deep Layers 5 and 6.

Figure C-19. Simulated Steady-State Flow Field Near Waste Management Area A-AX in Model Layer 6 of the Central Plateau Groundwater Model Version 8.4.5.

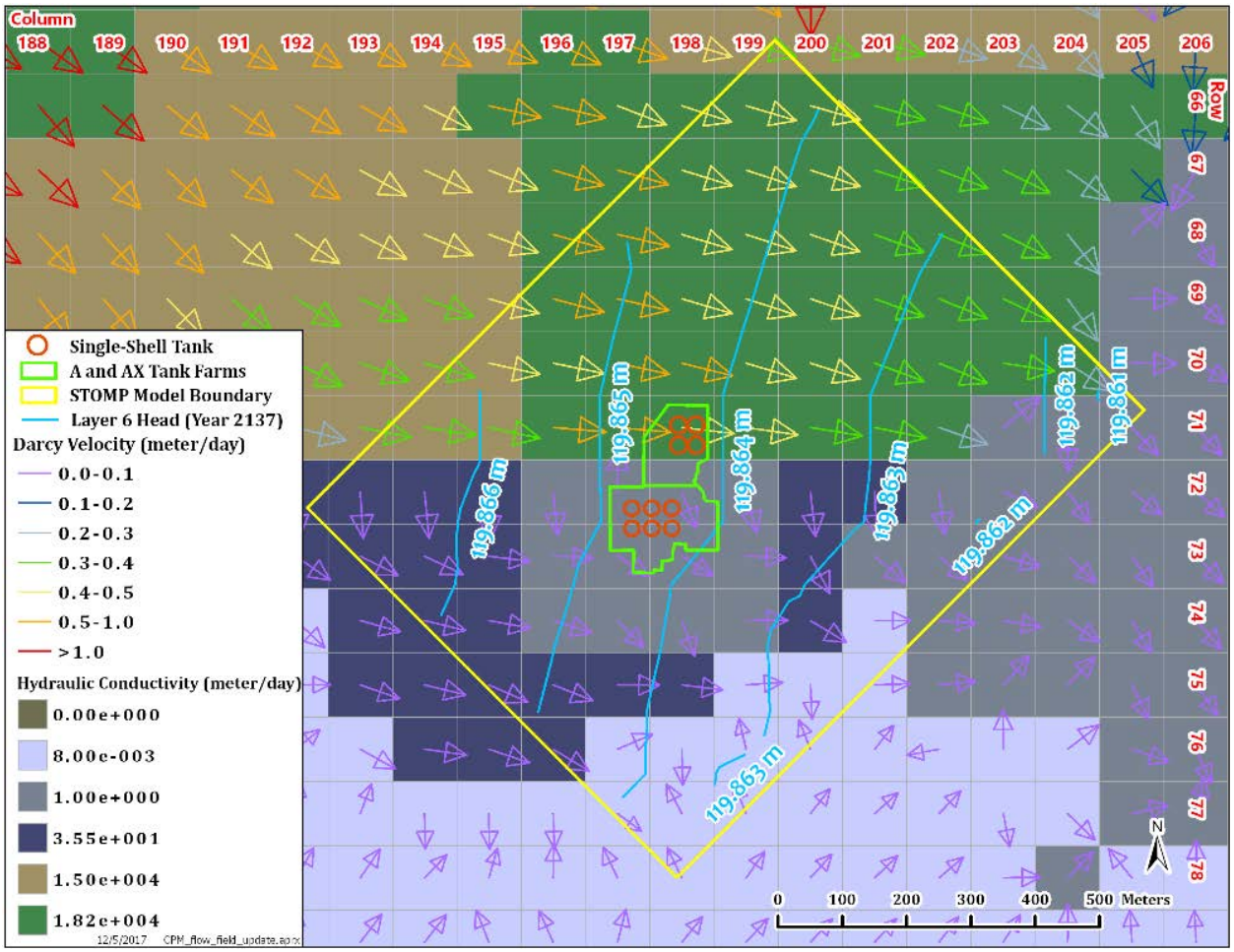

Source: Based on results in ECF-200W-17-0043, *Capture-Zone and Particle-Tracking Analysis for the 200-UP-1/200-ZP-1 Areas using the 2017 Updated Central Plateau Model.*

Subsurface Transport Over Multiple Phases (STOMP) is developed and distributed by Battelle Memorial Institute.

C.7 METHOD OF CALCULATING SATURATED ZONE BOUNDARY CONDITIONS

The STOMP model Layers k=1 through k=5 below an elevation of 106.75 m NAVD88 contain only basalt and Rwia and are therefore not expected to transmit any significant portion of the total saturated zone flow, given the hydraulic properties of saturated HSUs in Section C.5. Since the PA calculates groundwater concentrations in the upper 5 m of the saturated zone, eliminating layers below 106.75 m NAVD88 from simulations leaves an additional 7.75 m of saturated HSUs, mostly Rwia, in which to represent contaminant transport below the calculation interval that may potentially occur. Any potential contaminant flux into deeper portions of the Rwia below 106.75 m NAVD88 may lower concentrations near the water table but is expected to be small relative to advection-dominated flux in the shallower CCUg. Therefore, Layers k=1

through k=5 are assumed to be overwritten with inactive cells in the calculations of boundary conditions which follow, although the modelers have the alternative to reverse that assumption by simply substituting the total cross-sectional area of Rwia (including in Layers k=1 through 5 and higher layers) for the truncated area. Assuming the bottom 5 layers are inactive establishes a no flux boundary at the bottom of Layer 6 by default. The contact between basalt in Layer 6 or higher and other rock/soil zones is likewise a no flux boundary.

Figure C-20. Simulated Steady-State Flow Field Near Waste Management Area A-AX in Model Layer 7 of the Central Plateau Groundwater Model Version 8.4.5.

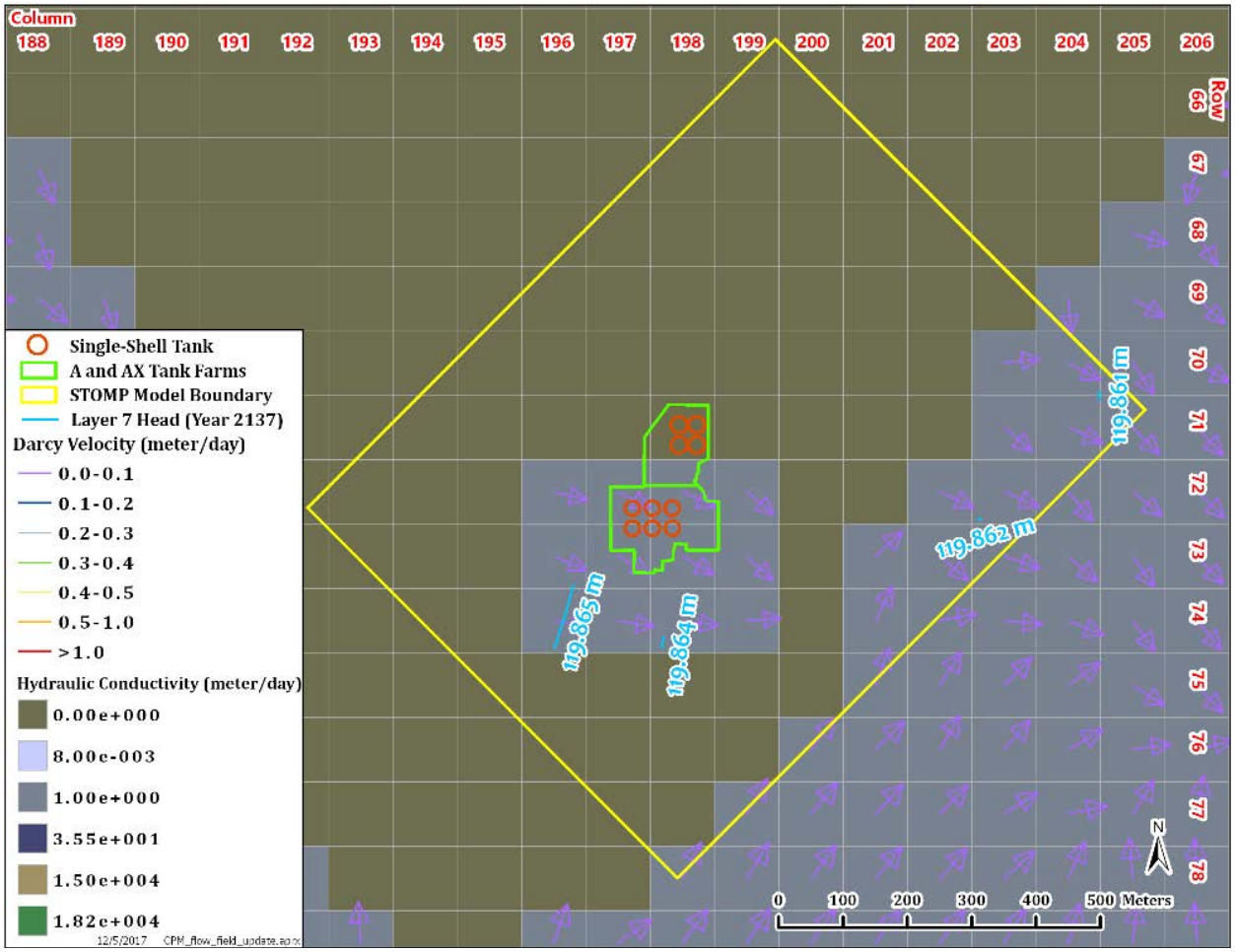

Source: Based on results in ECF-200W-17-0043, *Capture-Zone and Particle-Tracking Analysis for the 200-UP-1/200-ZP-1 Areas using the 2017 Updated Central Plateau Model*.

Subsurface Transport Over Multiple Phases (STOMP) is developed and distributed by Battelle Memorial Institute.

Recharge across the water table is calculated within STOMP according to infiltration rates prescribed at the top of the vadose zone (see Section 3.1.5). If no local releases of water or local increases in infiltration rate near the vertical domain boundaries are simulated, then infiltration is expected to move generally downward and become recharge rather than leave the domain, whether boundary conditions on the sides of the vadose zone are specified as zero flux or Dirichlet-type boundary conditions such as the "seepage face" option. In simulations used in this

model package report, after establishing the initial steady-state flow field, the default zero-flux condition applies to the vertical vadose zone boundaries except for one model layer above the water table (Layer k=19) where the "seepage face" option is used on the southeast boundary and the "initial condition" option is used on the northeast and southwest boundaries. These boundary conditions allow infiltration to leave the domain before reaching the water table (mainly as a precaution for potential simulation of different transient conditions than considered here), but in practice only a minimal fraction of infiltration exits at Layer k=19.

For the saturated zone, the upgradient, northwest boundary (model west) up to Layer k=18 is a prescribed flux boundary. The elevation of 119.5 m NAVD88 corresponding to the top of Layer k=18 is assumed to be the steady-state water table elevation at the upgradient boundary. The downgradient, southeast boundary (model east) is a prescribed head boundary using the "seepage face" option up to Layer k=19. Applying the estimated steady-state hydraulic gradient of -5×10^{-6} m/m with groundwater flow toward the southeast (Section C.3) over the 812.606-m length of the domain, the head at the southeast boundary equals 119.4959 m NAVD88. The cross-gradient, northeast (model north) and southwest (model south) boundaries are prescribed head boundaries up to Layer k=19 such that the water table is within Layer k=18 with heads varying from node to node. The heads along the cross-gradient boundaries are estimated using the model itself by running the flow field to steady state in an initial simulation with zero flux prescribed at these boundaries and then restarting to run to a new steady state in a second simulation with the simulated heads now prescribed using the "initial condition" option and without restricting flux.

The total groundwater flux of 1,052 m^3/day across the northwest STOMP model domain boundary determined from the steady-state CPGWM flow field (as described in Section C.6) is allocated among the CCUg and Rwia according to their cross-sectional areas given in Section C.4 and their hydraulic conductivities given in Section C.5. The greatest flux is expected to occur through the CCUg based on the respective hydraulic properties of the HSUs. Assuming the basalt is essentially impermeable relative to the other HSUs, the balance of the total groundwater flux is allocated to the Rwia (whether using the total cross-sectional area or just the area of Rwia above k=5 as in the calculation that follows). From Darcy's law, the volumetric flux (Q) in each saturated HSU is the product of the hydraulic conductivity (K), the hydraulic gradient (i), and the cross-sectional area (A) of the saturated HSU perpendicular to the direction of flow:

$$Q = K \times i \times A$$

For each HSU, the Darcy flux (q) equals the volumetric flux divided by the cross-sectional area:

$$q = \frac{Q}{A} = K \times i$$

The total volumetric flux across the northwest model domain boundary is equated to the sum of volumetric fluxes in the CCUg and Rwia as follows:

$$Q_{total} = K_{CCU_g} i_{CCU_g} A_{CCU_g} + K_{R_{wia}} i_{R_{wia}} A_{R_{wia}}$$

There is uncertainty in each of the variables needed to calculate the flux to be prescribed for each HSU at the northwest boundary. At the resolution of the CPGWM, the Rwia was not modeled to be present at the location of the STOMP model northwest boundary, so fluxes to prescribe for each HSU are not directly available. However, the total flux across that boundary from the CPGWM appears reasonable based on the model calibration (CP-47631) and the approximate consistency with upgradient fluxes estimated for steady-state conditions at WMA C (RPP-ENV-58782). The cross-sectional areas of the HSUs have uncertainties associated with geologic interpretation of borehole data and interpolation between boreholes, but these uncertainties from the GFM relying on a finite number of boreholes with reasonable-quality logs are small compared to uncertainties in flux, gradients, and hydraulic conductivities. Although there is large uncertainty in the local values of the hydraulic conductivities of the HSUs, the pumping test and regional groundwater model calibration discussed in Section C.5 provide a reasonable basis for the estimates. Given estimates of the areas and hydraulic conductivities, the uncertainty in the future steady-state hydraulic gradients is much the same as the uncertainty in the flux.

Whereas the current hydraulic gradient in the CCUg is known from monitoring wells and provides a means to evaluate whether the steady-state gradient modeled in the CPGWM is reasonable, there are no wells screened entirely in the Ringold near WMA A-AX with which to measure hydraulic heads and estimate the current gradient in the Rwia, and the CPGWM does not include an extensive layer of Rwia below WMA A-AX in which to model a steady-state gradient applicable to the Rwia in the STOMP model. Rather than specify the exact values of the gradients in each HSU, if they may be assumed equal, then the flux in each HSU can be estimated as a proportion of the total flux.

Assuming the hydraulic gradients in both HSUs are equal, and dividing both sides of the previous equation by the Darcy flux in the CCUg, the equation becomes:

$$\frac{Q_{total}}{q_{CCU_g}} = A_{CCU_g} + \frac{K_{R_{wia}}}{K_{CCU_g}} A_{R_{wia}}$$

Multiplying both sides by the hydraulic conductivity of the CCUg gives:

$$\frac{Q_{total} K_{CCU_g}}{q_{CCU_g}} = K_{CCU_g} A_{CCU_g} + K_{R_{wia}} A_{R_{wia}}$$

Thus, the Darcy flux in the CCUg can be obtained by scaling the total volumetric flux by a factor representing the proportion of total flux expected from the hydraulic conductivity of the HSU:

$$q_{CCU_g} = \frac{Q_{total} K_{CCU_g}}{K_{CCU_g} A_{CCU_g} + K_{R_{wia}} A_{R_{wia}}}$$

$$q_{CCU_g} = \frac{(1052\ m^3/d)(18{,}200\ m/d)}{(18{,}200\ m/d)(7{,}570\ m^2) + (1.0\ m/d)(3{,}916\ m^2)} = 0.139\ m/d$$

Similarly, the Darcy flux in the Rwia is obtained from:

$$q_{R_{wia}} = \frac{Q_{total} K_{R_{wia}}}{K_{CCU_g} A_{CCU_g} + K_{R_{wia}} A_{R_{wia}}}$$

$$q_{R_{wia}} = \frac{(1052\ m^3/d)(1.0\ m/d)}{(18{,}200\ m/d)(7{,}570\ m^2) + (1.0\ m/d)(3{,}916\ m^2)} = 7.64 \times 10^{-6}\ m/d$$

The assumption that the hydraulic gradient is the same in the Rwia as it is in the CCUg has the logical consequence that the calculated Darcy flux is five orders of magnitude lower in the Rwia than in the CCUg, given that the hydraulic conductivity is five orders of magnitude lower. In this case, the CCUg is essentially the only pathway for groundwater flow, and almost all groundwater will flow over and around the Rwia.

Dividing the Darcy flux for each HSU by its hydraulic conductivity, the hydraulic gradient estimated across the northwest boundary is 7.64×10^{-6} m/m, which is reasonably consistent with the magnitude of 5×10^{-6} m/m estimated across the model domain and with the apparent flattening of the gradient from northwest to southeast across the 200 East Area as seen in Figure C-2 through Figure C-5.

It is possible that the hydraulic gradient is higher within the Rwia than within the CCUg, in which case the Darcy flux in the Rwia would be higher than calculated in this section. However, the flux in the Rwia would still be expected to be much lower than that in the CCUg due to the large contrast in hydraulic conductivity. Without data available for hydraulic heads in the Rwia in the local area around WMA A-AX, the fluxes calculated assuming equal hydraulic gradients in the two HSUs are conceptually reasonable.

C.8 TRANSPORT PROPERTIES OF SIMULATED GROUNDWATER CONTAMINANTS

In addition to hydraulic parameters affecting groundwater flow and advective contaminant transport in the saturated zone, parameters that affect advective-dispersive contaminant transport include sorption parameters, macrodispersivity, effective diffusivity, and the effective porosity for transport. Radioactive decay also affects transport, but radionuclide half-lives depend only on the radionuclide and not the media (half-lives may be found in "ICRP Publication 107: Nuclear Decay Data for Dosimetric Calculations" [ICRP 2008]). Most details necessary to select the transport parameter values have been previously covered in this model package report, except in the case of the saturated zone macrodispersivity, which is discussed later in this section.

Sorption in the saturated zone is based on the same linear adsorption model and assumptions adopted for the vadose zone. Sorption is assumed to be fully reversible, as described and quantified by a soil-water partition coefficient (K_d) that is corrected for the gravel content of the saturated zone HSUs (Equations 2.3 and 2.4 in PNNL-17154, *Geochemical Characterization Data Package for the Vadose Zone in the Single-Shell Tank Waste Management Areas at the Hanford Site*). The relatively low "high-salinity" vadose zone K_d values are assumed to be

sufficient for the relatively brief time that contaminants are transported in groundwater to the points of calculation. An alternative assumption is that the high-salinity conditions in the vadose zone do not persist in the aquifer. In this case, K_d values applicable to the aquifer HSUs are determined from the K_d values appropriate for chemically-unimpacted far-field sediments, which are identified in the same data sources used for the vadose zone HSUs (Tables A.1 and A.2 in PNNL-17154 for the gravel-dominated HSUs and the Rlm, respectively). The importance of this assumption and its impact on the results can be evaluated as part of a sensitivity analysis.

Effective diffusivity is calculated internally in STOMP from the specified molecular diffusion coefficient, which as for the vadose zone is assumed to be 2.5×10^{-5} cm^2/s for all species in groundwater (WHC-SD-WM-EE-004, *Performance Assessment of Grouted Double-Shell Tank Waste Disposal at Hanford*, Table 3.22), and which is consistent with, and representative of, values used in other Hanford PAs (RPP-ENV-58782; WCH-520, *Performance Assessment for the Environmental Restoration Disposal Facility, Hanford Site, Washington*; WHC-EP-0645, *Performance Assessment for the Disposal of Low-Level Waste in the 200 West Area Burial Grounds*; and WHC-SD-WM-TI-730, *Performance Assessment for the Disposal of Low-Level Waste in the 200 East Area Burial Grounds*). Given the preponderance of gravel-dominated HSUs in the saturated zone of the WMA A-AX PA model domain, the effective porosity for transport is assumed to equal the total porosity for each HSU, as determined from the specific yields from CPGWM Version 8.4.5 presented in Section C.5.

Heterogeneities that exist at various length scales result in a scale dependence of macrodispersivities (Figure C-21; "A Critical Review of Data on Field-Scale Dispersion in Aquifers," [Gelhar et al., 1992]). Dispersivities increase with time (e.g., over years or decades), or equivalently with distance, until they tend to converge on unique asymptotic (large time) values of practical interest in PA simulations involving millennial or greater timescales or large travel distances of 100 m or greater. The use of a constant (asymptotic) macrodispersivity is thus considered appropriate in PA simulations (NUREG/CR-6114, *Auxiliary Analyses in Support of Performance Assessment of a Hypothetical Low-Level Waste Facility: Groundwater Flow and Transport Simulation*, Vol. 3).

As in the WMA C PA (RPP-ENV-58782), the longitudinal and transverse macrodispersivity estimates in the saturated zone are based on a review of three widely-cited general relationships ("Universal Scaling of Hydraulic Conductivities and Dispersivities in Geologic Media" [Neuman 1990]; "Longitudinal Dispersivity Data and Implications for Scaling Behavior" [Schulze-Makuch 2005]; and "Use of Weighted Least-Squares Method in Evaluation of the Relationship between Dispersivity and Field Scale" [Xu and Eckstein 1995]) that quantify the dependence of this parameter on measurement scale (Ls). For the 100-m scale of transport calculations considered in the PA effort, which is the minimum distance of transport from source areas to the edge of the buffer zone, the calculated values of longitudinal dispersivity fall within the range of 3.5 to 17 m (Table C-3). A value of 10.5 m is considered representative and the midpoint of the range of values presented in Figure C-21 and Table C-3. The ratio of longitudinal to transverse macrodispersivity is assumed to be 10, consistent with previous modeling analyses (including but not limited to those in RPP-ENV-58782 [see pp. 3-68 therein] and DOE/EIS-0391 [see Appendix O therein]). RPP-20621, *Far-Field Hydrology Data Package for the Integrated Disposal Facility Performance Assessment* and PNNL-23711, *Physical,*

Hydraulic, and Transport Properties of Sediments and Engineered Materials Associated with Hanford Immobilized Low-Activity Waste indicate that a value of 10 represents a reasonable estimate of the ratio of longitudinal to transverse macrodispersivity.

Figure C-21. Longitudinal Macrodispersivity in Saturated Media as a Function of Overall Problem Scale with Data Classified by Reliability.

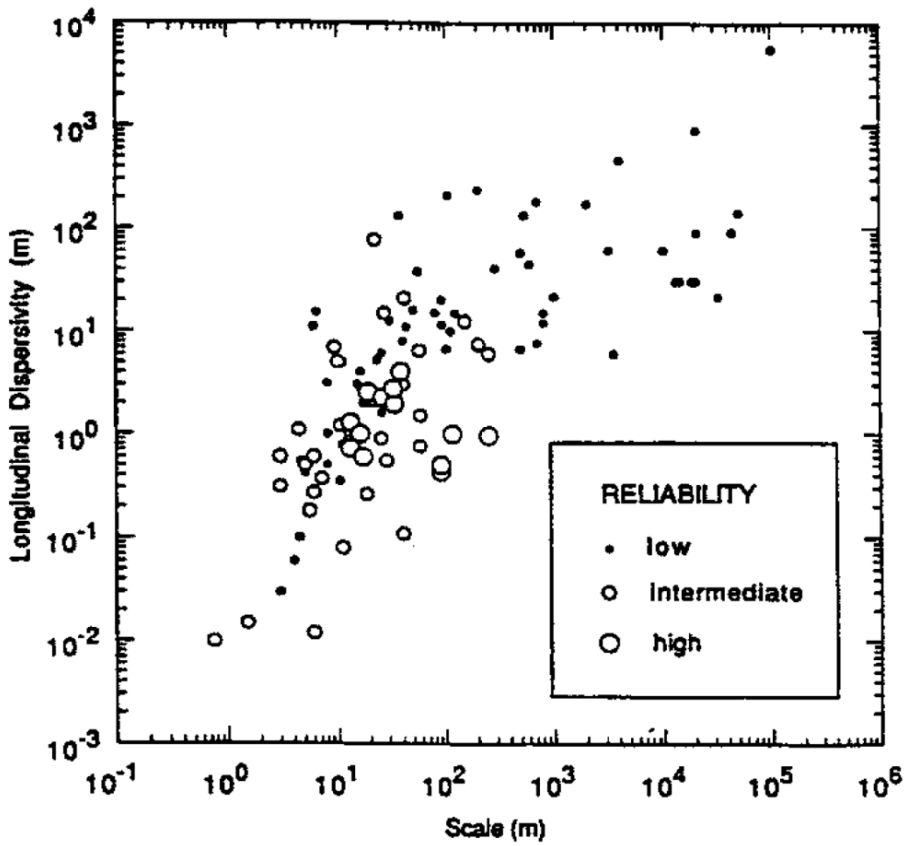

Source: "A Critical Review of Data on Field-Scale Dispersion in Aquifers" (Gelhar et al. 1992).

Although a network of monitoring wells is present that is capable of detecting impacts to groundwater near the water table, groundwater contamination at WMA A-AX is not defined in a manner that could reliably be used to validate local dispersivity values. There are no wells at WMA A-AX screened exclusively within the Rwia, so the vertical extent of existing groundwater contamination is not characterized locally. The horizontal extent of existing groundwater contamination is less widespread and, as a result, not as well delineated as at WMA C. Therefore, it is necessary to rely on empirical relationships, past modeling, and experience elsewhere on the Hanford Site in lieu of localized field data to estimate dispersivity values.

Table C-3. Relationship Between Saturated Longitudinal Macrodispersivity (α_L) and Scale of Measurement (L_s).

Reference	Relationship	Origin	Saturated Longitudinal Macrodispersivity Estimate (m) for 100-m Scale
Neuman (1990)	$\alpha_L \approx 0.017 L_s^{1.5}$	"Universal relationship" established considering both field and laboratory data (excluding modeling results)	17
Schulze-Makuch (2005)	$\alpha_L \approx 0.085 L_s^{0.81}$	Established considering field and modeling results (all reliabilities) and excluding laboratory data	3.5
Xu and Eckstein (1995)	$\alpha_L \approx 0.94 (\log_{10} L_s)^{2.693}$	Established considering the same data set as Neuman (1990) including numerical model results	6.1

References:
"Universal Scaling of Hydraulic Conductivities and Dispersivities in Geologic Media" (Neuman 1990).
"Longitudinal Dispersivity Data and Implications for Scaling Behavior" (Schulze-Makuch 2005).
"Use of Weighted Least-Squares Method in Evaluation of the Relationship between Dispersivity and Field Scale" (Xu and Eckstein 1995).

C.9 SOLUTION CONTROL CRITERIA FOR NUMERICAL SOLUTIONS

Model convergence (ability to solve the coupled flow and transport equations), numerical stability of transport solutions (sufficient accuracy and precision to avoid oscillating solutions), and limiting numerical dispersion (small enough time steps that solutes travel no more than one cell length between iterations) in the finite difference solutions to the transport equations in STOMP are dependent on selection of appropriate solution control criteria. The selection requires modeler expertise to balance these objectives with sufficient computational efficiency to allow the large model (on the order of one million cells) to complete multiple simulations of 10,000 years or more for the necessary base case and sensitivity cases for the PA within a reasonable project schedule.

There are multiple valid solver options in the CH2M HILL Plateau Remediation Company (CHPRC) Build 6 of STOMP; experience has shown that the "cgst" (SPLIB conjugate gradient stabilized) solver is a good option to achieve stable solutions efficiently for large problems. The only approved solver option in CHPRC Build 6 of extreme-scale STOMP (eSTOMP) is PETSc. Depending on input details for a given model application, solute mass balance may not be maintained in the saturated zone with the default PETSc settings for the tolerance for convergence, in which case the modeler may use the eSTOMP option to specify stricter values for the PETSc tolerances until results show appropriate mass balance. It is therefore recommended for modelers running the PA model with eSTOMP for decision-affecting calculations to verify that their selected PETSc parameters yield acceptable accuracy for their specific problems, for example by showing that results are consistent with the SPLIB cgst solver in serial STOMP.

To limit numerical dispersion of simulated contaminants, besides directly specifying a maximum time step size for a given simulation time period, use of the Courant-number-limited transport option in STOMP provides a flexible, efficient method that allows the time step size to increase as long as the model solution converges and the specified Courant number limit is satisfied. The Courant number (C_r) is given by Equation 3-2 from PNNL-11216, *STOMP Subsurface Transport Over Multiple Phases: Application Guide*:

$$C_r = \frac{v\Delta t}{\Delta x}$$

where v is the average linear velocity, Δt is the time step, and Δx is the grid spacing. Maintaining the Courant number less than or equal to 1 is frequently recommended for finite difference models in the literature to ensure numerical stability and/or limit numerical dispersion (e.g., Computational Techniques for Fluid Dynamics [Fletcher 1991]). The stability criterion is applicable to explicit finite difference schemes, but STOMP's default Patankar method is an implicit scheme which is unconditionally stable, so the acceptable Courant number limit is determined only by numerical dispersion considerations (Fletcher 1991; PNNL-12030, *STOMP Subsurface Transport Over Multiple Phases Version 2.0 Theory Guide*, Section 6.0). It may be necessary to relax the limit to some maximum value greater than 1 in the large PA simulations to avoid excessive simulation times (potentially multiple weeks for a 10,000-year simulation with a single solute in serial STOMP or even in eSTOMP, depending on the particular computing resources used), provided the modelers can demonstrate that any loss of accuracy is of tolerably small significance to the PA objectives.

The Courant number restriction is more severe for the saturated zone than for the vadose zone, given the high groundwater fluxes and low infiltration rates typical of the Hanford Site. The limiting dimension in the model for such a restriction is the 4.355-m minimum grid spacing in the x-direction aligned with the generally southeastward groundwater flow, and the most severe restriction occurs in cells of that size in the highest-flux portion of the flow field expected where the CCUg, the highest-conductivity medium, occurs. The CCUg has an estimated hydraulic conductivity of 18,200 m/day and an estimated effective porosity of 0.25. At a hydraulic gradient of ~5×10^{-6} m/m, the Darcy flux in the CCUg is 50.8 m/yr (0.139 m/day) and the average linear velocity is 203 m/yr (0.556 m/day). The time step corresponding to a Courant number of 1 in a 4.355-m-long cell under such conditions is 0.0215 yr (about 8 days). A 10,000-year transport simulation would thus contain more than 450,000 time steps, representing a significant computational expense for a model on the order of one million cells. Reducing the number of active cells—e.g., by inactivating deep layers containing only basalt and Rwia—is one measure available to retain tighter constraints on the solution accuracy in exchange for the loss of some detail. Conversely, relaxing the solution control to allow higher maximum Courant numbers, especially in parts of the domain outside of the main solute transport pathways, may be a necessary measure to obtain reasonable computational efficiency, provided it can be demonstrated that the model retains acceptable accuracy for a given problem.

The Peclet number, representing the ratio of advective transport to diffusive transport, is given by Equation 3-3 from PNNL-11216:

$$P_e = \frac{v\Delta x}{D}$$

where D is the hydrodynamic dispersion tensor, and Δx is a characteristic length for a given problem. When Δx is equal to the finite difference model grid spacing, P_e is known as the grid Peclet number. The Peclet number will necessarily assume relatively high values for the advection-dominated transport conditions caused by the high groundwater fluxes described in the saturated CCUg.

At high Peclet number, the total variation diminishing (TVD) scheme, a third-order scheme for the finite difference transport solution, may better limit numerical dispersion than STOMP's default, first-order Patankar solution scheme (PNNL-12030). Note that the higher-order terms of the TVD solution which limit numerical dispersion have the effect of predicting higher solute concentrations in a plume's center of mass near the source and lower concentrations near the plume's fringe relative to a first-order solution (e.g., see PNNL-11216, Section 3.1). As with the Courant-number-limited transport option, invoking the TVD scheme incurs greater computational expense than a first-order scheme, and the potential gain in accuracy should be weighed against the expense using the significance to the PA objectives as the basis for any decision.

In addition to characterizing the relative significance of advective transport versus diffusive transport, the grid Peclet number is cited in literature as a basis for stability criteria or accuracy criteria depending on the solution scheme, often with an upper limit of about 2 (e.g., Fletcher 1991; PNNL-11216, Section 3.0), which would require a smaller grid spacing the higher the groundwater velocity or the lower the hydrodynamic dispersion. A smaller grid spacing would in turn require smaller time steps for a given Courant number limit; thus, there will often be a tradeoff between computational efficiency and accuracy, even if the solution scheme is unconditionally stable. In the case of high velocity, diffusion becomes less significant, so the grid Peclet number can be approximated by the ratio of the grid spacing to the longitudinal dispersivity (α_L):

$$P_e = \frac{\Delta x}{\alpha_L}$$

Applying this equation with a longitudinal dispersivity value of 10.5 m from Section C.8, the saturated zone Peclet number values for the PA model range from ~0.41 for the minimum horizontal spacing of 4.355 m to ~1.9 for the maximum spacing of 20 m. The relatively low values suggest that the saturated zone spatial discretization is adequate. Uncertainty in the dispersivity means the values could potentially be somewhat higher, but since the grid spacing is tighter between the contaminant sources and the points of calculation than near the domain edges, the saturated zone discretization is reasonable for the range of dispersivity values discussed in Section C.8.

C.10 REFERENCES

CP-47631, 2015, *Model Package Report: Central Plateau Groundwater Model Version 6.3.3*, Rev. 2, INTERA, Inc., Richland, Washington.

CP-47631, 2017, *Model Package Report: Central Plateau Groundwater Model, Version 8.4.5*, Rev. 4, CH2M HILL Plateau Remediation Company, Richland, Washington.

DOE/EIS-0391, 2012, *Final Tank Closure and Waste Management Environmental Impact Statement for the Hanford Site, Richland, Washington*, U.S. Department of Energy, Office of River Protection, Washington, D.C.

DOE M 435.1-1, 1999, *Radioactive Waste Management Manual*, U.S. Department of Energy, Washington, D.C.

DOE O 435.1, 2001, *Radioactive Waste Management*, U.S. Department of Energy, Washington, D.C.

DOE/RL-2011-01, 2011, *Hanford Site Groundwater Monitoring Report for 2010*, Rev. 0, U.S. Department of Energy, Richland Operations Office, Richland, Washington.

DOE/RL-2015-75, 2016, *Aquifer Treatability Test Report for the 200-BP-5 Groundwater Operable Unit*, Rev. 0, U.S. Department of Energy, Richland Operations Office, Richland, Washington.

DOE/RL-2016-09, 2016, *Hanford Site Groundwater Monitoring Report for 2015*, Rev. 0, U.S. Department of Energy, Richland Operations Office, Richland, Washington.

DOE/RL-2016-66, 2017, *Hanford Site RCRA Groundwater Monitoring Report for 2016*, Rev. 0, U.S. Department of Energy, Richland Operations Office, Richland, Washington.

ECF-200W-17-0043, 2018, *Capture-Zone and Particle-Tracking Analysis for the 200-UP-1/200-ZP-1 Areas using the 2017 Updated Central Plateau Model*, Rev. 0, INTERA, Inc. for CH2M HILL Plateau Remediation Company, Richland, Washington.

ECF-HANFORD-16-0013, 2017, *Hydraulic Gradients and Velocity Calculations for RCRA Sites in 2015*, Rev. 0, CH2M HILL Plateau Remediation Company, Richland, Washington.

ECF-HANFORD-16-0139, 2017, *Hydraulic Gradients and Velocity Calculations for RCRA Sites in 2016*, Rev. 0, CH2M HILL Plateau Remediation Company, Richland, Washington.

Environmental Dashboard Application, Queried 07/17/2017, https://ehs.hanford.gov/eda/.

Fletcher, C. A. J., 1991, Computational Techniques for Fluid Dynamics, 2nd Edition, Springer-Verlag, Berlin, Germany.

Gelhar, L. W., C. Welty, and K. R. Rehfeldt, 1992, "A Critical Review of Data on Field-Scale Dispersion in Aquifers," *Water Resources Research*, Vol. 28, Issue 7, pp. 1955–1974.

HGIS Hanford Geographic Information System, Queried 06/26/2017, [HMAPS Interactive Maps], [redacted]

ICRP, 2008, "ICRP Publication 107: Nuclear Decay Data for Dosimetric Calculations," *Annals of the ICRP*, International Commission on Radiation Protection, Vol. 38, No. 3, pp. 7–96.

NAVD88, 1988, North American Vertical Datum of 1988, National Geodetic Survey, U.S. Department of Commerce, National Oceanic and Atmospheric Administration, Silver Spring, Maryland.

Neuman, S. P., 1990, "Universal Scaling of Hydraulic Conductivities and Dispersivities in Geologic Media," *Water Resources Research*, Vol. 26, Issue 8, pp. 1749–1758.

Nevulis, R., S. Sorooshian, and D. R. Davis, 1987, "Task 4.2: Effects of Surface Waste Disposal Activity on Ground-Water Levels in the Saddle Mountain Basalt," Department of Hydrology and Water Resources, University of Arizona, Tucson, Arizona; in Appendix B, Exhibit 1 of PNNL-13641, 2001, *Uncertainty Analysis Framework - Hanford Site-Wide Groundwater Flow and Transport Model*, Pacific Northwest National Laboratory, Richland, Washington.

NUREG/CR-6114, 1994, *Auxiliary Analyses in Support of Performance Assessment of a Hypothetical Low-Level Waste Facility: Groundwater Flow and Transport Simulation*, Vol. 3, U.S. Nuclear Regulatory Commission, Washington, D.C.

Open-File Report 90-392, 1990, *A Computer Program for Calculating Subregional Water Budgets Using Results from the U.S. Geological Survey Modular Three-dimensional Finite-difference Ground-Water Flow Model*, United States Geological Survey, Reston, Virginia.

Open-File Report 99-238, 1999, *Procedures and Computer Programs for Telescopic Mesh Refinement Using MODFLOW*, U.S. Geological Survey, Tucson, Arizona.

PNNL-11216, 1997, *STOMP Subsurface Transport Over Multiple Phases Application Guide*, Pacific Northwest National Laboratory, Richland, Washington.

PNNL-12030, 2000, *STOMP Subsurface Transport Over Multiple Phases Version 2.0 Theory Guide*, Pacific Northwest National Laboratory, Richland, Washington.

PNNL-13641, 2001, *Uncertainty Analysis Framework - Hanford Site-Wide Groundwater Flow and Transport Model*, Pacific Northwest National Laboratory, Richland, Washington.

PNNL-15837, 2007, *Data Package for Past and Current Groundwater Flow and Contamination Beneath Single-Shell Tank Waste Management Areas*, Pacific Northwest National Laboratory, Richland, Washington.

PNNL-16407, 2007, *Geology of the Waste Treatment Plant Seismic Boreholes*, Rev. 1, Pacific Northwest National Laboratory, Richland, Washington.

PNNL-17154, 2008, *Geochemical Characterization Data Package for the Vadose Zone in the Single-Shell Tank Waste Management Areas at the Hanford Site*, Pacific Northwest National Laboratory, Richland, Washington.

PNNL-23711, 2015, *Physical, Hydraulic, and Transport Properties of Sediments and Engineered Materials Associated with Hanford Immobilized Low-Activity Waste*, RPT-IGTP-004, Rev. 0, Pacific Northwest National Laboratory, Richland, Washington.

Resource Conservation and Recovery Act of 1976, 42 USC 6901, et seq.

RHO-RE-ST-12P, 1984, *An Assessment of Aquifer Intercommunication in the B Pond-Gable Mountain Pond Area of the Hanford Site*, Rockwell Hanford Operations, Richland, Washington.

RPP-20621, 2004, *Far-Field Hydrology Data Package for the Integrated Disposal Facility Performance Assessment*, Rev. 0, CH2M HILL Hanford Group, Inc., Richland, Washington.

RPP-CALC-60497, 2016, *Peak Groundwater Concentrations for Tank Farm 241-AX TWRWP Risk Assessment*, Rev. 1, INTERA, Inc., Richland, Washington.

RPP-ENV-58578, in process, *Summary of the Natural System at Waste Management Area A-AX*, Rev. 1, Washington River Protection Solutions, LLC, Richland, Washington.

RPP-ENV-58782, 2016, *Performance Assessment of Waste Management Area C, Hanford Site, Washington*, Rev. 0, Washington River Protection Solutions, LLC, Richland, Washington.

RPP-RPT-58291, 2017, *Hanford Waste Management Area A-AX Soil Contamination Inventory Estimates*, Rev. 1, Washington River Protection Solutions, LLC, Richland, Washington.

RPP-RPT-58693, 2020, *Engineered System Data Package for Waste Management Area A-AX*, Rev. 0, Washington River Protection Solutions, LLC, Richland, Washington.

RPP-RPT-60171, in process, *Model Package Report: Geologic Framework Model used in WMA A-AX Performance Assessment and RCRA Closure Analysis*, Rev. 0, Washington River Protection Solutions, LLC, Richland, Washington.

Schulze-Makuch, D., 2005, "Longitudinal Dispersivity Data and Implications for Scaling Behavior," *Ground Water*, Vol. 43, Issue 3, pp. 443–456.

SGW-54165, 2014, *Evaluation of the Unconfined Aquifer Hydraulic Gradient Beneath the 200 East Area, Hanford Site*, Rev. 0, CH2M HILL Plateau Remediation Company, Richland, Washington.

WCH-520, 2013, *Performance Assessment for the Environmental Restoration Disposal Facility, Hanford Site, Washington*, Rev. 1, Washington Closure Hanford, Richland, Washington.

WHC-EP-0645, 1995, *Performance Assessment for the Disposal of Low-Level Waste in the 200 West Area Burial Grounds*, Westinghouse Hanford Company, Richland, Washington.

WHC-SD-WM-EE-004, 1995, *Performance Assessment of Grouted Double-Shell Tank Waste Disposal at Hanford*, Rev. 1, Westinghouse Hanford Company, Richland, Washington.

WHC-SD-WM-TI-730, 1996, *Performance Assessment for the Disposal of Low-Level Waste in the 200 East Area Burial Grounds*, Rev. 0, Westinghouse Hanford Company, Richland, Washington.

Xu, M. and Y. Eckstein, 1995, "Use of Weighted Least-Squares Method in Evaluation of the Relationship between Dispersivity and Field Scale," *Ground Water*, Vol. 33, Issue 6, pp. 905–908.

APPENDIX D

HORIZONTAL AND VERTICAL SPACING OF THE FINITE DIFFERENCE CELLS IN THE THREE-DIMENSIONAL WASTE MANAGEMENT AREA A-AX FLOW AND TRANSPORT MODEL DOMAIN

This page intentionally left blank.

APPENDIX D HORIZONTAL AND VERTICAL SPACING OF THE FINITE DIFFERENCE CELLS IN THE THREE-DIMENSIONAL WASTE MANAGEMENT AREA A-AX FLOW AND TRANSPORT MODEL DOMAIN

Northwest to Southeast Spacing; West Corner Coordinates = 574817.91 m Easting, 136075.33 m Northing (Lambert Coordinate System[1])									
I Index	Spacing	I Index	Spacing	I Index	Spacing	I Index	Spacing	I Index	Spacing
1	20 m	2	20 m	3	20 m	4	20 m	5	16 m
6	16 m	7	16 m	8	12 m	9	12 m	10	12 m
11	12 m	12	10 m	13	10 m	14	10 m	15	8 m
16	8 m	17	8 m	18	8 m	19	8 m	20	6 m
21	6 m	22	6 m	23	6 m	24	5.152 m	25	5 m
26	5 m	27	5 m	28	5 m	29	5 m	30	4.562 m
31	4.355 m	32	4.355 m	33	4.355 m	34	4.355 m	35	4.562 m
36	4.355 m	37	4.355 m	38	4.355 m	39	4.355 m	40	4.562 m
41	4.355 m	42	4.355 m	43	4.355 m	44	4.355 m	45	4.562 m
46	4.355 m	47	4.355 m	48	4.355 m	49	4.355 m	50	4.562 m
51	4.355 m	52	4.355 m	53	4.355 m	54	4.355 m	55	4.562 m
56	4.355 m	57	4.355 m	58	4.355 m	59	4.355 m	60	4.562 m
61	5 m	62	5 m	63	5 m	64	5 m	65	5 m
66	5 m	67	6 m	68	6 m	69	6 m	70	6 m
71	6 m	72	6 m	73	6 m	74	6 m	75	8 m
76	8 m	77	8 m	78	10 m	79	10 m	80	10 m
81	10 m	82	10 m	83	10 m	84	10 m	85	10 m
86	10 m	87	10 m	88	10 m	89	10 m	90	10 m
91	10 m	92	10 m	93	10 m	94	10 m	95	12 m
96	16 m	97	16 m	98	20 m	99	20 m	100	20 m

Southwest to Northeast Spacing; West Corner Coordinates = 574817.91 m Easting, 136075.33 m Northing (Lambert Coordinate System[1])									
J Index	Spacing	J Index	Spacing	J Index	Spacing	J Index	Spacing	J Index	Spacing
1	20 m	2	20 m	3	20 m	4	20 m	5	16 m
6	16 m	7	16 m	8	12 m	9	12 m	10	12 m
11	10 m	12	10 m	13	10 m	14	8 m	15	8 m
16	8 m	17	8 m	18	8 m	19	8 m	20	6 m
21	6 m	22	6 m	23	6 m	24	6 m	25	6 m

Southwest to Northeast Spacing; West Corner Coordinates = 574817.91 m Easting, 136075.33 m Northing (Lambert Coordinate System[1])									
J Index	Spacing	J Index	Spacing	J Index	Spacing	J Index	Spacing	J Index	Spacing
26	6 m	27	6 m	28	6 m	29	5 m	30	5 m
31	5 m	32	5 m	33	4.794 m	34	4.562 m	35	4.355 m
36	4.355 m	37	4.355 m	38	4.355 m	39	4.562 m	40	4.355 m
41	4.355 m	42	4.355 m	43	4.355 m	44	4.562 m	45	4.355 m
46	4.355 m	47	4.355 m	48	4.355 m	49	4.562 m	50	4.355 m
51	4.355 m	52	4.355 m	53	4.355 m	54	4.562 m	55	4.6 m
56	5 m	57	5.25 m	58	6 m	59	6.047 m	60	6 m
61	5.25 m	62	5 m	63	4.6 m	64	4.562 m	65	4.355 m
66	4.355 m	67	4.355 m	68	4.355 m	69	4.562 m	70	4.355 m
71	4.355 m	72	4.355 m	73	4.355 m	74	4.562 m	75	4.355 m
76	4.355 m	77	4.355 m	78	4.355 m	79	4.562 m	80	5 m
81	5 m	82	5 m	83	5 m	84	6 m	85	6 m
86	6 m	87	6 m	88	6 m	89	6 m	90	6 m
91	6 m	92	6 m	93	8 m	94	8 m	95	8 m
96	8 m	97	8 m	98	8 m	99	10 m	100	10 m
101	10 m	102	12 m	103	12 m	104	12 m	105	16 m
106	16 m	107	16 m	108	20 m	109	20 m	110	20 m
111	20 m	112	20 m	113	20 m	114	20 m	115	20 m
116	20 m	117	20 m	118	20 m	119	20 m	120	20 m

Vertical Spacing; Bottom Elevation = 95.25 m (NAVD88[2])									
K Index	Spacing	K Index	Spacing	K Index	Spacing	K Index	Spacing	K Index	Spacing
1	3 m	2	2.5 m	3	2.25 m	4	2 m	5	1.75 m
6	1.75 m	7	1.5 m	8	1.25 m	9	1.25 m	10	1 m
11	1 m	12	1 m	13	0.75 m	14	0.75 m	15	0.75 m
16	0.75 m	17	0.5 m	18	0.5 m	19	0.5 m	20	0.5 m
21	0.5 m	22	0.5 m	23	0.5 m	24	0.5 m	25	0.5 m
26	0.5 m	27	0.5 m	28	0.5 m	29	0.5 m	30	0.5 m
31	0.5 m	32	0.5 m	33	0.5 m	34	0.5 m	35	0.5 m
36	0.5 m	37	0.5 m	38	0.5 m	39	0.5 m	40	0.75 m
41	0.75 m	42	0.75 m	43	0.75 m	44	0.75 m	45	1 m

Vertical Spacing; Bottom Elevation = 95.25 m (NAVD88[2])									
K Index	Spacing	K Index	Spacing	K Index	Spacing	K Index	Spacing	K Index	Spacing
46	1 m	47	1 m	48	1 m	49	1 m	50	1 m
51	1 m	52	1 m	53	1 m	54	1 m	55	1 m
56	1 m	57	1 m	58	1 m	59	1 m	60	1 m
61	1 m	62	1 m	63	1 m	64	1 m	65	1 m
66	1 m	67	1 m	68	1 m	69	1 m	70	1 m
71	1 m	72	1 m	73	1 m	74	1 m	75	1 m
76	1 m	77	1 m	78	1 m	79	1 m	80	1 m
81	1 m	82	1 m	83	1 m	84	1 m	85	1 m
86	1 m	87	1 m	88	1 m	89	1 m	90	1 m
91	1 m	92	1 m	93	1 m	94	1 m	95	1 m
96	1 m	97	1 m	98	1 m	99	1 m	100	1 m
101	1 m	102	1 m	103	1 m	104	1 m	105	1 m
106	1 m	107	1 m	108	1 m	109	1 m	110	1 m
111	1 m	112	1 m	113	1 m	114	1 m	115	1 m
116	1 m	117	1 m	118	1 m	119	1 m	120	1 m
121	1 m	122	1 m	123	1 m	124	1 m	125	1 m

Vertical Node and Cell Face Elevations; Bottom Elevation = 95.25 m (NAVD88[2])									
K Index	Spacing (m)	Node Elevation (m NAVD88)	Cell Bottom Elevation (m NAVD88)	Cell Top Elevation (m NAVD88)	K Index	Spacing (m)	Node Elevation (m NAVD88)	Cell Bottom Elevation (m NAVD88)	Cell Top Elevation (m NAVD88)
1	3	96.75	95.25	98.25	64	1	153.25	152.75	153.75
2	2.5	99.5	98.25	100.75	65	1	154.25	153.75	154.75
3	2.25	101.875	100.75	103	66	1	155.25	154.75	155.75
4	2	104	103	105	67	1	156.25	155.75	156.75
5	1.75	105.875	105	106.75	68	1	157.25	156.75	157.75
6	1.75	107.625	106.75	108.5	69	1	158.25	157.75	158.75
7	1.5	109.25	108.5	110	70	1	159.25	158.75	159.75
8	1.25	110.625	110	111.25	71	1	160.25	159.75	160.75
9	1.25	111.875	111.25	112.5	72	1	161.25	160.75	161.75
10	1	113	112.5	113.5	73	1	162.25	161.75	162.75
11	1	114	113.5	114.5	74	1	163.25	162.75	163.75

Vertical Node and Cell Face Elevations; Bottom Elevation = 95.25 m (NAVD88[2])									
K Index	Spacing (m)	Node Elevation (m NAVD88)	Cell Bottom Elevation (m NAVD88)	Cell Top Elevation (m NAVD88)	K Index	Spacing (m)	Node Elevation (m NAVD88)	Cell Bottom Elevation (m NAVD88)	Cell Top Elevation (m NAVD88)
12	1	115	114.5	115.5	75	1	164.25	163.75	164.75
13	0.75	115.875	115.5	116.25	76	1	165.25	164.75	165.75
14	0.75	116.625	116.25	117	77	1	166.25	165.75	166.75
15	0.75	117.375	117	117.75	78	1	167.25	166.75	167.75
16	0.75	118.125	117.75	118.5	79	1	168.25	167.75	168.75
17	0.5	118.75	118.5	119	80	1	169.25	168.75	169.75
18	0.5	119.25	119	119.5	81	1	170.25	169.75	170.75
19	0.5	119.75	119.5	120	82	1	171.25	170.75	171.75
20	0.5	120.25	120	120.5	83	1	172.25	171.75	172.75
21	0.5	120.75	120.5	121	84	1	173.25	172.75	173.75
22	0.5	121.25	121	121.5	85	1	174.25	173.75	174.75
23	0.5	121.75	121.5	122	86	1	175.25	174.75	175.75
24	0.5	122.25	122	122.5	87	1	176.25	175.75	176.75
25	0.5	122.75	122.5	123	88	1	177.25	176.75	177.75
26	0.5	123.25	123	123.5	89	1	178.25	177.75	178.75
27	0.5	123.75	123.5	124	90	1	179.25	178.75	179.75
28	0.5	124.25	124	124.5	91	1	180.25	179.75	180.75
29	0.5	124.75	124.5	125	92	1	181.25	180.75	181.75
30	0.5	125.25	125	125.5	93	1	182.25	181.75	182.75
31	0.5	125.75	125.5	126	94	1	183.25	182.75	183.75
32	0.5	126.25	126	126.5	95	1	184.25	183.75	184.75
33	0.5	126.75	126.5	127	96	1	185.25	184.75	185.75
34	0.5	127.25	127	127.5	97	1	186.25	185.75	186.75
35	0.5	127.75	127.5	128	98	1	187.25	186.75	187.75
36	0.5	128.25	128	128.5	99	1	188.25	187.75	188.75
37	0.5	128.75	128.5	129	100	1	189.25	188.75	189.75
38	0.5	129.25	129	129.5	101	1	190.25	189.75	190.75
39	0.5	129.75	129.5	130	102	1	191.25	190.75	191.75

Vertical Node and Cell Face Elevations; Bottom Elevation = 95.25 m (NAVD88[2])									
K Index	Spacing (m)	Node Elevation (m NAVD88)	Cell Bottom Elevation (m NAVD88)	Cell Top Elevation (m NAVD88)	K Index	Spacing (m)	Node Elevation (m NAVD88)	Cell Bottom Elevation (m NAVD88)	Cell Top Elevation (m NAVD88)
40	0.75	130.375	130	130.75	103	1	192.25	191.75	192.75
41	0.75	131.125	130.75	131.5	104	1	193.25	192.75	193.75
42	0.75	131.875	131.5	132.25	105	1	194.25	193.75	194.75
43	0.75	132.625	132.25	133	106	1	195.25	194.75	195.75
44	0.75	133.375	133	133.75	107	1	196.25	195.75	196.75
45	1	134.25	133.75	134.75	108	1	197.25	196.75	197.75
46	1	135.25	134.75	135.75	109	1	198.25	197.75	198.75
47	1	136.25	135.75	136.75	110	1	199.25	198.75	199.75
48	1	137.25	136.75	137.75	111	1	200.25	199.75	200.75
49	1	138.25	137.75	138.75	112	1	201.25	200.75	201.75
50	1	139.25	138.75	139.75	113	1	202.25	201.75	202.75
51	1	140.25	139.75	140.75	114	1	203.25	202.75	203.75
52	1	141.25	140.75	141.75	115	1	204.25	203.75	204.75
53	1	142.25	141.75	142.75	116	1	205.25	204.75	205.75
54	1	143.25	142.75	143.75	117	1	206.25	205.75	206.75
55	1	144.25	143.75	144.75	118	1	207.25	206.75	207.75
56	1	145.25	144.75	145.75	119	1	208.25	207.75	208.75
57	1	146.25	145.75	146.75	120	1	209.25	208.75	209.75
58	1	147.25	146.75	147.75	121	1	210.25	209.75	210.75
59	1	148.25	147.75	148.75	122	1	211.25	210.75	211.75
60	1	149.25	148.75	149.75	123	1	212.25	211.75	212.75
61	1	150.25	149.75	150.75	124	1	213.25	212.75	213.75
62	1	151.25	150.75	151.75	125	1	214.25	213.75	214.75
63	1	152.25	151.75	152.75	—	—	—	—	—

Vertical Node and Cell Face Elevations; Bottom Elevation = 95.25 m (NAVD88[2])									
K Index	Spacing (m)	Node Elevation (m NAVD88)	Cell Bottom Elevation (m NAVD88)	Cell Top Elevation (m NAVD88)	K Index	Spacing (m)	Node Elevation (m NAVD88)	Cell Bottom Elevation (m NAVD88)	Cell Top Elevation (m NAVD88)

[1] NOAA Manual NOS NGS 5, State Plane Coordinate System of 1983, National Geodetic Survey, U.S. Department of Commerce, National Oceanic and Atmospheric Administration, Rockville, Maryland.

[2] North American Vertical Datum of 1988, National Geodetic Survey, U.S. Department of Commerce, National Oceanic and Atmospheric Administration, Silver Spring, Maryland.

Note: To approximately align the model with the general direction of groundwater flow, the STOMP input files use a coordinate system rotated 135 degrees east of north about the node of cell (1,1,1) such that geographic northwest is model west, geographic southwest is model south, the x-coordinate of the west boundary of the grid in STOMP is -10 m, and the y-coordinate of the south boundary of the grid in STOMP is -10 m.

Subsurface Transport Over Multiple Phases (STOMP) is developed and distributed by Battelle Memorial Institute.

ATTACHMENT 1

SOFTWARE INSTALLATION AND CHECKOUT FORMS

This page intentionally left blank.

CHPRC SOFTWARE INSTALLATION AND CHECKOUT FORM

Software Owner Instructions:

Complete Fields 1-13, then run test cases in Field 14. Compare test case results listed in Field 15 to corresponding Test Report outputs. If results are the same, sign and date Field 19. If not, resolve differences and repeat above steps.

Software Subject Matter Expert Instructions:

Assign test personnel. Approve the installation of the code by signing and dating Field 21, then maintain form as part of the software support documentation.

GENERAL INFORMATION:

1. Software Name: eSTOMP (Parallel - Subsurf. Trans. Over Mult. Phases) Software Version No.: Bld 6

EXECUTABLE INFORMATION:

2. Executable Name (include path):

Test: [redacted]estomp-w-petsc-chprc06i.x
Production: [redacted]estomp-w-petsc-chprc06i.x
MD5 file signature: c4429b6a23dd26537f59d15594e5fc3f

3. Executable Size (bytes): 12824187

COMPILATION INFORMATION:

4. Hardware System (i.e., property number or ID):

Tellus Subsurface Modeling Platform

5. Operating System (include version number):

Linux tellusmgmt.rl.gov 2.6.18-308.4.1.el5 #1 SMP Tue Apr 17 17:08:00 EDT 2012 x86_64 x86 64 x86 64 GNU/Linux

INSTALLATION AND CHECKOUT INFORMATION:

6. Hardware System (i.e., property number or ID):

Tellus Subsurface Modeling Platform

7. Operating System (include version number):

Linux tellusmgmt.rl.gov 2.6.18-308.4.1.el5 #1 SMP Tue Apr 17 17:08:00 EDT 2012 x86_64 x86 64 x86 64 GNU/Linux

8. Open Problem Report? ◉ No ○ Yes PR/CR No.

TEST CASE INFORMATION:

9. Directory/Path:

[redacted]build-06 estomp

10. Procedure(s):

CHPRC-00211 Rev. 3, "STOMP Software Test Plan"

11. Libraries:

[redacted]

12. Input Files:

[redacted]

13. Output Files:

[redacted]

Page 1 of 2 A-6005-149 (REV 0)

CHPRC SOFTWARE INSTALLATION AND CHECKOUT FORM (continued)

1. Software Name: eSTOMP (Parallel - Subsurf. Trans. Over Mult. Phases) Software Version No.: Bld 6

14. Test Cases:

ATC-STOMP-1 (Water Mode with Transport) only

15. Test Case Results:

Pass

16. Test Performed By: WJ McMahon

17. Test Results: (•) Satisfactory, Accepted for Use ( ) Unsatisfactory

18. Disposition (include HISI update):

Accepted; Installation noted in HISI for users WE Nichols, TJ Budge, WJ McMahon, S Mehta

Prepared By:

19.	WE Nichols	1 OCT 2018
Software Owner (Signature)	Print	Date

20. Test Personnel:

	WJ McMahon	10/01/18
Sign	Print	Date
Sign	Print	Date
Sign	Print	Date

Approved By:

21.	N/R (per CHPRC-00211, Rev. 3)	
Software SME (Signature)	Print	Date

CHPRC SOFTWARE INSTALLATION AND CHECKOUT FORM

Software Owner Instructions:

Complete Fields 1-13, then run test cases in Field 14. Compare test case results listed in Field 15 to corresponding Test Report outputs. If results are the same, sign and date Field 19. If not, resolve differences and repeat above steps.

Software Subject Matter Expert Instructions:

Assign test personnel. Approve the installation of the code by signing and dating Field 21, then maintain form as part of the software support documentation.

GENERAL INFORMATION:

1. Software Name: STOMP (Subsurface Transport Over Multiple Phases) Software Version No.: Bld 6

EXECUTABLE INFORMATION:

2. Executable Name (include path):

```
All executable files installed in directory[redacted]
--------------------------------  ---------------------------
MD5 File Signature                Executable File Name
--------------------------------  ---------------------------
2aed5deebf96f2acd085ee5b8c035107  estomp-w-bcgs-chprc06i.x
```

3. Executable Size (bytes): MD5 signatures above uniquely identify each executable file

COMPILATION INFORMATION:

4. Hardware System (i.e., property number or ID):

Olive Linux Cluster

5. Operating System (include version number):

Linux olive 4.4.0-38-generic #57~14.04.1-Ubuntu SMP Tue Sep 6 17:20:43 UTC 2016 x86_64 x86_64 x86_64 GNU/Linux

INSTALLATION AND CHECKOUT INFORMATION:

6. Hardware System (i.e., property number or ID):

Olive Linux Cluster

7. Operating System (include version number):

Linux olive 4.4.0-38-generic #57~14.04.1-Ubuntu SMP Tue Sep 6 17:20:43 UTC 2016 x86_64 x86_64 x86_64 GNU/Linux

8. Open Problem Report? ◉ No ○ Yes PR/CR No.

TEST CASE INFORMATION:

9. Directory/Path:

[redacted]

10. Procedure(s):

CHPRC-00211 Rev 1, STOMP Software Test Plan

11. Libraries:

N/A (static linking)

12. Input Files:

Input files for ATC-eSTOMP-1
(Baseline for comparison are results files from ATC-eSTOMP-1 prepared on Green Linux Cluster during acceptance testing)

13. Output Files:

plot.* files produced by eSTOMP in testing

14. Test Cases:

ATC-eSTOMP-1

Page 1 of 2 A-6005-149 (REV 0)